Science, Medicine and Industry
Innovating for the Future.

ABSTRACTS
ASAIO 62nd ANNUAL CONFERENCE

SAN FRANCISCO, CA
JUNE 15 – 18, 2016

7

Flow-induced Coating Erosion and Fibrinogen Fouling

A. Belanger,[1] A. Decarmine,[2] S. Jiang,[3] K. Cook,[4] K. Amoako.[5] *[1]Mechanical Engineering, University of New Haven, West Haven, CT; [2]Chemical Engineering, University of New Haven, West Haven, CT; [3]Chemical Engineering, University of Washington, Seattle, WA; [4]Biomedical Engineering, Carnegie Mellon University, Pittsburgh, PA; [5]Mechanical and Industrial Engineering, University of New Haven, West Haven, CT.*

Study: Shear-induced erosion of non-fouling coatings can limit biomaterial fouling resistance. In this study, fibrinogen (Fg) fouling on zwitterionic polycarboxybetaine (pCB)-coated Polydimethylsiloxane (PDMS) membranes was evaluated under shear stress using a flow system.
Methods: PDMS were coated using graft-to dip coating methods. The flow system comprising acrylic flow cells, 3/16'' ID Tygon tubing, roller pumps, flow meters and probes imposed 1,6,and 10 dynes/cm^2 physiological shears on uncoated and coated PDMS (N=5/membrane, 8.89 cm x 2.54 cm) during recirculation of deionized water (ρ=1g/cm^3, pH 7.34) at 60, 150, and 230 mL/min for 8 hrs. Fg fouling, by standard ELISA, was reported as percent of fouling on uncoated PDMS.
Results: Pre-flow fouling on coated PDMS (5.73% ± 1.97%) was significantly lower compared uncoated PDMS (100%, p < 0.001). This level of fouling, although lower, was not different from fouling on coated PDMS exposed to 1 (9.55% ± 0.09%, p = 0.23), 6 (15.92% ± 10.88%, p = 0.14), and 10 dynes/cm^2 (21.62% ± 13.68%, p = 0.08). Our initial results indicate that pCB coating on PDMS were stable, under the test flow conditions, with minimal erosion. Future studies will evaluate other coatings using different biomarkers.

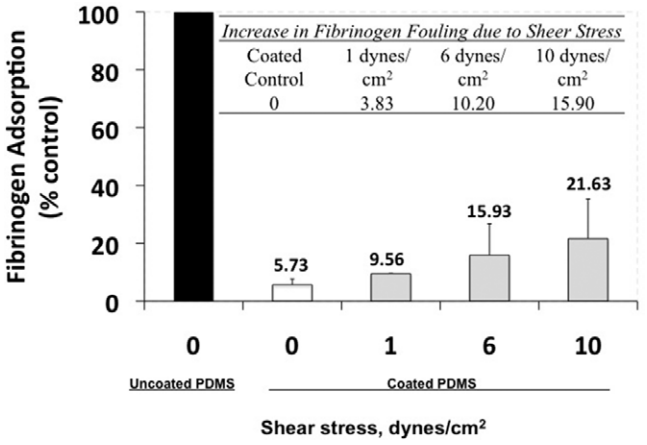

17

Ex Situ Perfusion of Human Limbs for 24 Hours

N. L. Werner,[1] F. Alghanem,[1] S. L. Rakestraw,[1] D. Sarver,[2] B. Nicely,[3] R. E. Pietroski,[3] P. A. Lange,[3] S. M. Rudich,[3] C. Mendias,[2] A. Rojas-Pena,[4] J. Magee,[4] R. H. Bartlett,[1] K. Ozer.[2] *[1]Department of Surgery, University of Michigan, Ann Arbor, MI; [2]Department of Orthopedic Surgery, University of Michigan, Ann Arbor, MI; [3]Gift of Life Michigan, Ann Arbor, MI; [4]Section of Transplantation, Department of Surgery, University of Michigan, Ann Arbor, MI.*

Study: Currently vascularized composite allografts (VCA) are cold preserved (4°C) until transplantation. This process is time limited, as the tissue has to be revascularized within 4–6 hours to minimize ischemia reperfusion injury. The purpose of this study was to evaluate ex situ perfusion as an alternate technique of VCA limb preservation.
Methods: Four human forearms were procured from brain-dead adult donors under tourniquet control. Following elbow disarticulation, the brachial artery was cannulated. The limb was flushed with heparinized saline and connected to a temperature controlled (30–33°C) ex situ perfusion system (Figure) for 24 hours. The perfusate was plasma-based and red blood cells added to target a hemoglobin (Hb) concentration of 4–6 g/dL. Hemodynamics were monitored continuously, perfusate samples analyzed hourly, and nerve stimulation performed every 2 hours. Muscle biopsies (flexor carpi radialis) were obtained at 0, 12, and 24 hours of perfusion.
Results: Average warm ischemia time was 76 minutes. Average arterial systolic pressure was 98 ± 2 mmHg, perfusion flow 319 ± 18 mL/min (~6–10% of the donor's estimated cardiac output), and vascular resistance 158 ± 18 mmHg/mL/min. Perfusate had an average pH of 7.43 ± 0.04, pCO_2 32 ± 1 mmHg, pO_2 317 ± 18 mmHg, and Hb 4.8 ± 0.4 g/dL. Electrolytes (sodium, potassium, chloride) remained within a physiologic range. Lactate increased steadily throughout the experiment; however, neuromuscular electrical stimulation revealed ongoing contraction throughout the experiment. Biopsy results are pending.
Conclusions: All limbs appeared viable after 24 hours of near-normothermic ex situ perfusion. While no assumptions can be drawn about the long-term function of the extremity, this approach could help extend VCA transplantation to a wider geographic area and may prevent the cellular injury associated with cold preservation.

22

Hemodynamic Performance of Vena Cava Filters with Helical Flow Inducers of Different Thread Pitches: A Numerical Study

Y. Chen, X. Deng. *Key Laboratory for Biomechanics and Mechanobiology of Ministry of Education, Beihang University, Beijing, CHINA.*

Study: The build-up of thromboses in vena cava filters after deployment presents serious problem to the patients. We propose a vena cava filter in which helical flow is induced in the filter's working zone in order to minimize filter blockage by trapped clots and facilitate the lysis of trapped clots. In present study, we compared five filter models with helical flow inducers of different thread pitches in terms of blood flow patterns in the vena cava.

Methods: The 5 filter models (Figure 1) with different thread pitches were created using the computer-aided design software, Pro-E and assumed to be deployed in the vena cava that was simplified as a cylindrical tube. Then the flow patterns in the vena cava with the filters were analyzed by numerical computation and compared. The numerical simulations of the flow patterns were carried out under laminar flow condition. The models were meshed using a mixture of tetrahedral and hexahedral volume meshes. The iterative process of computation was terminated when the residual of continuity and velocity were all less than the convergence criterion 1.0×10^{-5}. Velocity distribution, helicity and wall shear stress (WSS) were compared among the 5 models.

Results: The numerical simulation (Figure 2) revealed that the helical flow inducers of the filters can effectively create helical flows in the working zones of the filters, thereby enhancing blood flow velocity, subduing the filter structure's adverse disruption to blood flow and increasing flow-induced shear stress in the filter. Moreover, it was found that helical flow inducer with smaller thread pitch could induce flow rotation both in clockwise and counterclockwise directions.

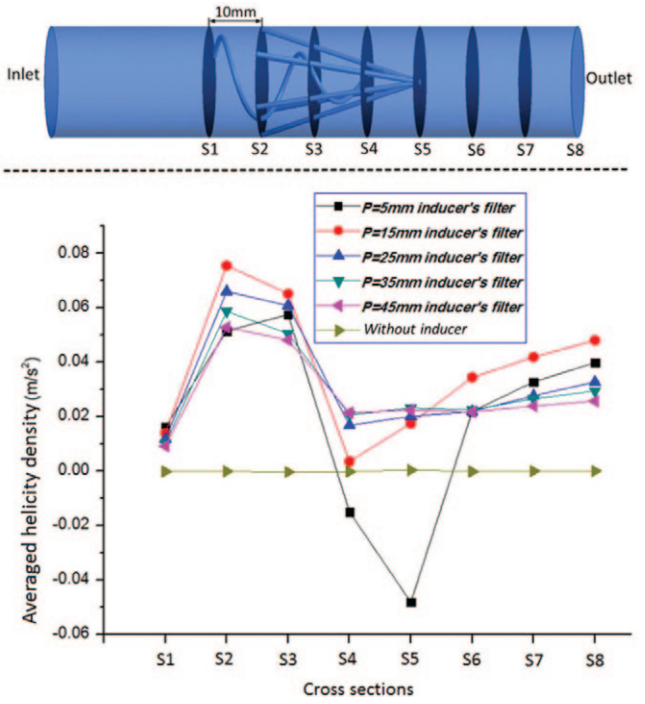

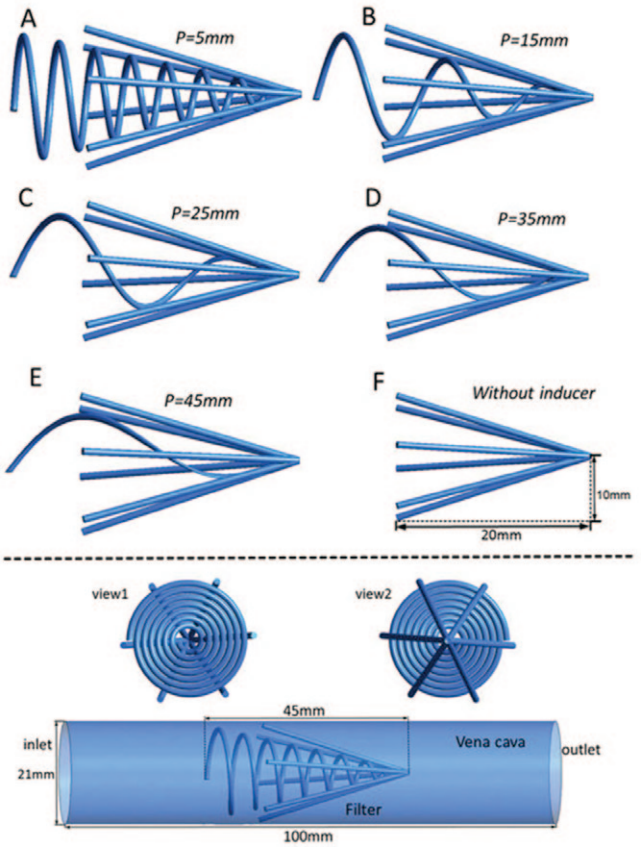

25

Time-frequency Analysis of Swallowing Sounds in Non-invasive Evaluation of Swallowing Function

M. Kani, S. Yamauchi, Y. Motohashi, T. Sato, T. Agishi. *Graduate School of Engineering, Toin University of Yokohama, Yokohama, JAPAN.*

Study: We have used acceleration sensors attached to the surface of the throat to measure swallowing sounds when the subject swallowed, using wavelet transformation of the resulting sound signals to conduct time-frequency analysis. Based on the results, we are investigating testing methods for non-invasive and quantitative evaluation of swallowing function. This study defined parameters expressing the temporal positional relationship of the three components of swallowing sounds, by approximating swallowing sound signals with a three-dimensional spline curve, and proposes a method for quantifying swallowing function.
Methods: Swallowing sounds were measured using a biological sound analyzer (BSA) developed by the authors. Acceleration sensors were affixed to the outer side of the trachea under the annular cartilage, as the position recommended for measurement of swallowing sounds, using the cervical auscultation method. Smoothing was carried out on the swallowing sound signals that were obtained, then every 16th amplitude peak was sampled. Intervals between sampling points were interpolated using a three-dimensional spline function, and an approximation curve of the swallowing sound signals was created. The time of the peak between the first and third sounds was taken as T1 and that between the first and second sounds was taken as T2. Swallowing function was then quantified using the equation T = T2/T1. Next, we asked the subject to swallow twice in succession within the BSA measurement time of 10 s and applied a typical swallowing sound signal detection function developed in relation to that signal group. We examined whether a signal representing the swallowing function for that subject could be selected.
Results: The T expressing the relative position of the second sound to the continuous time of the overall swallowing sound was determined from the T1 and T2 obtained from the approximation curve, enabling quantitative evaluation of swallowing function.

26

Computational Evaluation of Thrombosis Risk After Ventricular Remodeling with Long-term Mechanical Support

S. L. Jessen,[1] J. D. Horn,[1] A. C. Caruso,[2] F. J. Clubb, Jr.,[2] B. R.Weeks.[2] *[1]Department of Biomedical Engineering, Texas A&M University, College Station, TX; [2]Department of Veterinary Pathobiology, Texas A&M University, College Station, TX.*

Study: With the growing use of long-term ventricular assist device (VAD) therapy, effects of myocardial remodeling on ventricular flow and thrombosis risk must be considered. During months or years of mechanical support, cardiac remodeling may alter ventricular flow patterns, resulting in mural thrombus formation or dislodgement of pre-existing thrombi. We created a computational model to examine the effect of various VAD cannula implantation depths and orientations on intra-cardiac flow. Thrombogenic and embolic risks were estimated by examining computed regions of stasis and recirculation in dilated and normal human left ventricles (LV).
Methods: Two-dimensional computational representations of dilated and remodeled LVs were created with the VAD cannula either in-line with or at an angle to the mitral valve (MV) inserted into the ventricle at varied depths. Computational Fluid Dynamics (CFD) software (Star-CCM+) was used to predict flow patterns, stagnation, and recirculation as LV walls periodically contracted.
Results: In simulations representing dilated cardiomyopathy, cannula placement in the apex with minimal lumenal protrusion yielded the best washout and minimized stagnation and recirculation (Fig 1A). Alternatively, placing the VAD cannula at an angle to the MV resulted in decreased LV washout and larger areas of stagnation (Fig 1B). For each cannula orientation/depth examined, the remodeled LV of smaller lumen size demonstrated improved washout with less stagnation (Fig 1C-D). Ongoing risk for mural thrombus formation is maintained in dilated hearts due to large regions of stagnant flow. Washout improves as the heart remodels to a smaller volume. Periodic monitoring of myocardial remodeling during long-term VAD implantation may prove valuable for assessing changes in the risk for thromboembolic complications.

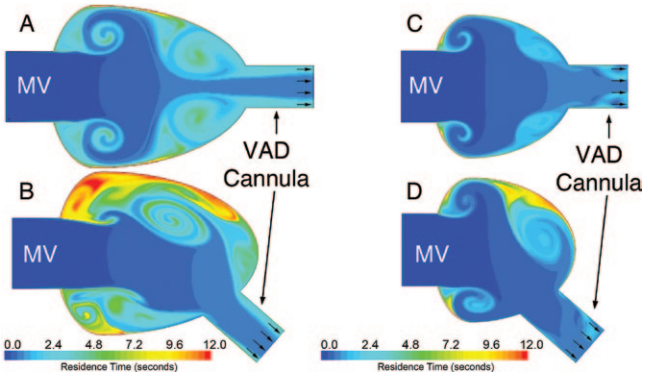

Fig 1. Areas of stagnation (denoted by orange-red) in dilated (A-B) and remodeled (C-D) LVs with implanted cannula.

28

Optimized Settings for Side Holes to Ensure Actual Blood Flow Through 17G Indwelling Needles for Hemodialysis

Y. Taguchi, S. Yamauchi, Y. Motohashi, T. Sato, T. Agishi. *Graduate School of Engineering, Toin University of Yokohama, Yokohama, JAPAN.*

Study: In order to perform ongoing hemodialysis while minimizing puncture pain and maintaining satisfactory vascular access (VA) function over the long term, an indwelling needle with small diameter should be used. However, as the diameter decreases, differences reportedly occur between the set blood flow rate and the actual rate. Companies commercially marketing indwelling needles have tried to correct this problem using various approaches. We believe that side holes in indwelling needles play a large role in ensuring the set blood flow rate, and have created several prototype 17G indwelling needles with different numbers of side holes and with the side hole apertures in various locations. We then conducted experiments to determine whether these differences affect the ability to ensure the actual blood flow rate.
Methods: One side hole with a diameter of 0.5 mm was provided at a position 3.3 mm from the tip of the needle. A second side hole was positioned 1.3 mm away from the first hole, with the needle rotated 90 degrees. This indwelling needle was our Type 1 prototype. We then created another prototype, Type 2, that had one side hole 3.3 mm from the tip, and a second side hole with the needle rotated 180 degrees. Next, we created a Type 3 prototype with one hole located 3.3 mm from the tip and two side holes located every 1.3 mm from that position, with the needle rotated 90 degrees, and a fourth prototype, Type 4, with three side holes. For the pseudo-blood vessel, we used a polyvinyl chloride tube with an inner diameter of 12 mm, and we circulated water through the pseudo-blood vessel at a flow rate of 700 ml/min. We then positioned the prototype needle in the pseudo-blood vessel.
Results: We found that the actual blood flow rate that can be ensured increases as the number of holes increases but that the amount of increase may differ depending on the locations of the holes.

29

A Study of the Effects of Side Holes in Indwelling Needles for Hemodialysis on Actual Blood Flow Rate Using Computational Fluid Dynamics Analysis

N. Shimazaki, S. Yamauchi, Y. Motohashi, T. Sato, T. Agishi. *Graduate School of Engineering, Toin University of Yokohama, Yokohama, JAPAN.*

Study: A larger set blood flow rate for hemodialysis corresponds to a larger discrepancy between the set and actual blood flow rates at which blood can be removed. To compensate for this discrepancy, indwelling needles tend to have larger aperture diameters. Providing side holes in the indwelling needle is an effective means for increasing the actual blood flow rate without changing the diameter of the indwelling needle. We are seeking theoretical optimization of side holes using computational fluid dynamics (CFD) analysis.
Methods: We created a model for analysis in which a 17G indwelling needle with an effective length of 30 mm and no side holes was positioned in a blood vessel with an inner diameter of 12 mm. We also prepared an experimental model with the same conditions as the analysis model. Using a manometer, we measured blood removal pressure at the blood removal exit of the indwelling needle in relation to the blood flow rate set for the roller pump, and the resulting blood removal pressure was set for the blood removal exit of the analysis model. Next, we created an analysis model of an indwelling needle with one side hole that was round, with a diameter of 0.5 mm, located 3.3 mm from the tip of the indwelling needle. We also created models with two and three side holes, and conducted CFD analysis to assess the impact of the number and locations of side holes on the actual blood flow rate.
Results: In order to achieve consistency between analysis results and experimental results, we defined a resistance force for the blood removal exit of the indwelling needle, based on the pressure loss coefficient and flow velocity. Because the pressure loss coefficient is determined on the basis of the shape of the indwelling needle, the results suggest that for the 17G indwelling needle used in our study, the impact of side holes can be theoretically investigated using the pressure loss coefficient.

30

A Theoretical Analysis of Shape Optimization to Minimize Clinging of Double Lumen Catheters with Side Holes

Y. Marushita, S. Yamauchi, Y. Motohashi, T. Sato, T. Agishi. *Graduate School of Engineering, Toin University of Yokohama, Yokohama, JAPAN.*

Study: During blood purification therapy using a double lumen catheter (DLC), the DLC sometimes clings to the blood vessel wall, resulting in a reduced volume of blood removed via the DLC. If this happens, a sufficient volume of blood removal can sometimes be ensured by changing the DLC connection from a forward connection to a reverse connection, so that therapy can be continued. A basic investigation into optimization of the DLC in order to keep the DLC from clinging to the blood vessel wall was conducted. In this investigation, the flow-structure interaction of a side-hole type DLC (SH-DLC) was analyzed using the finite element method (FEM).
Methods: For the analysis, ANSYS CFD, which is general-purpose finite element analysis software, was used. An analysis model in which a commercially available SH-DLC was positioned in the center of a vein with an inner diameter of 12 mm was created. The analysis conditions were as follows: the blood flow rate in the vein was set at 400 ml/min, and four rates were defined for the blood removal flow rate using the DLC: 150 ml/min, 200 ml/min, 250 ml/min, and 300 ml/min. The mean venous pressure at the outflow port of the vein was defined as 0 Pa, and water was defined as the fluid in the blood vessel. A constraint was complete immobilization at a location 10 cm from the tip of the SH-DLC. In order to re-create the conditions under which the DLC clings to the blood vessel wall, the suction force of the side hole in the SH-DLC was first determined, and that suction force was defined as the bending force of the tip portion of the SH-DLC.
Results: As the volume of DLC blood removal increased, the suction force of the side hole also increased, and that force caused the tip of the DLC to approach the blood vessel wall. It was possible able to re-create this in the analysis. Similar results were obtained in experiments using pseudo-dialysis systems under the same conditions as the analysis, and the efficacy of the analysis was confirmed.

31

Non-invasive Detection of Coagulation in Blood Circuits Based on Measurement of Light Absorbance

H. Sakamoto, S. Yamauchi, Y. Motohashi, T. Sato, T. Agishi. *Graduate School of Engineering, Toin University of Yokohama, Yokohama, JAPAN.*

Study: As one technique for non-invasive detection of coagulation in circuits, we focused on the fact that the color of blood changes from bright red to dark red when coagulation occurs in a circuit, and investigated the possibility of detecting coagulation in circuits from changes in light absorbance before and after coagulation.
Methods: For measurement, we used cannonball-shaped light-emitting diodes (LEDs) at wavelengths of every 100 nm in the range from 400 nm to 1,000 nm on the light-emitting side of the optical sensor. On the light-receiving side, we used a Si PIN photodiode that covers wavelengths from 320 nm to 1,100 nm. We inserted the hemodialysis circuit in a straight configuration between the light-emitting and light-receiving sides, and covered the optical sensor with a black jig used to obstruct external light. We had measured the relationship between sensor output voltage and light power in relation to the optical sensors at each wavelength in advance, and based on the results, adjusted the light-emitting power of the LED so that a high sensitivity of detection could be obtained in relation to changes in absorbance. Sixty seconds after starting circulation of bovine blood, we added calcium chloride to induce coagulation. At the same time that circulation began, we also began measuring the output voltage of the optical sensor, and continuously measured the output voltage for 10 min.
Results: When the calcium chloride was added, a sharp drop in optical power was seen, and optical power subsequently continued to gradually decrease as coagulation progressed. After blood coagulation had ended and the roller pump was stopped, we saw that optical power gradually recovered. However, if the ratio of optical power before and after coagulation is taken as the change in absorbance, we realized that, because the results differed for different wavelengths, an optimum wavelength exists for detecting changes in absorbance before and after coagulation.

33

Hemodynamic Numerical Simulations of Spiral Flow within a Patient-specific Abdominal Aortic Aneurysm Model

M. Liu, A. Sun, X. Deng. *School of Biological Science and Medical Engineering, Beihang University, Beijing, CHINA.*

Study: Abdominal Aortic Aneurysms (AAA) are localized, irreversible enlargement of the infrarenal aortic wall, and hemodynamics is thought to be a significant factor in the formation, progression and rupture of AAA. Since the blood flow in the human aorta is in the form of spiral flow that rotates clockwise in the systolic phase and anti-clockwise in the diastolic phase, this certainly would alter the hemodynamics within the AAA and the spiral flow with different streamwises may bring significant different effect on AAA. The present study is designed to investigate the effect of spiral flow on hemodynamic parameters in a patient-specific AAA model by using a computational fluid dynamic (CFD) method.
Methods: A 3-D AAA model with bilateral renal arteries were constructed based on CT images of a patient. Spiral flow profiles with varying swirling intensities and directions (clockwise, anti-clockwise) were imposed as the inlet flow condition to perform the CFD simulations. The hemodynamics in the aortic model under different inlet flow conditions were analyzed and compared.
Results: The results indicate that in the normal section of the aorta, clockwise spiral flow could reduce the area of low wall shear stress, therefore reduce the risk of atherogenesis hence suppressing the progression of aneurysm, while anti-clockwise spiral flow has the opposite effect. On the other hand, in the aneurysm section, clockwise spiral flow would enlarge the zone of low wall shear stress, while the anti-clockwise would reduce it. The opposite effects of spiral flow for the normal section and the aneurysm part were attributed to the existence of aneurysm neck with high torsion angle which forces the spiral flow to take the same spiral direction of the torsion angle. In conclusion, when analyzing the hemodynamics in an AAA, both the rotation direction of the spiral flow and the geometric feature of the AAA should be taken into consideration.

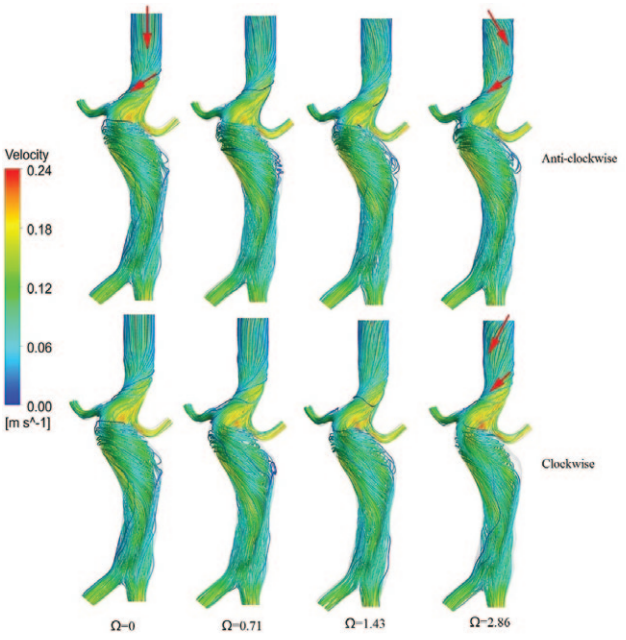

Figure 1. Velocity streamlines within the patient specific AAA model for different cases (Ω represents the swirling intensity; red arrows show the direction of blood flow).

36

Silicon Nanopore Membranes (SNM) Provide Islet Immunoisolation Under Convective Transport

S. Song,[1] G. Faleo,[2] R. Yeung,[1] R. Kant,[1] A. Posselt,[2] T. Desai,[1] Q. Tang,[2] S. Roy.[1] *[1]Department of Bioengineering and Therapeutic Sciences, University of California, San Francisco, San Francisco, CA; [2]Department of Surgery, University of California, San Francisco, San Francisco, CA.*

Study: Type 1 diabetes (T1D) results from autoimmune destruction of insulin-producing β cells. Islet transplantation by directly infusing cadaveric islets into the recipient has become a viable T1D treatment. However, shortage of donor cells, use of immunosuppressive drugs, and their side effects remain as major challenges. Using a semi-permeable membrane to encapsulate islets could potentially achieve immune isolation while supporting the function of encased cells. Our silicon nanopore membranes (SNM) exhibit monodisperse pore size distribution with 1% variation, which enables superior selectivity relative to conventional polymeric membranes. In this study, we investigated the feasibility of using SNM as an immune barrier to prevent islets from cytokine-induced cell death under convective transport.
Methods: A closed loop fluid circuit with SNM assembled in a flow cell device under physiological pressure was used to recapitulate local blood circulation. A combination of β cell-toxic cytokines, TNF-α (1000U/mL), IL-1 β (50U/mL), and IFN-γ (1000U/mL), was added to the circuit for analyzing sieving coefficients through SNM. Mouse islets were loaded into SNM-encapsulated flow cell device and islet viability was assessed using fluorescein diacetate and propidium iodide. Islets directly exposed to cytokines under static culture were used as controls.
Results: A 80% reduction in cytokine passage through SNM under convective transport was observed compared to bovine serum albumin (100% reduction). SNM protected islets from cytokines and retained islet viability over 6 hours. Direct exposure of islets to cytokines in static control cultures led to significant increase in cell death ($p<0.05$). These data demonstrates the feasibility of using SNM to protect islets from pro-inflammatory cytokines. SNM could potentially reduce or even eliminate the required immunosuppressants and open the possibilities of using alternative cell sources to overcome donor shortage for T1D treatment.

37

In-vitro Evaluation of Drug Sequestration in the Extracorporeal Membrane Oxygenation (ecmo) Circuit

J. Park, D. Shin, J. Lee, H. Kim. *Seoul National University, Seoul, KOREA, REPUBLIC OF.*

Study: In order to investigate significant changes in pharmacokinetics of drugs during extracorporeal membrane oxygenation (ECMO) treatment, various in-vitro and in-vivo experiments have been carried out. However, most previous studies were limited to focusing on the entire ECMO circuit rather than individual components of the circuit and failed to find out the most influential constituents that cause drug sequestration. In this study, we aim to quantify influences of each element that composes the circuit on drug sequestration by exclusively focusing on the interactions between materials and drugs.

Methods: We considered tubes and oxygenators from two different brands, Maquet Inc. and Terumo Inc. By identifying components that contact with blood, we decomposed oxygenator into gas membrane, water membrane, and housing. Each component shredded into ~1 gram was submerged into solutions of drugs dissolved in distilled (DI) water. Experimental drugs include heparin, dexmedetomidine, and meropenem with initial concentration of 1U/ml, 0.0075ug/ml, and 0.015mg/ml respectively, which were chosen based on the actual amount of dose used for patients receiving ECMO treatment. Three different tubes cut into ~6cm were filled with the solution by clamping both sides of the tube. Each experimental component was then delivered into water bath to maintain 37°C for 1, 6, 12, and 24 hours. Drug concentrations of the dexmedetomidine and meropenem were measured using liquid chromatography (LC) system and those of heparin were measured using UV spectrometer after post treatment with toluidine blue sample.

Results: As a result of preliminary experiment, concentrations seem to be unstable due to incomplete mixing of the solution at each experiment. However, the preliminary result shows that tubes might be the most influential factor that causes drug sequestration. Sequestration rate of dexmedetomine was the highest among others (Fig. 1).

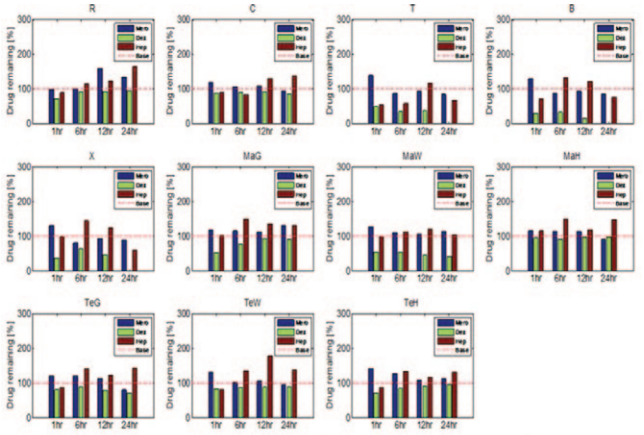

Fig 1. R: room temperature; C: control (at 37° without any material included); T: tygon tube; B: Bioline tube from Maquet Inc.; X: Xcoating tube from Terumo Inc.; MaG: Maquet oxygenator gas membrane; MaW: Maquet oxygenator water membrane; MaH: Maquet oxygenator housing; TeG: Terumo oxygenator gas membrane; TeW: Terumo oxygenator water membrane; TeH: Terumo oxygenator housing

39

FDA Benchmark Flow Models to Support Computational Fluid Dynamics Techniques in the Evaluation of Medical Devices

R. Malinauskas,[1] P. Hariharan,[1] S. Day,[2] L. Herbertson,[1] M. Buesen,[3] U. Steinseifer,[3] K. Aycock,[4] B. Good,[4] S. Deutsch,[4] K. Manning,[4] B. Craven.[1] *[1]US Food & Drug Administration, Silver Spring, MD; [2]Rochester Institute of Technology, Rochester, NY; [3]RWTH Aachen University, Aachen, GERMANY; [4]The Pennsylvania State University, University Park, PA.*

Study: Computational fluid dynamics (CFD) is increasingly being used to develop and evaluate blood-contacting medical devices. However, the lack of reliable standardized methods for validating CFD simulations and blood damage predictions limits its applicability in the safety evaluation of new products.

Methods: As part of an ongoing FDA initiative, two flow models (Study #1: nozzle, Study #2: blood pump) were developed and tested over a range of flow conditions in multiple labs to provide experimental velocity and hemolysis data to support CFD validation. In each study, computational simulations were performed by over 20 separate groups from around the world to assess current CFD techniques and limitations. Marked discrepancies between the CFD results and the measured velocities in the nozzle study motivated the development of "best practice" CFD guidelines (see https://fdacfd.nci.nih.gov) and an FDA Guidance Document on what to consider when reporting computational studies of devices (www.fda.gov/RegulatoryInformation/Guidances/ucm371016.htm).

Results: For Study #2, CFD simulations of the centrifugal blood pump model at six flow and rpm conditions (from 2.5–7 Lpm) demonstrated good general agreement between the computational estimates of pressure head and the experimentally measured pressures when using porcine blood (% Error between the mean values was less than 11% for all six test conditions). As was done for the nozzle model, a comparison between the CFD simulations and the measured velocity fields at multiple locations within the pump model will be reported. The goal of this project has been to improve computational techniques and blood damage predictions by providing benchmark flow model data in a publicly accessible database, and to collaboratively develop guidelines on proper validation and use of CFD simulations in the assessment of medical devices.

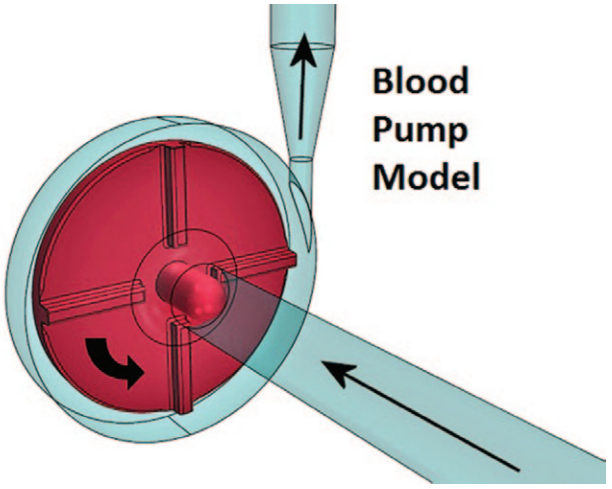

41

The Impacts of Left Ventricular Assist Device Design and Operation on Pump Acoustics

G. L. Yost,[1] T. Royston,[2] G. Bhat,[1] A. Tatooles.[1] *[1]Heart Institute, Advocate Christ Medical Center, Oak Lawn, IL; [2]Bioengineering, University of Illinois at Chicago, Chicago, IL.*

Study: There are several prevalent LVAD designs including axial and centrifugal flow systems, and as popularity of this new generation of pumps increases, a complete understanding of differences in device mechanics and operation will be pivotal to patient care. Previous work has demonstrated the utility of using acoustic data for the detection of changes in amplitude and spectral energy distribution following simulation of thrombus in the LVAD conduit. Noting the differences in design and operation between the HeartMate II (HMII), the HeartWare HVAD (HW) LVADs, we compared the acoustic characteristics of both pumps.
Methods: Pump sounds were recorded using a Littmann 3200 Electronic Stethoscope over the mitral area in patients supported with the HMII and HW pumps. Data were uploaded to an acoustic analysis program and were displayed as spectrograms for comparison.
Results: Device acoustics and resultant spectrograms were found to differ greatly between the two pump designs. The HMII is typically operated in the range of 8400–9800 RPM, corresponding to a first harmonic frequency range of 143.3–163.3 Hz. Spectrographic analysis revealed the presence of harmonic bands at all integer values between 1 and 12 (Figure 1) with harmonic frequency dependent on device operating speed. The presence of consistent harmonic bands at all integer values in the HMII may be a result of asymmetric pressure fluctuations generated via interaction between the fixed stator vanes and the rotating impeller. The HW operates between 1,800–4,000 RPM, and, accordingly, generated first harmonic frequencies between 30 and 66 Hz. Only iterations of the 4th harmonic occurred in the spectrogram however, due to the 4 bladed design of the HW impeller (Figure 2). Interestingly, a pulsatility is observed in the amplitude of the HW spectrogram, which is periodic with ventricular contraction. This is likely due to cyclic loading and unloading of this pre-load dependent pump.

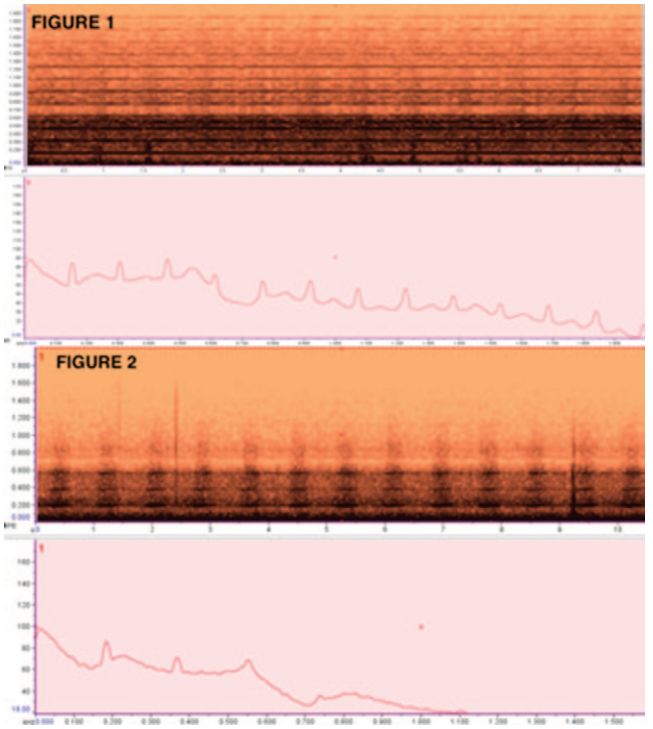

42

In Vitro and In Vivo Hemocompatibility Assessment of Thin Film Sulfobetaine and Carboxybetaine Zwitterionic Coatings

Z. Iqbal,[1] S. Kim,[2] W. Moses,[3] E. Kim,[1] J. Park,[1] W. Fissell,[4] S. Roy.[1] *[1]Bioengineering, University of California - San Francisco, San Francisco, CA; [2]Nephrology, University of California - San Francisco, San Francisco, CA; [3]Surgery, University of California - San Francisco, San Francisco, CA; [4]Medicine, Vanderbilt University, Nashville, TN.*

Study: Silicon nanopore membranes (SNM) for use in renal replacement, islet therapy, and membrane oxygenation applications require blood contacting surfaces that are non-activating and non-fouling. Polyethylene glycol (PEG) is widely used as a surface coating to improve hemocompatibility, but its degradation characteristics over time limit performance. Zwitterionic polymers such as poly(sulfobateine methacrylate) (pSBMA) and poly(carboxybetaine methacrylate) (pCBMA) have shown promise for long-term reduction of protein and cell adhesion. This study examines the performance of sub-5nm thickness pSBMA and pCBMA coatings on silicon surfaces.
Methods: Atom transfer radical polymerization was used to graft pSBMA and pCBMA on silicon substrates. Surface modification was verified using contact angle (n = 6) and x-ray photoelectron spectroscopy (XPS) (n = 3). Coating thickness (n = 6) was measured via ellipsometry. Protein adsorption was measured by incubating surfaces (n = 2) in 1 mg/ml fibrinogen and quantifying adsorption using enzyme-linked immunosorbent assay. Cell adhesion was evaluated by exposing surfaces to blood for 6 hours in an extracorporeal porcine circuit. Scanning electron microscopy (SEM) and immunohistochemistry (IHC) was then conducted on the substrates to examine adhesion of cells.
Results: The XPS, contact angle and coating thickness data is shown in Table 1 and indicate that the coating process for pSBMA and pCBMA was successful. Fibrinogen adsorption decreased to 50.4% with PEG and 13.5% with pSBMA, while there was no significant change with pCBMA compared to uncoated silicon substrates. SEM and IHC results following blood exposure demonstrate that pSBMA performance is comparable to PEG. Therefore, modification with pSBMA may be a viable option for application on SNM. In contrast, pCBMA underperformed in both in vitro and extracorporeal studies compared to pSBMA, which may be due to a lower degree of polymerization.

		No Coating	PEG-Silicon	pSBMA-Silicon	pCBMA-Silicon
Contact Angle (H_2O)		52.8 ± 2.6°	43.8 ± 1.0°	8.5 ± 2.4°	39.3 ± 5.5°
Thickness (nm)		--	0.8 ± 0.2	3.46 ± 0.64	1.7 ± 0.11
Elemental Composition (%)	Si, 2p	56.8 ± 0.8	52.1 ± 3.1	20.6 ± .4	31.5 ± 1.8
	O, 1s	28.5 ± 1.8	32.2 ± 0.4	27.6 ± 0.5	30.0 ± 0.4
	C, 1s	14.0 ± 2.2	15.6 ± 2.8	44.9 ± 0.6	35.6 ± 1.9
	N, 1s	0.4 ± 0.1	0.2 ± 0.1	3.9 ± 0.1	2.5 ± 0.1
	Br, 3d			0.2 ± 0.1	0.5 ± 0.1
	S, 2p			2.8 ± 0.1	

48

Formal Usability Methods to Support the Expedited Access Paradigm: A Pediatric Blood Pump Case Study

A. Abbate,[1] E. Bass,[2] A. Throckmorton.[1] *[1]Biomedical Engineering, Drexel University, Philadelphia, PA; [2]Computing & Informatics, Nursing & Health Professions, Drexel University, Philadelphia, PA.*

Study: Mechanical circulatory support systems involve the interaction of automated devices, healthcare providers, and patients. Human-automation interaction and formal methods researchers are developing methods to inform the design of such technology while considering human limitations and performance. As a new approach, we present a computational framework that supports safety and usability analyses for medical devices early in the development process.
Methods: We demonstrate this framework with a case study for a pediatric axial flow blood pump including its patient handbook. We created five models to represent the patient interacting with the device, external components of the device, the pump, possible patient actions, and the device control interface. We formally modeled the patient-device interaction using a written procedure provided in the handbook. We also developed finite state automata (FSA) representation of the controllers, batteries, alarms, cable connections, and the location of components relative to the patient. To model the pump, we encoded a set of functions that compute flow rate, pressure, and rotational speed.To model possible actions and device controls, we generated FSA representations of affordances (e.g. connectibility for cables) and of signifiers (e.g. a button pointing up meaning "increase speed").
Results: The composition of these models coupled with safety and usability specifications support formal analysis of system performance including the human operator, the device and external components including the handbook. To facilitate the design and development of high-risk, high-reward systems such as heart pumps, this unique approach provides insight into complex human-interactive systems including human factors considerations critical to patient safety.

50

Novel Magnetically Levitated Right Ventricular Assist Device

N. Murad,[1] C. Fox,[1] R. Stevens,[2] **A. Throckmorton**.[1] *[1]Biomedical Engineering, Drexel University, Philadelphia, PA; [2]Pediatrics, Cardiothoracic Surgery, Drexel University, Philadelphia, PA.*

Study: Thousands of pediatric and adults patients in the U.S. are diagnosed with congestive heart failure secondary (CHF) due to acquired or congenital heart disease. A substantial number of these patients also develop right-sided heart failure secondary to the left-sided failure or dysfunction. Treatment strategies consist of drug therapy, heart transplantation, or mechanical circulatory support devices. To address the latter, we are developing a novel, magnetically levitated, right ventricular assist device (RVAD) that is designed to improve blood flow to the lungs.
Methods: We designed an axial flow blood pump utilizing magnetic bearings to levitate the impeller of the RVAD and a set of motor magnets to induce rotation. The axial blood pump consists of 4 bladed regions: inducer, impeller, diffuser, and flow straightener. Computer simulations were performed using ANSYS software to estimate the hydraulic performance of the RVAD, fluid forces exerted on the rotor, shear stresses, and blood damage levels.
Results: The modeling results demonstrated that the RVAD is able to deliver 5–65 mmHg of pressure rise for a flow range of 3–7 L/min and rotational speeds of 7000-13,000 RPM. Radial and axial fluid forces were less than 0.60 Newton over the operational range. Shear stresses and blood damage indices were within acceptable levels. These findings are encouraging and support further development of the new RVAD for long-term support.

58

How Different Configurations of the Intra-Aortic Balloon (IAB) Can Influence the Aortic Flow

M. Caruso,[1] A. Renzulli,[2] **G. Fragomeni**.[2] [1]*DIMEG, University of Calabria, Arcavacata di Rende (CS), ITALY;* [2]*Medical and Surgical Sciences, Magna Graecia University, Catanzaro, ITALY.*

Study: Intra-aortic balloon pump (IABP) is the most used circulatory assist device for cardiac diseases, placed in the descending aorta with its tip 2 to 3 cm distal to the left subclavian artery origin. Furthermore, as reported by Maquet, the suitable balloon size must be chosen considering the patient height, but in literature, some studies report different complications due to the IAB-induced obstruction of abdominal arteries. So, a computational analysis was carried out in order to evaluate the effects on aortic flow of the IAB-induced obstruction of visceral district compared to the non-obstructive IAB.
Methods: To create the two computational models, two sizes of LINEAR 7.5Fr. IAB and two positions were considered. The non-obstructive IAB has a volume of 25 cc and is placed at 2 cm, whereas the obstructive IAB is a 34 cc balloon, positioned at 3 cm. The balloon inflation was numerically reproduced by means of a parametric study. Moreover, the boundary conditions were chosen in order to analyze the flow changes only due to the two configurations.
Results: The numerical results highlighted that the IAB-induced obstruction increases the perfusion of head and arms of about 8% and 10%, respectively, whereas it decreases the blood flow in abdomen and in the legs of about 4% and 23%, respectively. Indeed, a very low blood flow rate occurs in case of obstructive IAB, both in the abdominal vessels and in the iliac bifurcation. Since in clinical practice, the blood flow reduction distally to the balloon, the low output syndrome and the embolization of calcified debris from the aorta may cause acute ischemic events in the visceral and peripheral arterial districts, we concluded that the positioning and the size of IABP have a key role in the improvement of patients' outcome.

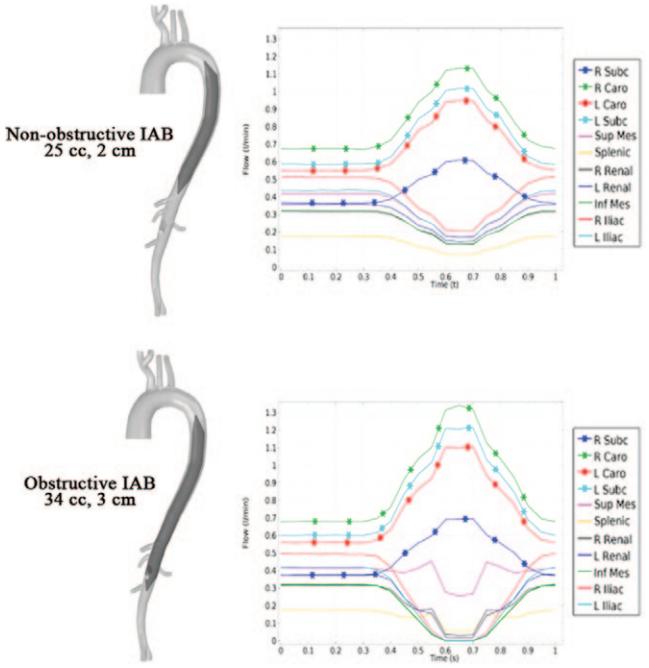

70

A Method for Identification of Pumping States in an Implantable Rotary Blood Pump: Experimental Validation for the LVAD Sputnik

D. Petukhov, D. Telyshev, S. Selishchev. *Department of Biomedical Systems, National Research University of Electronic Technology, Zelenograd, RUSSIAN FEDERATION.*

Study: The aim of this work is to experimental validation of the previously developed method for identification of pumping states in an implantable rotary blood pump (RBP): the backflow of blood, partial and full assist of the ventricle, partial and full collapse of the ventricle during a cardiac cycle. The fundamental idea of method is to analysis of blood flow dynamics through the pump using the mathematical model of RBP, which was a theoretical model formerly. This work rest on the experimental results of the first clinically approved Russian left ventricular assist device Sputnik.
Methods: The LVAD was investigated on the hydrodynamic mock loop in dynamic conditions at Helmholtz-Institute for Biomedical Engineering (RWTH Aachen University). The developed mathematical model uses measured pump speed and pressure head as input parameters. An optimization routine based on the differential evolution algorithm was developed and used for improve model accuracy (e.g. $R^2 > 0.995$). In accordance with basic idea of method the dynamics of derivatives, obtained from the pump model, was analyzed at different pump speeds. Comparison with hemodynamic curves are revealed correlation between pumping states and the certain dynamics of derivatives. Indices of derivatives were introduced for more indicative description of these dynamics, such as $S_{AV}(dQ/dt\ dQ/dH)$ where Q - pump flow, H - pressure head.
Results: The method was tested using experimental data obtained through the hydrodynamic mock loop at two different initial states corresponding to the various ventricular contractility (contractilityFactor, cF). Accurate identification of pumping states is possible in both cases. An example of partial and full assist states identification is shown on Fig. 1.

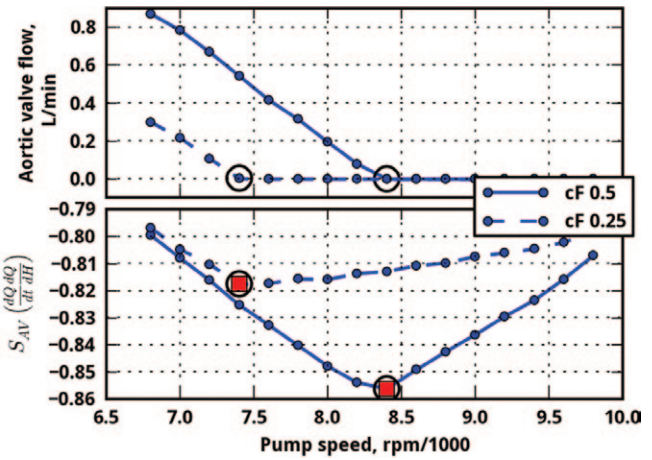

Figure 1. Identification of partial and full assist states, where red square marker denotes the change in the dynamics of S_{AV} index and transition from the partial to the full assist state (with zero aortic valve flow).

100

Feasibility Study and Application of a MEMs Accelerometer Sensor for Acquisition of Vibration Signs in Pivot Bearing

J. C. Sousa,[1] R. L. Souza,[1] B. Nishida,[1] E. Drigo,[2] T. F. Leão,[1] E. G. Bock.[1] *[1]Lab. Bioeng, Federal Institute of Technology in Sao Paulo, São Paulo, BRAZIL; [2]Institute Dante Pazzanese of Cardiology, São Paulo, BRAZIL.*

Study: The MEMS Accelerometers have great commercial impact, have application in many fields, the principal use is the automotive industry. These accelerometers are based on the measurement of the Cartesian vector components of gravitational acceleration. They are miniaturized, have low power, low cost and great response to dynamic acceleration resulting from motion. A recent study suggested for diagnosis of a centrifugal pump for thrombus simulation areas inserted in the pump rotor and points identified by vibrational analysis. The study evaluated use of a MEMS accelerometer sensor ADXL335 (Analog Devices, Norwood, MA, US) and development of a data acquisition system embedded in exclusive hardware to identify wear on the set of hydrodynamic bearings of a Implantable Centrifugal Blood Pump (ICBP) used as a long term Ventricular Assist Device (VAD).
Methods: A test workbench developed in our laboratory was used to simulate the function of the pivot bearings and the accelerometer sensor inserted into its structure to acquire the vibration signals arising from the motion. Different biomaterials were evaluated in the performed tests of this workbench with controlled rotation and contact force calibrated by load cell system; after acquiring the data were plotted in graphs and compared in the following situations: life and surface wear.
Results: The results were considered satisfactory from the point of view of an initial technical feasibility study of the use of monitoring vibration for MEMS in the rotation of the ICBP. In future studies, this monitoring will be applied as a tool for supervisory control, fault diagnosis and possible thrombus prediction tool around the pump rotor and predict failures or adverse events.

102

A Feasibility Study of a Novel Autologous Heart Valve

Y. Takewa,[1] Y. Nakayama,[2] H. Sumikura,[1] N. Naito,[1] K. Iizuka,[1] E. Tatsumi.[1] *[1]Department of Artificial Organs, National Cerebral and Cardiovascular Center, Osaka, JAPAN; [2]Department of Biomedical Engineering, National Cerebral and Cardiovascular Center, Osaka, JAPAN.*

Study: We are developing a novel autologous heart valve (Biovalve) with a unique in-body tissue engineering method. This may provide more biocompatible heart valves for the valvular disease. In this study, we evaluated the feasibility of them in a large animal experiment.
Methods: We created many kinds and sizes of plastic molds for Biovalves with 3D printer easily and quickly, and embedded them in the subcutaneous spaces of adult goats for 2 months. After confirming encapsulation of membranous tissue around the molds, we extracted them with the tissue and removing the molds only, and finally got beautiful tri-leaflet valves made by completely autologous connective tissues and fibroblasts. We selected 3 types of Biovalve (a conventional type, a full-root type and a valve with a metallic stent for transcatheter implantation) in this study. Five cases of conventional Biovalves were implanted in the aorta under cardiopulmonary bypass, 8 cases of full-root type were implanted in the apico-aortic bypass, and 22 cases of stent valve type were implanted with transcatheter technique into in situ the aortic or pulmonary valve.
Results: In each type, Biovalves were successfully implanted and showed smooth movement of the leaflets with a little regurgitation for maximum 15 months. Histological examination showed the autologous cells covering the laminar surface of the Biovalve leaflets and also getting into the connective tissues. In conclusion, the Biovalves have a potential to be used for valve surgery and satisfy the higher requirements of the systemic and pulmonary circulation maintaining the histological character as autologous tissues.

115

A Sensorless Control Algorithm for Physiologic Control, Flow Balance, and Suction Prevention for Rotary Biventricular Assist Devices

Y. Wang,[1] S. C. Koenig,[2] M. S. Slaughter,[3] **G. A. Giridharan**.[1] *[1]Bioengineering, University of Louisville, Louisville, KY; [2]Bioengineering and Cardiovascular and Thoracic Surgery, University of Louisville, Louisville, KY; [3]Cardiovascular and Thoracic Surgery, University of Louisville, Louisville, KY.*

Study: Biventricular assist devices (BiVAD) using continuous flow rotary blood pumps are becoming clinically accepted for the treatment of advanced biventricular failure. To improve efficacy, safety, and reliability, we propose a novel sensorless control algorithm integrated into the BiVAD controller for regulating physiologic perfusion, maintaining left-right sided balance, and preventing ventricular suction.
Methods: The proposed control algorithm consists of two gain-scheduled and proportional-integral controllers, extended Kalman filter and Golay-Savitsky filter for left and right ventricular assist devices (LVAD, RVAD) and only requires intrinsic pump parameter variables (pump speed, power). The controllers maintain target differential pump pressures across LVAD and RVAD (ΔP_L, ΔP_R) to provide physiologic perfusion and left-right balance, and differential pump speeds (ΔRPM_L, ΔRPM_R) above the user-defined thresholds to prevent ventricular suction. Efficacy and robustness of the proposed algorithm were tested *in silico* using (1) 2% pump speed noise, (2) excessive $\Delta P_L/\Delta P_R$ and $\Delta RPM_L/\Delta RPM_R$ setpoints, (3) a rapid three-fold increase in pulmonary vascular and/or vena cava resistances, and (4) transient responses from exercise to rest.
Results: The study successfully demonstrated that the proposed sensorless algorithm maintained physiological perfusion by matching pump output to cardiac demand, inherently balanced left and right sided flow rates, and prevented LV and RV suction using only intrinsic pump parameters without the aid of pressure and/or flow sensors (Figure 1). The algorithm also does not require pump or inlet/outlet cannula modifications and may be directly applied to existing LVAD and RVAD.

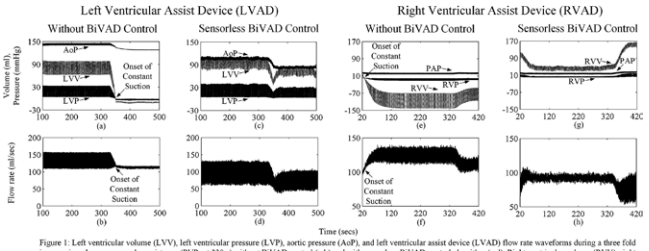

Figure 1: Left ventricular volume (LVV), left ventricular pressure (LVP), aortic pressure (AoP), and left ventricular assist device (LVAD) flow rate waveforms during a three fold increase in pulmonary vascular resistance (PVR, at 330 s) without BiVAD control (a,b) and with sensorless BiVAD control algorithm (c,d). Right ventricular volume (RVV), right ventricular pressure (RVP), pulmonary artery pressure (PAP), and right ventricular assist device (RVAD) flow rate waveforms during a three fold increase in PVR (at 330 s) without BiVAD control (e,f) and with sensorless BiVAD control algorithm (g,h).

118

Development of Simulated Ascites for the Training of Procedure and Evaluation of Machines for Cell-free and Concentrated Ascites Reinfusion Therapy (cart)

T. Okahisa,[1] **D. Tanaka**,[2] M. Sogabe.[3] *[1]Department of General Medicine and Community Health Science, Tokushima University Graduate School, Tokushima, JAPAN; [2]Department of General Medicine and Community Health Science, The Tokushima University, Tokushima, JAPAN; [3]Department of General Medicine and Community Health Science, The University of Tokushima Graduate School, Tokushima, JAPAN.*

Study: cell-free and concentrated ascites reinfusion therapy (CART) involves filtration, concentration, and reinfusion of drained ascites from a patient with refractory ascites. Usually, filtration and concentration step of ascites during CART is complicated and requires experience. However, it is difficult to obtain the patient ascites for the training of this procedure. In this study, we created simulated ascites using commercially available infusions, and evaluated the particle size, permeability and stability of this simulated ascites. In addition, we verified whether it is possible to reproduce the clogging of filtration filter and concentrator during filtration and concentration process using this simulated ascites.
Methods: To create the simulated ascites, intravenous fat emulsion (soybean oil), substitute plasma agent (hydroxyethylated starch) and saline were used. A laser diffraction particle size analyzer (SALD-2300, SHIMADZU CORPORATION) was used for the measurement of the particle size distribution. Confirmation of concentrator permeability of substitute plasma agent was carried out by iodine starch reaction.
Results: Particle diameter of intravenous fat emulsion is greater than 0.2 μm (the maximum pore size of the filter hollow fiber), the difference in particle size by lot or diluted solution was not found. Fat micelles did not pass through the hollow fiber membrane of filtration filter. The clogging of the filter by the fat emulsion, the clogging of the concentrator by substitute plasma agent, the clogging of both filter and the condenser by a mixture of fat emulsion and substitute plasma agent, were reproducible. These results indicate that simulated ascites using a commercially available infusions allows the reproduction of filtration and concentration step, including the clogging of the filtration filter and the concentrator, which is useful in the evaluation and education of the CART machines.

121

LVAD Outflow Graft Configuration Influences Thrombogenic Potential

A. R. Prisco,[1] **V. Chivukula**,[2] P. McGah,[2] J. A. Beckman,[3] G. Garcia,[1] N. A. Mokadam,[4] C. Mahr,[3] A. Aliseda.[2] *[1]Biotechnology and Bioengineering Center, Medical College of Wisconsin, Milwaukee, WI; [2]Mechanical Engineering, University of Washington, Seattle, WA; [3]Division of Cardiology, University of Washington, Seattle, WA; [4]Division of Cardiothoracic Surgery, University of Washington, Seattle, WA.*

Study: The prevalence of medical-therapy refractory advanced heart failure, coupled with a stagnant pool of donor hearts have resulted in increased use of Left Ventricular Assist Devices (LVADs). Significant advances in LVAD design and management have achieved 1-year survival rates approaching 90%. Neurologic events remain among the most devastating complications of VAD support. Thrombogenesis associated with flow patterns in the aortic root have shown a strong patient-to-patient variability that has proven difficult to predict. Current LVAD implantation strategies do not incorporate outflow graft angle optimization, which may influence thrombosis risk.

Methods: Unsteady computational fluid dynamics (CFD) are used in combination with virtual surgery to analyze the flow inside 3D patient-specific models of the aortic arch and great vessels for different LVAD outflow graft configurations, ranging from 45° - 90°. Wall shear stress indices (high/low wall shear stress, low Oscillatory Shear Index and high Wall Shear Stress Gradient) are computed to evaluate the thrombogenic risk. Additionally, a novel Lagrangian particle tracking method is applied to platelet surrogates in the data to calculate thrombogenicity through shear stress histories (SH) and residence times (RT).

Results: Hemodynamics parameters, averaged over at least 10 cardiac cycles, show a complex, non-monotonic, evolution with outflow graft angle. Wall shear stress cannot be minimized globally. Rather, the shear stresses on the aortic wall and on the ostia of the great vessels are minimized for different outflow graft anastomosis angles, with the size of the recirculation regions that develop in the proximal side of the ostia increasing and then decreasing with graft angle. Lagrangian tracking of platelets, however, reveals a clear trend, with strong reduction of cumulative platelet SH and RT observed for the most acute (~45°) angle studied. Thus, an acute outflow graft angle effectively minimizes thrombogenic potential.

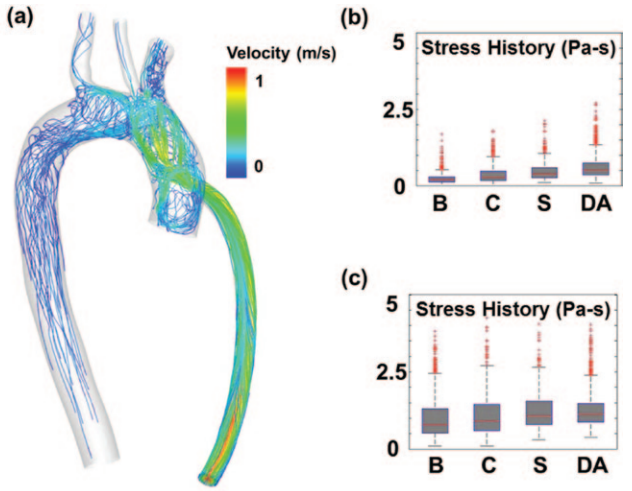

Figure 1: (a) Pathlines depicting paths traversed by particles entering the aortic arch for a 90° LVAD outflow graft configuration. A recirculatory flow pattern is clearly seen just proximal to the aortic valve. (b) and (c) Box-and-whisker plots of cumulative platelet stress histories after 3 cardiac cycles for 45° and 90° cases, respectively. Note the reduced cumulative shear stress histories and tighter distributions for the acute (45°) case. B: brachiocephalic, C: common carotid, S: subclavian and DA: descending aorta

127

Examination of Mechanism Underlying Shunt Sound Using Numerical Computation

N. Nakane, N. Shimazaki, S. Yamauchi, Y. Motohashi, T. Agishi. *Clinical Engineering, Toin University of Yokohama, Yokohama, JAPAN.*

Study: We have tried "time-frequency analysis" by wavelet transformation for shunt sound signals measured using an acceleration sensor attached to the skin surface of dialysis patients as a method for quantitatively evaluating shunt sounds. The differences which were suggested to agree qualitatively with past research were identified, the past studies were experimental and numerical computation using the finite-element method about the linear para-angiostenosis model that was imitated only the stenotic part. This study therefore performed numerical computations for a para-defect stenosis model imitating the stenotic part of an artificial blood vessel shunt, and inspected the utility of numerical computations for the occurrence of vibrations at the vascular wall and the spread of vibrations.

Methods: We made a U-shaped model imitating an artificial blood vessel and tried "fluid-structure interaction analysis" using a finite-element method (FEM). We assumed that the inside diameter was 6 mm and the thickness was 1 mm each for artificial blood vessels and outlet passage veins, and a 67% stenosis was present in the outflow passage. In addition, we set a pressure fluctuation with a period of 0.5 s (assuming a systolic pressure of 120 mmHg, a diastolic pressure of 80 mmHg, and heart rate of 60 beats/min in general adults), and defined the fluid within according to the physical properties of water.

Results: We confirmed backward flow with increasing pressure caused by expansion from the stenotic part, and the turbulence occurred with backward flow at downstream of the stenotic part. In addition, we confirmed flow through the stenotic part became a high-speed jet and part of the flow collided with a vascular wall with the fluctuating pressure caused by the heartbeat and turbulent flow. We confirmed that vibration of the vascular wall downstream of the stenotic part is produced where flow collides with the vascular wall.

129

Membrane Ventilators with Integrated Biofunctionally Modified Hollow Fibers That Avoid Material-mediated Neutrophil Activation

M. Scholz,[1] E. Novosel,[2] E. Reinauer,[1] J. Böhm,[2] G. Matheis.[2] *[1]R+D, Leukocare AG, Martinsried/Munich, GERMANY; [2]Xenios AG, Heilbronn, GERMANY.*

Study: Lung assist devices based on plasma-activated tight hollow fibers (Novalung iLA®, Xenios AG) are successfully used in patients with respiratory failure. However, the immunogenicity of blood contact surface materials in such devices bears the potential to improve durability in conjunction with improved fluid pathways. Therefore, a biofunctional heparin-free surface coating has been established to avoid material-mediated neutrophil activation during respiratory support.
Methods: Covalent coupling of an agonistic FasL molecule that rapidly reduces neutrophil activation after contacting the hollow fiber surface was achieved. The stabilizing and protecting solutions (SPS®) technology platform (LEUKOCARE AG) was utilized to enable stability and functionality of the biomolecule even after EtO sterilization and subsequent prolonged storage of the Novalung iLA® device.
Results: A standard neutrophil migration assay (modified Boyden chamber) revealed a significant reduction of IL-8-mediated chemotaxis of neutrophils (>10%) after contact with the functionalized surface. Moreover, an ELISA was established that enabled the highly sensitive and reproducible monitoring of homogenous molecule distribution on the material surface. No leaching of the biofunctional coating was detectable by means of a sandwich ELISA with a sensitivity of 0,1 ng/ml. The proprietary coating has been adapted to serial production processes and can be transferred to other material surfaces used in blood contacting devices in order to reduce unappreciated material-induced immunogenic responses.

141

Improving Safety Acceptance Criteria for *in vitro* Hemolysis Testing of Medical Devices

R. Malinauskas, P. Buehler, L. Herbertson, R. Brown, I. Mahmood, Y. Huang, N. Dereje, B. Tunick. *US Food & Drug Administration, Silver Spring, MD.*

Study: Damage to red blood cells as they flow through medical devices can release hemoglobin and result in adverse patient events. To evaluate their hemolytic potential, blood-contacting devices (e.g. oxygenators, catheters, ventricular assist pumps) undergo premarket benchtop testing under simulated clinical use conditions. Device safety is often based on determining whether the *in vitro* level of hemolysis is comparable between a new device and a similar, legally marketed device when tested in a paired fashion using the same blood pool (due to variations in blood preparation and quality between different animals). To account for instances when a relative hemolysis comparison is not feasible or ideal, FDA is exploring whether more clinically-relevant safety acceptance criteria for *in vitro* hemolysis levels can be established for different patient-device interactions.
Methods: Methods under investigation include (1) statistically determining state-of-the-art levels of *in vitro* hemolysis for different devices based on data mining of hemolysis studies in FDA premarket submissions and the biomedical literature, and (2) pharmacokinetic modeling of toxic free plasma hemoglobin levels in device patients. Implicit in these analyses is the need to appropriately extrapolate *in vitro* hemolysis test results (using animal blood) to patients while incorporating factors of safety.
Results: When validated, these new tools have the potential to help FDA and the biomedical industry supplement current practices for evaluating the *in vitro* hemolytic potential of new devices relative to previously marketed devices by establishing clinically relevant dose levels of *in vitro* free plasma hemoglobin as applied to different device types and patients.

142

Creating a Modular LVAD Equipment Tracking System

W. Hejl. *Heart Specialty Care and Transplant, Seton Health Medical Center, Austin, TX.*

Study: With a growing number of patients supported by LVADs, there will be an increased need to refine the methods used to manage durable VAD equipment of both the implanting center and the individual patient. Currently, many centers use industry driven software programs or have developed in-house, time consuming, procedures (many utilizing Microsoft Excel) to track this equipment. These techniques have their disadvantages. Industry driven software is specific to the manufacturers' device which creates extra work when a center begins to implant devices from multiple manufacturers, as each device will be tracked on its own platform. Therefore we sought to develop a platform for device tracking that allows the users to track devices from multiple manufacturers while also maintaining the automated functionality of industry provided platforms.
Methods: Microsoft Excel was used due to its ubiquitous use across centers as well as staff being competently trained in its basic use. Another advantage of Microsoft Excel is it's built in automation capabilities. Visual Basic for Applications (VBA) code was developed by the department Biomedical Technologist to automate and streamline the functions of the database in the form of user forms and macro's. The raw data (name, equipment type, etc.) is stored in a table and pivot tables are used to visualize the data. This allows the user to search and sort the data quickly. Many functions have been automated including entering a new patient and their equipment into the database, checking to see if the patient is due for maintenance and automatically alerting the user, and checking if hospital owned equipment is expired or needs servicing.
Results: Although the implementation of this program is still in its early phase and more applications are being developed, we have found that using the Excel based program has saved time and has condensed all of the center's equipment information into one viewable format. The modular nature of VBA is also amenable to creating new applications and refining hospital procedures.

143

Applied Technicians to Keep the VAD Control System on a Safety Condition

A. C. Cavalheiro,[1] D. J. Santos Filho,[2] A. Andrade,[3] E. Bock.[4] *[1]Engineer, Fundação Santo André, Santo André, BRAZIL; [2]Engineer, Universidade de São Paulo, São Paulo, BRAZIL; [3]Engineer, Instituto Dante Pazzanese de Cardiologia, São Paulo, BRAZIL; [4]Engineer, Instituto Federal de São Paulo, São Paulo, BRAZIL.*

Study: Several heart diseases could compromise a human life, then the VAD must possess very high safety levels. But it could have been avoided if these systems had controllers designed specifically to maintain the safety levels in case of fault.

Methods: The propose control monitoring the system fail as a Discrete Event System (DES). Considering VAD fails as a DES able to apply technicians to keep the system on a safety condition if part of the system fails. The technicians applied on this control be: (i) Input Conditioning Method (Figure A) is suggest under an abnormal state of a VAD system can become a normal state before restarting this process, another action will be executed first to maintain the VAD on a safety condition. (ii) Alternate Path Method (Figure B) is suggest when exist a alternate path (also called, error avoidance) that there is another way to avoid the fail which can modify an abnormal state directly into a normal state in the system. (iii) Backward Error Recovery Method (Figure C) is suggest under the assumption that the state is normal but a alternative solution can be executed and a new faulty state results. But this state can become a normal state after an operation is executed. (iv) Forward Error Recovery Method (Figure D) is similar to the backward error recovery method but suppose that a faulty state results after rectification action.

Results: This approach can be directly transformed into a normal state after the execution of a safety control operates. Applying the above four theorems imply that the structural properties of a VAD controller remain if are applied, and suitable recovery actions are taken. This approach allows diagnosis and treatment VAD failures in VAD systems which can degenerate or regenerate the system to a safe condition depending on the criticality of failure. In vitro and in vivo tests using this approach are being performed at the Dante Pazzanese Institute of Cardiology.

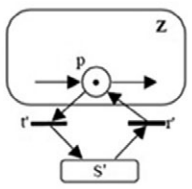

Figure A

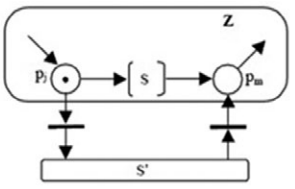

Figure B

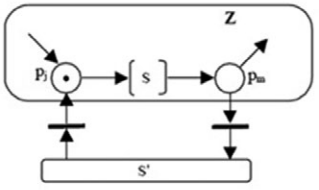

Figure C

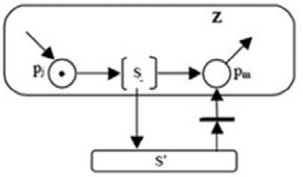

Figure D

147

Development of a Novel Paracorporeal Artificial Lung with Enhanced Flow Mixing

P. Fernando,[1] H. Cheriyan,[2] J. Toomasian,[2] J. Arens,[3] J. L. Bull,[1] R. H. Bartlett.[2] *[1]Biomedical Engineering, University of Michigan, Ann Arbor, MI; [2]Surgery, University of Michigan, Ann Arbor, MI; [3]Department of Cardiovascular Engineering, RWTH Aachen University, Aachen, GERMANY.*

Study: The effectiveness and life span of a paracorporeal artificial lung (AL) can be greatly increased by generating secondary flows, which enhance blood mixing, thereby reducing thrombogenecity and improving efficiency of gas transport. This study investigates a novel AL with gated junctions designed to cause bifurcations in flow that enhance flow mixing.

Methods: ALs with varying configurations were modeled, and a finite element method was used to solve the governing equations for flow through the ALs. The blood inlet flow was a pulsatile wave. The fiber bundle was modeled as a porous media with varying permeability to study the effects of fiber packing density. The resulting flow profiles were used to optimize the design, which was then prototyped using stereo-lithography and centrifugal potting; the AL featured a fiber bundle surface area of 0.28m^2. The blood-gas exchange performance of the AL was evaluated in vitro using a single-pass circuit with bovine blood at standard venous conditions. The sweep gas comprised 100% O_2. The O_2 and CO_2 transfer was evaluated for a range of blood and gas flows.

Results: Resulting flow profiles for the proposed AL design show a significant increase in secondary flows. The path length travelled by the fluid was maximized when consecutive gates were placed 180^0 apart from each other. Increasing the number of gates increases mixing and resistance across the AL, while increasing the permeability of the fiber bundle increases mixing and reduces resistance and shear stress across the AL. The in vitro blood-gas exchange studies demonstrate a rated flow of 2.0L/min and a CO_2 clearance of >180mL/min at the rated flow. These results demonstrate a highly efficient gas exchange capability and suggest that the proposed AL design has enhanced mixing by secondary flows, thereby showing potential to reduce thrombogenecity. Future work is currently underway to evaluate thrombogenecity of the AL in an in vivo model.

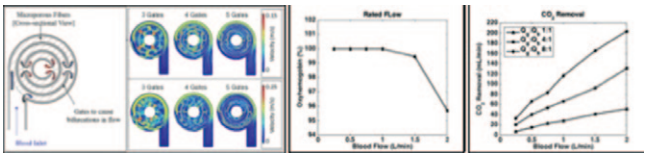

158

An Empirical Model to Estimate Blood Damage in Turbulent Flow in Medical Devices

M. Ozturk, E. A. O'Rear, D. V. Papavassiliou. *Chemical, Biological, and Materials Engineering, University of Oklahoma, Norman, OK.*

Study: Turbulent blood flow in artificial hearts and ventricular assist devices (VAD) cause red blood cell (RBC) damage, which is a major concern when designing prosthetic heart devices. Although the effects of specific turbulent flow characteristics on the blood cells are uncertain, it is generally known that turbulence affects RBCs causing trauma and hemolysis. In this work, contributing factors for RBC damage in turbulence were investigated by simulating jet flow experiments. A number of groups have explored Kolmogorov length scale, KLS, as an indicator of hemolysis. In this study, we have searched for relationships with hemolysis using extensive quantities such as the total surface area from subpopulation distributions of eddies with different KLS. Moreover, we propose a hemolysis model based on experimental results from 3 distinctly different devices: a jet, a Couette viscometer, and a capillary tube.
Methods: A computational technique (FLUENT with k-ω SST model) that can predict the detailed structure of turbulence has been used to investigate the effect of turbulent eddy structures on cell damage. In this study, observing extensive measures like total eddy areas for specific KLS was used to provide a more general understanding of hemolysis. Therefore, relation between the hemolysis to the characteristics of turbulence in the flow was investigated by using k-ω SST turbulence model to simulate jet flow hemolysis experiments.
Results: Findings showed that dissipative eddies comparable or smaller in size to the RBCs cause hemolysis and that hemolysis corresponds to the number and the surface area of eddies that are associated with KLS smaller than about 10 µm. The size of KLS eddies was used to define a turbulent flow extensive property, and a new hemolysis model was proposed. This empirical model is in agreement with hemolysis results for well-defined systems that exhibit the different exposure times and flow conditions found in Couette flow viscometer, capillary tube, and jet flow experiments.

160

Determination of Reynolds Shear Stress Level for Hemolysis

C. Jhun,[1] J. O. Taylor,[2] J. D. Reibson,[1] E. E. Yeager,[1] R. K. Newswanger,[1] K. B. Manning,[2] S. Deutsch,[2] W. J. Weiss,[1] G. Rosenberg.[1] *[1]Surgery, Penn State College of Medicine, Hershey, PA; [2]Biomedical Engineering, The Pennsylvania State University, University Park, PA.*

Study: Reynolds shear stress (RSS) has served as a metric for turbulence effect on hemolysis. Forstrom (1969) and Sallam (1984) determined the RSS threshold for hemolysis to be 50,000 dyne/cm^2 and 4,000 dyne/cm^2, respectively, using a turbulent jet. Despite the order of magnitude discrepancy, the Sallam's threshold has been frequently cited for hemolytic potential in blood pumps. We recreated both Sallam apparatus (SA) and Forstrom apparatus (FA) to resolve this discrepancy and provide additional data to be used in developing a more accurate hemolysis model.
Methods: Hemolysis was measured over a large range of Reynolds number (Re) conditions in both SA (Re=1000–80000) and FA (Re=1000–30000). Washed bovine red blood cells (RBCs) were resuspended in phosphate buffered saline (PBS) to achieve a hematocrit (HCT) of 50% and 5% for SA and FA, respectively. For SA, washed RBCs were injected into the free jet of PBS, and samples were collected at (x/d_e=6.5, y/r_e=1.2), where, d_e is the jet diameter (3 mm) and r_e is the jet radius. For FA, 2 ml of PBS was injected into a 30 ml syringe containing 7 ml of 5% HCT washed RBCs. The jet diameter was 0.33 mm. Hemolysis was quantified using a percent hemolysis, H_p=h(100-HCT)/Hb, where, h [mg/dl] is free hemoglobin and Hb [mg/dl] is total hemoglobin. Principal RSS was calculated at (x/d_e=6.5, y/r_e = 1.2) for SA using 2D laser Doppler velocimetry. For FA, RSS values were approximated using, RSS = 0.017ρU_e^2, developed by Schlichting, where ρ is density and U_e is jet exit velocity.
Results: In SA, the RSS value of ≥ 30,000 dyne/cm^2 corresponding to Re of ≥ 60,000 appeared to cause hemolysis. In FA, the RSS value of ≥ 50,000 dyne/cm^2 corresponding to Re of ≥ 6,000 appeared to cause hemolysis. Both RSS thresholds (30,000 dyne/cm^2 and 50,000 dyne/cm^2) are similar to Forstrom's RSS threshold, and an order of magnitude greater than Sallam's RSS threshold. This study resolved a long-standing discrepancy regarding the critical values of RSS for hemolysis, and may provide a foundation for a more accurate hemolysis model.

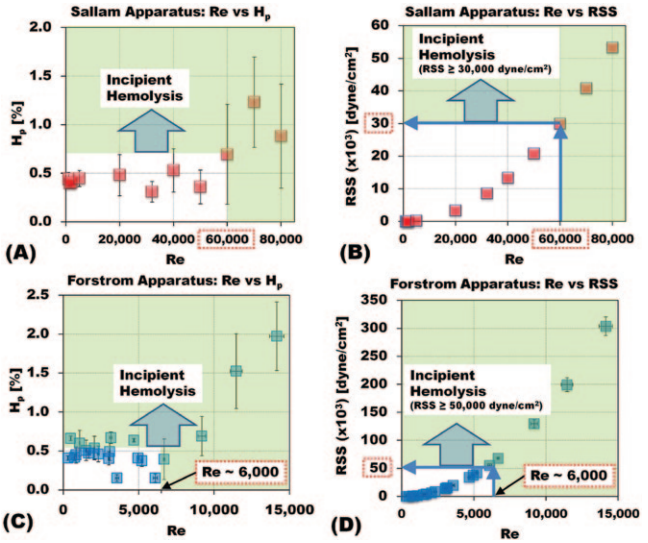

164

Control Strategy for the Inductively Coupled Wireless Power Transfer Circuit for Implants

H. Jiang,[1] **Y. W. Wu**,[1] A. Franco,[1] K. Bai,[1] J. Ye,[1] X. R. Zhang,[1] R. Fechter,[2] M. Harrison,[2] S. Roy.[3] *[1]Engineering, San Francisco State University, San Francisco, CA; [2]Surgery, University of California San Francisco, San Francisco, CA; [3]Bioengineering and Therapeutic Sciences, University of California San Francisco, San Francisco, CA.*

Study: An innovative control strategy of the inductively coupled wireless power transfer circuit is investigated with various operating conditions, e.g., different distances and geometrical alignments between two coils, different tissue environments and different coils. These operating conditions have profound impacts on the performance, however they hardly can be precisely controlled in the application. The control strategy is to stabilize the raised voltage across the receiving coil before the rectification by adjusting the duty cycle of the switch that is placed across the receiving coil, as depicted in Fig. 1.
Methods: The output voltage of the described circuit is able to constantly output 2V across a 25 KOhm resistor by adjusting the switch's duty cycle. The experiments have been conducted in the following conditions: (1) Different Operating Distances: The receiving coil has been placed in various distances from the transmitting coil. By changing the switch's duty cycle, the output voltage/power is able to remain constant; (2) Different Coil Orientations: The receiving coil has been placed in various orientations with respect to the transmitting coil. By changing the duty cycle, the output voltage/power remains constant; (3) Different Environments: The receiving coil has been placed inside the saline, comparing to the air. The output voltage/power is still able to remain constant by tuning the switch's duty cycle; (4) Different Receiving Coils: Four different receiving coils are winded. Their inductances range from 0.2mH to 2mH. They are all able to output the same voltage/power.
Results: The investigation suggests that the control strategy, adjusting the duty cycle of the controlling switch, is able to produce constant output voltage and power even when the receiving coil operates at different distances and geometrical orientations to the transmitting coil, different environments, and with different receiving coils.

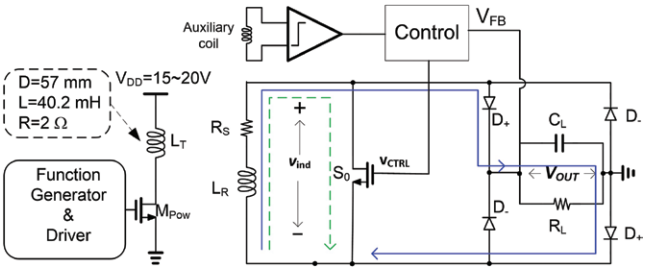

170

A Physics-Based Hemolysis Model Using Energy Dissipation

C. Jhun,[1] B. A. Craven,[2] J. D. Reibson,[1] E. E. Yeager,[1] R. K. Newswanger,[1] W. J. Weiss,[1] G. Rosenberg.[1] *[1]Surgery, The Penn State College of Medicine, Hershey, PA; [2]Biomedical Engineering, The Pennsylvania State University, University Park, PA.*

Study: A commonly used hemolysis model for blood pumps is a (Reynolds shear) stress-based power-law model. This stress-based power-law model depends on flow conditions and lacks accuracy over the wide range of Reynolds numbers (Re) found in circulatory support devices. We hypothesize that hemolysis is the result of energy dissipation resulting from viscous forces and the energy dissipated as heat. This study is to demonstrate that a single physics-based hemolysis model can accurately predict hemolysis in laminar through turbulent flow.
Methods: A submerged free jet apparatus recreated based on Sallam (1984) was used to hemolyze red blood cells (RBCs) over a wide range of Re conditions (Re = 1000 - 80000). The lysed RBCs were collected through an aspirator located at (x/d_e=6.5, y/r_e=1.2), where, d_e is jet diameter (3 mm) and r_e is jet radius. Hemolysis was quantified using a percent hemolysis, H_p=h(100-HCT)/Hb, where h [mg/dl] is free hemoglobin, HCT [%] is hematocrit, and Hb [mg/dl] is the total hemoglobin. Large eddy simulation (OpenFOAM) was used to calculate the energy dissipation at the sampling location for each Re condition. The CFD results were validated using 2D laser Doppler velocimetry. Accuracy in predicting hemolysis of the dissipation-based and stress-based models was also compared.
Results: A dissipation-based hemolysis model ($\varphi = FK\varepsilon$) was derived from the relationship between H_p and dissipation, ε, where, φ is the rate of free hemoglobin production, F is the fragility factor, and K is an empirical production coefficient. The model was then implemented in a transport equation. With a single constant K, the dissipation-based hemolysis model predicted H_p well (95% confidence interval) from laminar through turbulent flow. The stress-based power-law model severely under-predicted hemolysis as Re increased. The clinical impact of this dissipation-based hemolysis model will be to provide a tool for the design of improved ventricular assist devices (VADs) or any cardiovascular device where shear stress is important.

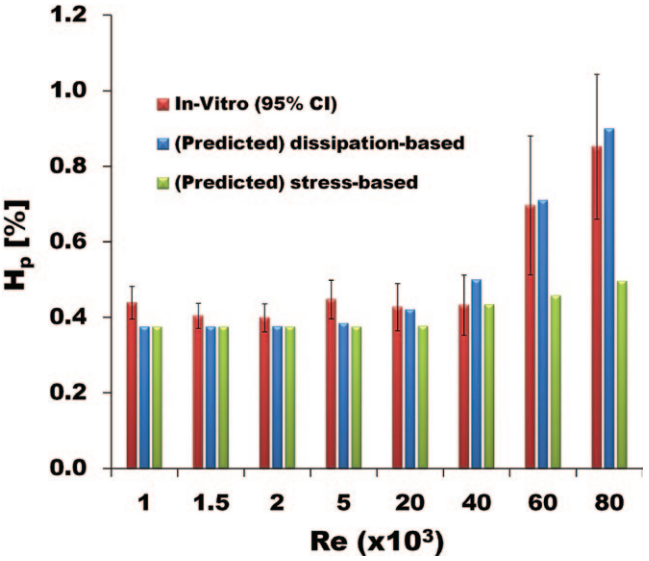

172

Modulation of RBC Traffic Using Blood Soluble Drag Reducing Polymers as Potential Treatment for Sickle Cell Disease (SCD)

D. Crompton,[1] S. H. Gudla,[1] M. A. Jimenez,[2] P. Sundd,[2] J. H. Waters,[3] M. V. Kameneva.[1] *[1]Bioengineering, University of Pittsburgh, Pittsburgh, PA; [2]Vascular Medicine Institute, University of Pittsburgh, Pittsburgh, PA; [3]Department of Anesthesiology, The Magee Women's Hospital of UPMC, University of Pittsburgh, Pittsburgh, PA.*

Study: SCD is an inherited hemolytic disorder that alters hemoglobin within red blood cells (RBCs), causing them to become rigid and 'sickle' shaped. Sickled RBCs (S-RBCs) occlude microvessels leading to severe pain. Current treatments are limited to chronic hydroxyurea (HU) and donor blood transfusion, which are often associated with complications such as alloimmunization and HU related toxicity. We are investigating a novel rheological approach which would enable the modulation of RBC traffic through small microvessels, reducing the number of S-RBCs entering capillaries.
Methods: In microvessels with diameters below ~300 micron, deformable RBCs tend to move toward the vessel center creating a cell-free layer (CFL) near the vessel wall, leaving less-deformable cells such as S-RBCs closer to the vessel wall. This results in an increase in number of S-RBCs entering the microvessel branches and obstructing capillaries. We have demonstrated that nanomolar concentrations of soluble high molecular weight (> ~106 Da) molecules (drag reducing polymers or DRPs) provide equal distribution of all RBCs across the vessel lumen and can reduce the relative number of S-RBCs near the vessel wall. Our current study investigates the DRP effect on flow of normal and rigidified RBC suspensions at 20–30% hematocrit in bifurcating microchannels.
Results: Preliminary studies demonstrated the existence of the CFL and its disappearance with the addition of DRPs via significant changes in hematocrit of samples collected from branchs. Further studies with RBC suspensions containing normal and heat treated rigid RBCs (R-RBCs) are being performed. The proportion of R-RBCs which have exited through each outlet is determined by analysis of cell deformability (Linkam Shearing Stage, Linkam Scientific Instruments, UK). A decrease in R-RBCs and increase of normal RBCs in branch outlets suggests that DRPs can be therapeutically effective in shunting S-RBCs past the capillary system.

176

Qualitative Method Using EDX Analysis with Fluorophore-conjugated Antibodies to Differentiate Cells in a Mixed Cellular Population

M. Rivas-Bustamante,[1] M. T. O'Brien,[2] B. R. Weeks,[2] F. J. *Clubb.*[2] *[1]Biomedical Engineering, Texas A&M University, College Station, TX; [2]Veterinary Pathobiology, Texas A&M University, College Station, TX.*

Study: Fluorophore-conjugated antibodies are commonly used for a variety of cellular imaging, identification, and phenotyping purposes. These antibodies are often readily available and relatively inexpensive. However, a metal-conjugated antibody is generally necessary for Scanning Electron Microscopy (SEM) of cellular identification/phenotyping. Although metal-conjugated antibodies and kits to provide conjugation can be purchased, these are expensive and sometimes require the use of a secondary antibody. Furthermore, the lack of commercially available metal-conjugated antibodies for a given purpose can impede the use of these entities. Although most commonly used fluorophore molecules do not contain distinct metallic components, the Energy Dispersive X-ray Spectroscopy (EDX) signature on SEM may sufficiently characterize these molecules and consistently differentiate between fluorophore-labeled and unlabeled cells.
Methods: Three sample sets of cells (labeled A, B, and C) were obtained. Set A had no antibody labeling and was used as a control. Set B was stained with an antibody conjugated to a fluorophore. Set C consisted of a mixture of unlabeled and antibody labeled cells. Cells were dehydrated in a series of graded ethanol. A low-vacuum scanning electron microscope at 5 to 15kV was used to obtain an EDX analysis; images were captured at magnifications of 300 to 4000x.
Results: Cells labeled with a fluorophore-conjugated antibody may have an EDX elemental signature that is sufficiently different from unlabeled cells that allow for consistent identification in a mixed cellular population of labeled and unlabeled cells. This suggests that the use of fluorophore-conjugated antibodies provide an inexpensive method for differentiating cells that can be used in a clinical setting.

177

Flow Visualization at the Outlet of the HeartMate II Left Ventricular Assist Device Using Particle Image Velocimetry

G. W. Rowlands, B. C. Good, S. Deutsch, K. B. Manning. *Biomedical Engineering, The Pennsylvania State University, University Park, PA.*

Study: Ventricular assist devices (VADs) are implanted in patients with a diseased ventricle to maintain peripheral perfusion or as a bridge to cardiac transplant. However, patients with an implanted VAD, such as the HeartMate II (HMII), have experienced bleeding episodes in the abdomen. These incidents are likely caused by the cleavage or breakdown of von Willebrand Factor (vWF), a protein in the clotting cascade. *In vitro* studies were conducted to quantify the flow at the outlet of the HMII under steady and pathophysiological conditions to determine their potential contribution to vWF mechanical destruction.
Methods: Particle image velocimetry was used to quantify velocities, stresses, and turbulence intensities in an acrylic model of the HMII outlet at three planes including the centerline and ±2 mm from the centerline. This *in vitro* study measured these parameters at the pump's outlet under steady and pathophysiological conditions. In the steady experiment, the HMII was connected in series with a compliance chamber and operated with an 80 mmHg rise across the pump. The latter experiment included a pulsatile pump with the VAD and compliance chamber inducing pulsatility through the HMII. The pulsatile pump operated at a rate of 95 beats per minute with a stroke volume of 40 mL.
Results: The steady experiment results were compared to the pathophysiological experiment results over various time points in the cardiac cycle. In the three planes, the pulsatility induced during the study produced, at times, shear stresses and turbulence intensities an order of magnitude greater in comparison to its steady counterpart. This study reveals the importance of not only the flow within a rotary pump, but the flow exiting can be harmful too.

179

The Relationship of Blood Viscosity to Hemolysis Index *in vitro* Hemolysis Test

X. Li, I. Saito, T. Yurimoto, S. Hara, Y. Abe. *The University of Tokyo, Tokyo, JAPAN.*

Study: Hemolysis (blood damage) is one of the most important parameters to evaluate medical devices' hemocompatibility. Assessment of hemolysis in vitro has been specified by ASTM. However, only pump drive condition has been written for ASTM. As for blood viscosity, it's not been considered. It's well-known that blood is damaged by shear stress in blood pump. Variations of blood viscosities have been associated to output of blood pump as well as shear stress. In this study, we investigate the relationship between the hemolysis index and blood viscosity.
Methods: Fresh porcine blood of 4 different hematocrits (5, 15, 25, 35%) was produced with 0.9% saline. Gentamicin and Heparin were given for antibacterial and anticoagulant. In a vitro mock loop, the blood pump (IBC FloPump 6000, International Biophysics Corporation, Texas, USA) was operated for 3h under 5L±0.1/min, 100 ± 3mmHg condition. Blood samples were collected at every 1h to measure plasma free hemoglobin. The blood viscosity was measured at the beginning of hemolysis test. Measuring the plasma free hemoglobin of blood samples by Cripps method, the normalized index of hemolysis (NIH) and modified index of hemolysis (MIH) were calculated.
Results: NIH/viscosity/ (viscosity-0.74) and Ht had a strong correlation with a coefficient of fit of 0.93. Moreover, the coefficient fit of MIH/viscosity versus Ht was 0.92. The relationship of blood viscosity to NIH and MIH in hemolysis test was investigated. For this result, it is considered necessary to adjust blood viscosity in hemolysis test.

185

Computational Prediction for Effects of Valvular Regurgitation on IABP Function Using 3D Cardiac Mechanics Model

C. Kim, K. Lim. *Kumoh National Institute of Technology, Gumi, KOREA, REPUBLIC OF.*

Study: We investigated the effects of aortic and mitral regurgitation on the function of intra-aortic balloon pump (IABP) using a three-dimensional electromechanical model of the failed canine ventricles. We incorporated valve regurgitation condition and IABP function into a previously developed electromechanical model of the ventricle with a lumped model of the circulatory system. Under normal condition, IABP therapy group showed less contractile ATP consumption and left ventricular (LV) peak pressure (ventricular unloading effect) and larger arterial blood pressure during diastole (coronary circulation improvement effect). However, the effects of IABP therapy decreased under aortic regurgitation condition due to backflow from aorta to LV cavity, while they are not much affected by mitral regurgitation. These results may be used as a reference data when considering the use of IABP for the heart failure patient with clinically doubtful valve regurgitation.
Methods: We used previously developed canine electromechanical model based on magnetic resonance imaging. Canine ventricular geometry model is combined with electromechanical components and cardiovascular model. Electromechanical model is combined with myocardial filament model. The IABP component was modeled as the time-varying compliance of the systemic arteries. To generalize the patterns of inflation and deflation of an IABP, a harmonic waveform was used for the time-varying compliance of the systemic arteries.
Results: IABP treatment increased ventricular pressure unloading and SV and EF at all degree of MR conditions. However, in case of AR, it had small effect of ventricular pressure unloading, but stroke volume and ejection fraction were reduced or maintained. IABP reduced ATP consumption and tension distribution of ventricular wall in MR condition, but not much in AR case. Therefore, we conclude that AR reduced the function of IABP more than MR condition.

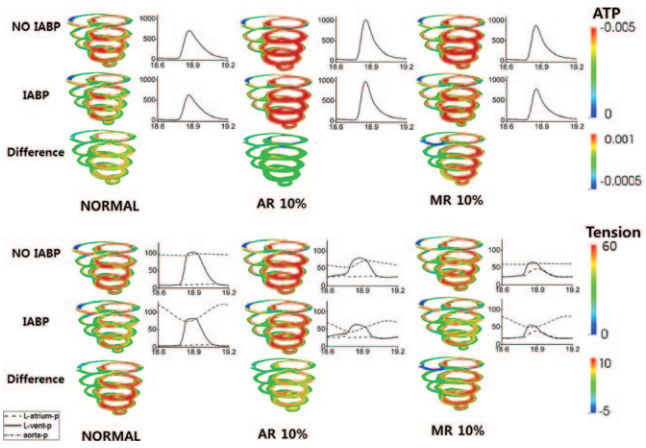

190

The Effect of 3-dimential Micro-geometrical Structures of Bio-material Surface on Flow and Adhesion Phase in Thrombus Cascade

A. I. Oota,[1] **T. Masuzawa**,[1] T. Shibata.[2] *[1]Ibaraki University, Department of Mechanical Engineering, Hitachi Ibaraki, JAPAN; [2]Toyohashi University of Technology, Toyohashi, Aichi, JAPAN.*

Study: The relationship between thrombus formation and micro morphology on bio-material surfaces is studied. Reactions of thrombus formation on bio-material surfaces with structures are complicated and have not yet revealed completely. The contributions of surface roughness on the blood compatibility have been reported that not only to cause thrombosis but also to inhibit thrombosis such as 'textured surface'. We assume the flow generated by micro-morphological structures on bio-material surface affects the platelet adhesion. The objective of this study is to investigate micro flow around 3-Dimentional micro-geometrical structures and adhesion phenomenon affected by the micro-flow.
Methods: Silicon test pieces with simple cylindrical micro-structures (columns) were constructed by Micro Electro Mechanical System (MEMS). The flow field and particle path lines around the columns on the test piece were calculated by Computational Fluid Dynamics (CFD) analysis. Adhesion tests using albumin microbeads which simulate platelets were conducted using a perfusion circuit with shear rate conditions of 0, 250 and 500 S^{-1} to investigate the effect of flow around the micro-columns on adhesion phenomenon. Averaged adhesion rate on the area around columns and on the plane area are measured using an image processing software Image J.
Results: The vortex and flow toward bottom surface around a column are identified by the CFD simulation. The experimental adhesion results with albumin microbeads indicated that the averaged adhesion rate around the columns is higher than the plane area, and the averaged adhesion rate increases with increasing flow rate in the perfusion circuit. High adhesion rate around columns are affected by the micro vortex and flow toward bottom surface around the column. The effect of the 3-Dimential micro-geometrical structures on the flow and adhesion rate is confirmed.

191

Short Term *in vivo* Studies with a Centrifugal Apico-Aortic Blood Pump

B. Utiyama,[1] T. Leão,[1] J. F,[1] R. de Sá,[1] E. Leal,[1] E. Drigo,[1] G. C. Andrade,[2] D. S. Filho,[3] J. R. Cardoso,[3] A. J. Andrade.[1] *[1]Bioengineering Division, Instituto Dante Pazzanese de Cardiologia, São Paulo, BRAZIL; [2]University São Judas Tadeu, São Paulo, BRAZIL; [3]University of São Paulo, São Paulo, BRAZIL.*

Study: Apico-Aortic Blood Pump (AABP) is a centrifugal intrathoracic LVAD under development in our laboratories. In order to observe organism physiological response and device behavior in real conditions, short term *In Vivo* experiments were performed.
Methods: AABP was implanted in 7 pigs (gender not defined, weight: 140 to 180 lb). AABP's inlet cannula was connected directly to the left ventricle apex and outlet cannula was connected to the ascending aorta. Animals were maintained for 6 hours, during this time, besides physiological parameters, AAPB's flow output, rotational speed and current consume were registered.
Results: In 4 of 7 experiments, none complication was registered and the planned 6 hours of experiment were achieved. In the other 3 experiments, complications were observed, including: - Animal's death during implantation caused by damage in the right coronary artery during anastomosis; - Animal's death during implantation caused by presence of air in the tubes. - Animal's death before the implantation during thoracotomy. Monitored device parameters indicated none failure in AABP's performance. Several events of inlet cannula obstruction by suction were observed. Implantation time dropped from 2 hours at the first two experiments to 30 minutes at the last two.
Conclusion: Results indicated that AABP's presented satisfactory performance during these short term *In Vivo* experiments. Suction events could be avoided using echocardiography during inlet cannula positioning. Shorter implantation time may be related to surgical team experience but also by the usage of specific surgical instrumentation, which were developed during this study.

194

A Novel Coil with Flexibility for Transcutaneous Energy Transmission System of Artificial Hearts

H. Murakami, I. Saito, Y. Abe. *Department of Biomedical Engineering, The University of Tokyo, Tokyo, JAPAN.*

Study: Artificial hearts need a percutaneous driveline for power supply. The driveline causes serious infection as well as inconvenience in life. Transcutaneous Energy Transmission System (TETS) is a solution to eliminate the driveline by electromagnetic induction. Previous TETS has a problem of reduction in transmission efficiency by positional displacement between internal and extracorporeal coils, due to difficulty of fixing previous hard and thick coils. The previous imbedding coils also damage patients' bodies by pressure. In this study, we developed a new coil for TETS made of Flexible Printed Circuits (FPC). This flexible and thin coil is easily fixed, and prevents positional displacement by embedding into side chest; too narrow to insert for the previous coils and moreover, it anatomically fits the embedding part. However, the flexible coil has difficulty to reduce resistance compared with the previous because of thinness. In this paper, we investigated relevant flexible coils form minimizing equivalent series resistance (ESR) regarding equivalent inductance.
Methods: We made twelve types of air-core coils of FPC, their diameter was 78–126 mm, internal diameter was 32–84 mm, number of turns was 2–36, number of slits was 0, 8, 25, 50. And, we measured the coils as single and the connected coils to same form in parallel or series.
Results: ESR of a single side coil was 2.15-fold compared with a double side coil of equivalent size and inductance. ESR of the smaller internal diameter coils was larger than the bigger ones under equivalent diameter and inductance. And, comparing double side coils in parallel and series connection, under equivalent size and inductance, ESR of the coils in series 0.47-fold as small as parallel. In conclusion, it was shown that double side coils connected in series, had larger internal diameter, enabled to reduce ESR compared with a single coil or coils connected in parallel those diameter and inductance were equivalent.

197

Design Optimization of a Dimpled Membrane for an Endothelializable Oxygenator Using Computational Fluid Dynamics

F. Hesselmann,[1] J. G. Wintersohle,[1] S. Groß-Hardt,[1] C. Neusser,[2] S. Djeljadini,[3] C. Cornelissen,[4] U. Steinseifer,[1] J. Arens.[1] [1]*Department of Cardiovascular Engineering, Institute of Applied Medical Engineering, RWTH Aachen University, Aachen, GERMANY;* [2]*Institut für Textiltechnik, RWTH Aachen University, Aachen, GERMANY;* [3]*Chemical Process Enineering, RWTH Aachen University, Aachen, GERMANY;* [4]*Department for Internal Medicine - Section for Pneumology, Medical Facultiy, RWTH Aachen University, Aachen, GERMANY.*

Study: The endothelialization of oxygenator membranes promises an improved hemocompatibility and, thus, offers great potential for the long-term use as an implantable lung. The development of such a biohybrid artificial lung faces new challenges such as retaining a functional cell layer under shear stress. The additional diffusive resistance of the cellular monolayer needs to be overcome for an adequate gas transfer. In this study, laminar vortex mixing through pulsatile flow over a structured membrane was evaluated and optimized numerically to achieve a maximum oxygen uptake in a physiological wall shear stress range (WSS).
Methods: A dimpled membrane surface was parameterized (sphere diameter D, normal membrane distance s, depth of spheres m, distance between spheres a). Blood flow pulsatility was described by three additional input parameters (Strouhal number, peak and mean Reynolds number). A validated numerical model for the gas exchange developed by our group was implemented to solve the flow and gas transfer simulations simultaneously. Design of Experiments (DoE) and response surface based multi-objective optimization with 280 design points were applied to maximize the oxygen uptake per exchange area for a constrained WSS below 15 Pa. Mesh, pulse and time step independence were assured prior to this study.
Results: The parameter sensitivity analysis shows a high impact of the peak Reynolds number and an opposed influence of the membrane distance s on the maximum WSS. The normalized gas transfer is mainly affected by the distance between the spheres. The optimized design shows compared to an unstructured design only a slight improvement in oxygen uptake with elevated WSS values by 28.4%. The results indicate that no laminar vortices occur in the specified range of acceptable WSS. Ongoing studies promise an improved shear resistance of the cellular layer and, therefore, this study will be extended to investigate laminar vortex mixing for increased WSS thresholds.

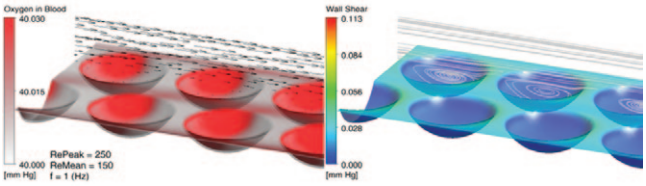

198

Liposome-Encapsulated Tacrolimus Ameliorates Total Brain Ischemia and Reperfusion Injury in the Rat

A. T. Kawaguchi,[1] H. Endo,[2] M. Yamano,[3] T. Fukuta,[4] T. Ishii,[4] N. Oku.[4] *[1]Cell Transplantation and Regenerative Medicine, Tokai University School of Medicine, Isehara, JAPAN; [2]Public Health, Tokai University School of Medicine, Isehara, JAPAN; [3]Osaka Prefecture University, Habikino, JAPAN; [4]Department of Medical Biochemistry, University of Shizuoka School of Pharmaceutical Sciences, Shizuoka, JAPAN.*

Study: Liposome-encapsulated Tacrolimus (LET) has been reported to accumulate in the damaged brain tissue. We tested its effect(s) in a rat model of total brain ischemia and reperfusion (I/R).
Methods: Wister rats of excellent Sidman avoidance test (SAT) performance underwent abrupt and total cerebral ischemia by intrathoracic vessel clipping for 5 minutes, received intravenous saline (2 mL/kg, n=7), LET (100 mcg/kg, n=8) or liposome-encapsulated hemoglobin with high O_2 affinity (LEH 2 mL/kg, n=8) while additional rats received thoracotomy alone without ischemia as the non-ischemic control (n=7). All rats were followed by repeated SAT in the next day and 6 weeks later when Morris water maze test were repeated before sacrifice for morphological studies.
Results: Treatment with LET or LEH was mildly preserving SAT performance on the next day between the ischemic and non-ischemic controls, which became equivalent in all 6 weeks later. In the Morris water maze tests, LET-treated rats required 4.0 ± 0.8 times on the average before reaching submerged platform in 8 seconds (=correctly locate and swim directly to the platform across the pool), equivalent to the non-ischemic control rats (3.9 ± 1.5 times, *P*=0.812) or LEH-treated rats (4.8 ± 2.0 times, *P*=0.334), and favorably compared to saline-treated rats (9.0 ± 5.1 times, *P*=0.016). Semi-quantitative morphological studies (0 to 4) showed damages in all rats undergoing I/R except for amygdala in LET-treated rats, which was not statistically different from rats without ischemia. Severity of the hippocampal CA1 lesion showed significant correlation with the Morris water maze trials required to reach submerged platform in 8 seconds (r=0.39) and in 10 seconds (r=0.48). In conclusion, these results suggest that LET in a much smaller dose for immunosuppression may be protective of total brain I/R injury presumably not by O_2 delivery, but by attenuating inflammation and preserving hippocampus and amygdala from delayed cell death.

200

Measurement of Cannula Centering Forces for Transvalvular Ventricular Assist Devices

M. H. Stoiber, P. Aigner, F. Moscato, **H. Schima**. *Medical University of Vienna & Ludwig Boltzmann Cluster for Cardiovascular Research, Vienna, AUSTRIA.*

Study: In transvalvular positioned cardiac support devices the cannula-leaflet interaction is of special interest and importance. Valve damage, backflow and thrombus formation might be improved if the cannula is kept in a central position within the valve orifice.In a pulsatile in-vitro setup, forces acting on transvalvular cannulas were identified and the influence of cannula diameter and transvalvular pressure were investigated.
Methods: Radial and tangential forces acting on transvalvular cannulas were measured in a pulsatile setup. Fresh native porcine, bioprosthetic and artificial pericardial tissue valves were mounted in a test rig. The cannula position was deflected from a central position to the wall in 10° rotational step for the whole circular range. Further the cannula diameter (4, 6, 8 mm) and transvalvular pressure (40 - 100 mmHg) were varied.
Results: Centering forces of the aortic cusps in the direction of the coaptation point were identified. At the mid of the leaflets and at the largest deflection the forces were highest (up to 0.8 N). In the commissures lower forces (up to 0.2 N) were measured. In symmetric valves with equal cusp sizes (pericardial tissue valve) the position of the commissures and cusps were clearly pronounced by the force distribution. Natural variations in the valve leaflets affected these distributions but lowest forces were always found in the commissures. A change in cannula diameter had only a minor influence. However rising transvalvular pressure linearly increased the forces, but did not alter the distribution patterns.
Conclusion: Centering forces that act on transvalvular cannulas were identified in an in-vitro setup for several valves and valve types. Lowest centering forces were found in the commissures and highest forces were found directly at the cusps. At low pressures low centering forces and an increased cannula movement can be expected.

203

Exogenous Nitric Oxide Supplementation to Enhance the Outcome of Fluid Resuscitation From Hemorrhagic Shock

J. Crump,[1] J. Briceño,[1] P. Cabrales.[2] *[1]Biomedical Engineering, Universidad de Los Andes, Bogota, COLOMBIA; [2]Bioengineering, University of California, San Diego, La Jolla, CA.*

Study: Nitric oxide (NO) production is impaired in hemorrhagic shock (HS) by: reduction on endothelial shear stress; free radicals that uncouple endothelial NO synthase; and hypoxia. We propose to supplement NO during resuscitation, using nanoparticles (NO-np). This study investigated the systemic and microcirculation changes and 8-day survival outcome of NO-np infusion in a murine model and then a scale up of the best dosage strategy to a swine hemorrhagic shock model.
Methods: In the first model, Syrian hamsters with dorsal window chamber were used. Microcirculatory parameters were evaluated. Blood chemistry, systemic parameters, and NO bioactive isoforms were monitored. Survival study group was followed for 8 days. In the second animal model, Yorkshire pigs were used. Complete blood chemistry and systemic parameters were monitored. All measurements were performed at baseline, after shock, and after fluid resuscitation.
Results: MAP, HR, CO, venular blood flow and diameter were affected by NO-np, indicating vasodilatation and chronotropic effect of NO. With NO supplementation, pH, BE and lactate improved indicating acid-base restoration. FCD, which is the key parameter in determining the functionality of microcirculation improved by two fold. These effects show the microvasodilatation, shunt prevention and improved perfusion effect of NO-np. NO bioactive isoform concentrations were dramatically increased and 8-day survival was dramatically improved, showing NO homeostasis in the circulatory compartment benefiting HS outcome. NO alters organ function by regulating regional blood flow and organ perfusion. NO prevented cardiovascular collapse, allowing animals to maintain superior systemic and microvascular hemodynamic conditions and increasing survival rate.

207

Design, Fabrication and *in vivo* Evaluation of a Structural Reinforced Small Intestinal Submucosa Regenerative Vascular Graft for Hemodialysis Access

K. T. Valencia Rivero,[1] J. Jaramillo,[1] F. J. Cedano,[1] R. López,[1] N. F. Sandoval,[2] J. C. Briceño.[1] *[1]Bogotá D.C., Universidad de los Andes, Bogotá D.C., COLOMBIA; [2]Bogotá D.C., Fundación Cardioinfantil Instituto de Cardiología, Bogotá D.C., COLOMBIA.*

Study: Chronic Kidney Disease affects about 13 % of the population in USA, around 370.000 patients are in Hemodilysis (HD) for its treatment and need a vascular access (VA). VA gold standard are autologous grafts, but this approach is limited by donor tissue availability and morbidity. Synthetic Vascular Grafts (SVG) are other option, but a high rate of infections, deficient long term functionality, thrombogenesis and graft wall stiffness mismatch with the native vessels, are major limitations. The objective of this study was to design and fabricate a Tissue engineered regenerative vascular graft (RVG) and to evaluate its *in vivo* patency in a previously defined animal model.
Methods: It was used Small Intestinal Submucosa (SIS) as a biological scaffold to make a RVG with reinforced structure. A preliminary graft design was implanted in swine (n=6). The final RVG was implanted in 50 kg swine (n=3) between the right carotid artery and the jugular vein to construct an arteriovenous fistula and a SVG was implanted on the contralateral side as control. Weekly ultrasound was performed until graft's patency loss. SIS graft was explanted with native vessels to evaluate regeneration by histology and wall stiffness by biaxial mechanical test.
Results: A C-shaped SIS graft was designed as a tubular conduit with 4 mm diameter, 150 mm length, smooth lumen and an external structural SIS reinforcement. SIS grafts remained patent 46 ± 7 days against the control (30 ± 3 days). Histological results showed neovascularization and compared to the control reduced thrombus formation and inflammation. Biaxial tests demonstrated no significant difference in Young moduli between SIS grafts (Ec = 2.5 ± 1.0 MPa, El = 5.7 ± 2.6 MPa) and SVG (Ec = 4.6 ± 1.4 MPa, El = 5.3 ± 1.5 MPa) as well as native artery (Ec = 1.4 ± 0.8 MPa, El = 5.5 ± 1.1 MPa) in both directions, indicating similar wall stiffness. These results show the viability of biological scaffolds as vascular grafts for HD access.

209

Evaluation of the Aachen Couette Shearing Device Using Transient CFD Analysis

P. Wu,[1] F. Boehning,[2] S. Gross-Hardt,[2] P. Hsu.[1] *[1]Artificial Organ Technology Lab, Bio-manufacturing Research Centre, Soochow University, Suzhou, CHINA; [2]Department of Cardiovascular Engineering, Institute of Applied Medical Engineering, RWTH Aachen University, Aachen, GERMANY.*

Study: Hemolysis is one of the most persistent problems for the development of artificial organs. Reducing the level of hemolysis is one of the key goals particularly during the development of blood pumps. In this study, transient CFD simulations are employed to estimate the influence of the Couette device run-out on the deviation of the index of hemolysis (IH). Many experimental studies have been conducted to explore and quantify the hemolytic mechanism of blood cells. It is commonly believed that the level of hemolysis depends both on to the amplitude of shear stress and exposure time. In recent years, much attention has been paid to the Couette shearing device due to its ease to control the shear rate and achieve a uniform level of shear stress. Recently, Boehning and his collaborators developed a laminar flow through Couette shearing device. Even though special attention is paid to the material and manufacturing process to achieve a high precision, the maximum run-out of the inner cylinder of the Couette flow device is around 10µm, accounting for 20% of the gap width, which may lead to high standard deviations of the IH with increased shear stress.

Methods: To estimate the influence of the alignment uncertainties in Aachen Couette device on the deviation of IH, the maximum run-out is set as 20µm, and decreased to 10µm and 5µm. Transient CFD approach combined with transient Lagrangian particle tracking is employed to study the unsteady flow physic in this Coeutte device.

Results: The local shear stress fluctuations decrease as the run-out is reduced. Higher standard deviations in shear stress are observed with increased run-out. The run-out are found to have considerable influence on blood damage. This work provides an insight into the uncertainties caused by an inevitable run-out of the Couette device when measuring IH. Run-out should be taken into account in the evaluation of blood damage in blood shearing devices and hydrodynamic bearings, as well as in the construction of blood damage models.

211

Reducing Water Transmission of Dynamically Loaded Polyurethane (PU) Using Multilayer Barrier Coatings Applied by Plasma-Enhanced Chemical Vapor Deposition (PECVD)

C. Lierath,[1] L. Kleines,[1] D. Kirchheim,[2] U. Steinseifer,[1] R. Dahlmann,[2] C. Hopmann.[3] *[1]Department of Cardiovascular Engineering, Institute of Applied Medical Engineering, RWTH Aachen University, Aachen, GERMANY; [2]Centre for Analysis and Testing of Plastics, Institute of Plastics Processing, RWTH Aachen University, Aachen, GERMANY; [3]Institute of Plastics Processing, RWTH Aachen University, Aachen, GERMANY.*

Study: Reducing water transmission (WT) through PU membranes used in medical devices by barrier coatings is a challenge if the membrane is mechanically loaded. Applying single barrier coatings, such as silicon oxide (SiO_x) used as barrier film for polymer food packaging, leads to low reduction of WT due to its low resistance against elongation. For applications on PET, the resistance against elongation can be improved by combining organic and inorganic coatings. Accordingly, multilayer barrier coatings were applied on PU to generate a barrier coating resisting elongations up to 10 %.

Methods: Multilayer coatings consisting of inorganic SiO_x and organic $SiO_xC_yH_z$ layers were applied on 0.2 mm thick PU samples by PECVD. Water Vapor Transmission Rate (WVTR) was measured to compare the barrier properties of the coatings in dependence of layer thickness, amount of dyads and order of layer type. Samples with different coatings were uniaxially loaded up to 7 %. The samples were analyzed by Laser-Scanning-Microscopy in order to compare the cracking behavior of the coatings. After these measurements the coatings with promising results were dynamically tested in a durability tester over 3 weeks to determine the WT. The samples were dynamically loaded up to 10 % elongation. The results were compared to those of untreated samples and to those with single barrier coatings.

Results: By using multilayer coatings, WT was reduced up to 16 % compared to untreated samples and up to 12 % compared to those with single barrier coatings due to the dynamical load. The WVTR was reduced up to 71 % and 40 %, respectively. Further investigations need to be performed to determine long term behavior.

218

***In vitro* Evaluation for Impeller Configuration Selection for a Temporary Circulatory Support Device**

J. Leme, J. Fonseca, B. Utiyama, E. Drigo, T. Leão, R. Sá, G. Andrade, J. F. Biscegli, A. Andrade. *Institute Dante Pazzanese of Cardiology, São Paulo, BRAZIL.*

Study: A temporary circulatory support device (TCSD) has been developed and tested to be used as bridge to decision or bridge to recovery. Golden ratio was used to calculate TSCD's external housing and mechanical component dimensions. This study shows hydrodynamic performance and hemolysis test for TSCD's impeller selection.
Methods: Three different impeller models with different blade curvatures were created: straight blades (impeller 1), low curvature blades (impeller 2) and high curvature blades (impeller 3). A mock loop circulation system was used for hydrodynamic performance test, were pressures, flows and rotational speeds were registered. Total pressure head (ΔP) versus flow curves were generated at different rotational speeds for each impeller. A standardized closed circuit was used to evaluate hemolysis, flow was maintained at 5 L/min under ΔP of 100 mmHg. Normalized Index of Hemolysis (NIH) was calculated.
Results: Results showed similar hydrodynamic performance for low rotational speeds for all impellers. However, better hydrodynamic performance at high speeds was observed in impeller 1 and 3. Hemolysis tests showed lower NIH for impeller 3 (0.00332 ± 0.00136 g/100L), NIH was 0.03951 ± 0.03031 g/100L for impeller 1 and 0.05115 ± 0.03147 g/100L for impeller 2.Conclusion: Impeller 3 with high curvature blades showed better hydrodynamic performance and NIH than impeller 1 and 2. Therefore, impeller 3 was chosen to be used at TCSD.

221

Stretchable Electronics Conformal Skin-adherent Wearable Patches: A Novel Tool for Quantifying Human Motion

K. R. Ammann,[1] A. L. Sweedo,[1] M. J. Slepian.[2] [1]*Biomedical Engineering GIDP, University of Arizona, Tucson, AZ;* [2]*AZ Center for Accelerated Biomedical Innovation, University of Arizona, Tucson, AZ.*

Study: Human mobility is an essential life function often compromised with injury, disease progression and aging. Motion capture is an emerging tool for analyzing human movement and extremity articulation, providing quantitative information on gait and range of motion. Currently, popular motion capturing techniques rely on optical or magnetic methods, limiting the amount of equipment and processing needed to obtain accurate measurements. Here we introduce a novel wireless approach to personalized motion capture utilizing skin-adherent wearable patches incorporating stretchable electronics, accelerometers, data capture and telemetry. Wearable patches were utilized to measure and define the "motion envelope", i.e. range, volume and shape of the motion space of the upper extremity.
Methods: Skin patches (BioStamp, MC10) were applied to the arm or forearm of normal volunteers. Arms were moved over the range of normal motion using five different motion categories: 1) vertical abduction/adduction 2) horizontal abduction/adduction 3) flexion/extension 4) medial/lateral rotation 5) circumduction. Data were streamed and recorded, revealing the pattern of movement in three separate axes.
Results: Motion extent and velocity for all five movements tested were readily quantified and captured utilizing the patch constructs. Accelerometry data for vertical abduction/adduction (Figure 1a) and horizontal abduction/adduction (Figure 1b) are shown. Each of the motion categories studied had a distinct pattern with identifiable qualitative and quantitative differences. Integration of all movement categories allowed construction of a motion envelope defining and quantifying (range, volume and shape) motion of the upper extremity. Wearable conformal skin adherent patch constructs allow on-body, mobile, personalized determination of motion and flexibility parameters. This tool and method hold promise for providing motion "biomarker" data in health and disease.

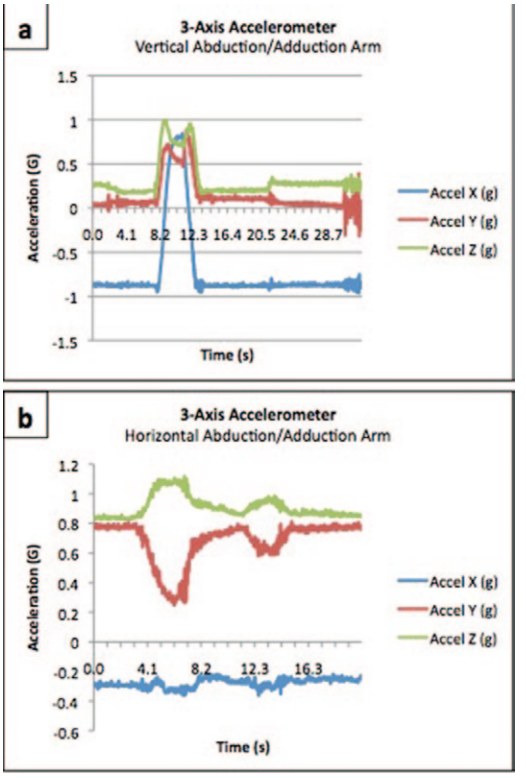

227

The Effect of Mitral Prosthesis Design and LVAD Support on Intraventricular Flow

J. Campos, R. Montes, J. Moon, K. May-Newman. *Mechanical Engineering, San Diego State University, San Diego, CA.*

Study: Some heart failure patients require implantation of a Left Ventricular Assist Device (LVAD), a mechanical pump that boosts blood flow. Often these patients have a heart valve prosthesis (HVP) due to chronic cardiovascular disease. Little is known on how these devices alter the blood flow field in the heart when combined, and the correlation to thrombus development. Our goal in this study is to quantitatively describe how the LVAD alters intraventricular flow combined with HVP.
Methods: Particle Image Velocimetry of a cardiovascular mock loop is used to measure the flow field in a silicone model of the LV supported with a HeartMate II LVAD. A porcine bioprosthetic valve (BPV) is placed in the aortic position, and a variety of HVP are tested in the mitral position including a BPV, a tilting disc valve (TDV), and a bileaflet mechanical valve (BMV). Two conditions are studied, representing low LVAD speed of 8 krpm and high LVAD speed of 11 krpm.
Results: During low speed, a portion of the flow during systole bifurcates towards the LVAD outflow at the apex. During diastole, the normal vortex pattern with the BPV starts with two counter rotating vortices. The clockwise anterior vortex grows during diastole, developing a large positive circulation and KE, while the counterclockwise posterior vortex dissipates against the LV free wall. The BMV and TDV exhibit a similar vortex pattern but lower LVAD outflow during systole when oriented towards the free wall. When the TDV is oriented toward the septum, the vortex pattern completely reverses and the LVAD outflow bifurcates from the opposite side of the LV closer to the septum rather than the free wall as observed in the BPV. With high speed, the results follow the same pattern observed for low LVAD speed but all of the flow exits through the LVAD. Additional analyses to evaluate pulsatility and areas of flow stasis will compare the efficiency of each HVP with the LVAD in order to predict the risk of thrombus formation for patients with this combination of cardiovascular medical devices.

233

Study of Coating Diamond Like Carbon in Polycarbonate for Devices Assist Circulatory

R. C. de Sá, **Sr**.[1] V. Trava Airoldi,[2] E. Drigo,[1] T. Leão,[3] J. Fonseca,[1] B. Utiyama,[1] E. Leal,[1] J. Moro,[3] A. Andrade,[1] E. Bock,[4] *[1]Centro de Engenharia em Assitência Circulatória, Instituto Dante Pazzanese de Cardiologia / Fundação Adib Jatene, São Paulo, BRAZIL; [2]Centro de Engenharia em Assitência Circulatória, Institute National for Space Research, São José dos Campos, BRAZIL; [3]Instituto Federal de São Paulo, São Paulo, BRAZIL; [4]Engenharia Mecânica, Instituto Federal de São Paulo, São Paulo, BRAZIL.*

Study: Ventricular Assist Device (VAD) are designed and developed at the Institute "Dante Pazzanese" Cardiology to assist hemodynamic stabilization of patients with severe heart failure. The circulatory support can be applied before, during and / or after corrective surgery or cardiac transplantation. As biofunctionality of a blood pump, apply appropriate and reliable biomaterials; the physical and chemical properties of these biomaterials should ensure high stiffness to resist internal pressure in pump 100 mmHg, high corrosion resistance due to the corrosion potential the blood, inert and smooth surface to prevent hemolysis and platelet aggregation and biocompatible. Surface modification techniques are applied to improve the biofunctionality of VAD's.
Methods: By the National Institute for Space Research, the Chemical Vapour Deposition technique was applied to coat a rotor of Spiral Pump® with a film the diamond like carbon (DLC). The properties chemical, physical and biological of the polycarbonate, virgin and coated with DLC, were obtained by analysis in Raman spectroscopy, wettability and surface energy by a goniometer and activated clotting time; The reológic influence of the viscous friction in polycarbonate can be compared in vitro assay by electric current consumption analysis in torque required by mechanical circulatory assistance.
Results: The amorphous carbon film on the polycarbonate can provide properties such as low coefficient of friction, greater hardness, chemical inertness, biocompatibility and antibacterial action.

234

The Investigation of Fluid Shear Stress and Subsequent Conformational Changes of Von Willebrand Factor Observed in an Optical Trap

X. J. Candela, D. Arginteanu, W. O. Hancock, P. J. Butler, K. B. Manning. *Biomedical Engineering, The Pennsylvania State University, State College, PA.*

Study: Thousands of ventricular assist devices (VADs) are implanted in patients with advanced heart failure in the U.S. each year. One complication associated with the use of these devices is the development of Acquired von Willebrand Syndrome (AVWS), a condition that arises when von Willebrand factor (vWF) fails to adequately recruit platelets and arrest bleeding. Elevated shear stresses introduced by the VADs are believed to cause the conformational change and subsequent inefficiency of the protein. Determining the threshold shear stresses necessary to induce a conformational change in the vWF protein would allow developers of cardiac prosthetic devices to avoid introducing such forces, and thus, reduce the incidence of AVWS. An experimental setup with an optical trap can be used to quantify the relationship between shear stress and the degree of conformational change observed in vWF.
Methods: VWF is extracted from human plasma, purified through column chromatography, identified using Western Blotting, and finally attached to 2 micron diameter polystyrene beads. The polystyrene beads are then fixed in place by the use of an optical trap. The stiffness of the trap is calculated and the beads' motion is tracked within a flow chamber of DPBS solution. Movement of a piezoelectric stage applies shear. Phase shift (between fluid velocity and bead motion) and bead displacement are measured for vWF-coated beads under varying shear rates of $59.57s^{-1}$, 185.23^{-1}, and 310.74^{-1}.
Results: The results show a difference in both phase shift and bead displacement between the three shearing conditions. This is presumably caused by an increase in the functional radius of the bead due to the characteristic unraveling of the vWF protein under significant amounts of shear stress. This information can be used to establish a relationship between shear rates and the associated degree of conformational change of vWF, ultimately being of use to device designers.

236

CFD Comparison of Blood Trauma in CF-VAD Under Constant and Pulse and Modulated Speed Rotation Conditions: A Numerical Study

Z. Chen, S. K. Jena, S. C. Koenig, M. S. Slaughter, Z. J. Wu. *Department of Cardiovascular and Thoracic Surgery, University of Louisville School of Medicine, Louisville, KY.*

Study: Pulse modulated rotation of continuous flow ventricular assist devices (CF-VAD) can generate pulsatile flow that may offer physiologic benefits; however, it is unclear whether pulse modulation increases the risk for blood trauma. The aim of this study was to compare the flow fields and blood damage potential of CF-LVAD during continuous and modulated rotation.
Methods: Computational fluid dynamics (CFD) was used to calculate flow in the HeartWare HVAD at constant speed and pulse modulated rotation. The pulse modulated speed varied from 2400-4000rpm at a period of 3 sec. The average speed of the pulse modulated rotation was the same as the constant speed condition. For the entire cycle length, pulsatile pressures (60 beats/min) mimicked ventricular and aortic pressures at the HVAD inlet and outlet, respectively. The wall shear stress (WSS) on rotor surface, scalar shear stress (SSS) and hemolysis within the HVAD were compared. The average hemolysis was calculated by integrating the instantaneous hemolysis at discrete time frames over the entire pulse modulated cycle.
Results: During constant speed rotation, the rotor surface WSS and the SSS distribution and velocity inside the pump varied over a small range due to the pulsatile inlet and outlet boundary conditions, while the same variables varied with high fluctuations due to transient speeds during pulse modulated rotation (Figure). The time average value of flow rate and hemolysis over the pulse modulated cycle were comparable at constant and pulse modulated speed rotation. Pulse modulated rotation may be a useful method to create physiologic pulsatility in the CF-VAD without increasing the risk for blood damage.

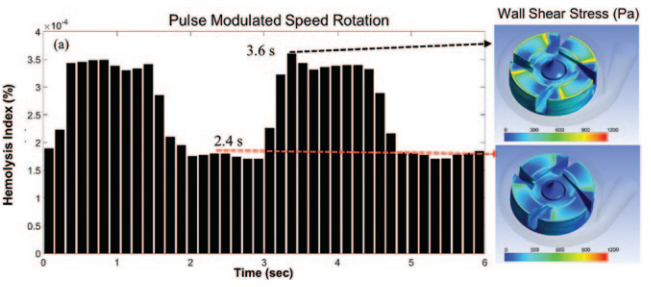

237

Physicochemical and Biological Characterization of Small Intestinal Submucosa Scaffolds for Wound Dressing Applications

V. A. Talero,[1] D. M. Narváez,[2] H. Groot,[1] R. López,[3] D. M. Tabima,[1] J. C. Briceño.[1] *[1]Biomedical Engineering, Universidad de los Andes, Bogotá, COLOMBIA; [2]Human Genetics Laboratory, School of Science, Universidad de los Andes, Bogotá, COLOMBIA; [3]School of Medicine, Universidad de los Andes, Bogotá, COLOMBIA.*

Study: Deep wounds generate tissue separation causing irregular geometry injuries, currently they cause about 9.5% of annual deaths in the world. Tissue engineering search treatments from scaffolds based on natural materials as Small Intestinal Submucosa (SIS) given its extracellular matrix-like environment. The aim of this study was to determine the influence of SIS and crosslinking agent concentration on physicochemical and biological properties of the scaffolds.
Methods: SIS scaffolds (0.5 and 1% w/v) were prepared using glutaraldehyde (GA) (0.02 and 0.2%) and (1-ethyl-3-(3-dimethylaminopropyl) carbodiimide hydrochloride) (EDC) (50 and 100 mM) as crosslinking agents. Physicochemical tests included scaffolds water uptake, pH evaluation of the aqueous environment to test stability, and bulk porosity. Kidney fibroblasts were cultured during 1, 3 and 6 days to study cells adhesion and proliferation. Adhered cells and scaffolds structure were identified using hematoxylin-eosin staining (H&E) and scanning electron microscopy (SEM).
Results: Water uptake ranged from 3000–5000%. Scaffolds crosslinked with EDC had better water uptake than GA scaffolds. All samples showed physiological pH ranges after 3 days and bulk porosity over 93%. The *in vitro* model showed fibroblasts adhesion and proliferation for all days. H&E showed limited adhesion of fibroblasts. Scaffolds crosslinked with EDC appeared to have healthier looking cells than the GA scaffolds. Generally, SIS scaffolds present an interconnectivity structure with physicochemical and biological properties in line with other biomaterials to use as wound dressing. On the other hand, *in vitro* model showed promising results in cell adhesion and proliferation. However, is necessary to perform an *in vivo* study to show the effectiveness of the biomaterial as compared to current treatments.

238

Evaluation of Ceramic Pivot Bearings of Implantable Centrifugal Blood Pump

E. Bock,[1] A. Marques,[1] J. Sousa,[1] R. Sa,[1] B. Nishida,[1] E. Drigo,[2] M. Barboza,[1] T. Leão,[1] J. Fonseca,[2] A. Andrade.[2] *[1]Federal Institute of Technology in Sao Paulo, Sao Paulo, BRAZIL; [2]Institute Dante Pazzanese of Cardiology, Sao Paulo, BRAZIL.*

Study: The Implantable Centrifugal Blood Pump (ICBP) with ceramic pivot bearings has original features for a long term Ventricular Assistance Device (VAD) such as dual impeller. The ICBP project started in 2006 at Baylor College of Medicine as part of an international and multicenter study involving Brazil and United States of America. This work presents the evaluation of ceramic pivot bearings of ICBP.
Methods: Methodology was based first in prediction of forces acting in pivot bearings by computational numerical simulations and electromechanical actuator assessment in dynamometer. Thus, a workbench was designed to mock the wear under controlled conditions like axial force in pivot bearings, rotational speed and vibration. Several bearings and rotor shafts with predefined dimensions were developed and tested. During the in vitro evaluation, it provided precise control of the contact pressure between the bearings and the rotor shaft for applying a constant force. A load cell sends an analog signal to an electronic circuit that converts this signal strength and shows it in a liquid crystal display.
Results: The results of tribological testing of pivot bearing pairs improved the selection of materials seeking greater mechanical durability for ICPB. Previously, human blood experiments were conducted for measurement of Normalized Index of Hemolysis (NIH) and pivot bearing showed good results with no trace of irregular mechanical induced trauma. The ICBP design is considered simple and robust, mechanically reliable, and safe in terms of hemolysis and hydraulically efficiency. In future, tests conjugating vibration and wear will be performed for a more accurate assessment of the friction inside the pump and its relation with possible deleterious vibrations.

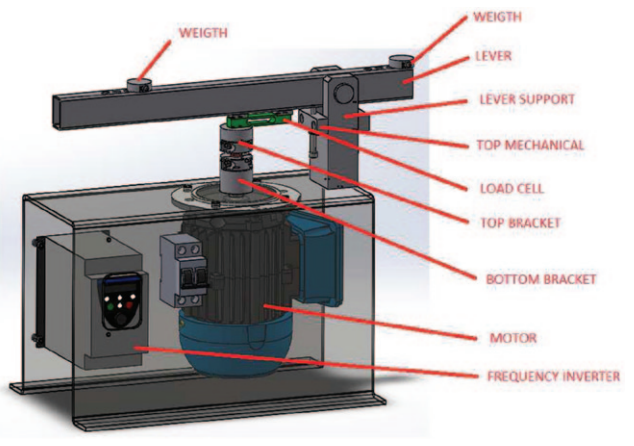

240

Wearable Sensor to Monitor Breathing Pattern

A. Arun, J. Imamura-Ching, M. Harrison, S. Roy. *Surgery, University of California San Francisco, San Francisco, CA.*

Study: Many people suffer from breathing disorder. It is estimated that 1 in 15 people suffer from obstructive sleep apnea, a disorder in which there is repeated upper airway obstruction during sleep, resulting in potentially significant adverse impacts on health and daily function. The diagnosis of breathing disorders is done by a sleep study also called polysomnography in a sleep facility. We are developing wearable sensors that can monitor breathing pattern and diagnose sleep apnea in the home setting. It will help the patient to identify the severity of his/her condition and seek immediate treatment.

Methods: The wearable apnea sensor uses a 3-axis accelerometer. We used the accelerometer MPU9150 by Invensense Inc with high sensitivity (16,384 LSB/g) and low power consumption of 3 mW. The movement of the neck muscle is correlated to the breathing pattern of the patient to indicate the occurrence of sleep apnea event. The sensor itself is encapsulated in a casing approximately 1 inch (W) x 1 inch (L) x 0.3 inch (H). It was designed to be compact so that it does not hinder the patients sleep experience. It was placed on to the patient's body using a clinical grade adhesive on top of the hyoid bone. Tests were performed with the accelerometer resting on the table (baseline measurement) and on healthy subjects without sleep apnea condition. For the bench top test the accelerometer was connected to a memory drive to store the data through electrical cable. In the next generation the sensor will communicate wirelessly to a smartphone to save the data on a HIPAA compliant database.

Results: The baseline output with the accelerometer resting on the table shown in Figure 1a. The output response is flat and represents the noise floor of the system. The result with the sensor placed on healthy patients is shown in Figure 1b. We were able to correlate the movement of the neck muscle recorded by the accelerometer with the patient breathing pattern. We will next perform a sleep study on sleep apnea patients and correlate the accelerometer data with the polysomnography data.

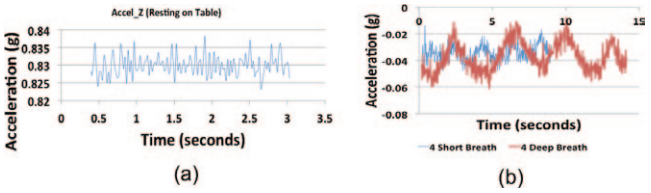

245

Hemodynamics in a Pediatric Aorta Model with Asynchronous PVAD Pumping

B. Good, K. Manning. *Biomedical Engineering, Pennsylvania State University, University Park, PA.*

Study: Penn State University is developing a pulsatile pediatric ventricular assist device (PVAD) to help the 1.35 million born annually with congenital heart disease. The PVAD is attached via an anastomotic graft to the ascending aorta but has been linked to long-term failure from intimal hyperplasia (IH). Additionally, the pulsatility generated in the aorta under bypass has been linked to organ development in pediatric patients. Previous computational work has studied these problems but assumed synchronized heart and PVAD beating. The Penn State PVAD, however, is not synchronized with the heart and begins its next systolic phase as soon as it has filled with blood. To understand the range of hemodynamics and pulsatility that can occur, asynchronous beating conditions need to be studied.

Methods: A pediatric patient's aorta model with an attached PVAD cannula is used in a computational study along with a viscoelastic blood model. Physiological pediatric heart and PVAD waveforms are initially scaled to 120 bpm and 0.5 lpm and synchronized. The PVAD waveform is then shifted 90°, 180° and 270° out of phase. Important hemodynamic parameters of vascular remodeling (wall-shear stress (WSS), time-averaged WSS (TAWSS) and oscillatory shear index (OSI)) are compared along with the pulsatility (surplus hemodynamic energy (SHE)) generated between the flow conditions.

Results: High OSI regions are prone to IH and can be seen on the toe and floor of the anastomosis (peak values of 0.44 and 0.48, respectively, in the 90° flow). Graft failure has also been linked to high WSS and TAWSS (peak values of 2360 and 528 dyne/cm^2, respectively, in the synchronized flow) at the anastomotic toe. The highest pulsatility occurs during synchronized flow and decreases with each PVAD shifted flow. The decrease in pulsatility during asynchronous pumping could lead to problems in peripheral organ development while the high OSI during asynchronous flow and high WSS and TAWSS during synchronous flow could lead to higher rates of long-term graft failure.

246

Long-term Ultrafiltration

C. F. An-Li,[1] Y. F. Qu,[1] R. F. von Gutfeld,[1] **E. F. Leonard**.[2] *[1]Chemical Engineering, Columbia University, New York, NY; [2]Columbia University, New York, NY.*

Study: Volume removal remains the bête noire of intermittent dialysis therapy and cannot be resolved intradialytically. A wearable ultrafilter could provide an interdialytic approach that could even produce approximate euvolemia. A scaled-down hollow-fiber device could serve, but only if adequate hydraulic permeability could be maintained for 48–72 hr. Long-term data from devices optimized for interdialytic volume control are not available. Here we:

Methods: 1. Provide *in-vitro* data that show, for miniature hollow-fiber devices, long-term fouling rates as a function of blood-side flowrate, ultrafiltration flux, and different combinations of fiber numbers and lengths.2. Report on several simple designs for a veno-venous flow circuit that incorporates a wearable ultrafiltration device. The circuit is designed to accommodate devices capable of removing 1–3 ml/min, steadily. Pressure drops, shear rates, transmembrane pressures, and filtration rates are reported as functions of fiber number and length and the blood-side flowrate.3. Describe a less-simple design that would allow, within the interdialytic period, one or more patient-implemented replacements of the working ultrafiltrator.

Results: Optimal performance, as seen *in vitro* depends on the combination of filter fiber length and diameter, with total areas between 500 and 70 cm^2. Long, possibly awkward fiber lengths are needed if an external flow restrictor is to be avoided. Fouling is least at high shear and blood flows greater than 10 x filtration rate. Long-term fouling remains problematical and a scheme for user introduction of fresh filtration area is described.

252

Synthesis and Physicochemical Characterization of Small Intestinal Submucosa Hydrogels for Deep Wound Regeneration

M. Pineda,[1] **J. Jaramillo**,[1] V. A. Talero,[1] O. A. Álvarez,[2] J. C. Briceno.[1] *[1]Biomedical Engineering, Universidad de los Andes, Bogota, COLOMBIA; [2]Chemical Engineering, Universidad de los Andes, Bogota, COLOMBIA.*

Study: Deep wounds cause soft tissue separation and injuries with different geometry. Current treatments only promote wound size reduction and scar formation, but cannot adapt to injury morphology, compromise tissue functionality and do not enhance regeneration. Biomaterials like Small Intestinal Submucosa (SIS), which is abundant in collagen, can promote tissue remodeling. Thus, as a solution to the problems mentioned, the aim of this study was to synthesize SIS hydrogels that can undergo gelation *in vitro* and evaluate the effect of the crosslinking agent on hydrogels physicochemical properties.

Methods: Fabrication process was standardized. SIS 30% w/w hydrogels were prepared and crosslinked using 50 and 100mM of 1-Ethyl-3-(3-dimethylaminopropyl)carbodiimide (EDC) (n=3). Functional groups were identified by Fourier Transformed Infrared Spectroscopy (FTIR). Influence of temperature on collagen structure was assessed by thermogravimetry (TG). Rheological tests were held to study gelation. Morphology was assessed by Scanning Electron Microscopy (SEM). Swelling ratio and degradation tests were performed for *in vitro* water uptake and mass loss evaluation.

Results: SIS hydrogels were successfully prepared. FTIR spectra confirmed collagen functional groups. TG showed that transition temperature of the SIS collagen between a triple helix to a random coil conformation varied from 120–130°C, while increasing EDC. Rheological tests showed a pseudoplastic behavior suggesting gels injectability and solid-like behavior (G'> G"). Increasing EDC led to a greater G'. SEM results revealed a porous interconnected structure, suitable for cell infiltration. Swelling ratio (>50%) and degradation results showed no significant difference between formulations. SIS hydrogels that could undergo gelation *in vitro,* with appropriate properties to be used as a wound healing material, were fabricated. Future work includes *in vitro* and *in vivo* biological tests.

257

Evaluation of Oxygen Solubility of Perfluorooctylbromide (pfob) Emulsions

J. Tocarruncho Luque, S. C. Navarrete, O. A. Alvarez, J. C. *Briceño. Universidad de los Andes, Bogotá, COLOMBIA.*

Study: Blood substitutes are substances that have been designed as an alternative to meet the oxygen transport function of blood. In this project, emulsions used as blood substitutes based on perfluorooctylbromide (PFOB) and egg yolk lecithin were prepared. An experimental model for measuring oxygen solubility was developed and related to Henry's Law.
Methods: Oxygen bubbling was performed using an oxygen flow of 250 mL/min adapted with a rotameter gas flow. The prototype developed to evaluate oxygen solubility was used to compare two quantitative methods: Winkler, which is a titration to measure the oxidation of dissolved oxygen, and oximetry test, that is an optical technique to measure the amount of oxygen dissolved. In addition, the effect of emulsion aging on the oxygen carrying capacity was evaluated for 42 days.
Results: Results obtained showed the ability of PFOB emulsions to be loaded with oxygen. Data results were adjusted to Henry's Law model obtaining values for the oxygen solubility constant of 0.009 ± 0.002 mL O_2/kPa dL emulsion. Results, were higher than the oxygen solubility constant for plasma and are consistent with the findings by other authors. In addition, both methods were comparable and the emulsion aging processes do not affect the oxygen solubility capacity. Based on the evidence, PFOB emulsions provide an advantage to the oxygen solubility and transport in-vitro. Further studies are required to confirm this behavior for models in-vivo.

261

Impact of Hemocompatible Coatings on Oxygen Permeability of Polydimethylsiloxane (PDMS) for Membrane Oxygenation

E. Abada,[1] A. Dharia,[2] T. Yeager,[1] W. Moses,[3] J. Park,[1] C. Blaha,[1] N. Wright,[1] B. Padilla,[3] S. Roy.[1] *[1]UCSF Department of Bioengineering and Therapeutic Sciences, University of California, San Francisco, San Francisco, CA; [2]UCSF Department of Pulmonary and Critical Care Medicine, University of California, San Francisco, San Francisco, CA; [3]UCSF Department of Surgery, University of California, San Francisco, San Francisco, CA.*

Study: Current extracorporeal membrane oxygenation (ECMO) devices are insufficiently blood compatible, leading to the need for high anticoagulation and related patient complications. Our lab has developed a highly-efficient oxygenator design for improved hemocompatibility that uses silicon microporous membranes bonded with micron-thin polydimethylsiloxane (PDMS) arranged in parallel plate geometry. The PDMS layer can be modified with hemocompatible surface coatings that decrease membrane fouling and consequently improve gas permeability during blood contact, such as polyethylene glycol (PEG) and slippery liquid-infused porous surfaces (SLIPS), but the effects on the oxygen permeability of the PDMS-silicon membranes have not been well-studied. In these investigations, we examined the effect of PEG and SLIPS on oxygen permeability of our membranes.
Methods: To measure permeability, we developed a testing system in which oxygen transport was detected in real time across the membranes from gas into water using an optical probe. For the PEG and SLIPS groups, chips were oxygen plasma-treated before coatings were applied. We measured the oxygen permeability of PDMS coated with PEG, and SLIPS on days 0 and 5 after application. Controls were unaltered PDMS and plasma-treated PDMS.
Results: Oxygen permeability results are presented in Table 1. Compared to unaltered PDMS, all surface modifications reduced permeability on day 0. Both PEG and SLIPS coatings reduced permeability equally. Measurements on day 5 revealed negligible changes in gas permeability. Continuing ex vivo and in vivo blood studies will determine if the decreased fouling characteristics of PEG and SLIPS coatings will meaningfully benefit ECMO systems.

Table 1. Oxygen Permeability of Surface Coatings on PDMS.

	Gas Permeability (mL O_2 STP/min/m^2/cmHg)	
Coating	Day 0	Day 5
Unaltered PDMS	1.25 ± 0.12	1.10 ± 0.08
Plasma PDMS	0.86 ± 0.06	0.90 ± 0.10
PEG	1.04 ± 0.09	0.98 ± 0.05
SLIPS	1.05 ± 0.09	0.99 ± 0.07

268

"Intracellular Transplant": Replacement of Native Hemoglobin with Donor Hemoglobin in Autogenic RBCs for Potential Treatment of Sickle Cell Disease

L. A. Ziegler,[1] K. B. Zougari,[2] S. E. Olia,[2] J. H. Waters,[3] M. V. Kameneva.[2] *[1]McGowan Institute for Regenerative Medicine, Pittsburgh, PA; [2]Department of Bioengineering, University of Pittsburgh, Pittsburgh, PA; [3]Department of Anesthesiology, University of Pittsburgh, Pittsburgh, PA.*

Study: Sickle-cell disease (SCD) causes abnormal shape and rigidity of red blood cells (RBCs) due to pathological hemoglobin (HbS), which results in vaso-occlusion, tissue hypoxia and many other severe and painful complications. Current long-term treatments for SCD are limited: pharmacotherapy with hydroxyurea leads to both leukopenia and thrombocytopenia while repeated blood transfusion results in alloimmunization in over 50% of patients. We proposed to replace HbS in the SCD patient's RBCs with healthy donor Hb, and return these modified RBCs to the patient. With this therapy, it is hoped that vaso-occlusion and alloimmunization will be minimized or eliminated.
Methods: Ongoing experiments are using healthy donor RBCs. To maximize endogenous Hb removal, RBCs are processed using a novel two-cycle lysing and resealing process. Lysing is achieved by an osmotic pressure gradient, and resealing is completed by a specific combination of osmotic pressure gradients and temperatures. The majority of native Hb is removed from the RBCs in the first lysing and resealing cycle. These membranes are then re-lysed and refilled with either a pure Hb solution (experimental cells) or PBS (control cells). Degree of Hb encapsulation is evaluated by measurement of total hemoglobin concentration in the modified RBCs (OSM 3 Hemoximeter).
Results: Currently, encapsulated experimental RBCs reached an intracellular Hb concentration of ~25% of that in native RBCs, compared to the ~2% original intracellular Hb leftover present in the control RBCs. Based on the obtained results, encapsulation of much higher concentrations of Hb is expected and currently under examination in on-going studies. Preliminary observations indicate that rheological and morphological properties of these modified cells are comparable to normal cells, as investigated by use of light microscope and Linkam Shearing Stage device.

274

Development of Prediction Method of Thrombus Formation on Wall by High Shear Rate on Pipe Flow Through an Orifice with Considering Transportation of Concentration

M. Tamagawa. *Graduate School of Life Science and System Engineering, Kyushu Institue of Technology, Kitakyushu, JAPAN.*

Study: To suppress the hemolysis and avoid the thrombus is very important and serious problem in developing the rotary blood pumps. In our previous studies, effects of the thrombus formation rate on wall were examined. And it was found that the thrombus formation rates increasing linearly with shear rates. To understand this relation in detail, it is necessary to establish the computational model. This investigation describes the analysis of concentration transport process of species such as activated platelet, non-activated platelets and agonists etc. on blood flows.
Methods: Using the flow filed data, the concentration of species with chemical reaction were computed by finite difference method (FDM). Especially concentration of activated platelets was predicted and the deposition of activated platelets was also predicted. In our proposed model, the activation platelets turn on when shear rate is more than threshold and concentration of related species is more than other threshold. By setting the deposition model, number of deposited activated platelets was evaluated. Computational objects are 5 types of pipe flows through an orifice, which were same geometries in our previous observation experiments of thrombus formation.
Results: The distributions of concentration of activated platelets were obtained from these computations of several orifice geometries. Fig.1 shows typical distribution of the concentration. It was found that the concentration of activated platelet is high at the front of orifice and near the reattachment point of recirculation area. By accumulating the number of deposited activated platelet on the wall, the total number history of deposition of activated platelets was obtained. The deposition rate was compared with our previous experiment of thrombus formation rate. It was found that the deposition rate increases linearly with shear rates.

Fig.1 Typical distribution of concentration on orifice flow

275

Efficacy of Subcutaneous ECG Leads for Chronic Counterpulsation Therapy

S. Carnahan,[1] S. C. Koenig,[2] M. A. Sobieski,[3] E. Schumer,[3] G. Monreal,[1] Y. Choi,[1] B. Meuris,[4] L. Tompkins,[1] M. S. Slaughter,[3] **G. A. Giridharan**.[1]
[1]Bioengineering, University of Louisville, Louisville, KY; [2]Bioengineering and Thoracic and Cardiovascular Surgery, University of Louisville, Louisville, KY; [3]Thoracic and Cardiovascular Surgery, University of Louisville, Louisville, KY; [4]SCR Inc, Louisville, KY.

Study: Counterpulsation devices (CPD) require ECG lead implantation for timing device filling and ejection with the native heart. Non-implantable leads limit the scope of CPD treatment to short-term therapy. Standard transvenous/epicardial ECG leads increase the invasiveness of therapy. To overcome these limitations, chronic subcutaneous ECG leads were developed and tested in a bovine model.
Methods: ECG waveforms from clinical-grade epicardial (control) leads and subcutaneous (test) leads were simultaneously recorded in calves for 30-days (*n*=3), 10-days (n=2), and acute (*n*=3) resulting in 833 data epochs (30-s each) for a total of 44,743 heart beats. Device triggering using R-wave detection were calculated for each lead type and compared. Additionally, the hemodynamic benefits of CPD with aortic cannulation (n=3) was compared to carotid artery (equivalent to subclavian artery cannulation in humans) cannulation (n=9) during pharmacologically-induced heart failure, hypertension, hypotension, hypovolemia and hypervolemia test conditions.
Results: The subcutaneous leads provided 97% positive predictive value and 98% sensitivity compared to the epicardial ECG leads (Figure 1). The CPD cannulated to the aorta diminished left ventricular (LV) external work (up to 5.5%), LV end diastolic (170ml vs 252ml at baseline) and end systolic volumes (98ml vs 154ml at baseline) during pharmacologically induced heart failure (HF). Aortic mean, pulse pressures, and mean coronary artery flow were augmented by up to 28mmHg, 7.8%, and 31.5%, respectively. Similar trends were observed for all other test conditions. These findings demonstrate the feasibility of chronic use of subcutaneous EKG leads for CPD timing. The hemodynamic efficacy of the CPD cannulated to the aorta is equivalent or better than subclavian artery cannulation, which may increase the scope of CPD patient population.

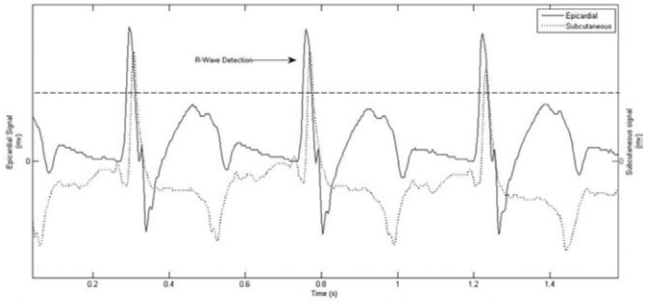

Figure 1: Comparison of subcutaneous (dashed line) ECG demonstrated a 97% positive predictive value and 98% sensitivity for counterpulsation timing compared to epicardial (solid line) ECG leads.

277

Modeling of Thrombus Formation in the LVAD-assisted Left Ventricle

B. Herold, C. Reider, K. May-Newman. *Bioengineering, San Diego State University, San Diego, CA.*

Study: Left ventricular assist devices (LVAD) can be used in some cases to treat heart failure in the absence of an available heart transplant. However, there are a series of adverse events associated with these devices, one of which is the risk of clotting, or thrombosis. This study aims to model thrombosis in the left ventricle using data obtained during a previous study via particle image velocimetry (PIV) of a mock cardiac loop. Our previous study, based on clinical data, showed that a small simulated clot, or thrombus, near the left ventricular outflow tract disrupted the normal fluid flow in the ventricle and created a region of stasis distal to the thrombus. This disruption increased both with higher LVAD support and larger thrombus.
Methods: The goal of the current study is to refine the time-varying velocity field data and process it using a Lagrangian Coherent Structure (LCS) approach via calculating finite-time Lyapunov exponent (FTLE) fields. These calculations are implemented in a combination of Python, C, and Matlab. LCS are structures within a fluid that have little to no fluid transport across them and maximize shear force in the region. These LCS can give insight into areas of maximum shear force and residence time of blood in the left ventricle, both of which are related to platelet activation and clotting.
Results: Preliminary results suggest a large LCS proximal to the clot, which would suggest that platelets are activated along this LCS. This LCS further suggests that distal to the thrombus is an area of high residence time. If these activated platelets were to get trapped on the other side of the LCS, they would be in a region of stasis, promoting platelet aggregation and thrombus growth.These results suggest a mechanism by which the thrombus in the clinical data inspiring this study may have grown.

282

Characterization of AV Tissue Biomechanics During LVAD Support and Implementation in a Bioreactor Design

K. May-Newman, X. Wang, M. Jamal. *Bioengineering, San Diego State University, San Diego, CA.*

Study: LVAD support has been linked to the development of aortic incompetence (AI), which develops in 25% of HeartMate II recipients within 12–18 months of implantation. We hypothesize that AI is the result of remodeling initiated by the altered loading produced during LVAD support. Our goal is to investigate the underlying mechanism of this problem using a tissue engineering approach, but first we require an accurate description of the stretch and shear stress changes to the AV produced by LVAD support, which we have investigated using a combination of experimental and computational models.
Methods: Measurements of valve stretch and opening area were performed of a porcine bioprosthesis in a mock circulatory loop that included a HeartMate II LVAD. Pressure and flow were measured during baseline and LVAD support conditions, and images recorded for measurement of valve opening area and stretch. An estimate of leaflet shear stress during peak flow conditions was made by combining valve biomechanics data with a CFD model developed in ANSYS. The 3D model geometry was prescribed to match the opening area measurements. A quasi-static analysis was assumed that corresponds to the point of maximum flow through the AV. Peak and average wall shear stress were calculated for each condition.
Results: The average AV tissue stretch cycles from 0 to 8% during the cardiac cycle under baseline conditions. As LVAD support increases, the duration of low strain decreases, and the magnitude increases, resulting in an overall increase in average, but not maximum, stretch to the tissue. The model shows that maximum shear stress decreases as LVAD support increases, in addition to being applied for a shorter duration. A bioreactor designed by SDSU students to study the effect of stretch and shear changes on valve cells has been validated for this range of stretch and shear and will be used to investigate the immediate response of valve tissue cells to altered loading.

284

Design, Testing, and Optimization of a Novel, Implantable RVAD

J. R. Stanfield,[1] T. A. Snyder,[2] J. Wu,[3] P. Coghill,[4] R. Wampler,[5] J. W. Long.[6] *[1]Mechanical Engineering, University of Utah, Salt Lake City, UT; [2]INTEGRIS Health, Oklahoma City, OK; [3]Advanced Design Optimization, Irvine, CA; [4]VADovations, Oklahoma City, OK; [5]Surgery, Oregon Health Sciences University, Portland, OR; [6]INTEGRIS Advanced Cardiac Care, INTEGRIS Health, Oklahoma City, OK.*

Study: Despite significant need, there are no implantable, durable Right Ventricular Assist Devices (RVADs) in the clinical marketplace that were designed specifically for Right Ventricular (RV) support. We report on the development of a miniaturized, implantable RVAD addressing challenges unique to right-sided support, incorporating a core blood pump designed for affordability and hemocompatibility.
Methods: The blood flow path of the miniaturized pump includes a rotating impeller, vaned diffuser, and unique radial inlet configuration within a 7mm hydraulic diameter. With an "inline pump" configuration, the motor and bearings are separated from the rotor, affording higher flows relative to pump diameter. Rotor suspension was achieved with a combination of hydrodynamic bearings and passive magnetics. RVAD blade geometry was optimized with computational fluid dynamics (CFD) to maximize hydrodynamic and hemocompatibility performance. Particle image velocimetry (PIV), mock circulation loops, durability testing, computational anatomic fit, and hemocompatibility testing were used to evaluate the design.
Results: CFD optimization returned a bladed geometry producing 3 L/min flow and 40 mmHg differential pressure at 15000 rpm with 35% hydraulic efficiency and normalized index of hemolysis (NIH) at .0023 g/100L. PIV showed a maximum residence time of 950 ns. Mock loop testing confirmed performance across a wide flow range, including enhanced pressure-sensitivity and peak flow of 6 L/min at 25000 rpm. Durability testing showed no signs of chronic wear or degradation at 6 months. Anatomic studies identified optimal implantation sites in the RV for both surgical and less-invasive approaches. Average in vitro hemolysis was .4 g/day, and in vivo plasma free hemoglobin was <5 mg/dL. Anatomic positioning, hemocompatibility, and hydrodynamic performance of the implantable RVAD were tested in acute and chronic ovine studies, indicating that the first implantable RVAD may be nearing readiness for clinical use.

287

The Modified Mechanical Fragility Index: A New Tool for Clinical Measurement of Red Blood Cell Mechanical Fragility

L. A. Ziegler,[1] S. E. Olia,[2] M. V. Kameneva.[2] [1]*McGowan Institute for Regenerative Medicine, Pittsburgh, PA;* [2]*Department of Bioengineering, University of Pittsburgh, Pittsburgh, PA.*

Study: Red blood cell (RBC) susceptibility to mechanically induced hemolysis, or RBC mechanical fragility (MF), is an important parameter in the characterization of erythrocyte membrane health. The rocker bead test and associated calculated mechanical fragility index (MFI) has proven to be a simple and reliable method for MF measurement. While we have recently made progress towards making the rocker bead test clinically applicable by reducing the blood volume requirements from 15.5 ml to 6.5 ml, the MFI produces hematocrit (Ht) dependent results, making direct measurement of blood from patients impossible. In the interest of applying the reduced volume rocker bead test in the clinic, we have developed the modified mechanical fragility index (MMFI), which is the equivalent of MFI at 'standard' Ht (40%).

Methods: The small volume rocker bead test utilizes 3.0 ml plastic collection tubes containing 2.0 ml of whole blood each. Two experimental tubes contain three 1/8" stainless steel beads while one control tube does not, and all tubes were rocked using a platform mixer (18 cycles/min ±17° from horizontal) for one hour. MFI was calculated as a function of total hemoglobin and the difference in free hemoglobin between experimental and control tubes. Four human donor blood units were measured (n=96) at hematocrits between 25–50%.

Results: A strong non-linear relationship was observed between sample Ht and the resultant MFI. After linearization, multivariate linear regression analysis yielded a highly correlated fit (r=0.965). The developed correction factor accurately predicted (R^2=0.923) MFI at 40% Ht from native hematocrit (**Figure 1**). With the MMFI equation, the small-volume rocker bead test may be used to compare blood samples between 25–50% Ht without normalizing for hematocrit.

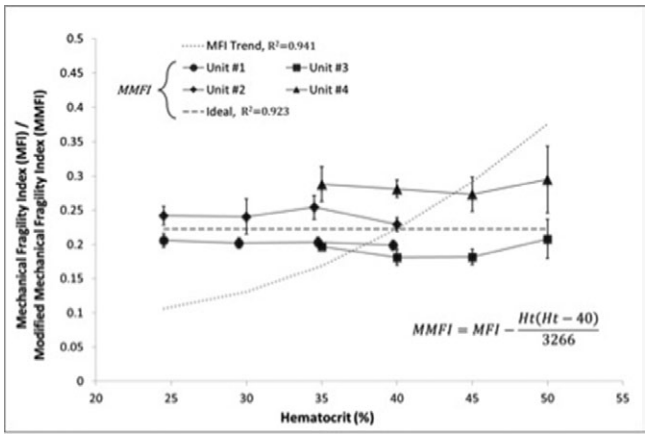

9

The Prognostic Utility of Brain Natriuretic Peptide in Patients with Left Ventricular Assist Device Implantation

G. Yost, B. Kyi, **G. Bhat**, A. Tatooles. *Center for Heart Transplant and Assist Devices, Advocate Christ Medical Center, Oak Lawn, IL.*

Study: Brain natriuretic peptide (BNP) is a cardiac neurohormone which is known to correlate with left ventricular dilation, decreased contractility, and increased stiffness. Consequently, BNP has been used to assess the degree of LV unloading for patients supported by continuous flow left ventricular assist devices (LVADs). We assessed the prognostic value of changes in BNP in the 2 weeks following LVAD implantation.
Methods: This retrospective study analyzed the laboratory findings and outcomes of 290 patients implanted with LVADs between 2005–2013. Patients were separated into two groups based on whether their serum BNP levels had improved from preoperative levels by postoperative day 14. Patients in group 1 had improvement in BNP levels, while patients in group 2 had no improvement or worsening in BNP.
Results: Average age was 59.5 ± 13.8 years in group 1 and 60.8 ± 11.2 years in group 2. There were no significant differences between the groups in age, gender, race, body mass index, or comorbidities. Group 1 had preoperative BNP 1125 ± 1078.3 pg/dL and postoperative BNP 440.2 ± 267.7 pg/dL (BNP= -693.09 ± 942.4 pg/dL), while group 2 had preoperative BNP 346.0 ± 309.1 pg/dL and postoperative BNP 631.57 ± 483.4 pg/dL (BNP= 289.32 ± 329.7 pg/dL). Despite significant decreases in BNP after LVAD implantation, postoperative survival in group 1 was significantly worse than in group 2 (Figure 1). This is presumably a result of worsened preoperative cardiac status causing elevated BNPs in these patients. Rates of right ventricular failure (RVF) were significantly higher in group 2, however (group 1: 39%, group 2: 52.7%, p=0.01). These results support the findings of previous work which indicate that elevated preoperative BNP is a risk factor for mortality in LVAD patients, but also suggests that lack of postoperative improvement in BNP may be related to the development of RVF. In these LVAD patients unchanged or worsened BNP may be indicative of continued right ventricular decompensation.

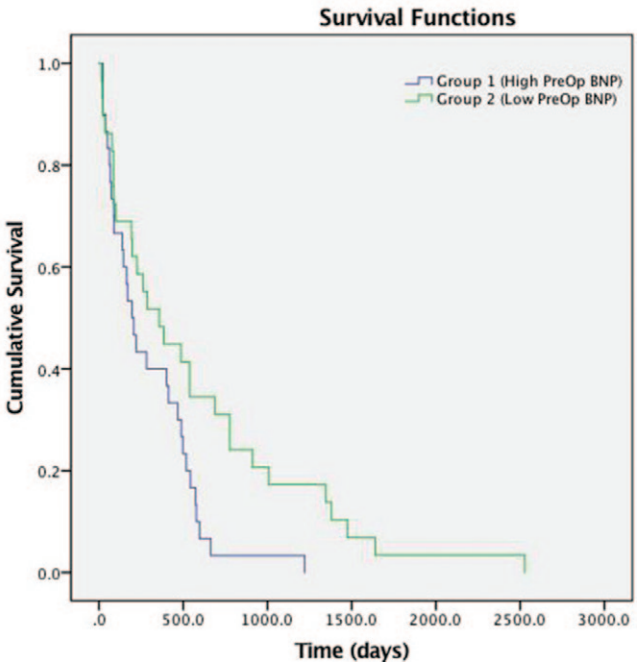

10

Infections After Total Artificial Heart Implantation

A. S. Cabasa,[1] D. L. Joyce,[1] S. Maltais,[1] J. M. Stulak,[1] L. D. Joyce,[1] K. S. King,[2] R. R. Razonable.[3] *[1]Division of Cardiovascular Surgery, Mayo Clinic, Rochester, MN; [2]Division of Biomedical Statistics and Informatics, Mayo Clinic, Rochester, MN; [3]Division of Infectious Diseases, Mayo Clinic, Rochester, MN.*

Study: Despite advancements in the peri-operative management after implantation of mechanical circulatory devices as bridge-to-transplantation, infection remains a substantial concern. We reviewed the epidemiology of infections following total artificial heart (TAH) implantation.
Methods: Clinical records of patients who received TAH for end-stage heart disease (ESHD) in 2010 to 2015 were reviewed. Continuous variables were expressed as mean ± standard deviation, while categorical data were expressed as percentage. Survival rates were estimated using Kaplan-Meier method.
Results: Fourteen patients received TAH (mean age 57 ± 6.2 years, range 42–63, 100% males), most commonly for non-ischemic dilated cardiomyopathy (7 of 14, 50%). Twenty-four counts of post TAH implantation infections (19 culture proven, 5 presumed) occurred in 9 of the 14 patients (64%). Majority (15 of 24, 63%) of infections occurred ≥30 days after device implantation. Central vascular access is the most common site of infections (6 of 24, 25%). Infection of the sternotomy wound and the driveline occurred only in 3 of the 24 infections (13%). Those who developed infections had a longer surgery time (7.9 ± 1.8 versus 6.9 ± 1.6 hours for those with and without infection, respectively). The 1 year survival probability in our series was 64.5%. Five out of the six patients who did not receive heart transplantation died within nine months and had a mean survival time of 5.4 ± 2.6 months while on TAH support.
Conclusion: Infections are common among TAH patients. Central vascular access was the most common site of infection post implantation. Our findings support the need for more stringent protocols on handling patient on mechanical circulatory support while on the transplant list.

Data summaries of Postoperative Infection

Variable	Overall (N=24)
Perioperative Infection (w/in 30 days), n (%)	
. No	15 (63%)
. Yes	9 (38%)
Culture Proven, n (%)	
. No	5 (21%)
. Yes	19 (79%)
Culture_study, n (%)	
. Blood	5 (21%)
. Sputum	5 (21%)
. Sternotomy site	1 (4%)
. Driveline site	2 (8%)
. PICC line tip	3 (13%)
. Arterial line	1 (4%)
. HD cath	2 (8%)
. Presumed infection	5 (21%)
Site of Culture, n (%)	
. Central line infection	6 (25%)
. Bacteremia	5 (21%)
. Respiratory	5 (21%)
. Operative site	3 (13%)
. Presumed	5 (21%)

12

The Tale the Controller Tells: Identifying Cause of Death Based on Controller History

S. V. Witthoefft. *Seton Heart Specialty Care and Transplant Center, Austin, TX.*

Study: An LVAD patient with past medical history of ischemic cardiomyopathy, repeated gastrointestinal bleeding with blood transfusions, recent iliac thrombosis with embolectomy, ICD shocks for ventricular tachycardia, and subtherapeutic INR, was pronounced dead in the ER following an unwitnessed cardiac arrest at a skilled nursing facility. At that time, we found that the driveline was not fully inserted into the controller and the controller was in sleep mode.
Methods: A root-cause analysis of the code was done to determine the cause of death. The family declined autopsy, so medical record review was utilized. Additionally, the controller was thoroughly interrogated and log files were sent to the manufacturer for analysis. We worked closely with the manufacturer's Biomedical Engineer to further review the data. We found that frequent low flow alarms, coupled with a significant drop in pump power, occurred for several hours before the patient was found unresponsive. These low flow alarms may not have lasted long enough to generate an audible alarm, but the SNF and EMS medical records did reflect at least one audible alarm during the code. Neither source mentioned who disconnected the controller and placed it in sleep mode or why, and the backup controller history showed that it was never connected to the patient.
Results: In the context of the clinical circumstances, the controller data is strongly suggestive of an inflow cannula thrombus causing a partial obstruction of flow through the pump; however, human error was undoubtedly an additional factor. If the controller had not been inappropriately disconnected, the patient may have arrived in the ER alive and undergone pump exchange. In conclusion, thorough interrogation of the controller and careful analysis of its data proved extremely helpful in the root-cause analysis of this complex and confusing case. It should be considered a valuable tool when attempting to discern a patient's cause of death, especially when circumstances are unclear.

14

tPA Titration to Waveform Analysis: Successful Fibrinolysis After Acute HeartWare LVAD Pump Thrombosis-case Study

L. L. Staley, L. Schroedl, D. E. Steidley, O. Pajaro. *Cardiothoracic Sugery, Mayo Clinic Hospital, Phoenix, AZ.*

Study: Pump thrombosis (PT) continues to be a problem in LVAD patients. Some patients progress to severe hemolysis and require pump exchange (PX) but may be poor candidates for PX.
Results: Suspected PT can be detected with LDH, clinical symptoms, and waveform analysis. This may allow for more rapid administration of tPA with beneficial results. Discontinuing tPA during infusion based on waveform analysis may help minimize the risk of hemorrhagic complications from fibrinolytic therapy.

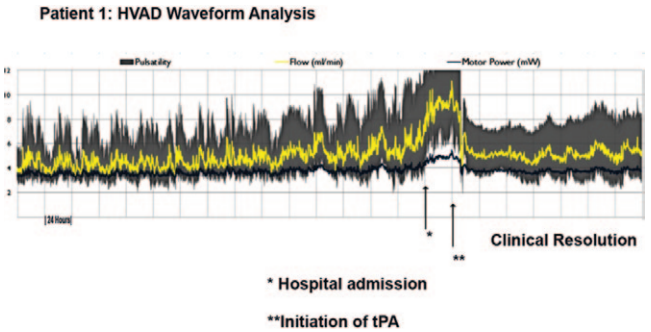

16

Beta Blockade Induced Heart Failure Provides a Model for Assessing Cardiac Support

B. A. Schmitt,[1] Y. Zhou,[1] S. A. Kerns,[2] L. J. Prochaska,[3] D. B. Reynolds,[4] M. P. Anstadt.[5] *[1]Biomedical Sciences PhD Program, Wright State University, Dayton, OH; [2]Department of Pharmacology and Toxicology, Wright State University, Dayton, OH; [3]Department of Biochemistry and Molecular Biology, Wright State University, Dayton, OH; [4]Department of Biomedical, Industrial and Human Factors Engineering, Wright State University, Dayton, OH; [5]Department of Surgery, Wright State University, Dayton, OH.*

Study: Beta-adrenergic blockade (BB) induced heart failure (HF) has been suggested as a means to assess the efficacy of circulatory support (CS) devices. However this model has not been well described and questions regarding its clinical relevance remain. The purpose of this study was to characterize acute effects of BB HF and establish its utility and relevance in assessing CS.
Methods: New Zealand white rabbits (n = 27) were anesthetized and instrumented for hemodynamics and transesophageal ultrasound imaging. Esmolol, a short-acting BB, was titrated to achieve HF cardiac outputs (50–60% baseline). Phenylephrine was used to preserve mean arterial pressures of 50–60 mmHg. HF was maintained for 30 (n = 5), 60 (n = 6), 120 (n = 11), and 180 (n = 5) mins. Animals were recovered for 30 mins and further assessed. LV tissue was assayed for proapoptotic and molecular stress indicators. Results were compared between groups using one-way ANOVA analysis.
Results:

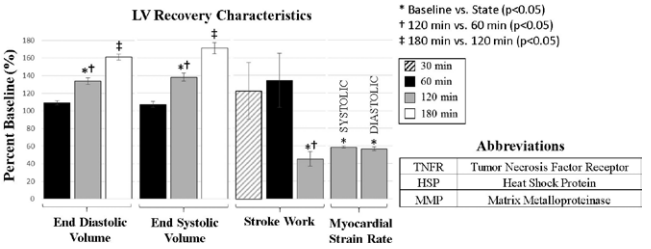

LV TNFR, HSP-70, Caspases 8 and 9, and MMP-9 progressively increased after 30 mins BB HF. Significant LV dilation and reductions in both stroke work and myocardial strain were observed following 60 mins HF (see figure). Recovery was relatively hyperdynamic after 1 hour and became significantly reduced with increasing duration of HF. Notably there were no acute effects on myocardial viability, which are important when evaluating potentially derogatory effects of CS devices. BB HF produces uniform cardiac dysfunction, controlled degrees of HF, and limits confounding variables such as ischemic injury when compared to other acute HF models. This study demonstrates that acute BB HF models clinically-relevant changes in LV function, morphology, and proapoptotic signaling useful for testing CS devices.

19

The Prognostic Nutrition Index is Predictive of Length of Stay Following Left Ventricular Assist Device Implantation

G. L. Yost,[1] A. Tatooles,[1] **G. Bhat**.[2] *[1]Heart Institute, Advocate Christ Medical Center, Oak Lawn, IL; [2]Center for Heart Transplant and Assist Devices, Advocate Christ Medical Center, Oak Lawn, IL.*

Study: The prognostic nutritional index (PNI) is a simple metric which utilizes serum albumin and total lymphocyte count to provide a basic indicator for nutritional status. It has recently garnered attention as a prognosticator of poor outcomes in many types of cancer including colorectal, T-cell lymphoma, hepatocellular, and others. We investigated the utility of the PNI as a prognostic marker for poor outcomes following left ventricular assist device (LVAD) implantation.
Methods: 288 consecutive patients implanted with continuous flow LVADs at our institution between 2005–2013 were included in this retrospective study. Laboratory, demographic, and outcomes data were collected. PNI was calculated for all patients (PNI= 10 x serum albumin (g/dL) + 0.005 x total lymphocytes (1000/mcL)). The population was split into two groups based on median PNI; group 1 with PNI < 30, and group 2 with PNI ≥ 30. Groups were compared using independent-samples T-tests, chi-squared analysis, and Kaplan-Meier survival analysis.
Results: Mean age was 60.3 years in group 1 and 59.8 years in group 2. Mean PNI was significantly different between groups 1 and 2 (26.0 ± 2.9 vs. 33.2 ± 2.8, $p<0.001$), indicating worse malnutrition in group 1. There were no significant differences between groups in terms of age, gender, race, or comorbidities. The mean PNI for the group as a whole was 30.1 ± 4.6, indicating pervasive malnutrition in this group of advanced heart failure patients. Group 1 had significantly longer postoperative length of stay than did group 2 ($p= 0.003$, Figure 1). Patients in group 1 also had higher rates of right ventricular failure (37.8% vs. 25.5%, $p=0.025$). Our results suggest the PNI may be an indicator for worsened outcomes in patients with advanced heart failure. These patients, who often suffer from chronic malnutrition, may experience worsened outcomes due to associated neurohormonal, muscular, and metabolic derangements.

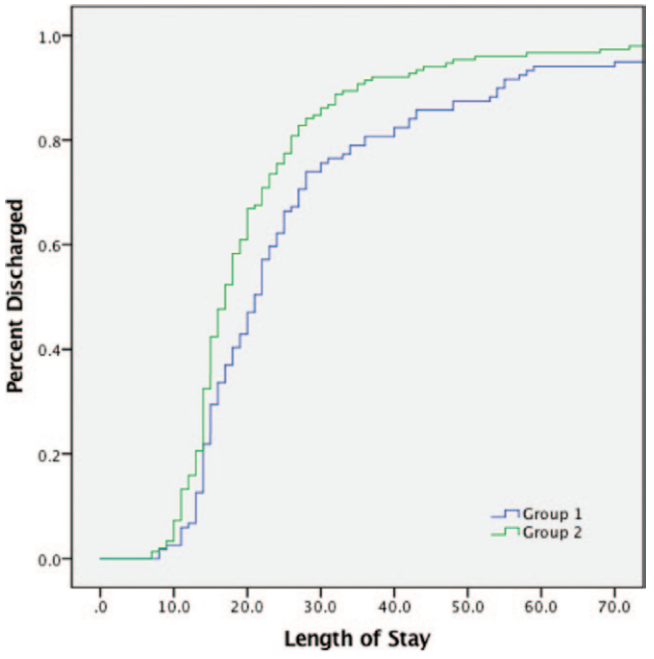

21

Neurocognitive Impairment Associated with Discordant Upper-lower Body Oxygenation or North-South Syndrome After Bailout Extracorporeal Membrane Oxygenator Support for Post-cardiotomy Shock

J. C. Mendez,[1] R. Malyala,[1] T. Chameogeorgakis,[1] S. A. Hall,[1] G. Patankar,[2] A. Bindra,[1] G. V. Gonzalez-Stawinski.[1] *[1]Simmons Transplant Institute, Baylor University Medical Center, Dallas, TX; [2]Baylor University Medical Center, Dallas, TX.*

Study: North-South Syndrome, (N-SS) is a physiological state associated with peripheral veno-arterial extracorporeal membrane oxygenator support, (pVA-ECMO), occurring when poorly-oxygenated blood from a recovering native circulation intermixes in the distal aortic arch with well-oxygenated blood advancing retrogradely from pVA-ECMO circulation. Consequently, upper-body arterial hypoxemia, (UBAH), ensues while the lower-body receives well-oxygenated blood. Neurocognitive impairment, (NI), resulting from discordant UABH is not described in the literature. We describe herein a case report of NI occurring in the absence of stroke or asystolic arrest:
Methods: 63-year-old man presents elsewhere with a myocardial infarction and cardiogenic shock. Coronary angiography revealed proximal LAD occlusion and multivessel disease. Percutaneous intervention proved unsuccessful and urgent bypass completed. By post-op day 2 pVA-ECMO bailout was required for refractory hypoxemia and shock. Tertiary-care referral occurred on post-op day 4, where UABH was recognized and the arterial pVA-ECMO limb repositioned from the femoral to right axillary site resolving UBAH. Multi-organ system failure ensued and a protracted post-op course followed. Cardiopulmonary function recovered allowing pVA-ECMO separation. Upon metabolic parameter normalization and neuroleptic withdrawal, serial Folstein Test, (FT), were completed beginning on post-op day 30. FT scores were <19 reflecting NI; assessed as hypoxemic, given no focal deficits and negative serial CNS imaging.
Results: Neurological injuries associated with p-VA-ECMO are invariably described as acute vascular events. To our knowledge this is the first case report of NI associated with UBAH or N-SS.

27

Hemodynamic Evaluation of Ventricular Support Using the Axial Flow Blood Pump Placed at Descending Aorta

E. Okamoto,[1] T. Yano,[2] Y. Shiraishi,[3] H. Miura,[3] T. Yambe,[3] Y. Mitamura.[1] *[1]Graduate School of Science and Engineering, Tokai University, Sapporo, JAPAN; [2]Faculty of Systems Science and Technology, Akita Prefectural University, Yurihonjo, JAPAN; [3]Institute of Development Aging and Cancer, Tohoku University, Sendai, JAPAN.*

Study: We have been advocated an axial flow blood pump called "valvo pump"that is implanted at aortic valve position. The valvo pump is unique because it is connected in series with a natural heart. In this study, we investigated hemodynamics under cardiac support using the current model of the valvo pump (valvo pump 2) connecting in series with the natural heart in in vivo.
Methods: The axial flow blood pump (diameter of 33 mm, length of 52 mm,anatomical occupation length of 33 mm) was anastomosed the descending aorta of the anesthetized goat (female, 43 kg) with PTFE cuffs. We measured systemic blood flow at inflow port of the pump, cerebral blood flow at left common carotid artery and coronary blood flow at left anterior descending artery.
Results: With increase in impeller rotational speed from 0 to 8000 rpm, aortic pressure at output port of the pump rose and systemic blood flow increased from 4 L/min to 6.7 L/min, and pulsatility of the blood flow was preserved regardless of increase of pump output. However cerebral blood flow decreased by 30%, also coronary blood flow decreased by 30%.The axial flow blood pump connected in series with a natural heart was able to achieve superior support blood supply to organs because of preserving pulsatilities of systemic blood flow regardless of increase of pump outflow. However cerebral blood flow and coronary blood flow decreased depending of pump output. In conclusion, the aortic valve position is best for implantation of the axial flow blood pump in series with a natural heart to increase not only systemic blood flow but also cerebral and coronary blood flow. Now we have been developing a new ultra-miniature axial flow blood pump that can be implanted at the aortic valve position.

34

Evaluation of Hemodynamics and Cardiac Metabolism Under LVAD Support with Aortic Valve Regurgitation in Acute Animal Experiments

K. Iizuka, N. Naito, H. Sumikura, T. Mizuno, T. Tsukiya, Y. Takewa, E. Tatsumi. *Department of Artificial Organs, National Cerebral and Cardiovascular Center, Osaka, JAPAN.*

Study: Aortic valve regurgitation (AR) is a serious complication under left ventricular assist device (LVAD) support. But change of hemodynamics and cardiac metabolism under LVAD support with AR is not clarified enough. We made animal model of LVAD with AR, and investigated change of hemodynamics and cardiac metabolism under LVAD support with AR in acute animal experiments.
Methods: 6 goats (53 ± 11kg) were investigated. Centrifugal type LVAD, EVAHEART implantation was performed with inserting inflow cannula to the left ventricular apex and suturing outflow graft to the descending Aorta. The AR model was established by placing a vena cava filter in the aortic valve. Aortic pressure (AoP), left ventricular pressure (LVP), LVAD pump flow, pulmonary artery flow (PAF), descending aortic flow (DAF) and coronary artery flow (CoF) were recorded as well as myocardial oxygen consumption (VO2), oxygen delivery (DO2), and oxygen extraction ratio (O2ER = VO2/DO2). We evaluated these value with changing pump rotation speed and controlling AR. AR+ was defined Sellers classification 3 or more.
Results: Though PAF and DAF didn't increase with increasing pump rotation speed, LVAD pump flow increased over systemic flow in AR+. It was considered that increasing pump rotation speed lead to increasing LVAD-left ventricular recirculation via AR and didn't contribute effective systemic circulation.Comparing AR+ and AR-, mean AoP was lower in AR+. LVP decreased with increasing pump rotation speed, but this decreasing tendency was weaker in AR+ than AR-. CoF was lower in AR+ than AR-, and this tendency became more marked with increasing pump rotation speed. O2ER in AR- decreased with increasing pump rotation speed, but O2ER in AR+ increased. These findings meant that AR caused disturbing cardiac assistance of LVAD support.

43

Endothelial Cell Glycocalyx Modulates Shear-induced Tubule Formation

P. Zhao, X. Liu, X. Deng. *School of Biological Science&Medical Engineering, Beihang University, Beijing, CHINA.*

Study: Vascular endothelial cells (ECs) are subjected to sustained mechanical stimuli, which play an important role in the homeostasis of circulatory system. It is well documented that blood flow induced shear stress may modulate the ECs sprouting and hence affect their angiogenic potential. However, the mechanism is still unclear. Glycocalyx is a bush like structure coating the luminal surface of vascular endothelium. Recent studies have shown that the endothelial glycocalyx acts as a mechanotransducer which implicated in fluid shear stress transmission and transduction. We believe that endothelial glycocalyx mediated mechanotransduction may be responsible for the mechanical simulated ECs angiogenesis.
Methods: A parallel plate flow chamber was employed to expose human umbilical vascular endothelial cells (HUVECs) monolayers to a physiological level of shear stress (15 dyn/cm^2) for 24 hours. Heparinase II (Hep. II) was applied to selectively degrade heparan sulfate on the ECs surface. Then, cells were used in Matrigel tubule formation assay and total tubule length was compared among the following four groups of cells: 1) untreated with no flow, 2) Hep.II treatment with no flow, 3) untreated with flow of 15 dyn/cm^2 exposure, and 4) Hep.II treatment with flow of 15 dyn/cm^2 exposure.
Results: Tubule formation was observed using a phase contrast microscope at 5x magnification and total tubule length was quantified using AngioTool. Results show that flow-induced shear stress significantly suppressed endothelial tubule formation in cells without Hep.II treatment, whereas the suppression was reduced in sheared, enzyme treated cells. No difference of total tubule length was found between enzyme treated and untreated cells in static state.

44

Mechanical Hemolysis Testing Across the Full Operating Range of a Centrifugal Blood Pump Model

L. Herbertson,[1] A. Paraloglou,[1] S. Day,[2] R. Malinauskas.[1]. *[1]Center for Devices and Radiological Health, U.S. Food & Drug Administration, Silver Spring, MD; [2]Department of Mechanical Engineering, Rochester Institute of Technology, Rochester, NY.*

Study: As part of an FDA initiative to provide experimental data to support the development of computational simulations in the safety evaluation of blood-contacting medical devices, a blood pump model was designed to be suitable for both hemolysis testing and particle image velocimetry (PIV) analysis. The housing and rotor of the centrifugal pump were fabricated out of polished clear acrylic for flow visualization, and to observe removal of bubbles from the pump prior to use with blood. The blood pump model is mechanically driven by a brushless motor and contains a mechanical shaft seal, which was developed through a series of experiments to limit seal-related hemolysis.
Methods: Mechanical hemolysis caused by the pump model was assessed over its entire operating range, and, as typically seen in regulatory submissions, testing was performed in parallel with a commercially available clinical pump. Critical dimensions of the pump model, such as the impeller blades, rotor to housing clearance gap, and outflow cut-water, along with the operating conditions, were controlled to determine if elevated, differentiable levels of flow-related blood damage could be obtained. All testing was performed for two hours using ACDA-anticoagulated, abattoir-derived porcine blood at 25°C and an adjusted hematocrit of 36%.
Results: To avoid complications from cavitation, limited motor performance, and non-pump related hemolysis, the useful operating range of this dynamic hemolysis model was determined to be from 2.5–7 L/min over a pump speed range of 2500–3500 rpm. As expected, the blood pump model was able to cause significantly more hemolysis than the commercial blood pump. Overall, this parametric study provided insight into which pump characteristics are critical to pump performance and how to better characterize flow-related hemolysis over the entire device operating range in a bench setting.

47

Heartmate II Inflow and Outflow Modifications to Augment Caval and Pulmonary Arterial Blood Flow: Implications for the Mechanical Circulatory Support of a Failing Fontan

M. Swartz, L. DiVincinti, R. Westcott, W. Harris, K. Smith, F. Gensini, G. M. Alfieris. *University of Rochester, Rochester, NY.*

Study: There are minimal circulatory support options for patients with a failing Fontan. The Heartmate II (HMII) left ventricular assist device (LVAD) in its packaged state cannot augment the caval/pulmonary arterial blood flow. We hypothesized that a modified HMII pump could augment caval and pulmonary arterial blood flow.
Methods: A bifurcated ringed gortex graft was sewn to the HMII inflow, and the outflow graft transected and tapered from 16 to 8 mm in diameter. In three sheep (50 kg, BSA-1.0m^2) the inflow and outflow grafts were anastomosed end-to-side to both cava and the pulmonary artery. Following baseline measurements, the speed of the HMII was increased by 400 RPM increments to achieve the optimal hemodynamics.
Results: With the grafts connected, and the pump off, there was 480 ± 309 cc/min of retrograde flow from the pulmonary artery into the cava. When the pump speed was increased, in all cases, optimal hemodynamics were obtained at 8,000 RPM's. Compared to baseline, there was no difference in mean arterial, central venous, or pulmonary arterial pressure once 8,000 RPM's was achieved. However, from baseline to 8,000 RPM's there was a decrease in right ventricular diastolic diameter (3.1 ± 0.1 vs. 1.8 ± 0.2 cm, R=0.6, p=0.02) and pulmonary arterial pulse pressure (8.5 ± 2.1 vs. 2.1 ± 2.9 mmHg, p=0.01) further demonstrating an absence of flow through the right ventricle. Similarly, as pump speed increased there was a corresponding increase in pump flow and power, with a decrease in pulsatility index. Maintenance of support at 8.000 RPM's for 4 consecutive hours demonstrated no suction events or significant changes in hemodynamics, flow, power, or pulsatility index. This suggests that the HMII may be modified to provide circulatory support to augment pulmonary arterial blood flow, and may have implications for patients in failing Fontan physiology.

60

Hemodynamic Contribution of HeartMate II and HVAD at Low Speed: Implications in Assessing Cardiac Recovery

G. Sunagawa, N. Byram, J. H. Karimov, D. Horvath, N. Moazami, R. C. Starling, K. Fukamachi. *Cleveland Clinic, Cleveland, OH.*

Study: Current protocols for evaluating cardiac recovery after left ventricular assist device (LVAD) implantation involve assessment of hemodynamics and cardiac reserve at the lowest operating speed of LVAD. Hemodynamic contribution of the pump at this speed is largely unknown.
Methods: The LVADs were operated in a mock loop at 6000, 8000, and 10000 rpm (for Thoratec HeartMate II) and 1800, 2400, and 3000 rpm (for HeartWare HVAD). We acquired pressure-flow curves in each steady state. A pulsatile pneumatic ventricle served as a heart simulator. Evaluations were done under conditions mimicking normal heart function and heart failure. LVAD flow, total flow, and aortic pressure (AoP) data were collected and analyzed at each pump speed condition and compared with those with no LVAD support (pump off with the outflow clamped).
Results: A large regurgitant flow during diastole was confirmed during normal heart function at lowest speed in both pumps which is greater than that in the heart failure condition (Figure); however, there was no difference in mean AoP and total flow between LVAD support at lowest pump speed and no LVAD support (Table). In contrast, in the heart failure condition, LVAD flow at lowest pump speed significantly contributed to mean AoP and total flow, because there was less regurgitant flow (Figure & Table). Regardless of the pump type (axial or centrifugal), net pump flow generated by the LVADs at lowest pump speed depends on the degree of residual left ventricular function and may be underappreciated. The LVAD operation at low speed is a different condition than pump-off with the outflow graft clamped, when the heart is not recovered well, thus assessing cardiac recovery at low speed is flawed unless measures are taken to prevent regurgitant flow.

Figure

HeartMate II **HVAD**

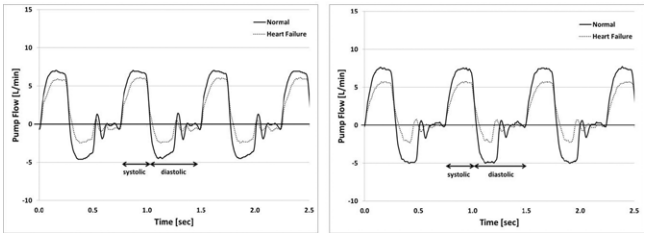

Table

	HeartMate II				HVAD			
Pneumatic heart condition	Normal Heart		Heart Failure		Normal Heart		Heart Failure	
Pump Speed [rpm]	Off with the outflow clamped	6000	Off with the outflow clamped	6000	Off with the outflow clamped	1800	Off with the outflow clamped	1800
Mean AoP [mm Hg]	100	102	77	86	99	100	72	83
Pump Flow [L/min]	0	0.76	0	0.99	0	0.99	0	1.35
Total Flow [L/min]	3.96	3.95	1.21	1.27	3.48	3.41	1.22	1.30

64

New Optimized Dual Lumen Self-Expanding Catheter Design

S. Abdel-Sayed, Sr.[1] J. Favre,[2] L. von Segesser.[1] [1]*Surgery, Cardiovascular Research, University Hospital-CHUV, Lausanne, SWITZERLAND;* [2]*Musculoskeletal Medecine, University Hospital-CHUV, Lausanne, SWITZERLAND.*

Study: Contribution of veno-venous ECMO to gas transfer is flow dependent. Catheter design is a key factor for optimal pressure/flow rate relationship. This study designed for assessment of an optimized self-expanding dual lumen catheter design versus the current standard.
Methods: Outlet pressure/flow rate and inlet pressure/flow rate for 24 F Smart catheter with self-expanding dual lumen design constricted to 23 F simulating an identical access orifice as for Avalon 23 F catheter (control) were compared on a computerized flow bench and calibrated sensors with a Biomedicus centrifugal pump. Flow, pump inlet-pressure and outlet-pressure were determined at 500, 1500, 2500, and RPM for self-expanding *versus* control.
Results: At 500 RPM, outlet-pressure was -3.12 ± 0.17 mmHg for self-expanding catheter *versus* -5.29 ± 0.07* for control; -62.25 ± 0.32 *versus* -75.24 ± 0.53* at 1500 RPM; and -114.01 ± 0.81 *versus* -206.61 ± 0.69* at 2500 RPM: $p<0.0001$. The flow values were 0.95 ± 0.02 l/min for self-expanding catheter *versus* 0.76 ± 0.02* for control at 500 RPM; 3.74 ± 0.17 *versus* 2.93 ± 0.01* at 1500 RPM; and 5.57 ± 0.22 *versus* 5.07 ± 0.07* at 2500 RPM: $p<0.0001$. At 500 RPM, Inlet pressure was 14.8 ± 0.13 mmHg for self-expanding catheter *versus* 15.88 ± 0.12* for control; 92.79 ± 1.02 *versus* 99.54 ± 0.82* at 1500 RPM; and -233.51 ± 0.82 *versus* -256.13 ± 0.69* for control at 2500 RPM: $p<0.0001$. The flow values were 0.99 ± 0.02 l/min for self-expanding catheter *versus* 0.82 ± 0.01* for control at 500 RPM; 2.63 ± 0.02 *versus* 2.12 ± 0.01* at 1500 RPM; and 4.34 ± 0.01 *versus* 3.36 ± 0.01* at 2500 RPM: $p<0.0001$. These results demonstrate that the optimized dual lumen self-expanding catheter requires lower catheter inlet and outlet pressures for higher flows as compaerd to the current standard.

65

Telemanaging for Anticoagulative Treatment in LVAD Patients - Our Daily Practise

J. Garbade, S. Eifert, A. Meyer, J. Hahn, J. Fischer, S. Lehmann, F. Mohr. *Cardiac Surgery, Heart Center Leipzig, Leipzig, GERMANY.*

Study: Optimal anticoagulation is essential for the outcome and frequency of thromb-embolic events of patients on left ventricular assist device (LVAD). Supervision and management of anticoagualative treatment may be difficult in these cases.
Methods: We want to report our results of telemonitoring and telemanaging by use of Vitaphone-remote-tele-platform in 50 out 146 ambulatory LVAD patients. INR range was set between 1.9 to 2.7.
Results: Fifty patients on LVAD (46 men, 4 women) were telemonitored over a median duration of 178 ± 118 days. INR measurements were carried out every 7 ± 9 days. Median number of INR measurements was 27 ± 32 over the entire time of the study. Vitaphone telemonitoring did detect a median frequency of absolute outliers of 6 ± 6 per patient. The percentage of wrong INR values was demonstrated in a percentage of 18.1 ± 16.1 of patients. Six of 50 patients did never have wrong INR levels. The lowest measured INR was 1.4 and the highest 5.6 in one patient each. Twenty seven of 50 patients did never drop below INR of 1.9. The lowest median INR of our study cohort measured 1.9 ± 0.18. Two of the included patients showed an LVAD thrombus and underwent successful thrombolysis.
Thirty seven patients exceeded our set upper INR level of 2.7. The highest median of INR was 3.1 ± 0.64. INR outliers received immediate modulated anticoagulative drugs. Telemonitoring- and telemanaging anticoagulation in LVAD patients is a novel, feasible and supportive measure to reach optimal therapeutic INR levels for this specific heart failure cohort.

66

Recurrent Ventricular Tachycardia After Implantation of a Left Ventricular Assist Device: A Interdisciplinary and Interventional Target

J. Garbade,[1] J. Fischer,[1] A. Meyer,[1] S. Lehmann,[1] A. Ayra,[2] G. Hindricks,[1] F. Mohr.[1] *[1]Cardiac Surgery, Heart Center Leipzig, Leipzig, GERMANY; [2]Electrophysiology, Heart Center Leipzig, Leipzig, GERMANY.*

Study: Ventricular tachycardia (VT) is a common finding following implantation of a continuous-flow left ventricular assist device (LVAD). We report our experience, technical feasibility and efficacy of endocardial VT-ablation to treat symptomatic patients with LVAD.
Methods: A retrospective analysis of all patients supported with a LVAD who were referred for catheter ablation to treat recurrent symptomatic VT was performed.
Results: Between 2012 and 2014, 159 patients underwent implantation of a LVAD. In eight patients (all of whom had an ICD before LVAD implantation) an ablation was indicated due to recurrent episodes of VT, leading to ICD shock or recurrent hemodynamic instability. A total of 11 ablation procedures were performed. The first ablation was performed after an average of 142 ± 130 days after LVAD implantation. Between the implantation of the LVAD and the first ablation procedure 24 ± 18 appropriate shocks per patient were delivered. For catheter ablation the CARTO 3 mapping system was utilized. Nine clinical VT episodes were able to be induced in four patients. Seven of these VT epsiodes (77.8%) were successfully ablated after activation mapping in these patients. In two patients a monomorphic VT origin was located in the epicardium and could not be ablated successfully, but only in one patient was it inducible at the end of the procedure (12.5%). In six patients voltage mapping was conducted. The low voltage area in four patients extended to the implantation area of the inflow cannula, and of these, all were rendered non-inducible after ablation. All patients remained hemodynamically stable during the procedure. Although the majority had a reduction in VA frequency, in two patients clinical VT recurred, making a second ablation necessary. There were no complications associated with the ablation procedures. The patients were free from ICD shock for an interval of 209 ± 193 days.

68

A Model of Anterograde Oxygenated Lung Blood Perfusion in Acardia

S. Marinakis,[1] M. Burki,[2] S. Abdel-Sayed,[2] L. K. von Segesser.[2] *[1]Cardiothoracic Surgery, CHU Charleroi, Londelisart, BELGIUM; [2]Department of Experimental Surgery, Centre Hospitalier Universitaire Vaudois, Lausanne, SWITZERLAND.*

Study: In extreme situations as hyperacute rejection of heart transplant or major heart trauma, the explantation of the heart and the hemodynamic support by extracorporeal membrane oxygenation (ECMO) might be the only means for survival. In our previous model of acardia, during ECMO, pulmonary artery (PA) was clamped and did not receive any anterograde blood flow. However, a model of anterograde PA perfusion might be necessary to avoid ischemic pulmonary damage in prolonged ECMO in acardia. From experimental data on big animals, it is known that the occlusion of a PA, even for long periods (one week), does not jeopardize lung viability. However, pulmonary reperfusion provokes acute lung injury, with microscopic alterations indicating cellular apoptosis. The aim of our present study was to describe the surgical technique and to determine the feasibility of an anterograde lung perfusion in acardia through the anastomosis of the right internal mammary artery (RIMA) to the PA.
Methods: A venoarterial cardiopulmonary bypass was established in 3 pigs (72 ± 2.6kg) by the transjugular insertion to the caval axis of a double staged cannula with a carotid artery return. Heart was excised, ECMO support was established and pressure and flow values were recorded. RIMA was harvested and anastomosed to the PA.
Results: Initial pump flow was 4.3 ± 0.17 L/min and Mean Arterial Pressure (MAP) was 43.3 ± 13.3 mmHg, dropping to 3 ± 1.2 L/min (P=0.16) and 27.7 ± 7.5 mmHg (P=0.05) 10 minutes after induction of ventricular fibrillation. After cardiectomy and RIMA anastomosis to PA, pump flow and MAP re-achieved baseline values (4.4 ± 0.5 L/min, P=0.73 and 50 ± 15 mmHg, P=0.08). Bronchial circulation's output during atria suture was 25 ± 2.5 ml/min representing 0.6 ± 0.03% of pump's output. RIMA's output was 93.3 ± 5.8ml/min which accounted for 2.2 ± 0.15% of pump's output. RIMA anastomosis to PA is a feasible, safe and easy to perform maneuver assuring an almost fourfold augmentation of anterograde lung perfusion in acardia.

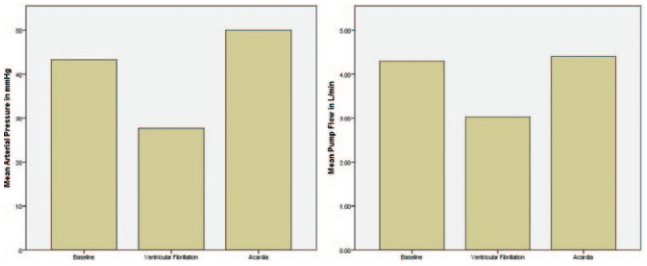

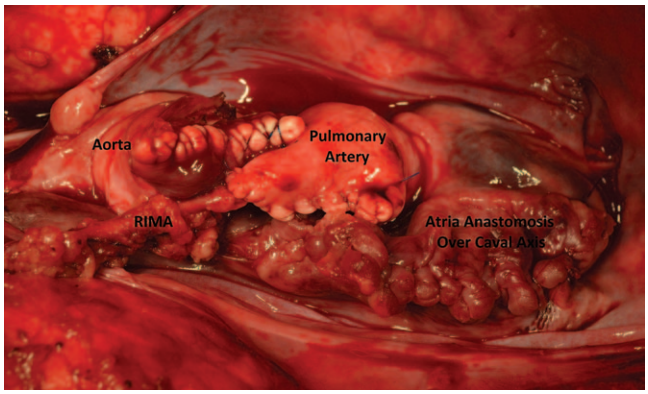

71

Less Invasive HeartMate II LVAD Exchange via Subxiphoid Midline Incision

V. Tchantchaleishvili,[1] J. Haswell,[1] W. Hallinan,[1] H. Massey.[2] *[1]University of Rochester, Rochester, NY; [2]University of Louisville, Louisville, KY.*

Study: The conventional surgical approach for pump exchange has been a redo median sternotomy. At our institution, we have been performing pump exchange through sternal sparing, subxiphoid incision, reserving reoperative sternotomy for procedures requiring LVAD inflow cannula revision and left ventricular apex recoring, or outflow graft revision.
Methods: We performed a retrospective review of patients who underwent HeartMate II left ventricular assist device (LVAD) exchange at our institution and analyzed their perioperative characteristics and postoperative outcomes.
Results: From June 2010 through June 2015, 230 patients underwent HeartMate II LVAD placement, and 30 (13%) required exchange, including one patient who underwent the exchange at an outside institution. Out of the remaining 29 patients, 28 required pump exchange once, and one patient twice. 24 (80%) LVAD exchanges were performed through subxiphoid sternal-sparing approach, and six (20%) through reoperative sternotomy. Median age at exchange was 56 years (IQR, 45–60) and 10.3% (3/29) were female. Predominant indication for pump exchange was suspected or confirmed pump thrombus (70%), followed by electromechanical pump dysfunction (20.7%). Median operative (238 min) and bypass (83 min) times, as well as need for blood products, were comparable between the two groups. None of the patients required reoperation for bleeding. Subxiphoid approach group had a significantly shorter median ICU (7 vs 37 days, p = 0.01) and hospital stay (29 vs 107 days, p = 0.01) compared to reoperative sternotomy. Overall 90-day mortality was 10%, including two patients (8%) in the subxiphoid group and one patient (17%) in the resternotomy group (p = 1.00). Kaplan-Meier analysis showed comparable survival of patients with pump exchange to the rest of the HeartMate II LVAD patients at our institution (p = 0.12).
Conclusions: Subxiphoid pump exchange is a viable option, resulting in shorter ICU and hospital stay and comparable survival to non-exchange patients.

73

A Novel Method for 3D Modeling of Left Ventricular Assist Device Inflow Cannula Malposition

J. Chuang,[1] O. Dur,[1] B. Lima,[2] T. Chamogeorgakis,[2] S. Hall,[2] G. Gonzalez-Stawinski,[2] D. Farrar,[1] K. Sundareswaran.[1] *[1]St. Jude Medical, Pleasanton, CA; [2]Baylor University Medical Center, Dallas, TX.*

Study: Optimal function of a left ventricular assist device (LVAD) depends on proper alignment of the inflow cannula (IC) in the left ventricle (LV). Quantitative guidelines for IC angulation are lacking due to variation in cardiac geometry and difficulty in analyzing the 3D cannula orientation relative to the LV. The study objective was to develop a method to provide 3D quantification of IC malposition.
Methods: Contrast enhanced cardiac computed tomography (CT) images of 5 normal and 5 clinically malpositioned IC cases were collected from patients with HeartMate II LVADs. Using Mimics image processing software (Materialise, Belgium), the native heart, major arteries, and LVAD were segmented to create 3D patient-specific models. To characterize the relationship between the IC and LV, a local curvilinear coordinate system was defined at the IC insertion point relative to the mitral valve and septum (Figure). The z-axis, which points from the insertion point to the mitral valve center, describes the ideal IC orientation. Deviation of the IC from the z-axis is defined by ϕ. In the transverse plane of the LV, θ describes the IC rotation towards the septal or lateral wall. The distance (D) from the cannula inlet to the proximal endocardium was also measured. All 3D measurements were performed with 3-matic^{STL} design software (Materialise, Belgium).
Results: Compared to normal cases, ϕ trended higher and D was significantly shorter in malpositioned cases (P<0.05). Four out of five malpositioned ICs met the following criteria: 1) ϕ ≥ 40° and 2) D ≤ 40 mm. None of the normal IC cases exhibited both of these characteristics. The developed 3D modeling technique allows one to quantitatively define IC malposition. Future applications of this method may improve clinical outcomes through earlier diagnosis of pump malposition or better preoperative planning.

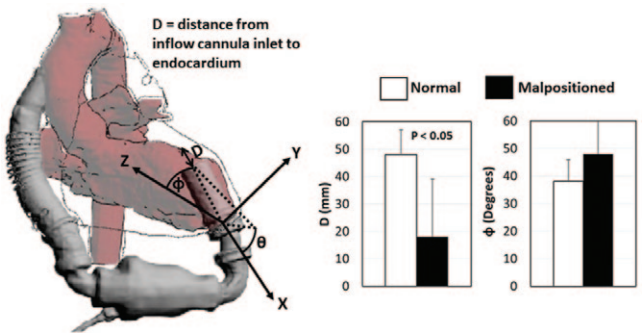

94

Prolonged Normothermic Ex-Situ Heart Perfusion with Live Animal Plasma Cross-circulation

J. T. Church, **F. Alghanem**, K. B. Deatrick, J. M. Trahanas, J. P. Phillips, E. M. Perkins, M. H. Song, R. H. Bartlett, A. Rojas-Pena, G. E. Owens, M. L. Bocks. *University of Michigan Health System, Ann Arbor, MI.*

Study: Prolonged normothermic *ex-situ* heart perfusion (NEHP) could revolutionize cardiac transplantation by prolonging preservation times and allowing assessment of pre-transplant organ function. We previously reported that whole blood cross-circulation with a live parallel, paracorporeal animal (pPA) results in improved cardiac function and physiology. To help identify perfusate components that might enable long-term perfusion, we compared hearts preserved with cross-circulated plasma to those with cross-circulated whole blood from a pPA, as well as to our closed-circuit NEHP system.

Methods: There were three groups: closed-circuit NEHP (CC, n=22), pPA whole blood cross-circulation (XC-Blood, n=6), and pPA plasma cross-circulation (XC-Plasma, n=2). In the CC group, porcine hearts were attached to a circuit consisting of a reservoir, roller pump, and membrane oxygenator, and perfused via the aortic root for 12 hours. XC groups used a similar circuit with the addition of a pPA under anesthesia. The XC-Blood group involved continuous circulation of whole blood between the pPA and reservoir. The XC-Plasma group involved plasma filtration of both the pPA and reservoir with continuous exchange of plasma between the pPA and reservoir at 1L/hr.

Results: Physiologic parameters were similar between the XC-Blood and XC-Plasma groups after 12 hours, including oxygen consumption (8.8 ± 5.8 vs. 9.1 ± 6.5 mL/min) and left ventricular systolic pressure (60.5 ± 18.5 vs. 69.8 ± 49.5 mmHg). Coronary vascular resistance in the XC-Plasma group appeared lower than in the XC-Blood group (0.6 ± 0.004 vs. 0.85 ± 0.3 mmHg/L/min; p=0.13), but higher than in the CC group (0.33 ± 0.45 mmHg/L/min; p=0.008). These early data suggest that cardiac function is equally robust with plasma and whole blood cross-circulation. The variance in vascular resistance between groups and factors influencing it will be evaluated in future experimentation.

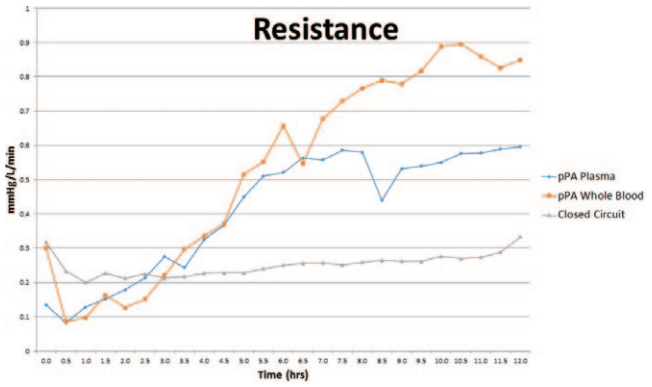

97

Managing the Total Artificial Heart via an Implantable Pulmonary Artery Pressure Monitor

D. L. Joyce, M. M. Redfield, S. S. Kushwaha, A. Behfar, B. A. Borlaug, G. S. Sandhu, R. C. Daly, L. D. Joyce. *Mayo Clinic Hospital- Saint Marys Campus, Rochester, MN.*

Study: Although reversal of pulmonary hypertension has been observed in patients who are bridged to transplant with a left ventricular assist device, implantation of a Total Artificial Heart (TAH) prevents subsequent right heart catheterization. Consequently, there is controversy over whether or not the prosthetic right ventricle improves or exacerbates pulmonary hypertension.

Methods: An implantable pulmonary artery pressure monitor was placed in two patients who underwent TAH implantation as a bridge to transplant. One patient demonstrated pulmonary hypertension at the time of implant, while the other demonstrated normal pulmonary pressures. Daily measurements were taken of the systolic, diastolic, and mean pulmonary arterial (PA) pressures over the duration of support.

Results: Patient #1 was supported for 101 days before expiring from abdominal ischemic complications. PA pressures remained consistent throughout the period of support from 26/17 (20) to 23/13 (17) at the time of death. Patient #2 remains actively listed for transplant after 28 days of support. PA pressures have steadily decreased from 55/39 (28) at the time of implant to 29/18 (7) currently (Figure 1). These findings suggest that implantation of a TAH may have a beneficial impact on the degree of pulmonary hypertension seen in patients who are bridged to transplant. The use of an implantable pulmonary artery pressure monitor may be useful in optimizing hemodynamics as well as planning the appropriate timing for transplantation in the setting of TAH support.

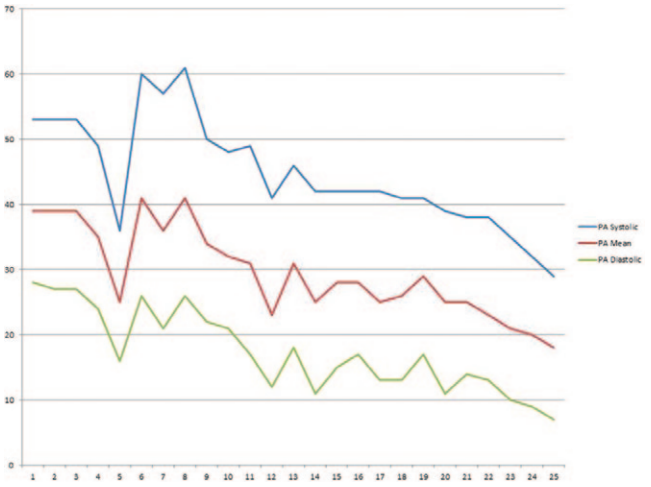

99

Infection, Oxidative Stress and Changes in Circulating Regulatory T Cells of Heart Failure Patients Supported by Continuous-flow Left Ventricular Assist Devices

N. K. Mondal,[1] M. Sobieski,[1] S. Pham,[2] B. P. Griffith,[2] S. C. Koenig,[1] M. S. Slaughter,[1] Z. J. Wu.[1] *[1]Department of Cardiovascular and Thoracic Surgery, University of Louisville School of Medicine, Louisville, KY; [2]Department of Surgery, University of Maryland School of Medicine, Baltimore, MD.*

Study: Infection is a common cause of morbidity and is the 2nd most common cause of death in heart failure (HF) patients with CF-LVAD support. The objective of this study was to investigate the changes in oxidative stress and circulating regulatory T cells (Tregs) of the immune system in CF-LVAD implanted patients with or without infection.

Methods: We recruited 16 CF-LVAD patients (5 with infection and 11 without infection) and 7 healthy volunteers. Pre and post implant blood samples were collected. Generation of reactive oxygen species (ROS) from leukocytes, superoxide dismutase (SOD) in erythrocyte, total antioxidant capacity (TAC) and oxidized low density lipoprotein (oxLDL) in plasma were measured. Circulating Tregs cells were evaluated by flow cytometry and defined as percent positive CD4+CD25+ T cells.

Results: HF patients had preexisting condition of oxidative stress than healthy volunteers as evident from higher leukocyte ROS, elevated oxLDL levels as well as depleted SOD and TAC (Figure). At baseline, HF patients had decreased % of circulating Tregs cells (5.12 ± 1.5 vs 8.14 ± 3.01 %, p<0.01) when compared to healthy volunteers. After CF-LVAD implantation, patients with infection illustrated 35% and 44% rise in ROS and oxLDL respectively, 31% decrease in TAC and marked rise in % of circulating Tregs cells (14.27 ± 3.17 vs 9.38 ± 3.41 %, p<0.01) when compared to patients without infection. Persistent oxidative stress and compromised immune system were found more confrontational in HF patients with infection after CF-LVAD implantation when compared to patients without infection. In conclusion, our findings suggest that appreciable rise in Tregs cells of the immune system and persistent oxidative stress may be important indicators of systemic response of the body to CF-LVAD among HF patients with infection.

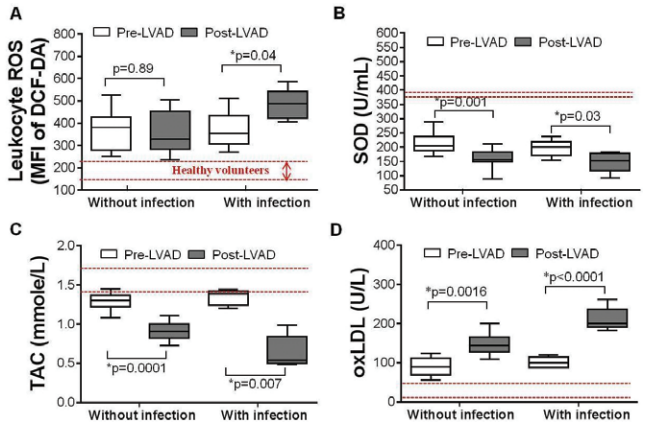

107

Diaphragmatic Left Ventricular Wall Placement of HeartWare Ventricular Assist Device

B. Soleimani, A. Werner, E. Stephenson, W. Pae. *Cardiothoracic Surgery, Penn State Hershey Medical Center, Hershey, PA.*

Study: Implantation of the Heartware ventricular assist device (HVAD) inflow cannula has conventionally been in the left ventricular apex. However, there are circumstances in which apical inflow cannula placement is not feasible. We describe our institutional experience with HVAD inflow cannula placement in the diaphragmatic wall of the left ventricle (LV).
Methods: Since May 2013, six patients received an HVAD with the inflow cannula placed in the diaphragmatic LV wall. Operation was performed on cardiopulmonary bypass with beating heart. Left ventriculotomy was made on the inferior wall 1/3 of the way from apex to base of the heart 1 cm left of the inferior interventricular septum. The outflow graft was anastomosed to the ascending aorta in the conventional way. We performed a retrospective chart review to determine the perioperative characteristics and outcomes of this group of patients.
Results: The baseline characteristics are depicted in the table. The median INTERMACS category was 2, with 3/6 patients supported on ECMO at time of implant. Reason for diaphragmatic LV wall approach was apical calcification from previous aneurysmectomy (3), ongoing antero-apical myocardial infarction (2) and small size patient (1). There were no cases of inflow cannula obstruction and target flows were achieved in all cases, with complete LV decompression and closure of the aortic valve. 3 patients required a temporary right ventricular assist device. There were no cases of hemolysis, pump thrombosis or embolic stroke. There was 1 early post-operative death due to hemorrhagic complications and one case of hemorrhagic stroke 7 months post-implant. One year survival was 62.5%. The overall median survival was 577 days including one successful transplant. In conclusion, diaphragmatic LV wall placement of the HVAD is a reasonable alternative to conventional apical placement in selected patients in whom the apex is not suitable due to calcification, recent myocardial infarction, or a small thoracic cavity.

Number of patients	6
Males	5 (83%)
Age (mean)	67 (range 58-75)
Ischemic Etiology	6 (100%)
INTERMACS Category (median)	2 (range 1-4)
Hemodynamic Support	3
ECMO	3
Intra-Aortic Balloon Pump	1
Reason for Diaphragmatic Wall Placement	
Acute antero-apical myocardial infarction	1
Subacute anterolateral LV free wall rupture following acute myocardial infarction	1
Calcified LV apex due to previous LV aneurysmectomy	3
Small size patient	1
Post-operative RV failure	4 (67%)
Inotropes for >1 week	3 (50%)
Temporary RVAD	3 (50%)
Re-operation for Bleeding	2 (33%)
Wound Infection	0
CVA (late)	1 (17%)
30-day Mortality	1 (17%)
One-year Survival	62.5%
Median Survival (days)	577

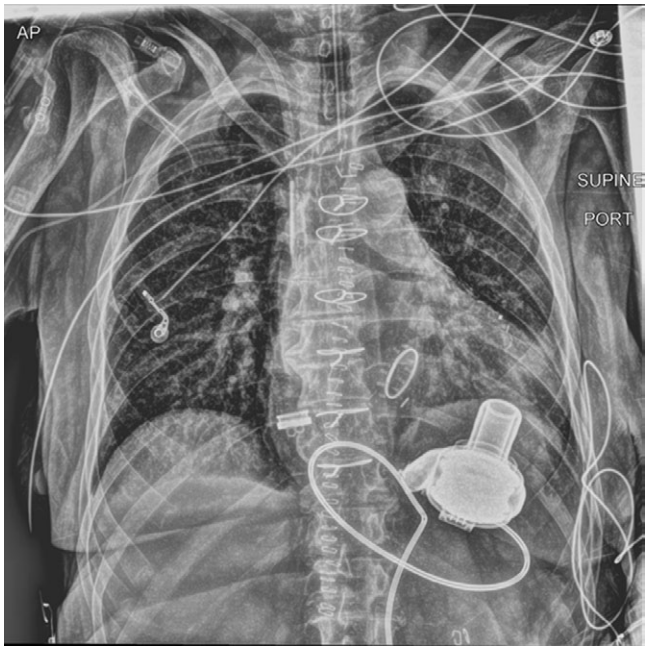

112

Remote Pulmonary Artery Hemodynamic Monitoring in Patients Supported with a Left VentricularAssist Device

A. Bindra,[1] S. Hall,[1] S. Mckellar,[2] S. Joseph,[1] J. Stehlik,[2] S. Drakos,[3] C. H. Selzman,[3] S. Carey,[1] O. Wever-Pinzon.[3] *[1]Baylor University Medical Center, Dallas, TX; [2]University of Utah School of Medicine, Salt Lake City, TX; [3]University of Utah School of Medicine, Salt Lake City, UT.*

Study: Background: LVADs are widely used in patients with advanced heart failure (HF) for Left Ventricular (LV) unloading, restoring systemic and pulmonary hemodynamics. This therapy improves functional class (FC), quality of life and survival in this patient population. CardioMEMS HF system (CM) is an FDA-approved device that is percutaneously implanted allowing for remote monitoring of PAP, a surrogate of LV filling pressures in patients with HF. Herein we describe 2 cases in different centers of simultaneous use of CM and LVAD implantation.

Methods: Case 1: A 21-year-old man, with idiopathic dilated cardiomyopathy, NYHA functional class III underwent implantation of CM to assist in medical optimization. The patient's condition declined requiring inotrope support and subsequently HeartMate (HM) II LVAD was implanted for destination therapy. Post VADdual implant, the patient's NYHA FC increased improved from IV-I, average PA pressures decreased from &gt 50 to &lt 30 mmHg, diuretics requirements decreased drastically, titration aided by CM. Case 2: A 56-year-old man with dilated, non-ischemic cardiomyopathy, underwent CM and subsequently on deterioration LVAD (HMII) implantation. Post VAD, the patient's NYHA class improved from IV-I, average PA pressures decreased from &gt 40 to &lt 20 mmHg. Additionally, we were able to identify/ treat episodes of paroxysmal atrial fibrillation wirelessly. VAD optimization was done using the CM in addition to echocardiography.

Results: Discussion: CM monitoring appears to be feasible and useful in post LVAD implantation management. Prospective studies are needed to determine if this combined technology would equate to a reduction of readmissions and adverse events in this patient population. LVAD speed optimization from another set of data points obtained from CM in addition to echocardiography seems plausible.

114

In-vivo Hemocompatibility Study of CH-VAD, an Ultra-Compact Fully Magnetically Suspended Centrifugal Blood Pump

P. Yang,[1] M. S. Slaughter,[2] **Z. J. Wu**,[2] S. C. Koenig,[2] M. A. Sobieski,[2] G. Monreal,[2] N. K. Mondal,[2] C. Chen.[1] *[1]CH Biomedical Inc, Suzhou Industrial Park, CHINA; [2]Cardiovascular and Thoracic Surgery, University of Louisville, Louisville, KY.*

Study: CH-VAD (CH Biomedical, Suzhou, China) is an ultra-compact centrifugal blood pump with full magnetic suspension. Its compact size (190g, 49mm diameter, 26mm height) facilitates pericardial implantation. The major electronic components are integrated inside the pump with a small (3.4mm diameter) flexible power and communication cable. The purpose of this study was to evaluate feasibility of the CH-VAD by investigating hemodynamic and hemocompatibility performance.

Methods: Two acute, two 14-day, and two 60-day animal studies were conducted in male Jersey calves (87-96kg). The inflow was placed in the apex of the left ventricle and the outflow graft was sutured to the proximal descending aorta. Device performance, end-organ function, and device hemocompatibility were assessed. Biomarkers for shedding of three key platelet adhesive receptors (GPIbα, GPVI, GPIIbIIIa) and multimer distribution of vWF in the plasma samples from the two 60-day animals were analyzed, representing important aspects of blood damage relevant to thrombosis and bleeding.

Results: The device fit well in the chest cavity and provided adequate circulatory support (flow: ~ 5 L/min at 3300 rpm). All animals successfully survived to the scheduled end point. Key laboratory tests and gross necropsy of the two 60-day animals suggested that the devices did not cause end-organ dysfunction or hemolysis (see Table). Biomarker analyses indicated no shedding of GPIbα and some degree of shedding of GPVI and GPIIbIIIa that were likely associated with pump inlet obstruction in one animal. All explanted pumps from the six animals were clean and free of any adherent emboli. Overall, the present studies successfully demonstrated feasibility of pump performance and acceptable hemocompatibility.

Variable	Data from calves Implanted with CH-VAD for 60 days (n=2)									
	Reference	Base	Day-1	Day-3	Day-6	Day-14	Day-28	Day-40	Day-50	Day-60
Alkaline phosphatase (U/L)	28 – 233	158±24	98.5±20.5	68±8.5	78.5±9.2	95±5.7	174.5±38.9	162±31.11	142.5±29	168±24
Alanine Aminotransferase (U/L)		51±7	109.5±72.8	63±0.0	48±35.4	28±8.5	47±8.5	44.5±16.3	45±4.3	49±8.5
Blood urea nitrogen (mg/dL)	10 – 25	4.5±2.1	11±1.4	3±1.4	3.5±2.1	4±2.8	2.5±0.7	5.5±0.7	5±1.4	12±1.4
Creatinine (mg/dL)	0.5 – 1.6	0.6±0.0	0.5±0.0	0.5±0.0	0.5±0.0	0.6±0.1	0.65±0.1	0.65±0.1	0.6±0.0	0.7±0.0
Total bilirubin (mg/dL)	0.0 – 0.7	0.2±0.1	0.1	0.15±0.07	0.15±0.07	0.3±0.0	0.15±0.07	0.15±0.07	0.1±0.0	0.3±0.0
Total protein (g/dL)	6.2 – 8.0	5.9±0.14	5.1±0.28	4.9±1.2	5.5±0.5	6.3±0.4	6.6±0.2	6.2±0.1	6.1±0.4	6.2±0.0
Creatine Kinase (U/L)	50 – 350	154.5±10.6	2026±14.1	366.5±145	80.5±17.7	98±14.1	69±14.1	78.5±13.4	67.5±2.1	111.5±2.1
Lactate dehydrogenase (U/L)		4786±992.8	7191	5926.5±447.6	6017.5±163.3	4893.5±122.3	3669.5±774.3	2994.5±487.2	3239.5±1068.4	3138±627.9
Plasma free hemoglobin (mg/dL)		5±7.1	2.5±3.5	0	5±7.1	5±0.0	7.5±3.5	7.5±3.5	7.5±3.5	5±0.0

116

Low-shear TORVAD Ventricular Assist Device Preserves von Willebrand Factor in Chronic Ovine Model

E. Larson,[1] J. R. Gohean,[1] R. G. Longoria,[2] M. Kurusz,[1] R. W. Smalling,[3] E. Larson,[1] C. R. Bartoli,[4] J. Kang.[4] *[1]Windmill Cardiovascular Systems, Austin, TX; [2]Mechanical Engineering, The University of Texas at Austin, Austin, TX; [3]The University of Texas Health Science Center at Houston, Houston, TX; [4]Division of Cardiovascular Surgery, Philadelphia, PA.*

Study: The TORVAD is a positive-displacement ventricular assist device that synchronizes with the cardiac cycle to deliver full support to a failing heart with a 30 ml counterpulse ejection. Pumping is achieved by rotating two pistons within a toroidal chamber on ceramic hydrodynamic bearings. The design achieves low-shear by virtue of controlled gaps and low rotational speeds (60–140 rpm). Blood pressure is measured using motor currents. This chronic animal study was performed to assess long-term performance, automatic control of pumping parameters, hematologic effects, and thrombogenicity of the TORVAD.
Methods: Three sheep were implanted with the TORVAD with a target study duration of 60 days. Blood samples were taken throughout the study for analysis of plasma free hemoglobin (PFHg) and von Willebrand Factor (vWF). Hemodynamic and pump parameters were relayed by the controller to a server for continuous remote monitoring.
Results: Animals 1 and 2 were weaned off heparin and onto warfarin. All anticoagulation was stopped on postoperative day (POD) 8 due to excessive anticoagulation with bleeding complications. Animal 3 was weaned off of heparin on POD 3 and no anticoagulation was given for the remainder of the study. The first animal was terminated on POD 9 due to non-device-related internal bleeding; the other two animals were supported for 62 and 60 days. Following stabilization, PFHg averaged 5.2 ± 2.3, 7.4 ± 5.8, and 4.4 ± 3.6 mg/dL for each animal. No loss in high molecular weight vWF was observed. Grafts and inflow cannulas were free from thrombus except for the inflow graft of animal 3, likely due to contamination prior to implantation. Infarcts were observed in the kidneys of animals 2 and 3, which may have resulted from a thrombus in a torus inner seam gap caused by deflection from O-ring forces. This will be corrected by laser welding the seam before any future studies. All other blood-contacting surfaces of the pump were free from thrombi, including the pistons and hydrodynamic bearings.

117

Thrombotic Depositions on Right Impeller of Double-ended Centrifugal Total Artificial Heart *in vivo*

J. H. Karimov,[1] D. Horvath,[1] S. Okano,[1] M. Goodin,[2] G. Sunagawa,[1] N. Byram,[1] N. Moazami,[1] K. Fukamachi.[1] *[1]The Cleveland Clinic, Cleveland, OH; [2]SimuTech, Cleveland, OH.*

Study: The development of Cleveland Clinic continuous-flow total artificial heart (CFTAH) is a complex undertaking that includes chronic biocompatibility assessment of the device. In this study we evaluated the CFTAH for signs of thrombosis and biological material deposition in four animals that had achieved the intended 14-, 30-, or 90-day durations in each respective experiment.
Methods: Thrombotic depositions from four animals (Jersey calves; weight range, 79.5–89.5 kg) that had been implanted with a CFTAH and that had achieved the intended durations were analyzed. The analysis included macroscopic evaluation of pump depositions, histology and computational flow dynamics of the device impeller.
Results: Four animals achieved the intended durations of 14 (case 1), 30 (case 2), or 90 days (cases 3 and 4). Detailed analysis at explant revealed the rotor, stator bore, both (left and right) pump housings, and rotating assembly had remained free of thrombus or depositions in all cases. The left impeller was free of depositions and thrombus. The right impeller was found to have some depositions in all four cases. The shape, configuration, consistency of the thrombi varied in each case. Thrombus depositions in the right pump of the total artificial heart continue to represent an important clinical issue. The right depositions can have multiple contributing factors that will require further investigation. Improved wash and lower residence time within the right impeller, upstream sources for thrombus migration, and increased speed modulation can be potential solutions. More research is necessary to elucidate the implications of a particular impeller design on the susceptibility of the pump to migrating clots.

120

Effects of Using a Torsional Ventricular Assist Device (tVAD) on the Global Hemodynamics of a Failing Heart

E. Soohoo,[1] L. K. Waldman,[2] D. R. Trumble.[1] *[1]Biomedical Engineering, Carnegie Mellon University, Pittsburgh, PA; [2]Insilicomed, Inc., La Jolla, CA.*

Study: The goal of this study was to evaluate the feasibility of using a torsional ventricular assist device (tVAD) to assist a failing heart. Specifically, we examined the effects of increasing angles of rotation applied to the apex of the ventricles on cardiac function, which was quantified in terms of left ventricular ejection fraction (EF), peak systolic pressure (PSP), end-systolic volume (ESV) and stroke work (SW).

Methods: An 80-element, high-order computational biventricular model of a beating heart based on clinical measurements of a patient with severe heart failure (HF) was created using ContinuityPRO modeling software (Insilicomed, Inc., La Jolla, CA). This cardiac model was attached to virtual closed-loop circulatory systems to complete the cardiovascular simulation circuit. By imposing dynamic boundary conditions on select apical nodes, we simulated a tVAD that covers 24% of the longitudinal distance between the apex and the base of the ventricles. The apical region of the ventricles was rotated counterclockwise for 187.5 ms during isovolumic contraction and most of ejection and rotated back during the remainder of the cardiac cycle (heart rate = 80 bpm). Four simulations were performed where three angles (45, 60 and 75 degrees) of systolic rotation were compared to a baseline HF case (NoVAD). Steady-state solutions were obtained after 10 cardiac cycles with concurrent contraction of the heart and the resulting EF, PSP, ESV, and SW were calculated for the last cardiac cycle.

Results: Applied apical rotation resulted in substantial increases in left-ventricular EF, PSP and SW and a decrease in ESV when compared to the NoVAD case (Table 1, Figure 1). These results indicate that apical torsion, when applied at appropriate rotation angles, may improve cardiac function in heart failure patients. Further work is needed to determine optimal ventricular coverage, rotation angle and timing to guide tVAD prototype development.

Rotation Angle	EF (%)	PSP (mmHg)	ESV (mL)	SW (mmHg*mL)
No VAD	20.3	122.6	200.3	2236
45°	22.2	127.5	184.8	2374
60°	24.0	138.4	175.8	2474
75°	27.5	159.8	160.8	3292

Table 1: Left-ventricular ejection fraction, peak-systolic pressure, end-systolic volume and stroke work of baseline HF and torsion simulations.

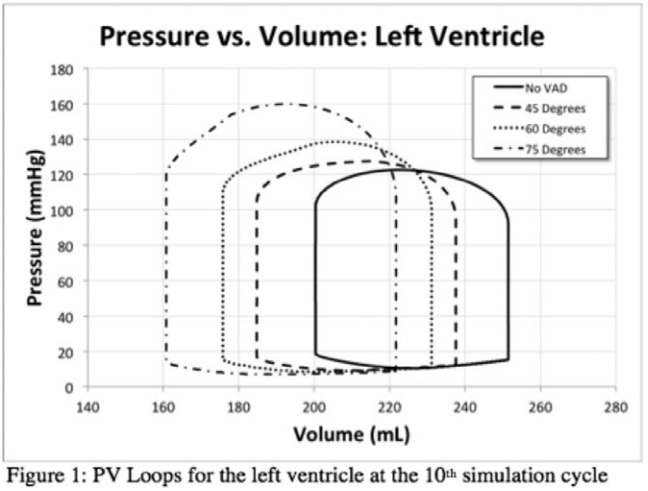

Figure 1: PV Loops for the left ventricle at the 10th simulation cycle

125

LVAD Consent Forms: Current Practices, Gaps, & Recommendations

K. K. MacKenzie,[1] **E. D. Delgado**,[2] M. Abraham,[1] J. S. Blumenthal-Barby,[2] S. E. Fedson.[2] *[1]Health, Humanism and Society Scholars, Rice University, Houston, TX; [2]Center for Medical Ethics & Health Policy, Baylor College of Medicine, Houston, TX.*

Study: The decision regarding LVAD implant has the challenge of complex medical decision-making combined with cognitive impairment due to underlying heart failure. The informed consent form (ICF) is one important part of this process because it is an educational resource given to patients (pts). The study purpose is twofold: 1) to compare LVAD ICFs in order to determine current practices; 2) to develop a new standard of LVAD ICF that provides the necessary clinical & lifestyle information, in a patient-centered format.

Methods: LVAD ICFs were collected from US LVAD programs paired with a transplant center. A rubric was developed to analyze ICFs based on previous assessments of expressed informational needs by LVAD pts. Relying on suggested standards for ICF, we assessed content, syntax, & layout. Content topics of interest were: purpose of LVAD, risks (surgical, short, & long-term), options for alternative therapies & end of life, as well as lifestyle factors. Syntax was evaluated for readability and use of technical jargon using the Flesch-Kincaid Formula & Simple Measure of Gobbledygook (SMOG).

Results: 19 ICFs representing all UNOS regions were analyzed (Table 1). 7 forms discuss medical management for pts that either decline or are later deemed ineligible for implant, though none discuss the risks/benefits of destination palliative care. 18 forms mention general risks of bleeding, and only 4 specifically referred to long-term GI bleeding. Also, limited info is provided to forecast lifestyle changes (e.g. psychosocial & device upkeep). In terms of pt accessibility, only one form is written at an 8th grade reading level (x=11th grade, SD=1.49). Overall, there is wide variation in LVAD ICFs, and notable omissions of benefits/risks. Our findings highlights the need for better surgical, short, & long-term benefit/risk stratification for LVAD vs alternatives. An ICF that includes content that pts find relevant, in addition to the necessary clinical information, could help with pt decision-making and should be implemented.

Table 1. Results

Criteria	#ICFs	Percent
Designation of DT or BTT	17/19	89.5%
Explanation that BTT Designation Does Not Guarantee a Transplant	5/19	26.3%
Destination Palliative Care as an Alternative	9/19	47.4%
Risks/Benefits of Palliative Care	0/19	0%
Gives Option of Deactivation	7/19	36.8%
Explanation of Psychosocial and Cognitive Changes	8/19	42.1%
Description of Overall Activity Restrictions	12/19	63.2%
Guide to Medication Regimes	6/19	31.6%
Explanation of Risk/Result of Infections	3/19	15.8%
Description of Body Image Changes	5/19	26.3%
Effective Explanation of Caregiver Burden and Role	7/19	36.8%
Differentiates and Explains Surgical, Short-Term and Long-Term Risks	4/19	21.1%
Acceptable Layout of Short Sections of Text with Subheadings	12/19	63.2%
No Use of Jargon, or Included Explanations of Necessary Terms	8/19	42.1%

126

Influence of a Novel Rotational Speed Modulation System Used with VA-ECMO on Left Ventricular Afterload and Coronary Arterial Flow

N. Naito,[1] T. Nishimura,[2] K. Iizuka,[1] Y. Takewa,[1] M. Ono,[3] E. Tatsumi.[1]
[1]Department of Artificial Organs, National Cerebral and Cardiovascular Center, Osaka, JAPAN; [2]Department of Cardiac Surgery, Tokyo Metropolitan Geriatric Hospital, Tokyo, JAPAN; [3]Department of Cardiac Surgery, The University of Tokyo Hospital, Tokyo, JAPAN.

Study: Veno-arterial extracorporeal membrane oxygenation (VA-ECMO) is widely used for cardiogenic shock. Although VA-ECMO is efficient with regard to maintaining blood flow through the body, retrograde blood flow increases left ventricular afterload (LVAL). On the other hand, we have developed rotational speed modulation (RSM) system used with continuous-flow LVAD, which changes rotational speed in synchronization with the native cardiac cycle. We conducted this study to evaluate our novel RSM system used with VA-ECMO.
Methods: VA-ECMO was installed via right atrial drainage and distal abdominal aortic perfusion in five adult goats weighing 43.2 ± 2.3 kg. After implantation of the device, cardiogenic shock was induced with beta-adrenergic antagonist infusion. IABP was placed in the thoracic descending aorta through the left carotid artery approach. Left ventricular stroke work (LVSW), left ventricular end-systolic pressure (LVESP), and blood flow of the left coronary artery main trunk (CoF) were evaluated. Data were collected under four conditions with a bypass rate of 70%; circuit-clamp (no ECMO support), continuous-mode (constant RS), counter-pulse mode (increases RS during diastole), and continuous-mode with IABP. LVSW, LVESP, and CoF were shown as percentages of those in circuit-clamp.
Results: LVSW was significantly lower in counter-pulse mode than in circuit-clamp (62.9 ± 18.3%; $p < 0.05$). LVESP was increased significantly in continuous mode than in circuit-clamp (119.2 ± 11.1%; $p < 0.05$). LVESP in counter-pulse mode was significantly lower than in continuous mode (107.3 ± 7.9% and 119.2 ± 11.1%, respectively; $p < 0.05$). Although statistically insignificant, CoF in counter-pulse mode tended to be higher than in the other modes. **Conclusion:** Counter-pulse mode increased coronary artery blood flow and decreased LVSW and LVAL. The results of this study imply that our RSM system may offer the effects of VA-ECMO and IABP only with one device.

130

Pressure-flow Performance Comparison of Specific Axial and Centrifugal Flow Rotary Pump Designs, the HeartMate II and HeartMate 3

C. Cotter. *R&D, St. Jude Medical, Burlington, MA.*

Study: As rotary VAD experience grows in terms of the number of supported patients and the number of pump designs, attempts have been made to identify pressure-flow (HQ) performance characteristics intrinsic to axial flow and centrifugal flow pumps with the ultimate goal of optimizing patient care. HQ curve slope is generally qualitatively characterized as steep for axial pumps and flat for centrifugal pumps. Here, pressure-flow performance is evaluated for the HeartMate (HM) II and 3 which are specific examples of axial and centrifugal pumps.
Methods: HQ curves were generated for the two pumps using a test loop containing 2.7 cP water and glycerin blood analog. The pump pressure difference and flow were measured with the HM II at fixed speeds from 8krpm and 12krpm in 400 rpm increments and the HM 3 at fixed speeds from 3krpm to 8krpm in 500 rpm increments. The absolute value of HQ curve slope was calculated, with slopes becoming flatter as the absolute value approaches zero, as well as shutoff pressure or the pressure at which pump flow becomes zero. For discussion, the tested flow range is divided into three smaller ranges: 0–3 lpm, 3–6 lpm and 6–9 lpm.
Results: The table details HQ curve slope ranges for all speeds as well as at a nominal speed within the typical speed range for each pump. While the HM II, an axial pump, has areas of steep slope and the HM 3, a centrifugal pump, has areas of flat slope, those general characterizations do not hold up across the flow range. Still generalizing, but perhaps more accurately, compared to HM II the data indicates that HM 3 HQ curve slope is more flat from 0–3 lpm, similar to steeper from 3–6 lpm and steeper from 6–9 lpm. At nominal speeds, HM II and HM 3 had similar shutoff pressures of 110 mmHg and 108 mmHg respectively.

HQ Curve Slope Absolute Value (mmHg/LPM)			
Pump/Speed	0–3 LPM	3–6 LPM	6–9 LPM
HM II, all speeds	7–24	6–12	7–23
HM 3, all speeds	3–14	6–25	15–35
HM II, 9200 rpm	8–18	7–10	10–22
HM 3, 5500 rpm	4–6	6–25	25–30

132

Impact of Outflow Graft Diameter and Aortic Incompetence on Cerebral Blood Flow in Continuous Flow Pumps: Relevance to Strokes

R. Krishna Kumar,[1] K. Balakrishnan,[2] S. Bhat.[1] *[1]Engineering Design, Indian Institute of Technology Madras, Chennai, INDIA; [2]Cardiac Sciences, Fortis Malar Hospital, Chennai, INDIA.*

Study: The reason for the difference in stroke rates between HVAD and Heartmate II has been a subject of much debate. We hypothesized that the difference in outflow graft diameters could be an important factor. A computational fluid dynamics (CFD) study of flow in the aortic arch and cerebral vessels was done to compare the pumps with normal pulsatile flow.

Methods: The CFD problem was treated as a fluid structure interaction finite element analysis and solved using the commercial package ADINA. A patient CT scan was converted into a 3D geometric model using Image Segmentation and Registration tool kit. Pressure boundary conditions were calculated using a whole body 0D electrical analogue so that flow into the neck vessels was *an output from the study*. The effect of aortic incompetence on cerebral blood flow was also studied. Blood stasis in the arch was compared by measuring the time taken for injected particles to move out of the system.

Results: Pulsatile flow through the aortic annulus showed normal perfusion of cerebral vessels with no stasis as compared to LVADs, which showed significantly more stasis. Cerebral blood flow was much more sensitive to angle of insertion in the aorta in a 10 mm graft compared to 14 mm. Flow in the innominate artery was severely compromised with a 10 mm graft, especially at an angle of 45°. Aortic incompetence affected cerebral blood flow non-linearly reducing it by almost 60% in certain angles. Thromboembolism due to stasis in the arch and cerebral hypo perfusion could be additional causative factors for stroke especially in pumps with smaller diameter outflow grafts. The effect of aortic incompetence on cerebral blood flow needs further investigation.

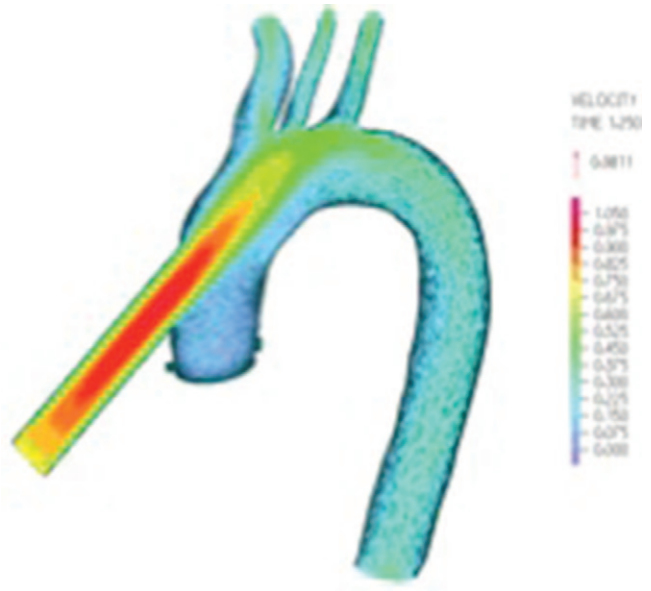

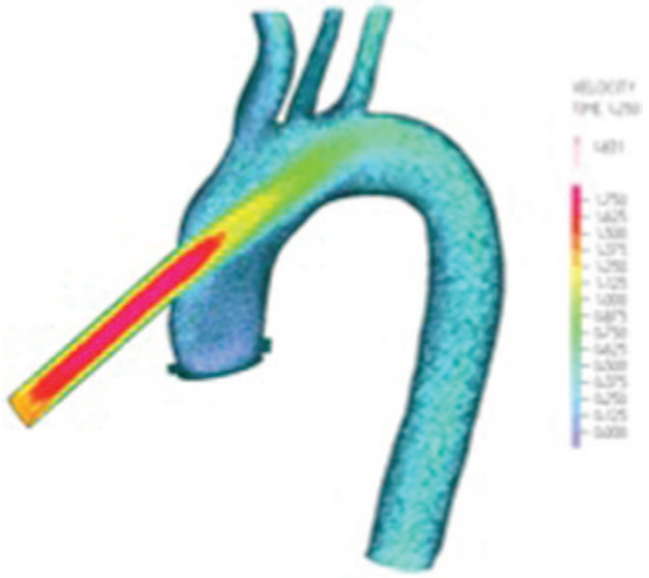

135

Pre-clinical Evaluation of the Calon Cardio MiniVAD

G. D. Foster, I. Pieper. *Calon Cardio-Technology Ltd, Swansea, UNITED KINGDOM.*

Study: The MiniVAD (Calon Cardio, Swansea, UK) is a new LVAD that utilises a novel device layout with passive maglev bearing technology to improve implantability, manufacturability and haemocompatibility. This study comprised both in-vitro and in-vivo evaluations to assess the haemocompatibility and end-organ effects of the MiniVAD. In-vivo evaluation was carried out in 5 adult sheep for 1 month. In-vitro evaluation comprised a suite of blood trauma assays and included the St Jude Heartmate 2 (HM2) and Heartware HVAD (HVAD) for comparison.

Methods: *In-vivo:* Adult sheep weighing 75–90 kg were implanted with the MiniVAD for 30 +/- 2 days. Implantation was via a left thoracotomy with the outflow graft anastomosed to the descending aorta. A flow probe was attached to the outflow graft. The sheep received no post-operative anticoagulation regime. *In-vitro:* Pumps were tested in a 500 ml circulatory loop using bovine blood for 360 minutes. Flow was maintained at 5 L/min, pressure at 100 mmHg and temperature at 37 deg C. Samples were collected at regular intervals and tested for: haemolysis by Harboe assay; leukocyte MPs and platelet activation by flow cytometry; vWF degradation by immunoblotting; and vWF activity by collagen binding assay.

Results: *In-vivo:* Of the 5 cases 4 reached the study term of 30 days. The first two cases experienced issues that were attributed to technical problems with the pump builds. The final three cases exhibited low haemolysis (<6mg/dl) and normal biochemistry / haematology throughout the study. The explanted pumps were clean and free from thrombus, and the kidneys were free from infarction. *In-vitro:* Haemolysis (NIH, g/100L): 0.02 ± 0.004 HM2 (n=9); 0.007 ± 0.0002 HVAD (n=5); 0.001 ± 0.0004 MiniVAD (n=14). Leukocyte MP (fold change to static control): 27.2 ± 11.2 HM2; 37.7 ± 15.2 HVAD; 15.7 ± 9.4 MiniVAD. Platelet activation (relative CAPP2A expression fold change to static control): 4.49 ± 1.15 HM2; 2.82 ± 0.93 HVAD; 1.65 ± 0.98 MiniVAD.

136

New Technology to Achieve True Physiologic Pulsatile Flow During Cardiopulmonary Bypass

G. Sunagawa,[1] J. H. Karimov,[1] R. Dessoffy,[1] N. Byram,[1] P. Grady,[1] M. Sinkewich,[1] J. Naber,[2] D. Vincent,[2] S. Okano,[1] R. Stewart,[1] S. Sale,[1] N. Moazami,[1] K. Fukamachi.[1] *[1]Cleveland Clinic, Cleveland, OH; [2]Design Mentor Inc., Pelham, NH.*

Study: The VENTRIFLO™ True Pulse Pump (Design Mentor, Inc., Pelham, NH) is the first blood pump designed to mimic the human heartbeat by recreating adjustable pulse waveforms. The pump is both preload and afterload sensitive and provides a period of relaxation with no flow during pump diastole similar to the native heart. The aim of this study was to demonstrate feasibility, safety, and efficacy of using this pulsatile pump in 6-hour cardiopulmonary bypass (CPB).

Methods: We studied 4 piglets (41.4–46.2 kg): 3 with VENTRIFLO pulsatile pump and one with ROTAFLOW non-pulsatile pump (Maquet GmBH & Co. KG, Rastatt, Germany) as a control. The first piglet with VentriFlo was excluded due to complications unrelated to the pump. Hemodynamics were monitored during 6-hour CPB support and 2-hour after CPB weaning. No vasoconstrictors were used during CPB. Plasma free hemoglobin and venous O_2 saturation levels were measured. Thereafter, histological analysis was performed.

Results: All included animals were successfully weaned from CPB. VENTRIFLO demonstrated physiologic pressure and flow (Figure) with arterial pulse pressure of 29.9 ± 5.2 mm Hg. Pump flows (2.0 ± 0.1 L/min in ROTAFLOW and 1.9 ± 0.1 L/min in VENTRIFLO) were comparable. Plasma free hemoglobin levels during the 8-hour study were also comparable (27.9 ± 12.5 mg/dl in ROTAFLOW and 28.5 ± 14.2 mg/dl in VENTRIFLO), but venous O_2 saturation levels seemed to be slightly lower during VENTRIFLO (36.8 ± 6.8%) than during ROTAFLOW (44.6 ± 36.8%), which may suggest VENTRIFLO perfused larger area of capillary beds. On histology, all the organs were normal, and there was no evidence of acute ischemic change or thromboembolism in the brain, lungs, heart, liver, spleen, and kidneys. In conclusion, this pilot study demonstrated that the VENTRIFLO generated pulsatile flow and maintained adequate perfusion of all organs during prolonged CPB. The potential benefit of improved microcirculatory perfusion with pulsatile flow needs to be assessed.

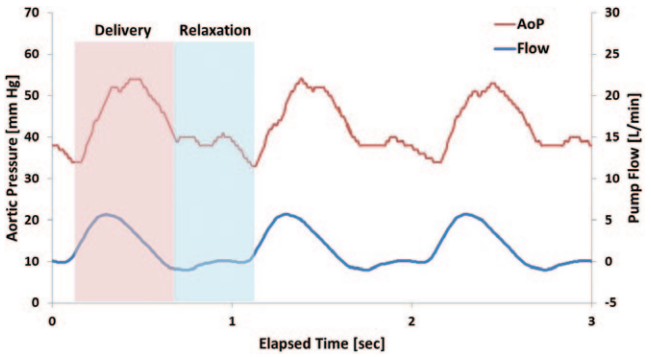

137

Investigating Shear Degradation of Von Willebrand Factor Induced by Ventricular Assist Device-related Flow Conditions in Well-defined Shear Systems

S. Yang,[1] Z. N. Demou,[1] J. Sheriff,[2] D. Bluestein,[2] V. Turitto.[1] *[1]Biomedical Engineering, Illinois Institute of Technology, Chicago, IL; [2]Biomedical Engineering, Stony Brook University, Stony Brook, NY.*

Study: Excessive degradation of von Willebrand Factor (VWF) induces impaired blood coagulation and higher bleeding tendency. Ventricular assist devices (VADs) characteristically produce lower VWF activity in patients. However, due to complexity of flow conditions in VADs, the mechanisms of VAD-induced enhancement of VWF degradation are not fully understood, nor are the critical flow conditions responsible for such degradation.

Methods: VWF degradation as a result of shear stress, exposure time and pulsatile shear frequency was explored under controlled shear stress conditions in a modified Couette viscometer at up to 550 dynes/cm^2. The role of proteases on VWF degradation under the corresponding shear levels was studied with EDTA inhibition of proteolysis. The relative degradation effect of shear stress versus exposure time was investigated in a capillary system under higher, more VAD-comparable shear levels (up to 5,000 dynes/cm^2) and exposure times (as low as 5ms). The VWF distribution was quantitatively analyzed with Western Blot and densitometry.

Results: VAD induced VWF degradation pattern was reproduced in the controlled systems. Increased shear stress above physiological level, prolonged exposure time and higher pulsatile shear frequency generated higher degradation. The shear degradation was mechano-enzymatic with a calcium-dependent protease function being necessary. Shear stress was identified to be more dominant than exposure time with respect to VWF degradation; and various shear regions demonstrated maximal degradation effect indicating these regions essential for degrading VWF multimers of various sizes.

138

Monitoring LVAD Performance in Globally Remote Areas

A. Sharma,[1] A. Hooda,[1] P. Dutta,[1] A. Jyoti,[1] S. K. Lakkipogu,[1] J. Hohenstein,[2] B. Lynch,[2] S. Parnis,[2] S. Attawar.[1] *[1]Fortis Memorial Research Institute, Gurgaon, INDIA; [2]ReliantHeart Inc., Houston, TX.*

Study: Monitoring of LVAD performance in patients after they are discharged from the hospital and return home is evolving. Patients who live in remote areas may not have access to experienced, high level mechanically circulatory support(MCS) care. To decrease hospitalizations and to curtail problems associated with complications which may occur as a result of lack of communication between patient and care givers, a monitoring system which connectsa web based application via wireless telephonic transfer of information from the controller allows review of LVAD system performance.
Methods: We have implanted three patients with the ReliantHeart HA5 LVAD who live in remote areas (Middle East and western Asia) that did not have easy available access to advanced MCS care with the ReliantHeart System.
Results: Through monitoring of the LVAD true flow waveform we have been able to evaluate LVAD function (flow, power and speed) and patient physiologic function such as arrhythmias, trends in cardiac contractility, aortic valve opening and left heart volume status. No pump malfunctions have occurred during this time. Periodic issues with device communication have been encountered, but this was due to the type of cell tower service. We were able to identify an erratic waveform caused by water egression into a connector after the patient showered. Pump function remained normal. Remote monitoring has allowed patients from distant areas to return home and still receive high level monitoring of their LVAD systems.

139

Deairing Techniques for Double-Ended Centrifugal Total Artificial Heart Implantation

J. H. Karimov,[1] D. Horvath,[1] N. Byram,[1] G. Sunagawa,[1] P. Grady,[1] M. Sinkewich,[1] N. Moazami,[1] S. Sale,[2] K. Fukamachi.[1] *[1]The Cleveland Clinic, Cleveland, OH; [2]CardioThoracic Anesthesiology, The Cleveland Clinic, Cleveland, OH.*

Study: The Cleveland Clinic continuous-flow total artificial heart (CFTAH) is a single-piece, valveless, pulsatile pump that provides self-regulated hemodynamic output. The unique device architecture requires specific air removal techniques during implant. The purpose of this study was to evaluate the air removal techniques for CFTAH in vivo implant.
Methods: The air removal techniques were evaluated in chronic in vivo (n=17) CFTAH implants (Jersey calves, weight range 77 - 93 kg). Techniques and pump design iterations consisted of developing the device priming method and addition of built-in deairing ports in early cases (n=5). In the remaining cases without air removal ports (n=12), the air removal was performed in a passive manner (without activation of the pump). First, the side branch (pressure line) of the right outflow graft was used to remove air from the right pump (before declamping the right outflow graft). Then, the air from the left pump was removed in a passive manner from the side branch of the left outflow graft. After removing the left outflow clamp, the CFTAH was started at the minimum speed (2,400 rpm).
Results: All CFTAH pumps were successfully primed with saline prior to implant to remove entrapped air. The deairing ports built-in the pump design were with limited success. There were no clinical signs of air embolism in the pulmonary or systemic circulation observed during the last 12 cases managed with passive deairing and side branches of the outflow grafts. Dedicated air removal ports were not essential design requirement. Careful device priming and passive deairing was found to be an effective measure with this pump design and may be applicable to other rotary pumps. The side branches in the outflow grafts were useful, but the presence in clinical device version would be highly questionable.

146

Monitoring LVAD Performance in Globally Remote Areas

S. Parnis. *none, Missouri City, ÅLAND ISLANDS.*

Study: Monitoring of LVAD performance in patients after they are discharged from the hospital and return home is evolving. Patients who live in remote areas may not have access to experienced, high level mechanically circulatory support care. To decrease hospitalizations and to curtail problems associated with complications which may occur as a result of lack of communication between patient and care givers, a monitoring system which connects a web based application via wireless telephonic transfer of information from the controller allows review of LVAD system performance.
Methods: We have implanted three patients with the ReliantHeart HA5 LVAD who live in remote areas (Middle East and western Asia) which did not have easy available access to advanced mechanical circulatory support care with the ReliantHeart System. Through monitoring of the LVAD true flow waveform we have been able to we evaluate LVAD function (flow, power and speed) and patient physiologic function such as arrhythmias, trends in cardiac contractility, aortic valve opening and left heart volume status. No pump malfunctions have occurred during this time
Results: Periodic issues with device communication have been encountered, but this was due to the type of cell tower service. We have been able to identify an erratic waveform caused by water egression into a connector after the patient showered. Pump function remained normal and the patient returned to our institution for a controller exchange which was performed without any issues. Remote monitoring has allow patients from distant areas to return home and still receive high level monitoring of their LVAD systems.

151

Blood Flow Stagnation at the Descending Aorta After Aortic Valve Bypass: A Patient-Specific Evaluation of Hemodynamics Using Magnetic Resonance Imaging Based Computational Fluid Dynamics Simulation

K. Kawahito,[1] N. Kimura,[2] M. Nakamura,[3] Y. Misawa.[1] *[1]Cardiovascular Surgery, Jichi Medical University, Tochigi, JAPAN; [2]Cardiovascular Surgery, Jichi Medical University, Saitama, JAPAN; [3]Mechanical Engineering, Saitama University, Saitama, JAPAN.*

Study: Descending aortic thrombosis is a rare but fatal potential complication of apico-aortic conduit (AAC). Although it may be caused by stagnation due to the completion of antegrade and retrograde flow, fluid dynamics after AAC have not been fully investigated.
Methods: We analyzed blood flow 1 month after AAC procedure using computational fluid dynamics modeling. Flow waveforms at the boundaries except the ascending aorta were obtained with time-resolved 3-dimensional phase-contrast magnetic resonance imaging. The simulation of aortic blood flow was performed using the SCRYU/Tetra™ software (CRADLE, Inc., Osaka, Japan).
Results: The streamlines showed that blood from the ascending aorta was mostly directed to the aortic branches, while the one from AAC flowed to the lower body. In the meanwhile, little flow was observed in the descending aorta throughout cardiac cycles due to competition of flows from the ascending aorta and AAC (Fig. left). Particle tracking color-coded according to particle residence time clearly visualized entrapment of particles in the descending aorta (Fig. right). Although cardiac output through the aortic valve might change the area of flow competition, the risk of thrombus formation in the descending aorta caused by stagnation must be recognized.

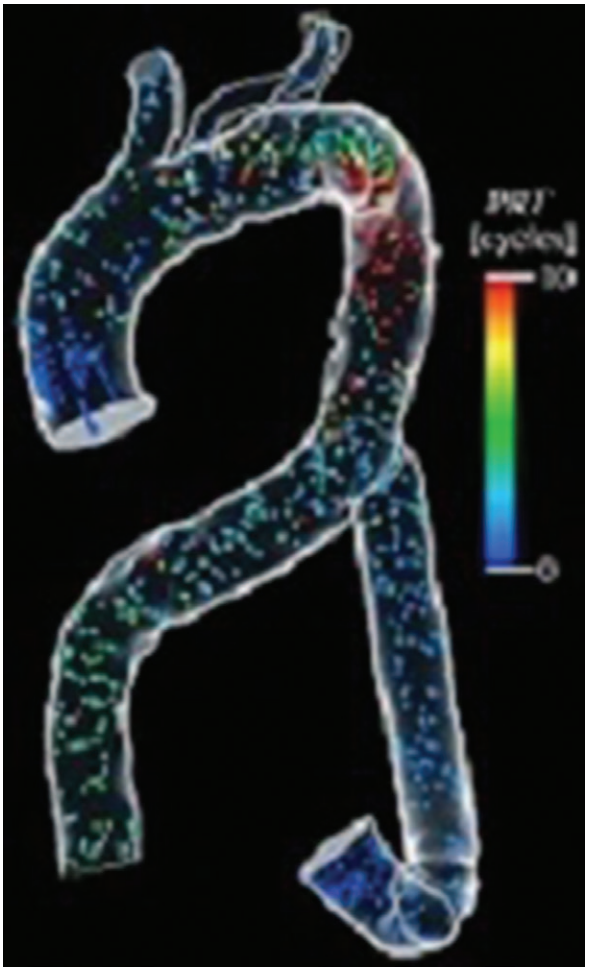

152

Rotational Speed Modulation for Centrifugal Left Ventricle Assist Device Based on Cardiac Cycle (MCC)

T. Leao,[1] J. Fonseca,[2] E. Bock,[1] B. Utiyama,[2] E. Drigo,[3] R. Sa,[1] A. Andrade.[3] *[1]Federal Institute of Sao Paulo, Sao Paulo, BRAZIL; [2]Institute Dante Pazzanese of Cardiology and Sao Judas Tadeu University, Sao Paulo, BRAZIL; [3]Institute Dante Pazzanese of Cardiology, Sao Paulo, BRAZIL.*

Study: This study presents a technique for Rotational Speed Modulation based on Cardiac Cycle (MCC) of Left Ventricular Assist Device (LVAD), allowing aortic valve to work properly. Modulation based on Time (MT) has been worldly studied "in vitro" and in clinical trials, reducing pump rotational speed to allow aortic valve opening.

Methods: An Apical-Aortic Centrifugal Blood Pump is being developed in our laboratory for destination therapy,MCC method has been applied, which uses: heart rate, estimated from variation in motor current; amplitude of rotation speed reduction, adjusted for each patient; number of beats in which rotation speed is reduced to allow opening of the aortic valve; and number of beats of the MCC; e.g., 2 beats cycle once per 20 beats in reduced rotational speed. Hybrid Cardiovascular Simulator (HCS) adjusted to simulate heart failure situations was used. Two types of modulations were compared: MCC and MT. For each modulation method two adjustments were used: 1 beat 20 beats and 2 beats in reduced rotation speed each 20 beats, for MCC; and 3 seconds in reduced rotation speed each minute and 6 seconds in reduced rotation speed each minute, in MT. Rotational speed reduction was 600 rpm for all modulation methods. Effectiveness of aortic valve opening, Mean Arterial Pressure (MAP) and mean flow were monitored for performance evaluation of both modulations.

Results: All modulations were able to allow aortic valve opening during periods of LVAD reduced rotation speed. Both techniques kept the mean flow at physiological level (5 L / min) for all modulations. MAP variation during tests were: MCC (96–101 and 94–101 mmHg); and MT (89–102 and 87–108 mmHg). MCC method was able to allow aortic valve opening at LVAD reduction of rotational speed, keeping mean flow and MAP at physiological condition. Comparing to MT method, MAP variations for LVAD controlled at MCC was smaller. According to literature, smallest changes in MAP can be beneficial to destination therapy and to bridge to recovery.

153

The Combination of Pulmonary Vascular Resistance and he Ratio of Central Venous Pressure to Pulmonary Capillary Wedge Pressure Is a Useful Predictor for Right Ventricular Assist Device Requirement

D. Nitta,[1] K. Kinugawa,[2] T. Imamura,[3] E. Amiya,[1] M. Hatano,[1] O. Kinoshita,[4] K. Nawata,[4] M. Ono,[4] I. Komuro.[1] *[1]Cardiovascular Medicine, The University of Tokyo Hospital, Tokyo, JAPAN; [2]Department of Internal Medicine 2, The University of Toyama, Toyama, JAPAN; [3]Therapeutic Strategy for Heart Failure, The University of Tokyo Hospital, Tokyo, JAPAN; [4]Cardiothoracic Surgery, The University of Tokyo Hospital, Tokyo, JAPAN.*

Study: Thus far right ventricular assist device (RVAD) requirement is associated with poor mortality among those who received left ventricular assist device (LVAD) implantation. Recently several important predictors have been reported, but there is still a controversy about the predictor of RVAD requirement. The purpose of this study was to investigate preoperative predictors for RVAD requirement among those who received LVAD implantation.

Methods: We conducted a retrospective review of 70 consecutive patients with sufficient perioperative clinical data who received extracorporeal pulsatile ventricular assist device (Nipro-VAD) implantation at the University of Tokyo Hospital between 2004–2015. The primary endpoint was RVAD requirement at the time of LVAD implantation as well as within 1 month after the operation. Among the preoperative variables, the ratio of central venous pressure to pulmonary capillary wedge pressure (CVP/PCWP), right ventricular stroke work index (RVSWI), pulmonary artery pulsatility index (PAPi) and pulmonary vascular resistance (PVR) were evaluated.

Results: RVAD requirements were recorded among 14 patients (20%). From the univariate analysis, lower PCWP, lower cardiac output, lower PAPi, lower RVSWI, smaller left ventricular diastolic diameter, higher PVR and higher CVP/PCWP ratio were significantly associated with RVAD requirement (all $p<0.05$). After the multivariate analysis, only PVR and CVP/PCWP ratio were significant predictors [PVR>4.5 (wood unit); p=0.013, OR 7.9, CVP/PCWP>0.8; p=0.001, OR 14.4]. From the odds ratio, we assigned 1 point to PVR>4.5 and 2 points to CVP/PCWP>0.8. These scores efficiently stratified the risk of RVAD requirement [score 0, 2/45 (4.4%); score 1, 2/7 (28.6%); score 2, 5/12 (41.7%); score 3, 5/6 (83.3%)]. The combination score using PVR and the CVP/PCWP ratio was a useful predictor for RVAD requirement.

154

The Effects of Various Gasses on Platelet P-selectin and Leukocyte CD11b Expression in a Rabbit Model of Cardiopulmonary Bypass

A. Mohammed, T. C. Major, J. Toomasian, E. Barletta, B. Drumright, R. H. Bartlett. *Robert H. Bartlett ECLS Laboratory, University of Michigan, Ann Arbor, MI.*

Study: Cardiopulmonary bypass (CPB) is a complex procedure that has been associated with adverse events including platelet activation and loss in platelet count as well as white blood cell activation and its resulting systemic inflammatory response syndrome (SIRS). Previous clinical work has shown that blood exposure to air leads to both platelet and leukocyte activation. However, the mediator of cell activation has not been assessed.

Methods: To determine the mediating effects of air exposure on platelets and leukocytes, an extracorporeal circuit (ECC) was developed in a rabbit model via an arteriovenous shunt with a blood/air reservoir. In addition, in-vitro positive control studies were also done by exposing rabbit blood to lipopolysaccharide (n=3). The ECC reservoir allowed for exposure of no-air (n=4), high-air (n=4), high-N_2 gas (n=4), high-O_2 gas (n=4), or high 100 ppm nitric oxide (NO; n=4). Each experiment was run for 4 hours under systemic heparinization with ACT > 250 s. Platelet count, platelet aggregation, monocyte CD11b expression, and granulocyte CD11b expression were measured at 4 hours.

Results: Platelet counts decrease from baseline for high-air and high-NO, while counts for no-air were preserved (figure 1). Ex-vivo collagen-induced percent platelet aggregation showed a downward trend for high-air indicating that platelets were being activated in-vivo from blood/air exposure (figure 2). CD11b expression from both monocytes and granulocytes was relatively unchanged (figure 3). We hypothesized that CD11b counts in the high-air model would be significantly higher than the no-air group. The surface area of the blood/air interface in our model may need to be increased to upregulate leukocyte activation, thereby increasing CD11b counts. We also hope to see attenuated CD11b counts in the high-NO group. The model does show activation of platelets with the high-air group, similar to CPB circuit.

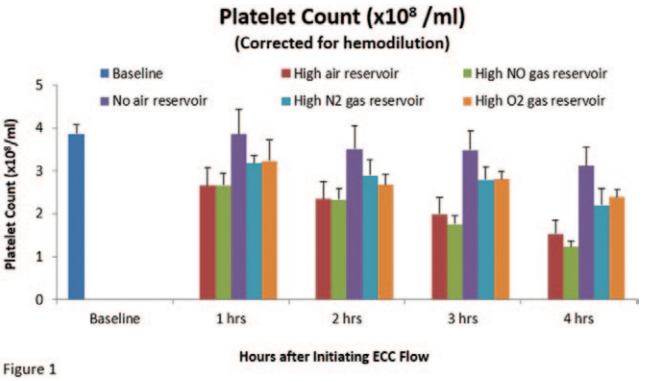

Figure 1

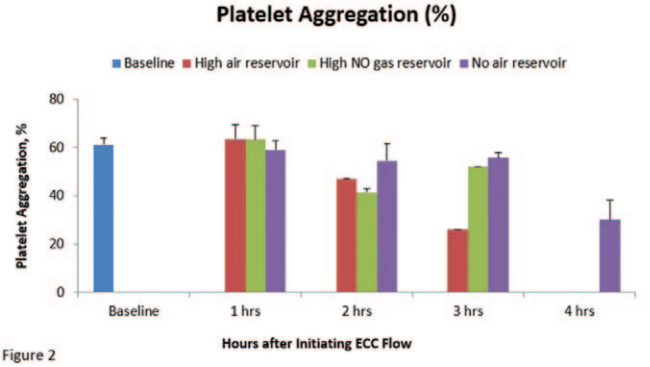

Figure 2

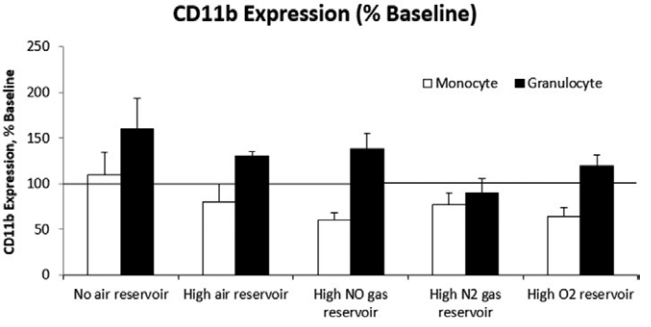

Figure 3

155

A Novel Device for Venous Retroperfusion of the Myocardium; Preliminary *in vitro* Results

G. Pantalos,[1] L. Cahalan,[2] M. Gartner,[2] P. Cahalan.[2] [1]*University of Louisville, Louisville, KY;* [2]*Ension, Inc., Pittsburgh, PA.*

Study: Approximately 15% of patients with coronary artery disease are not suitable for coronary artery bypass grafting (CABG) or percutaneous transluminal coronary angioplasty (PTCA). Ension is developing a system for these "no option" patients to re-establish flow of oxygenated blood to tissue that had been reduced due to stenosis or occlusion from emboli as an alternative or adjunct to PTCA, CABG, mechanical circulatory support, or transplantation. Ension's concept connects the left ventricle (LV) to the anterior interventricular vein (AIV) using a device specifically designed to achieve safe and effective myocardial venous retroperfusion. Preliminary *in vitro* evaluation of this device was conducted in a pulsatile mock loop to explore coronary flow over the cardiac cycle.
Methods: A mock circulation using a blood analogue was used to simulate normal and moderate heart failure. Flows and pressures in the aortic root (AoP), LV-AIV device, and a dynamic coronary resister (DCR) were measured using Transonic flow probes and Millar catheters. The DCR provided a cyclic increase in coronary vascular resistance coincident with LV systole as occurs physiologically. Normal cardiac function was simulated (cardiac output of 5 L/min with an AoP of approximately 120/80/95 and a heart rate of 72 beats/min) and moderate heart failure with reduced cardiac output (3.5 L/min) and AOP (100/50/65). For each condition, passive coronary flow (DCR off) and flow with DCR activated was investigated.
Results: Supplemental blood flow to the myocardium via the LV-AIV device for both normal and LV dysfunction was observed. When the DCR was activated, flow through the DCR branch to the myocardium, while diminished as expected, remained sufficient (25 to 30 mL/min) to augment myocardial retroperfusion, concomitant nutrient transport, and waste removal without excessive increase in venous vascular pressures.

157

Time-Resolved Detection of Platelet Activation and von Willebrand Factor Cleavage in Deep Suspensions

J. Biasetti,[1] K. Sampath,[1] A. Cortez,[2] A. Azhir,[1] A. A. Gilad,[2] T. Kickler,[2] J. Katz.[1] [1]*Johns Hopkins University, Baltimore, MD;* [2]*Johns Hopkins School of Medicine, Baltimore, MD.*

Study: High shear stresses generated in Left Ventricular Assist Devices (LVADs) are thought to enhance platelet (PLT) activation and von Willebrand factor (vWF) cleavage within them. The aim of this work is to develop optical techniques for time-resolved detection of PLT activation and vWF cleavage in deep suspensions of the same scales as those of LVADs. These tools are aimed at imaging these phenomena in transparent LVADs replica.
Methods: The calcium sensitive probe Indo-1 is employed for detecting PLT's intracellular calcium release, the first step in the activation process. Recombinant vWF-eGFP and human vWF labeled with a IgG:FITC are used to visualize vWF cleavage and its interaction with PLTs. LEDs with excitation filters illuminate the samples, and images are recorded by a high-speed, high-sensitivity EM-CCD camera equipped with long-range objectives and emission filters transmitting only the relevant fluorescence wavelengths. An in-house post-processing algorithm has been developed to enhance and track the signals.
Results: The labels and imaging methods readily track cells and vWF multimers in deep suspensions. Activation of Indo-1 loaded PLTs by thrombin causes a substantial increase in the fluorescence intensity of moving cells, demonstrating the viability of this approach. Shear-induced mechano-enzymatic cleavage increases the number of free floating rVWF-eGFP multimers by an order of magnitude, making the number of fragments a convenient method for detecting cleavage. Transition of vWF multimers from a globular to a stretched configuration is also observed. As for the PLT-decorated vWF:IgG:FITC strands, changes to their size provide clear evidence of both fragmentation and thrombotic processes induced by shearing.

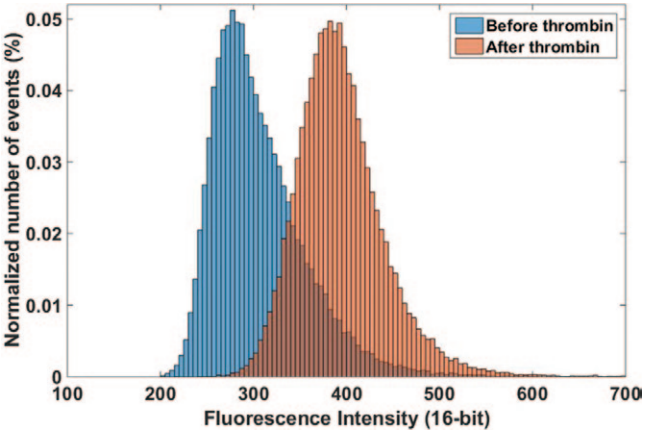

162

Native Cardiac Output May Influence Stroke Risk in LVAD Patients

V. Chivukula,[1] P. McGah,[1] A. Prisco,[2] J. Beckman,[3] G. Garcia,[2] N. Mokadam,[4] C. Mahr,[3] A. Aliseda.[1] *[1]Mechanical Engineering, University of Washington, Seattle, WA; [2]Biotechnology and Bioengineering Center, Medical College of Wisconsin, Milwaukee, WI; [3]Division of Cardiology, University of Washington, Seattle, WA; [4]Division of Cardiothoracic Surgery, University of Washington, Seattle, WA.*

Study: The prevalence of medical-therapy refractory advanced heart failure, coupled with a stagnant pool of donor hearts have resulted in increased use of Left Ventricular Assist Devices (LVADs). Significant advances in LVAD design and management have achieved 1-year survival rates approaching 90%. LVAD patients, however, remain at risk for neurologic events. Moreover, current standard-of-care does not include recommendations for LVAD management strategies permitting aortic valve (AV) opening and accounting for residual native cardiac output and blood pressure to reduce blood stasis and shear rate exposure, which may impact the thrombogenic potential of the device.
Methods: This study uses unsteady computational fluid dynamics (CFD), virtual surgery and Lagrangian analysis on 3D patient-specific models of the aortic arch and great vessels to evaluate the anti-thrombotic potential of intermittent aortic valve opening in a near-optimal LVAD outflow graft to aorta angle of 45°. In addition to global hemodynamic parameters, Lagrangian tracking of platelet surrogates (particles) is applied to the computational hemodynamics, and the particle's shear stress histories (SH) and residence times (RT) are calculated.
Results: Intermittent aortic valve opening, providing a small but measurable native cardiac output (~1 l/min), at a reduced frequency of 12 openings per minute has an immediate effect in reducing global aortic wall shear stress resulting from impingement of the LVAD outflow graft jet on the contralateral arterial wall. Lagrangian tracking of blood-suspended cells reveals that aortic valve opening significantly reduces SH and RT for cells that would otherwise stagnate in the aortic root region. This reduction in thrombogenicity at all angles of the LVAD outflow graft show that advanced VAD management strategies that enable intermittent aortic valve opening can lead to a more favorable aortic valve/root flow pattern and may decrease thrombotic risk.

163

Inflow Cannula Angulation Influences Risk of Thrombosis in LVAD Patients

J. Beckman,[1] **V. Chivukula**,[2] P. McGah,[2] A. Prisco,[3] G. Garcia,[3] A. Aliseda,[2] N. Mokadam,[4] C. Mahr.[1] *[1]Division of Cardiology, University of Washington, Seattle, WA; [2]Mechanical Engineering, University of Washington, Seattle, WA; [3]Biotechnology and Bioengineering Center, Medical College of Wisconsin, Milwaukee, WI; [4]Division of Cardiothoracic Surgery, University of Washington, Seattle, WA.*

Study: The prevalence of medical-therapy refractory advanced heart failure, coupled with stagnant heart donor numbers, have led to increased use of Left Ventricular Assist Devices (LVADs). Significant advances in LVAD design and management have achieved 1-year survival rates approaching 90%. LVAD patients, however, remain at risk for neurologic events. Our working hypothesis is that the implantation angle between LVAD inflow cannula and ventricular axis can significantly influence ventricular hemodynamics, leading to an increase in thrombosis risk.
Methods: Unsteady computational fluid dynamics (CFD) is used in combination with virtual surgery to study the hemodynamics in 3D patient-specific models of the left ventricle (LV) with a standard inflow cannula implanted at the ventricular apex. Novel Lagrangian analysis is used to evaluate the shear stress histories (SH) and residence times (RT) of particles (platelet surrogates) along their trajectories through the LV. Inflow cannula orientations between -21° and +14° are modeled and thrombogenic metrics along both the ventricular wall and the particle trajectories are compared to determine relative risk.
Results: Wall shear stress on the ventricular wall shows significant influence of the cannula angle: larger angles, particularly towards the septum, increase shear stress. While the average values of particles SH and RT do not change, a small but significant number of particles are found to stagnate within the LV for >10 cardiac cycles. The number of these long-residence-time platelets strongly depends on cannula angle. The strongly asymmetric flow into the cannula traps platelets in the narrow gap between the cannula and the ventricular wall, thus leading to increased RT/SH. LVAD inflow cannula surgical orientations that are misaligned with respect to the ventricular axis create conditions under which platelets can activate and agglomerate for long periods of time (~100s of seconds) increasing risk of thrombus entrainment into the LVAD.

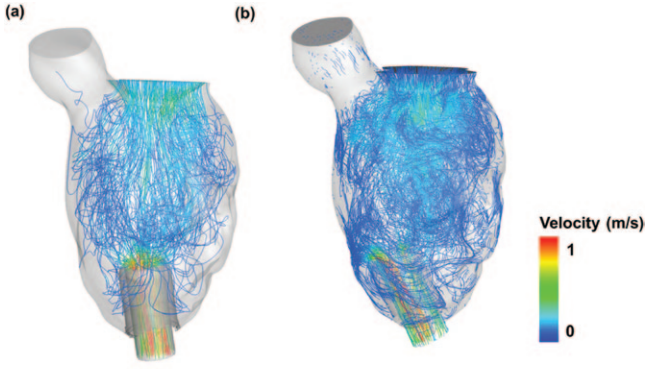

Figure 1: Pathlines depicting paths taken by particles traversing the ventricle for (a) 0^{o} and (b) -14^{o} inflow cannula orientation. A strong asymmetrical flow and recirculation regions can be observed for the -14^{o} case.

165

Left Ventricle Size May Impact LVAD Thrombosis Risk

A. Aliseda,[1] **V. Chivukula**,[1] P. McGah,[1] A. Prisco,[2] J. Beckman,[3] G. Garcia,[2] N. Mokadam,[4] C. Mahr.[3] *[1]Mechanical Engineering, University of Washington, Seattle, WA; [2]Biotechnology and Bioengineering Center, Medical College of Wisconsin, Milwaukee, WI; [3]Division of Cardiology, University of Washington, Seattle, WA; [4]Division of Cardiothoracic Surgery, University of Washington, Seattle, WA.*

Study: Treatment for end-stage heart failure (HF) patients with Left Ventricular Assist Devices (LVADs) approaches 90% survival at 1 year post-implantation. Inertia-driven blood flow inside the left ventricle (LV) can induce significant hemodynamic variability in the LV and inflow cannula. The coupling of the mitral valve vortex ring during ventricular filling and the quasi-steady suction from the LVAD determine residence times (RT) and shear stress histories (SH) of the blood-suspended cells entrained by the LVAD, influencing thrombosis risk. Our working hypothesis is that patients with smaller ventricles may be more prone to thrombosis due to the flow patterns established inside the left ventricle. The goal is to provide support for this clinical observation, and quantify this phenomenon, to aid in clinical decision-making

Methods: Unsteady computational fluid dynamics (CFD) is used in combination with virtual surgery to evaluate flow patterns in 3D patient-specific left ventricle models with a standard LVAD inflow cannula in an apical anastomosis. Novel Lagrangian analysis is applied to the CFD data to evaluate the thrombogenic potential as a function of patient's ventricular size. LV sizes ranging from 3 cm - 7cm are studied, and metrics for both the flow pattern of wall shear stress and the Lagrangian platelet-specific SH and RT are compared

Results: Trajectories for platelet surrogates are computed over 10 cardiac cycles in each of the patient-specific anatomical LV models. Higher wall shear stress is observed for smaller ventricles, along with extreme values in the distribution of platelet SH and RT. Platelets are trapped in the narrow space between the ventricle wall and the cannula, particularly near the ventricle apex. These platelets are subject to high SH and RT due to recirculation and only occasional mixing with bulk flow entering the LVAD, which increases risk of platelet activation and aggregation. Thus, LV size is an important factor in LVAD implantation, with significant implications for thrombosis risk.

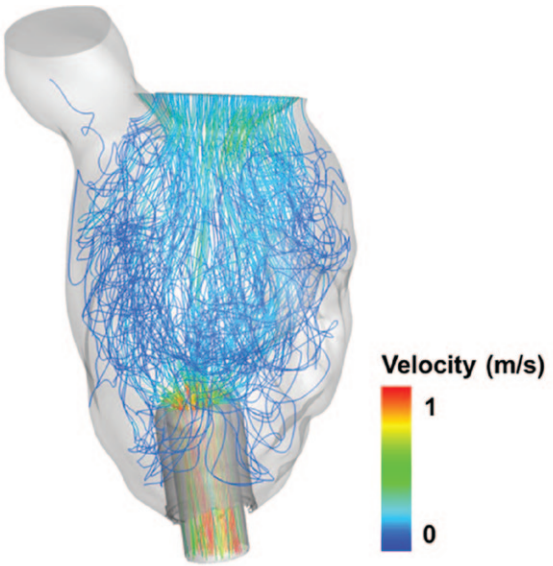

Figure 1: Pathlines for particles traversing a normal sized LV over 1 cardiac cycle with the inflow cannula aligned at 0° with respect to the surgical axis (line connecting LV apex to mitral valve) .

167

Hysteresis Levitation Motor for Adult and Pediatric Extracorporeal Life Support

M. Noh,[1] **M. Gartner**,[2] D. Trumper.[1] *[1]Mechanical Engineering, Massachusetts Institute of Technology, Cambridge, MA; [2]Ension, Inc., Pittsburgh, PA.*

Study: Magnetic levitation enables contact-free impeller operation thereby eliminating critical areas of wear and heat generation that can contribute to hemolysis and thrombosis. We propose an innovative magnetic levitation system for extracorporeal life support (ECLS) applications based on a hysteresis motor concept. Our design permits a smaller overall configuration, eliminates magnetic field safety concerns, reduces vibration, and locates the more costly rare earth magnetic elements in the reusable motor stator. The hysteresis motor design also facilitates simplified control algorithms for enhanced robustness and reduced power requirements to improve patient transport mobility. As the initial development step, this hysteresis motor will be integrated into Ension's pediatric cardiopulmonary assist system (pCAS) to evolve the current mechanically supported blood pump element of the system to a fully levitated design.

Methods: We have designed and fabricated a ring-shaped hysteresis rotor (D2 steel) accommodating a flux-biasing structure in the center to be utilized with an accompanying hysteresis motor and a LabVIEW based control system. The prototype hysteresis motor will be evaluated to characterize the full torque-speed performance and determine whether the motor satisfies the target specification and maximum static force.

Results: We intend to undertake preliminary testing to demonstrate the motor torque and stiffness capabilities as well as integrate the hysteresis motor into the current Ension pCAS impeller with minimal modifications.

168

Performance of the Heartmate II Risk Score in an External Validation Cohort

A. Taggarse, S. Schettle, L. D. Joyce, J. Stulak, S. Maltais, R. Daly, B. Lahr, S. Dunlay, D. L. Joyce. *Mayo Clinic Hospital- Saint Marys Campus, Rochester, MN*.

Study: The Heartmate II Risk Score (HMRS) predicts 90 day and 2 year mortality based on an assessment of pre-operative age, albumin, creatinine, INR, and center volume. We hypothesized that this model would be limited in practical application due its failure to account for clinically important risk factors that occur within a large volume tertiary referral center.

Methods: We retrospectively reviewed 192 implants from our institution over a five year period. Patients were included in the study if they underwent LVAD therapy as destination therapy (DT) or bridge to transplant (BTT) with one of the currently approved continuous flow devices. HMRS was calculated and analyzed using Kaplan Meier survival curves over 90-day and 2- year follow-up. The prognostic performance of HMRS was further evaluated with the use of logistic regression (including c-statistic) for predicting 90-day mortality and Cox regression for 2-year mortality.

Results: In 192 patients (median age, 62 years; 80% male) used to validate the prognostic ability of HMRS, the majority (61%) were classified as low risk from the applied score (median [range], 1.4 [-7.1 to 5.0]). For prediction of 90-day mortality in this external cohort the HMRS showed a comparable c-statistic (*c*=0.70) to the derivation data set, as well as significant differences in survival across risk strata (Figure 1, p=0.011). When extended to 2 years of follow-up, there is an overall survival difference among risk strata (Figure 2, p<.001) but no difference in the contrast between middle and high risk groups (p=0.96). The influence of individual HMRS factors on outcomes revealed marginal to significant associations for age, albumin and creatinine, but no association of INR with survival time for either 90-day (p=0.62) or 2-year (p=0.65) follow-up. These results demonstrate external validation for the 90-day score, with comparable c-statistics to the derivation data set. However, the utility of this risk model was diminished when making observations beyond 90 days.

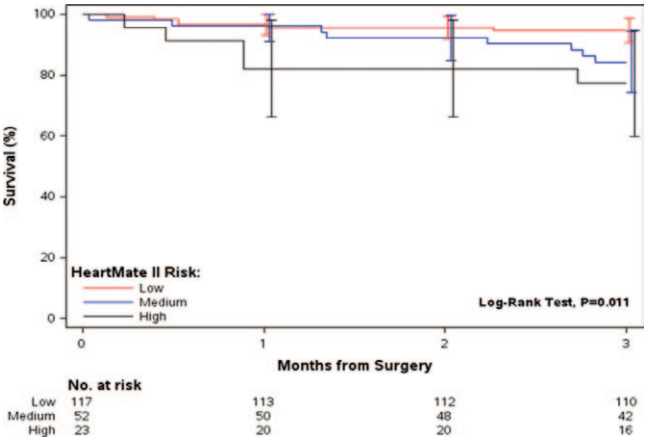

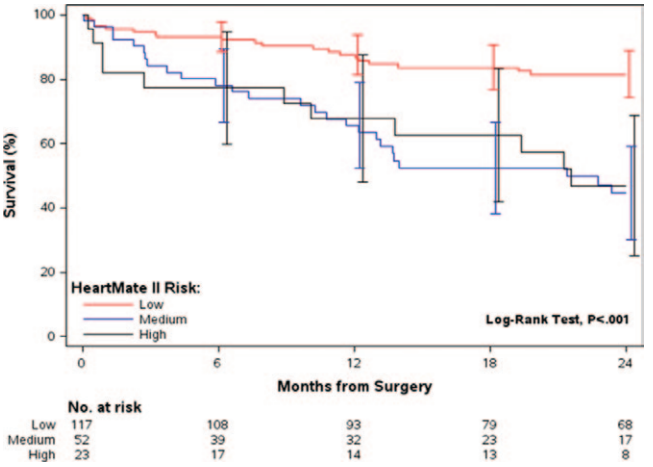

169

Destination Therapy by Choice: Patients' Perspectives on Why Ventricular Assist Device Therapy May Be Preferable to Cardiac Transplantation

L. A. Wilhelms, J. Blumenthal-Barby, E. D. Delgado, K. M. Kostick, C. R. Bruce. *Baylor College of Medicine, Houston, TX.*

Study: Left-ventricular assist device (LVAD) therapy is a growing mechanical circulatory support (MCS) therapy used to treat patients with advanced heart failure. There is a general assumption among clinicians that patients who are eligible for a heart transplant would prefer to accept a heart to other treatment. However, little research has been done to clarify the nuances of patient treatment preferences for LVAD therapy versus transplantation. The objectives of this retroactive study were to investigate this treatment preference assumption.
Methods: Sixty in depth, structured interviews following the Ottawa framework were conducted with patients currently living with the device (LVAD patients, n=15), patients making a decision about whether to receive the device (LVAD candidates, n=15), patients who declined LVAD implantation (LVAD decliners, n=15), and patient caregivers (caregivers, n=15). LVAD patient and candidate group consisted of both bridge-to-transplant (BTT, n=4), destination therapy (DT, n=22), and undesignated candidates (n=4). Interviews were analyzed with ATLAS.ti and coded independently by team members.
Results: Three themes emerged, suggesting that some patients become ambivalent in their treatment preference as they experience LVAD therapy or they may self-designate to LVAD therapy as a long-term treatment. 1) Unwanted consequences of multiple surgeries (n=19), 2) fears surrounding lifestyle changes of accepting a heart transplant (n=13), and 3) life satisfaction with an LVAD as a "new normal" (n=13). These findings were surprising given that the prevailing assumption among clinicians is that all eligible patients would prefer a heart transplant rather than continued therapy on the LVAD. Based on these findings, providers must reaffirm patients' values and goals at multiple points after LVAD placement as well as engage in shared decision-making in the context of those evolving values and goals.

171

Cardiopulmonary Bypass With Low-versus High-blood Contact Surface Area: Comparison of Cytokine Level DuringCardiopulmonary Bypass in a Rat Model

Y. Fujii,[1] M. Shirai,[2] Y. Takewa,[3] E. Tatsumi.[3] *[1]Department of Artificial Organs, Department of Clinical Engineering and Medical Technology, National Cerebral and Cardiovascular Center Research Institute, Niigata University of Health and Welfare, Suita, Niigata, JAPAN; [2]Department of Cardiac Physiology, National Cerebral and Cardiovascular Center Research Institute, Suita, JAPAN; [3]Department of Artificial Organs, National Cerebral and Cardiovascular Center Research Institute, Suita, JAPAN.*

Study: Systemic inflammatory responses in patients receiving cardiac surgery supported by cardiopulmonary bypass (CPB) significantly contribute to CPB associated morbidity and mortality. Previous studies have suggested that the interaction of blood and large artificial surface contributes to inflammatory response during CPB. As a result of a series of chain reactions, the numerous powerful inflammatory mediators are formed and released. We hypothesized that small CPB circuit which reduces blood contact surface area attenuates cytokine levels during CPB.
Methods: Rats were divided into the large surface area CPB (priming volume: 15 ml, surface area: 0.044 m^2) group and the small surface area CPB (priming volume: 7 ml, surface area: 0.036 m^2) group. CPB pump flow was maintained at 80 ml/kg/min. Blood samples were collected pre, 60 and 120 min after initiation of CPB. We measured the serum cytokine levels (TNF-α, IL-6, IL-10) and wet-to-dry (W/D) weight ratio of the left lung tissues postmortem after 120 min CPB.
Results: Pro-inflammatory markers (TNF-α, IL-6) and biochemical markers were significantly elevated in the large surface area CPB group compared with the small surface area CPB group at 60 min (TNF-α: large vs small: 856 ± 65 vs. 444 ± 34 pg/ml, IL-6: large vs small: 695 ± 62 vs: 292 ± 85 pg/ml). At 120 min, however, none of the markers was statistically different between the 2 groups (TNF-α: large vs small:1237 ± 61 vs. 1129 ± 137 pg/ml, IL-6: large vs small: 1226 ± 132 vs. 1158 ± 150 pg/ml). The W/D ratio increased significantly more in the large surface area (high priming volume) CPB group than in the small surface area (low priming volume) group (6.01 ± 0.11 vs 5.46 ± 0.09). These data suggested that in addtion to the blood contact surface area factor, the CPB exposure duration is also an important factor for causing the systemic inflammatory response.

173

Oxidative Stress and Endotoxemia Potentiate Free Hemoglobin (Hb)-induced Blood-Brain Barrier (BBB) Disruption

J. Simoni,[1] G. Simoni,[1] J. F. Moeller,[1] J. Gresham,[2] J. X. Castillo,[3] P. Simoni,[4] D. E. Wesson.[5] *[1]Texas HemoBioTherapeutics & BioInnovation Center, Lubbock, TX; [2]Texas A&M College of Veterinary Medicine and Biomedical Sciences, College Station, TX; [3]Universidad Autónoma de Guadalajara School of Medicine UAG, Guadalajara, MEXICO; [4]Texas Tech University Health Sciences Center and Covenant Medical Center, Lubbock, TX; [5]Texas A&M College of Medicine, Baylor Scott and White Health, Temple, TX.*

Study: To be neurotoxic, Hb released during excessive intravascular hemolysis must cross the BBB or result from lysis of extravasated RBC during intracerebral or subarachnoid hemorrhage. Hb has well-documented vasoconstrictive, pro-oxidative, pro-inflammatory and pro-apoptotic potentials and is known for its detrimental effect on endothelial cells (EC). Since the BBB is a highly selective permeability barrier with tight junctions between EC, it will be important to know if besides direct impact of Hb on EC, other factors facilitate Hb trafficking across.
Methods: Human brain capillary EC (Cambrex, Walkersville, MD) were cultured to confluence on 0.4 um polycarbonate membrane cell culture devices (Whatman, Clifton, NJ), unsiliconized glass coverslips and 12 well plates, and incubated with Hb (0.2 mM), endotoxin (10 EU/mL), hydrogen peroxide (100 uM), alone and in combinations. The BBB permeability was evaluated based on the diffusion rate of 125-I albumin (DPC, Los Angeles, CA) and Hb. Formation of gaps between EC was measured by photodensitometric technique. EC oxidative stress was monitored by intracellular GSH and lipid peroxidation. EC apoptosis was studied utilizing Apoptosis Detection Kit Annexin V-FITC (Sigma, St. Louis, MO). Saline treated EC served as a control. All experiments were done in triplicate and data subjected to statistical analyses.
Results: The observed changes are indicative of the detrimental effect of Hb on human brain capillary EC. Hb-induced EC oxidative stress correlated with increased BBB permeability. Endotoxin and hydrogen peroxide alone also carry ability to impact the BBB. Combination of Hb + endotoxin, Hb + hydrogen peroxide and Hb + endotoxin/hydrogen peroxide exponentially accelerated EC damage and compromised the BBB.
Conclusion: Oxidative stress and endotoxemia may significantly increase the BBB permeability to Hb, therefore facilitating its neurotoxic potential in subjects with excessive intravascular hemolysis.

174

Transcranial Detection of Signals (HITS/ MES) in an Implantable Pump Compared with a Non-implantable Pump (Preliminary Study)

K. Sato,[1] T. Nakajima.[2] *[1]Niigata Univ., Niigata Hsp, Niigata, Kashiwazaki, JAPAN; [2]NHO, Niigata Hsp, Kashiwazaki, JAPAN.*

Study: The severest complications in the postoperative management of cases with a left ventricular assist device are thromboembolism and bleeding. The control of anticoagulation has often been discussed, but reports of a practical approach to monitoring thromboembolism are rare. Transcranial detection of HITS/ MES (high intensity transient signals/ micro-embolic signals) for the prevention of cerebral infarction is clinically performed in patients with neuro-vascular disease and the nature of HITS/ MES has been clarified. Undoubtedly because the device cannot be directly seen, the approach may be more useful for patients with an implantable ventricular assist device.
Methods: In the second study, in patients who underwent implantation of new implantable pumps or a non-implantable pump, HITS/ MES were measured for 30 minutes using a Pioneer TC2020 ultrasound system at postoperative month 1 or later. A transcranial Doppler probe was placed on the right temporal window, i.e. at the right middle cerebral artery.
Results: Firstly, in patients supported with non-implantable Nipro-Toyobo-LVAS (Left Ventricular Assist System), the high-frequency counts in HITS/ MES were greater than the low-frequency counts (n=7, P=0.025) and both counts may increase with time. The high-frequency signals may imply air microemboli, confirmed for the first time in clinical cases with a ventricular assist device, without significant postoperative events in all patients. Secondly, in the long-term follow-up period, no HITS/ MES were determined in patients with the implantable new devices (EVAHEART, DuraHeart and Jarvik-2000), postoperatively uneventful, compared to many HITS/ MES in the patients with the non-implantable device (3 vs. 3, with significance). This suggests superiority for the prevention of embolic events of the new non-pulsatile devices and better intensive care in these cases.

180

Long Term Outcomes Following a Continuous Flow Left Ventricular Assist Device Exchange

L. Coyle, C. Gallagher, G. Bhat, P. Pappas, **A. Tatooles**. *Heart and Vascular Institute, Advocate Christ Medical Center, Oak Lawn, IL.*

Study: The goal is to examine long term outcomes of patients (pts) undergoing a CF-LVAD exchange at a single high volume center.
Methods: All pts (n=407) at our institution implanted with a CF-LVAD between March 2005 and February 2015 were retrospectively reviewed. Preoperative demographics, indication for device exchange, days on devices, surgical approach, and hospital length of stay, discharge placement, operative mortality, survival using the Kaplan-Meier analysis and cause of death were determined.
Results: A total of 56 (13.8%) pts (43 male, 13 female), average age 58 (range 26–80) underwent 59 device replacements, 3 pts required a 3rd device as a result of recurrent pump thrombosis. The majority (91%) of pts were implanted for destination therapy and had a Heartmate 2 LVAD (93%). Surgical indications for device exchange included percutaneous lead damage (28 events, 6.9%), device thrombosis (18 events, 4.4%), infection (9 events, 2.2%), and suspected device malfunction (1 event, .3%). The median time to device exchange was 651 days (range, 4-2188). A sternotomy was employed in 88% (n=49) of pts. The median length of stay postoperatively was 18 days (range 4–62). Discharge outcomes included 68% (n=38) to home, 12.5% (n=7) acute rehab, 7% (n=4) long term acute care hospital, 1.8% (n=1) subacute rehab, 1.8% (n=1) home with hospice and 8.9% (n=5) early operative mortalities (median days on device 18, range 7–42). The median length of support on second device was 521 days (range 1-1991). Overall actuarial survival after device exchange (n=56) was 75% at 1 yr and 62% at 2 yrs. Cause of death before 1 yr included: 37% (n=5) HCVA, 7% (n=1) ICVA, 21% (n=3) pump thrombosis, 14% (n=2) RV failure, 14% (n=2) MSOF, and 7% (n=1) cardiac tamponade. CF-LVAD exchange is required in a small cohort due to device related complications. Despite initial device failure, continued long term support is demonstrated with 1 and 2 year survival rates after device exchange approaching the same as those with an original implant.

184

Clinical Outcomes in Patients with a Mechanical Aortic Valve Undergoing Left Ventricular Assist Device Placement

R. Issa, G. Macaluso, A. Tatooles, P. Pappas, G. Bhat, S. Pauwaa. *Advocate Christ Medical Center, Oak Lawn, IL.*

Study: The presence of a pre-existing mechanical aortic valve (mAV) in patients undergoing left ventricular assist device (LVAD) implantation is considered to increase risk of thromboembolic complications (TEC). Replacement of a mAV with a bioprosthetic valve however increases the risk of surgery. There is minimal information on clinical outcomes of patients with mAV undergoing LVAD, especially those undergoing implantation for destination therapy (DT). We present a case series of 3 patients with mAV undergoing DT LVAD.
Methods: Following a retrospective review of 300 consecutive LVAD implants, we identified 3 patients with mAV in place at the time of DT LVAD implantation. Patient demographics, medical history, postoperative outcomes were examined.
Results: 3 patients with mAV underwent LVAD implantation for DT. The first is a 61 year-old male with history of cerebrovascular accident (CVA), atrial fibrillation (AF) and a mAV originally placed in 1992. He was implanted with a HeartMate XVE in 2008 which was replaced in 2009 with a HeartMate II (HMII) due to device malfunction. Pre-operative cardiac computed tomography revealed massive thrombosis in the ascending aorta (Figure 1). Over 2557 days of follow up he has not had any TEC. The 2nd patient is an 81 year old male with history of CVA, AF, and mAV placed in 1990. He underwent HMII implantation in 2014. At 703 days of follow up he has not had any TEC. The final patient is a 73 y/o male with history of AF and mAV placed in 1999. He underwent HMII implantation in 2016. At 36 days of follow up he has not had any TEC. All patients have been maintained on aspirin and Coumadin with a goal INR of 2–3.

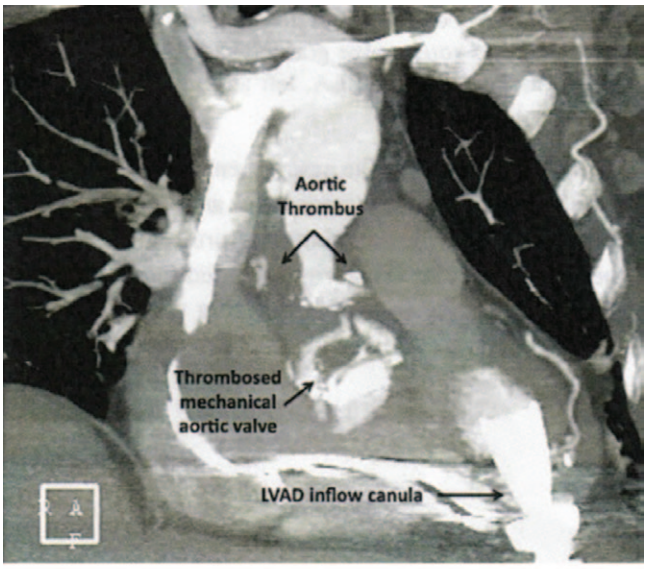

Figure 1 Maximum intensity projection image in the coronal plane (window width, 750; level, 150) showing extensive thrombus (116 HU) in the aortic trunk with a thrombosed aortic valve and the LVAD inflow canula anastomosed to the left ventricle.

201

International Normalized Ratio (INR): Time in Therapeutic Range for VAD Patients

J. Bennett, P. Combs, A. Hudson. *Heart Specialty Care and Transplant Center, Seton Medical Center Austin, Austin, TX.*

Study: Ventricular Assist Device (VAD) as a treatment for end-stage heart failure is becoming more widely accepted. Because of the function and structure of these devices, warfarin is necessary to prevent thrombosis within the pump. Some possible complications noted with this therapy are device thrombosis, cerebral vascular accident (CVA), gastrointestinal bleeding (GIB) and epistaxis. By measuring and analyzing time in therapeutic range (TTR), we hope to determine the relationship between bleeding/embolic complications and TTR. This study, using baseline data as the preliminary analysis will be used to compare with future data.
Methods: TTR is determined as the number therapeutic INRs divided by the number of INRs completed since July 1, 2014 until December 31, 2015 for 36 patients. The standard of care for INR testing is weekly but patients were tested more frequently if out of range. INR data was analyzed using descriptive analysis for each patient's INR goal. If the goal changed over time, it was noted in the patient's medical record.
Results outside TTR were broken down into values above and below TTR.
Results: There were 912 therapeutic INRs and 1934 INRs total with 56.61% of INRs within therapeutic range. The out of range INRs were further delineated to below range (19.64 %) and above range (19.95%). A limitation in the data is indication bias as more testing is completed to ensure INR is trending toward therapeutic range when INR is not in range. Determining TTR is a starting point for programs to assess INR management and complications that arise from warfarin in VAD patients. Additional data analysis is needed using chi-square analysis to test for an association to fully understand the relationship between TTR and complications in this patient population.

202

Liposome-encapsulated Hemoglobin Protects Ischemic Myocardium by Preserving Hemodynamics and Oxygen Consumption in the Rat - A Concept of Biological Circulatory Support

A. T. Kawaguchi,[1] M. Yamano.[2] *[1]Cell Transplantation and Regenerative Medicine, Tokai University School of Medicine, Isehara, JAPAN; [2]Osaka Prefecture University, Habikino, JAPAN.*

Study: Liposome-encapsulated hemoglobin (LEH), a cellular artificial O_2 carrier, has been reported to help contain extra O_2 in the plasma, preserve peripheral perfusion due to its nanometer size (250 nm) and increased O_2 affinity (targeted O_2 delivery), alleviate heart rate response on submaximal cardiopulmonary exercise, thereby help maintain hemodynamics by compensating decreased cardiac output in heart failure.
Methods: Rats underwent myocardial ischemia (MI) and reperfusion (I/R) by occlusion and release of the left anterior descending artery for 40 min under monitoring respiratory gas analyses for O_2 consumption (VO_2) and CO_2 production (VCO_2) as well as repeated left ventricular pressure-volume relationship (PVR) recordings for myocardial function. The animals were pretreated with LEH with high O_2 affinity (h-LEH, 10 mL/kg, n=8), low O_2 affinity (l-LEH, 0 mL/kg, n=7), homologous red cells (RBC, n=6) and saline (n=8) as controls. These monitoring were repeated before, 10, 20 and 40 min after induction of MI and 20 and 40 min after reperfusion, when whole heart was excised for histological studies.
Results: While VO_2 and VCO_2 were preserved steady in all animals regardless of infused solutions, ejection fraction, stroke volume and cardiac output were better preserved in the order of rats treated with saline, RBC, and LEHs regardless of O_2 affinity. Summed area of myocardial damages was larger and wider in the reversed order (Figure).
Summary: The results suggest that LEH may keep VO_2, VCO_2 and hemodynamics steady while cardiac performance is suppressed to eventually protect myocardium in I/R. Although these effects need to be studied as a therapeutic use after MI and followed longer to seek chronic and eventual benefits of LEH, these unique characteristics conform a treatment of myocardial I/R injury as a model of biological circulatory support.

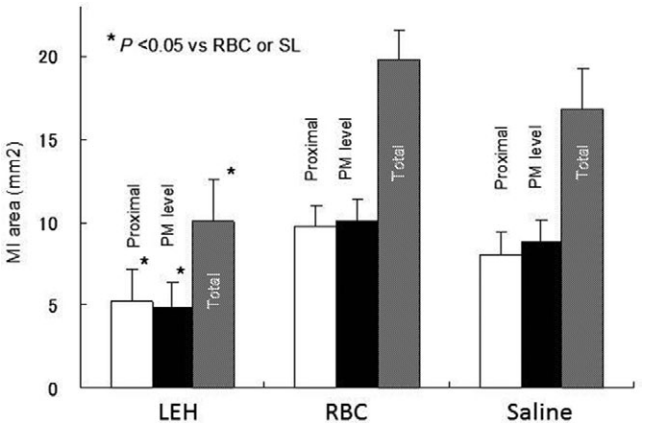

208

Impact of the HeartWare Ventricular Assist Device Lavare Cycle on Intraventricular Flow Patterns

P. Aigner,[1] F. Moscato,[1] M. Stoiber,[1] D. Zimpfer,[2] **H. Schima**.[1] *[1]Medical University of Vienna; Ludwig Boltzmann Cluster for Cardiovascular Research, Vienna, AUSTRIA; [2]Medical University of Vienna; Department of Cardiac Surgery, Vienna, AUSTRIA.*

Study: Thromboembolic events in mechanical cardiac support patients are often related to blood flow stagnation within the supported ventricle due to altered flow patterns. The HeartWare® Ventricular Assist Device (HVAD®) includes a periodic pump speed modulation (LavareTM cycle) to ameliorate flow patterns and reduce areas of potential blood stasis. Effects of these speed changes were investigated in an in-vitro model.
Methods: The impact of the Lavare cycle was investigated in a transparent left ventricular model and flow patterns were analyzed with Particle Image Velocimetry. A baseline speed of 2800 rpm was used and situations compared where the Lavare cycle was on (LON) and where the Lavare cycle was off (LOF). Fluid dynamics parameters (standard deviation σ over the measurement period for characterization of flow variation; angular dispersion r of the flow direction for identification of constant flow directions, stagnation index SI for washout) were calculated and compared for the two situations.
Results: Overall the flow patterns for both investigated cases were similar but the variation of flow was higher, when the Lavare cycle was turned on. With the Lavare cycle on the variation in the flow patterns was higher (LON σ=0.027 ± 0.019 m/s vs. LOF σ=0.015 ± 0.007 m/s). Additionally a less aligned and consistent flow orientation was identified by the angular dispersion (LON r=0.84 ± 0.18 vs. LOFF r=0.70 ± 0.19). Finally also the stagnation index showed a reduction (LON SI=3.05 ± 2.14s vs. LOFF SI=3.92 ± 4.98 s).
Conclusions: Fluid dynamical measurement showed that the activation of the Lavare cycle resulted in improved ventricular washout and higher flow variations that can reduce areas of stasis and might improve the patients outcome. This is congruent also with an elsewhere published analysis of the ReVOLVE clinical registry, where a statistically significant lower stroke rate was found in patients in case the Lavare cycle was turned on.

215

Driver Optimization to Decrease Hemolysis and Promote Urine Production in a Patient with a Total Artificial Heart on Hemodialysis - A Case Report

L. A. Schroedl, L. L. Staley, D. E. Steidley, O. E. Pajaro. *Mayo Clinic, Phoenix, AZ.*

Study: A 54 year old male implanted with a SynCardia Total Artificial Heart (TAH) as a bridge to transplant, was transferred to our facility post-op day 104. The patient was anuric and on hemodialysis (HD) since implantation. He required blood transfusions at a rate of 2.6 units per week due to chronic hemolysis with an average lactate dehydrogenase (LDH) of 3060 U/L and hemoglobin (Hgb) of 6.2 g/dL. His SynCardia Companion-2 Driver was set at a beat rate of 115 with a 45% systolic duration, right drive pressure of 85 mmHg, and left drive pressure of 180 mmHg with 0 mmHg vacuum. Upon device analysis, his average right fill volume was 55 ml, and left fill volume was 60 ml, with a combined average cardiac output of 6.6 LPM. We determined that there was an elevated average right dP/dt of 9170 mmHg/s, and left dP/dt of > 9999 mmHg/s.
Methods: On Post-op day 104 the patient was transitioned to the SynCardia CSS driver. Beat rate was set to 125 with a 52% systolic duration, right drive pressure of 60 mmHg, and left drive pressure of 210 mmHg with -6.5 mmHg vacuum. Average right fill volumes were 58 ml, average left fill volumes were 61 ml, with an average cardiac output of 7.6 LPM.
Results: LDH decreased to 777 U/L ($p < 0.0001$), blood transfusion rate has decreased to 0.3 units/week, average Hgb has increased to 6.9 g/dL ($p = 0.0062$), and urine output has increased to 374 ml/day ($p < 0.0001$). The TAH generates a significant amount of hemolysis due to high pressure gradients across four artificial heart valves. Close monitoring and management driver parameters can play a key role in minimizing this level of hemolysis and increase the patient's overall hemodynamic stability and end organ perfusion.

	LDH (U/L)	Plasma Hgb (mg/dL)	Urine (ml)	Hgb (g/dL)	Total Bilirubin (mg/dL)	Alanine Aminotransferase (U/L)	Transfusions (units/week)
Pre-Transfer	3060.0 (+-) 137.7	150.4 (+-) 20.0	0.0 (+-) 0.0	6.21 (+-) 0.33	1.10 (+-) 0.22	46.7 (+-) 0.9	2.63
Post-Transfer	776.8 (+-) 26.6	14.0 (+-) 2.1	373.8 (+-) 76.6	6.93 (+-) 0.27	0.43 (+-) 0.08	17.3 (+-) 1.5	0.29
p-Value	<0.0001	0.0028	<0.0001	0.0062	0.0048	<0.0001	

216

Neutrophil-to-Lymphocyte Ratio and the Risk of GI Bleeding in Patients with LVAD

F. Abou Obeid, A. Rifai, S. Pauwaa, G. Yost, A. Tatooles, **G. Bhat**. *Center for Heart Transplant and Assist Devices, Advocate Christ Medical Center, Oak Lawn, IL.*

Study: The increased risk of gastrointestinal (GI) bleeding after left ventricular device (LVAD) is multifactorial including acquired Von Willebrand factor deficiency and the use of warfarin to prevent thrombotic events. Right-sided heart failure after LVAD implantation has also been associated with increased risk of GI bleeding. Inflammation and malnutrition play an important role in the development and progression of congestive heart failure. The neutrophil-to-lymphocyte ratio (NLR) has recently been found to be a sensitive biomarker in acute decompensated heart failure and is associated with poor outcomes after LVAD placement. Our goal was to determine if a high NLR value prior to LVAD implantation correlates with a higher risk of GI bleeding after implantation.

Methods: We retrospectively reviewed the charts of 210 patients who underwent LVAD implantation between Jan 01, 2010 and Jan 01, 2015. Patients who were on ECMO and had biventricular VAD were excluded from this study. Absolute neutrophil count and absolute lymphocyte count were collected and NLR was calculated for every enrolled patient one day prior to LVAD implantation. The mean NLR was compared among patients who did and did not develop a GI bleeding event after the LVAD placement. Demographics are shown in Table 1.

Table I.

Gender	76.7% male	23.23% female	
Race	41.4% AA	51.5% Caucasian	8.1% other
Age at implant	59.67 yr, 95% Cl (56.45;62.9)		
Type of Device	71.9% HM II	17.6% HW	10.5% other
Hx of GI Bleeding prior to LVAD	90.4% No	9.6% yes	

Results:

Table II.

	No GI Bleeding	GI Bleeding	P value
NLR	6.25 with 95% Cl (5.12; 6.38)	8.35 with 95% Cl (5.11; 11.59)	0.11

There was a trend toward higher NLR in LVAD patients with GI bleeding episodes High NLR may reflect an intrinsic inflammatory state coupled with poor nutritional and immune status contributing to GI bleeding after LVAD implantation. Further studies are needed in a larger cohort to explore these findings.

217

VWF Hemocompatibility Testing of a Novel Miniature Implantable Blood Pump - Benchtop & *in vivo* Results

J. W. Long,[1] P. A. Coghill,[2] J. R. Stanfield,[2] R. K. Wampler,[3] T. A. Snyder.[2] *[1]Advanced Cardiac Care, INTEGRIS Baptist Medical Center, Oklahoma City, OK; [2]VADovations, Oklahoma City, OK; [3]Oregon Health & Science University, Portland, OR.*

Study: Improving hemocompatibility is a next, critical requirement to reduce complications of Ventricular Assist Devices (VADs). VAD-induced degradation of von Willebrand Factor (VWF) contributes to bleeding, which occurs in 20–30% of VAD patients each year, and is associated with shear-related blood trauma. In this study, we developed and applied bench-top and in vivo testing to analyze a newly developed VAD for preservation of VWF multimers and VWF collagen binding (VWF:CB) function.

Methods: Benchtop: Human blood bank plasma supplemented with dextran to achieve a viscosity of 3cP was circulated through flow loops with the new pump (V-O VAD), along with the Thoratec-SJM HeartMate II (HMII), Heartware HVAD and Levacor VAD while a control loop was rocked at 1 Hz. The pumps were set to generate 4L/min against an afterload of 75mmHg. Samples were collected pre-test, after 15, 30 & 60 mins, and then hourly until 6hrs. Multimer distributions were determined by electrophoresis and in-gel immunoflourescent staining. VWF:CB was quantified using available assay kits. In vivo: Plasma samples from ovines implanted with the V-O VAD were also analyzed for VWF:CB and VWF multimer distributions. Pre-op samples were used to define normal ovine VWF:CB values.

Results: Benchtop: VWF:CB was preserved, unchanged with the V-O VAD, Levacor, and control loops after 6hrs, but was significantly depleted with the HMII and HVAD to 54% and 64% of baseline. Likewise, hVWF multimers were preserved in the V-O VAD and Levacor but not the HMII and HVAD. In vivo: VWF:CB in V-O VAD implanted ovines was 0.77+/-0.26 U/mL at 30 days and 0.95U/mL at 90 days, preserved near the preop levels of 0.81+/-0.24 U/mL. VWF multimer distributions were unchanged. This is the 1st report of preservation of VWF multimer distribution and function in benchtop and animal tests of a continuous flow VAD. The data suggest the next-generation V-O VAD in development may deliver superior hemocompatibility.

219

Leukocyte Modulation: A Strategy During Cardiopulmonary Bypass to Mitigate Systemic Inflammatory-like Response

T. J. Johnson,[1] K. A. Johnston,[2] K. B. Deatrick,[1] M. S. Cornell,[1] J. M. Toomasian,[1] H. D. Humes,[3] J. W. Haft,[4] A. Rojas-Pena.[5] *[1]Surgery, University of Michigan, Ann Arbor, MI; [2]Innovative BioTherapies, Ann Arbor, MI; [3]Internal Medicine - Nephrology, University of Michigan, Ann Arbor, MI; [4]Cardiac Surgery, University of Michigan, Ann Arbor, MI; [5]Surgery - Section of Transplantation, University of Michigan, Ann Arbor, MI.*

Study: Cardiopulmonary bypass (CPB) is associated with a systemic inflammatory response and multi-organ failure. A Leukocyte Modulation Device (LMOD) able to down-regulate leukocytes via exposure to a low calcium environment reduces leukocyte activation during hemodialysis and in models of sepsis. We studied if the addition of LMOD therapy minimizes the systemic inflammatory response in a porcine model of CPB.
Methods: Nineteen healthy anesthetized pigs were instrumented and placed on standard CPB for 3hr (1hr CPB, 45min of cold cardioplegic arrest with cross-clamp, and 75min weaning off CPB). Animals were allocated into three experimental groups: ***CPB*** (n=6), standard CPB; ***CPB-3hr LMOD*** (n=7), CPB + 3hr LMOD therapy via CPB circuit venous line; CPB-8hr LMOD (n=6), ***CPB+8hr LMOD*** therapy via a double-lumen catheter in the femoral vein. All animals were followed for 5hr after CPB. Data collection included systemic hemodynamics and leukocyte counts. Leukocyte activation was assessed by flow cytometry for CD11b expression in blood and in cells eluted from the LMOD cartridge.
Results: All animals were successfully weaned from CPB. No differences between groups were observed in hemodynamics or vasopressor requirements. Normalized leukocyte count decreased during CPB in all groups, but at the end of the study was lower only in ***CPB+8hr LMOD***, Fig 1a. Neutrophil CD11b expression (measured as fold change) was lower at the end of CPB in ***CPB+8hr LMOD*** (2.0 ± 0.6) vs. ***CPB*** (3.6 ± 0.7) or ***CPB-3hr LMOD*** (2.6 ± 0.5). CD11b expression retuned to baseline at the end of the study in all groups. CD11b expression of cells eluted from the LMOD cartridge was higher at the end of CPB, Figure 1b. LMOD therapy during CPB decreased the expression of CD11b (in blood) and leukocyte count. Cells eluted from the LMOD cartridge had the highest levels of CD11b expression. A dose-dependent response to LMOD therapy was observed, suggesting that the longer it is applied, the more repression of CD11b can be achieved.

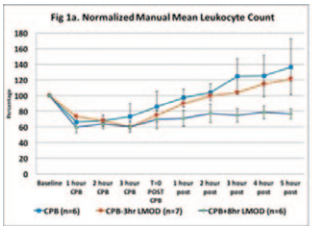

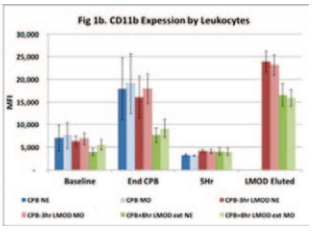

223

Analytical Estimate of Washout Characteristics in Conical Spiral Groove Bearings for Axial Flow Cardiac Assist Devices

S. Bieritz,[1] P. A. Smith,[1] J. Grande-Allen,[2] W. Cohn,[1] G. Tansley.[3] *[1]Texas Heart Institute, Houston, TX; [2]Rice University, Houston, TX; [3]Griffith University, Southport, AUSTRALIA.*

Study: Spiral groove bearings (SGBs) have the potential to replace or compliment magnetic bearing systems in miniature axial blood pumps to reduce power consumption and facilitate washout of secondary flow paths. The goal of this study was to optimize geometry of a conical SGB in order to promote washout of the bearing gap while providing radial and axial stiffness to an impeller in an axial blood pump.
Methods: Conical SGB designs were optimized for either washout or load capacity based on the analytical narrow-groove theory. A Poiseuille flow term was developed and added to Muijderman's pressure distribution equation for a conical SGB bearing, and an inertial correction was included. The resulting equations gave the transverse flow rate as a function of geometric parameters (SGB gap height, groove angle and depth, and conical half-angle), which were numerically solved to maximize flow rate. SGBs were then optimized for load capacity using the pressure distribution integrated over surface area.
Results: Washout optimization reduced blood residence time (BRT) in SGBs with small conical half-angles by 60% but sacrificed axial load capacity by 25%. Optimization for load capacity benefits flatter SGB designs more than steeply angled SGBs, and load capacity can be improved without sacrificing substantial washout in the bearing gap. Conical SGBs with larger half-angles had the highest load-bearing capacity and shortest BRT but sacrificed radial stiffness. Calculations will be compared to experimental data in future studies to determine their validity in predicting the behavior of conical SGBs. Conical SGBs optimized for washout may provide a lower-power alternative to magnetic bearing systems in axial rotary blood pumps, with minimal risk of hemolysis.

224

The Utility of Frequency Analysis of Sounds Produced by Left Ventricular Assist Devices to Detect Pump Thrombosis

S. Klesnik,[1] E. Nunez Centeno,[1] M. K. Jezovnik,[2] K. James,[1] S. Nathan,[2] V. Fikfak,[3] R. Radovancevic,[2] P. Loyalka,[2] B. Kar,[2] I. D. Gregoric.[2] *[1]Memorial Hermann Hospital, Houston, TX; [2]Center for Advanced Heart Failure, The University of Texas Health Science Center, Houston, TX; [3]Department of Surgery, The Houston Methodist Hospital, Houston, TX.*

Study: A reliable method for detecting insipient pump thrombosis (PT) in left ventricular assist device (LVAD) patients is lacking. An electronic stethoscope can reliably and non-invasively record sounds produced by LVADs. A correlation between acoustic spectra and in-vitro and in-vivo recordings has been shown. We aimed to investigate harmonic frequencies in patients with confirmed PT and to compare them with those of patients without PT.

Methods: A standardized auscultation method using a Littman electronic stethoscope was used for recording pump sounds in 30 patients with LVAD without PT (controls) and 8 patients with pathologically confirmed PT after pump exchange (PT patients). MATLAB software was used to create a proprietary script ecosystem designed to detect contribution of each harmonic frequency of rotation of the impeller. Levels of lactate dehydrogenase (LDH) and free hemoglobin (fHB) were measured.

Results: Thirty-eight patients (84% men) with HeartMate II, mean age 54.2 ± 11.7 years were included in the study. 142 recordings were analyzed, on average 3.6 recordings per patient. Peak intensity was significantly higher in PT patients at the 2nd ($p < 0.001$) and 5th harmonic ($p < 0.001$) of the detected rotary frequency of the LVAD (Figure 1). Pump speed, pump power, pulsatility index and fHB did not differ between groups. LDH was significantly higher in PT patients (411 ± 130 I.U. vs 374 ± 18.6 I.U., $p < 0.001$). In summary, peak intensity of harmonic frequency might be useful as an adjunctive tool to detect PT. Further studies are needed to investigate if changes in pump sounds can be detected prior to rises in clinical biomarkers of PT.

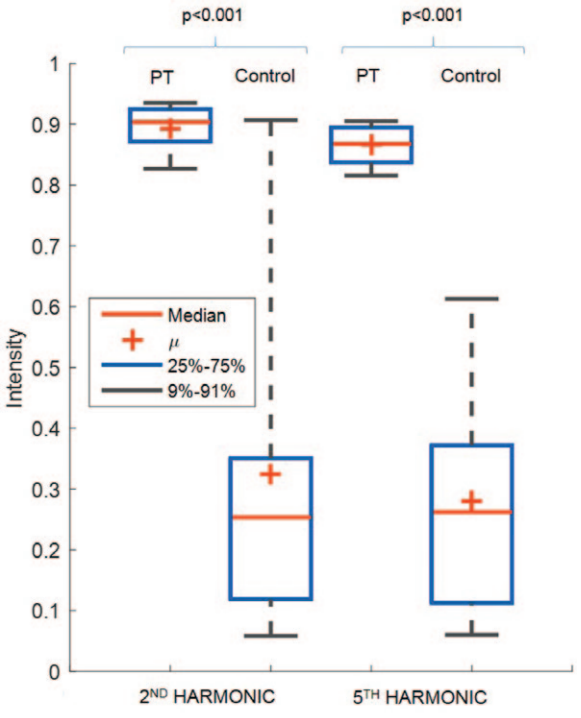

Figure 1. Peak intensity of harmonic frequency in patients vs. controls

232

Heart Wait Time Modeling Data

D. L. Joyce, L. Joyce, S. Kushwaha, B. Lahr, R. Daly. *Mayo Clinic Hospital-Saint Marys Campus, Rochester, MN.*

Study: An analysis of anticipated waiting time was undertaken to assist with decision making on timing of left ventricular assist device (LVAD) therapy in the bridge to transplant (BTT) population. A risk score model was developed based on the combined influence of blood type, patient size, regional donor availability, and listing status on expected waiting times.

Methods: We reviewed data from the United Network for Organ Sharing (UNOS) between 2009 and 2013 for 14,242 patients listed for isolated heart transplant. Body Mass Index (BMI), blood type, UNOS region, and listing status were pre-selected as predictor variables and evaluated for their influence on waiting time with multivariable Cox PH regression. Bootstrap re-sampling was used to internally validate this model, with performance evaluated based on bias-corrected measures of predictive accuracy and calibration. A scoring system was derived based on the presence of these risk factors, weighted in magnitude by the corresponding regression coefficients, and summed together to define an individual's risk score.

Results: In the fitted model all 4 predictor variables were significantly and independently associated with wait time ($P<0.001$ for each), showing adequate model discrimination (bias-corrected c-statistic=0.704) and calibration. Risk score points were assigned based on the regression coefficients from the derived model (Figure 1). Higher risk scores correlated with shorter waiting times (Figure 2). Risk scores correlated closely with observed rates of transplantation when plotted against the model-based predictions. The Risk Scores predict longer waiting time for lower listing status, larger patient size, some blood groups and some UNOS regions which may influence patient management decisions. The discrepancies in waiting times for some blood groups and UNOS regions reinforce the need for review of geographic allocation policy. This data may be informative as the proposed, new, UNOS allocation policy for hearts is reviewed this year.

Figure 1. Point System for Risk Score

* -1 point per each 5 kg/m² interval above the BMI reference range of 20-<25, and 1 point per interval below this reference (i.e., 0 points assigned to subjects with BMI 20-<25, -1 points to subjects with BMI 25-<30, -2 points for BMI 30-<35, etc.)

Parameter		HR (95% CI) [P-value]	β	β'	Points
BMI (per 5 kg/m²)		0.80 (0.78, 0.82) [<.001]	-0.22	-1.00	-1*
Blood type	A	1.71 (1.64, 1.80) [<.001]	0.54	2.42	2
	AB	3.08 (2.81, 3.37) [<.001]	1.12	5.05	5
	B	1.67 (1.57, 1.78) [<.001]	0.52	2.32	2
	O	1.0 (reference)	0	0	0
Region	1	1.0 (reference)	0	0	0
	2	2.00 (1.78, 2.24) [<.001]	0.69	3.11	3
	3	1.59 (1.41, 1.79) [<.001]	0.47	2.09	2
	4	1.56 (1.38, 1.76) [<.001]	0.44	2.00	2
	5	2.44 (2.17, 2.74) [<.001]	0.89	4.01	4
	6	1.70 (1.45, 1.99) [<.001]	0.53	2.38	2
	7	1.40 (1.24, 1.58) [<.001]	0.33	1.50	2
	8	2.02 (1.77, 2.30) [<.001]	0.70	3.15	3
	9	1.09 (0.96, 1.24) [0.184]	0.09	0.40	0
	10	1.52 (1.34, 1.73) [<.001]	0.42	1.90	2
	11	1.57 (1.39, 1.77) [<.001]	0.45	2.03	2
Listing Status	1A	3.07 (2.90, 3.24) [<.001]	1.12	5.04	5
	1B	1.99 (1.89, 2.09) [<.001]	0.69	3.08	3
	2	1.0 (reference)	0	0	0

Figure 2: Kaplan-Meier Estimated Wait Time By Risk Score Intervals

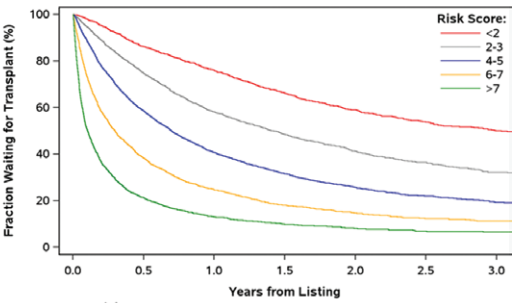

No. at risk

<2	1686	1298	1019	766	544	381	268
2-3	2962	1962	1341	987	634	410	274
4-5	3718	1875	1104	728	429	266	166
6-7	3309	1057	582	355	213	119	71
>7	2567	417	219	131	82	53	35

242

Examination of Damage to the Erythrocyte Membrane Using Microfluidic Channels and Flow Cytometry

J. P. Buerck,[1] D. V. Papavassiliou,[1] T. Snyder,[2] D. W. Schmidtke,[3] E. A. O'Rear.[1] *[1]University of Oklahoma, Norman, OK; [2]VADovations, Oklahoma City, OK; [3]The University of Texas at Dallas, Richardson, TX.*

Study: Blood flow in ventricular assist devices (VAD) exposes red blood cells (RBC) to supraphysiologic shear that increases the likelihood of RBC damage. Trauma to RBCs can result in membrane damage or hemolysis. VAD patient blood exhibits an increase in microparticles. One suggested reason for this phenomenon is that the erythrocytes use the microvesicle formation as a means to prevent premature clearance of still otherwise healthy cells. We employed novel microfluidic channels to replicate shear-time exposure conditions within VADs to investigate RBC microparticle generation.

Methods: Human RBCs were isolated, washed, and resuspended in isotonic, protein solutions, then perfused through microfluidic channels exposing cells to shear rates of 100,000 s^{-1} for 1–15 ms. The effluent was collected and stained using fluorescent markers, Annexin V and CD235A, then analyzed with a flow cytometer. Annexin V is a positive marker for exposure of external phosphatidylserine (PS) that suggests apoptotic activity in cells and a cell surface that supports coagulation cascade reactions. CD235A serves to absolutely mark RBCs and RBC microparticles.

Results: The data collected from the flow cytometer indicated a trend in RBC microparticle formation in the size range from 0.5 to 1.0 µm per RBC. The increase in microparticle formation from the control to the longest exposure time showed over a ten-fold increase. For the control channel, with no high shear region, the average RBC microparticle per 1,000 RBCs was 1.3. The other microfluidic channels had 2.2, 3.8, 4.7 and 14.5 microparticles per 1,000 RBCS for 1 ms, 5 ms, 10 ms and 15 ms respectfully. We can conclusively say microparticle formation with exposed PS occurs after high shear of 0–15 millisecond duration, identifying a sublethal marker for RBC damage, which may be useful in the evaluation of VAD design and operation.

247

Intracardiac Thrombus in Patients Undergoing Left Ventricular Device Implantation: Predictive Capability Correlated to Intraoperative Findings

R. H. Parrado,[1] S. Maltais,[2] S. Sharma,[3] S. M. Dunlay,[2] R. C. Daly,[1] D. L. Joyce,[1] L. D. Joyce,[1] J. M. Stulak.[1]; *[1]Division of Cardiovascular Surgery, Mayo Clinic, Rochester, MN; [2]Division of Cardiovascular Diseases, Mayo Clinic, Rochester, MN; [3]Medical Student, Department of Cardiovascular Surgery, Mayo Clinic, Rochester, MN.*

Study: Predicting presence of intracardiac thrombus is critical in patients undergoing left ventricular assist device implantation and may alter surgical approach. Few data exist examining ability of various echocardiographic modalities to identify intracardiac thrombus, especially depending on the location.

Methods: Between February of 2007 and September of 2009, 309 patients underwent primary CF-LVAD implantation and had preoperative echocardiography at our institution. Median age was 59 years (18–79) and 250 were males (81%). Preop echocardiography was performed using transthoracic echocardiograms (TTE) in 296 patients (96%) and transesophageal (TEE) in 13 patients (4%). Mean interval between preop echocardiography and implant was 21 ± 5 days. All patients underwent intraopTEE (IOTEE) at implantation.

Results: Intracardiac thrombus was identified on preoperative echocardiography in 20 patients (6%); 16/20 on TTE and 4/20 on TEE. Locations included left ventricle (LV) in 12/20 (60%), left atrial appendage (LAA) in 4/20 (20%), right atrium (RA) in 3/20 (15%) and right ventricle (RV) in 3/20 (15%). IOTEE identified thrombus in 57 patients (18%); LAA in 30/57 (53%), LV in 15/57 (26%), and RA in 12/57 (21%). At surgery, LV thrombus was found in 21 patients and LAA thrombus in 4 patients. For any thrombus, preopTTE had 29% sensitivity and 98% specificity while IOTEE had 65% sensitivity and 92% specificity. For LV thrombus, preop TTE had 33% sensitivity and 99% specificity which was similar to IOTEE with 43% and 99%, respectively. For LAA thrombus, preop TTE had 25% sensitivity and 99% specificity while IOTEE had 75% sensitivity and 94% specificity. IOTEE more often identifies intracardiac thrombus; LAA and LV are most common locations. Preop echo and IOTEE were similar for LV thrombus, while IOTEE was superior for LAA thrombus. Understanding these differences allows preoperative planning and alteration of the surgical plan if needed.

249

Simultaneous Laparoscopic Sleeve Gastrectomy in Morbidly Obese BTT Patients Undergoing Left Ventricular Assist Device Implantation

I. D. Gregoric,[1] S. Kumar,[1] R. Radovancevic,[1] M. Patel,[1] M. H. Akay,[1] J. A. Patel,[1] S. S. Nathan,[1] B. Akkanti,[1] I. Rajapreyar,[1] S. K. Shinil,[2] P. Loyalka,[1] K. S. Bajwa,[2] B. Kar.[1] *[1]Center for Advanced Heart Failure, The University of Texas Health Science Center, Houston, TX; [2]Department of Surgery, The University of Texas Health Science Center, Houston, TX.*

Study: There are increasing reports of weight loss surgery in morbidly obese patients undergoing implantation of left ventricular assist devices (LVAD). We analyzed our experience using laparoscopic sleeve gastrectomy (LSG) performed simultaneously with LVAD implantation in these patients.

Methods: We reviewed the charts of 10 patients (pts) at our center who underwent LVAD implantation immediately followed by LSG. LSG was performed using standard 4-port technique, avoiding the LVAD device and placing ports slightly lower than normal. Endoscopy was performed to check the caliber of the sleeve gastrectomy and to ensure no leaks or bleeding occurred. Pts were started on bariatric clear liquids after extubation. We compared preoperative and postoperative data with an emphasis on perioperative outcomes.

Results: Ten men and 3 women, age 46 ± 13 years, underwent HeartMate II (N=8) and HeartWare (n=2) LVAD implantation as a bridge-to-transplant (BTT) (n=2) and bridge to candidacy (BTC) (n=8). Four pts were INTERMACS Class 2 and 6 pts were Class 3. After LVAD implant (cardiopulmonary bypass time of 65 ± 35 min) they underwent LGS with total surgery time of 413 ± 67 min. Their body weight 30 days after surgery was significantly lower compared to before surgery: 126 ± 35 vs 138 ± 35 kg; p<0.0001 (BMI: 40 ± 7 vs 45 ± 6). During surgery and postoperative period there were no major complications. Two BTC patients received heart transplants 290 and 313 days after LVAD implant. Other pts are alive on LVAD 323 ± 276 days. In conclusion, it seems that LGS performed concomitantly with LVAD implantation offers these pts the opportunity to receive heart transplants after weight loss. Larger prospective studies are needed to evaluate long term benefits of this technique.

250

Early Echocardiography After Left Ventricular Assist Device Implantation: Indications, Resultant Interventions and Utility

R. H. Parrado,[1] S. Maltais,[2] S. Sharma,[3] S. M. Dunlay,[2] R. C. Daly,[1] D. L. Joyce,[1] L. D. Joyce,[1] J. M. Stulak.[1] *[1]Division of Cardiovascular Surgery, Mayo Clinic, Rochester, MN; [2]Division of Cardiovascular Diseases, Mayo Clinic, Rochester, MN; [3]Medical Student, Department of Cardiovascular Surgery, Mayo Clinic, Rochester, MN.*

Study: Optimal early management after continuous-flow left ventricular assist device (CF-LVAD) implantation is critical to avoid subsequent morbidity and mortality. Adjustments in care are guided largely by clinical assessment, but echocardiography is also utilized. Few data examine indications and utility of early echocardiography in these patients and subsequent interventions that are undertaken as a result.

Methods: Between February 2007 and September 2015, 312 patients underwent primary CF-LVAD implantation at our institution. Median age was 59 (18–79) and 252 were (81%) males. Early echocardiography was defined as done within the first 72 hours post-implant; 182 echocardiograms were obtained in 153/312 patients (49%). One echocardiogram was obtained in 126 patients (82%), 2 in 25 (16%) and 3 in 2 (2%).

Results: Within the 1st 24 hours post-implant, 77 (42%) of echocardiograms were obtained, 51 (28%) in the 2nd 24 hours, and 54 (30%) in the 3rd 24 hours. Echocardiography was transthoracic in 160 patients (88%) and transesophageal in 12%). The most common indications included elective speed optimization in 51 patients (28%), right heart failure in 50 (27%), left heart failure in 24 (13%), hypotension in 17 (9%), suspected tamponade in 14 (8%) and arrhythmia in 13 (7%). The most common resultant interventions included speed change in 66 (36%), medications adjustment in 52 (26%), transesophageal echocardiography in 9 (5%). and reoperation in 7 (4%). No subsequent interventions were performed in 61 patients (34%). Early echocardiography was utilized in approximately half of the patients with most undergoing a single study. The most common indications included speed optimization, heart failure, tamponade and arrhythmias. Although echocardiography led to no intervention in approximately 1/3 of patients, the majority resulted in a subsequent intervention most commonly including speed and medication optimization, as well as emergent reoperation.

259

Population-driven Design of a Right-sided Blood Pump

C. Zarins. *Abiomed, Danvers, MA.*

Study: The Impella RP is a right-sided blood pump which sits across the right heart. The inflow sits in the inferior vena cava (IVC) and the outflow in the pulmonary artery (PA). This project describes a method for designing new a shape based on a population of patients as well as validation of the new shape with device users in benchtop models.

Methods: A set of 50 EKG-gated CT scans was collected from a representative sample population. The right heart was segmented using Mimics (Materialise, Leuven, Belgium). Datum points were assigned to key cardiac landmarks. The centerpoint of the tricuspid annulus was taken as the primary datum. The scans were aligned and the other landmarks were mapped relative to this datum. MATLAB (MathWorks, Natick, MA) was used to create 3-dimensional binary matrices representing the right-side bloodpool of each patient, specifying an identical coordinate system for each. A matrix summation was performed. The result of this summation was a 3-dimensional "heat map" of right-sided cardiac anatomy. The value of each point corresponded to the number of patients whose anatomy shared this point.

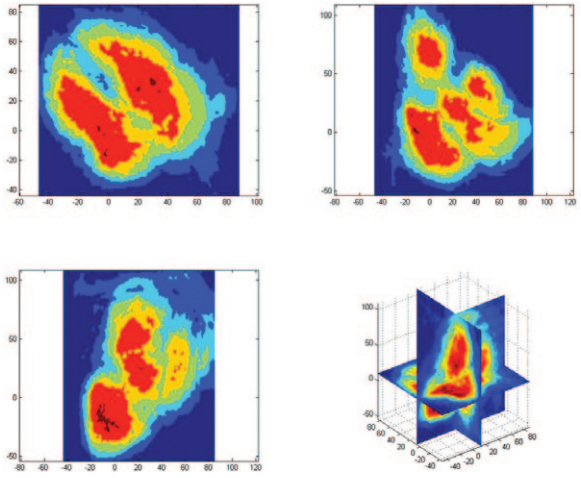

Contour plots (eg. anatomy common to 95% of sample population) were generated and the device was fit to this geometry.

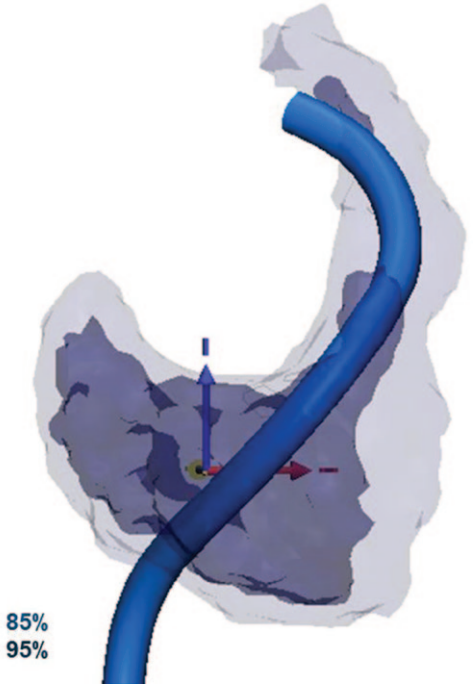

We selected "challenge" anatomies and created benchtop models via 3D printing. Simulated deliveries were conducted to observe the dynamics of delivery and identify challenge points. The new design was adjusted based on observations in the models. Iterating the design allowed us to optimize the final position as well as minimize the challenges observed at each step of delivery. Simulated implantations were conducted with device users to validate the new shape.

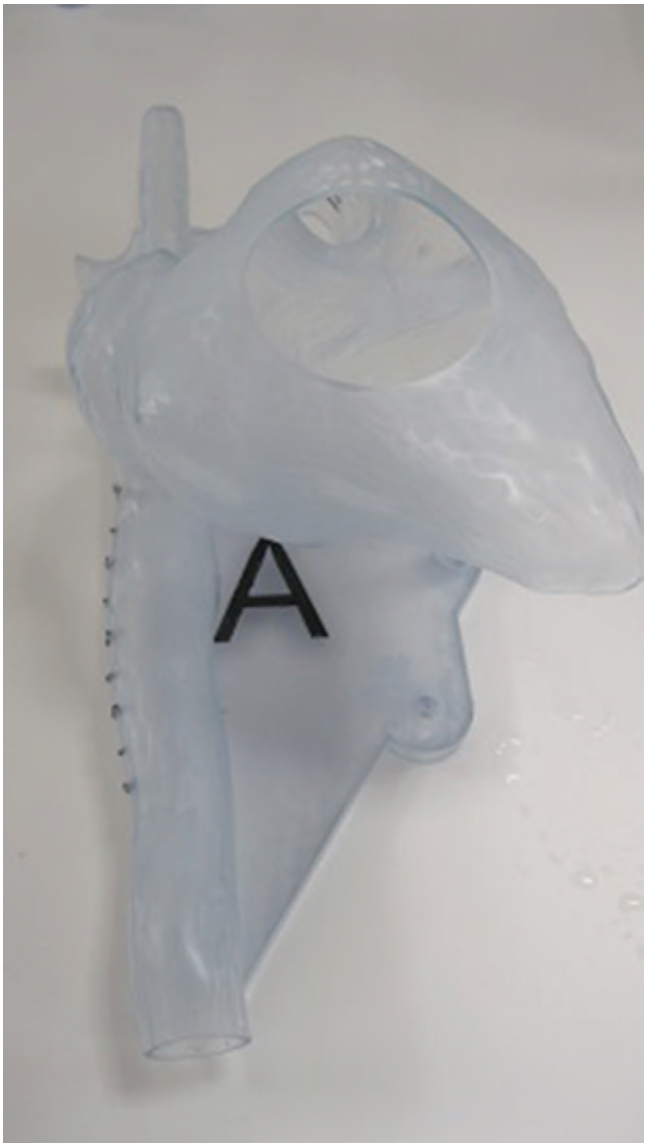

Results: The analysis identified an access path common to 95% of the sample population. A new cannula design was developed which retained optimal fit in the population and had improved deliverability. Testing with device users showed a significant improvement in ease of implantation.

260

The Implantable Rotary Continuous Flow Blood Pump ReligaHeart ROT First *in vitro* Investigation

M. Gonsior, R. Kustosz, M. Darłak, I. Altyntsev, M. Gawlikowski, M. Glowacki. *Artificial Heart Laboratory, Foundation for Cardiac Surgery Development, Zabrze, POLAND.*

Study: The centrifugal blood pump, ReligaHeart ROT (RH ROT), has been developed as implantable LVAD. The RH ROT prototype, with magnetically and hydro-dynamically suspended rotor, produces flow up to 10 l/min with efficiency varied from 30 to 45%. The surface engineering was used to create blood pump elements surfaces structure, reducing inside pump blood clothing.
Methods: The Titanium Nitride surfaces were manufactured on blood contacting surfaces, with roughness of Ra=80nm. The RH ROT functional tests: pump head, electrical power consumption, and energetic efficiency were performed using different fluid viscosity. The long term evaluation was done, using mock circulation stand, simulating the pulsatile pressure between RH ROT inflow and outflow. The dynamic gravity overloading was applied to validate rotor suspension accuracy. The acute 6 hours trombogenicity test on fresh animal blood was performed to validate the pump embolization risk.
Results: The pump pressure head varied in range starting from 50 Pa (at 2k RPM) to 190 Pa (at 4k RPM), ending at value of 20 Pa for maximum flow varied from 1 l/min to 3 l/min (2k RPM) and 10 l/min (4k RPM). The power consumption varied from 2 W (5 l/min; 2k RPM) to 9 W (10 l/min; 4k RPM). The maximum pump efficiency varied from 16% (2k RPM) to 26% (4k RPM). The long term work test, expanded with dynamic gravity overloading up to 3G, confirmed TiN surface layer resistance against accidental rotor - house collision. The acute trombogenicity test confirmed blood clotting freedom inside the pump, including impeller. The micro emboli were observed at surface technological defects. The RH ROT prototype investigations confirmed the pump expected properties. The further work for human device construction and manufacturing technology development will be carried out.Acknowledgements. This work has been supported by the Polish National Centre for Research and Development - project no. PBS1/A5/20/2012 and project RH ROT (STRATEGMED2/266798).

262

The Numerical Flow Analysis Utilization for Pediatric Ventricular Assist Device ReligaHeart Ped Development

W. Bujok, A. Kapis, A. Szuber-Dynia, R. Kustosz, M. Gonsior. *Foundation for Cardiac Surgery Development, Zabrze, POLAND.*

Study: The good results of MCS for adults resulted in increased interest in using this technique for treatment of HF in children. The only available pediatric pulsatile VAD is the device with PU valves. Therefore, a novel pulsatile VAD with titling disc valves was developed in Poland.
Methods: CAD models of 2 pumps ReligaHeart: PED45 (45cc SV) and PED30 (30cc SV), and family of tilting disc valves were developed. Numerical analyzes were performed assuming pump walls and valve components as non-deformable. Non-Newtonian blood model was used. Blood viscosity model: for values close to 0 shear rate value did not reached infinity, and at value greater than 327 s^{-1} was equal to the dynamic viscosity of a Newtonian model (η = 0.00345 Pa·s). As the main indicator of flow quality and accuracy the streamlines were considered. Secondary indicator was stagnation area defined as the place where blood moves at a speed of less than 0.0001 m/s. Flow structure numerical analyzes were performed for different valves size and angle position. For the best VADs construction the in vivo pump evaluation was performed on 8 animals (pigs) for 30 days.
Results: A new pumps PED45 and PED30 with various connector's angles were developed. The original tilting disc valves sizes of 14 to 20 mm for pediatric pumps were successfully developed. The best flow quality of analyzed pumps was obtained for: PED45 with valves size 18/20 and the angle set 70/90, and PED30 with valves size 16/18 and the angle set 70/90, which were designated for *in vivo* investigations. *In vivo* investigations confirmed numerical and in vitro results. The next step is the clinical investigations.
Conclusions: Numerical analyzes allowed to select the appropriate diameter and the angular position of the valves and their settings. The use of numerical methods led to significant reduction of the time required to develop the final design of prostheses. This work has been supported by NCBiR within the projects: PBS1/A7/1/2012 and 13–0118/10/2011.

263

Patient-Specific Models for TAVI Planning Assistance

J. Sánchez-P,[1] J. Forero,[2] J. Cabrales,[2] J. Briceño.[1] *[1]Universidad de los Andes, Bogotá, COLOMBIA; [2]Fundación Cardioinfantil, Instituto de Cardiología, Bogotá, COLOMBIA.*

Study: Transcatheter aortic valve implantation (TAVI) is a minimally invasive alternative to open-heart surgery, currently performed only on high risk patients suffering from severe aortic stenosis. As a new and successful technology, there is an exponential increase in the number of patients treated, medical centers offering the procedure and physicians being trained to perform it. TAVI's success depends heavily on the positioning of the prosthesis along the aortic root and misplacement may result in paravalvular leakage or obstruction of the coronary ostia. The objective of this study was to develop 3D patient-specific models (computational and 3D printed) of the aortic root and left ventricle of the heart of TAVI patients. With these models, physicians could, prior and during the procedure, become familiar with the anatomy, and evaluate models, sizes and locations of the prostheses, thus reducing complications and increasing overall success.
Methods: The aortic root and left ventricle were reconstructed from coronary CT images using Slicer3D, MeshLab, Blender and Autodesk Inventor. Aortic and annular dimensions were computationally measured and compared to those obtained by the radiologist in the CT examination process, validating the reconstruction. The 3D printed 1:1 models were handed in to the physician to simulate prosthesis selection, positioning and implantation prior and during the procedure.
Results: Up to now this tool has been successfully tried in one TAVI patient (Fig. 1), indicating that the use of a patient-specific 3D model could be a valuable tool for providing: 1) additional information about the patient's anatomy and 2) an in vitro anatomic model for simulation of the procedure in the planning process of TAVI. Therefore, the implementation of these models could cause overall impact on the procedural success in TAVI patients. The geometrical model is also being used to develop CFD simulations of the procedure which could further enhance this planning tool.

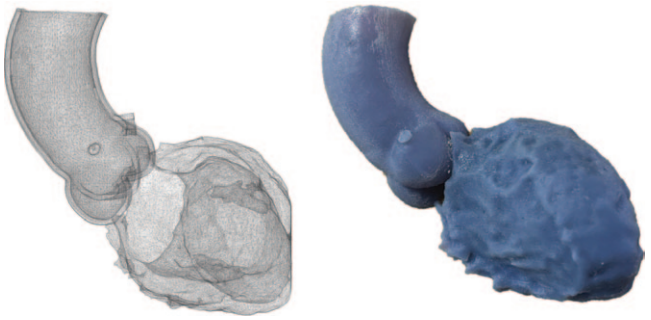

Fig. 1. Computational and 3D printed models.

267

Super Computer Simulation for Evaluating EVAHEART Augmented Pulsatility

T. Motomura,[1] T. Hisada,[2] T. Washio,[2] S. Sugiura,[2] D. Ogawa,[3] H. Kanebako.[3] *[1]Evaheart, Inc., Houston, TX; [2]UT-Heart Corp, Tokyo, JAPAN; [3]Sun Medical Technology Research Corp, Nagano, Suwa, JAPAN.*

Study: EVAHEART is a continuous flow ventricular assist device generating augmented pulsatility with a constant pump speed. This study aimed to simulate the hemodynamic response and understand the mechanism of EVAHEART (EVH) augmented pulsatility.
Methods: The Total Cardiac Mock Loop Circuit (LabHeart NCVC, Iwaki, Co, Tokyo) was used to obtain the dynamic hydrodynamic performance in addition to static HQ curve analysis, and numerical modeling was applied to 600K-cores super computer system (UT-Heart Corp, Tokyo) for two LVADs simulation (EVH vs axial flow pump). Ventricular myofibril was reduced 40% to simulate a dilated heart failure condition. Pulsatility was evaluated by pulse pressure [PP], dp/dt and EEP (energy equivalent pulse pressure: mmHg), also examined aortic valve opening, pressure-volume loop (the left and right ventricle), pump & left ventricular (LV) work [J], and ATP consumption.
Results: EVH showed approximately 4L higher systolic instantaneous peak flow, higher PP (13.6 vs 8.8 mmHg), and higher dp/dp (117 vs 70 mmHg), however EEP showed no difference (82 vs 81 mmHg). EVH tends to demonstrate higher end-diastolic volume and lower end-systolic volume. Based upon LV pressure-volume loop analysis, both of pumps unloaded the LV, and LV work was 0.45 [J] in EVH and 0.37 [J] in axial flow pump. At mid pump speed (1,800 RPM), EVH demonstrated 2-fold higher forward flow through the aortic valve compared to axial flow pump (9,000 RPM). In conclusion, Evaheart generated higher pulse pressure and dp/dt by intrinsically augmented systolic peak flow. This may contribute to prevent aortic remodeling and advancement of aortic valve insufficiency.

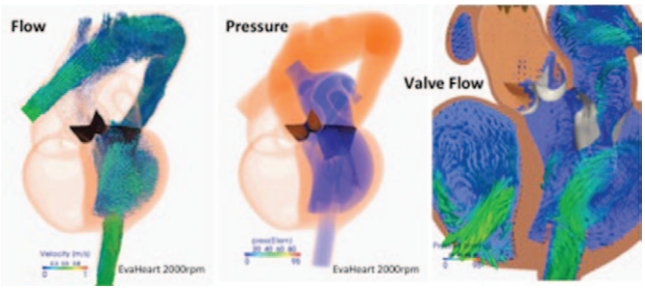

269

Comparing Sequential Organ Failure Assessment (SOFA) Score versus Respiratory Extracorporeal Membrane Oxygenation Survival Prediction (RESP) Score for Predicting In Hospital-Mortality for Patients Requiring Extracorporeal Membrane Oxygenation (ECMO)

R. M. Hasson Charles,[1] B. A. Whitson,[1] G. S. Phillips,[2] M. Farneman,[1] R. Tripathi,[1] S. Moffatt-Bruce.[1] *[1]Divisions of Cardiac and Thoracic Surgery, The Ohio State University, Columbus, OH; [2]The Ohio State University, Columbus, OH.*

Study: To evaluate the use of SOFA score versus RESP score for predicting In-hospital mortality in patients requiring ECMO.
Methods: Patients with respiratory failure underwent placement of VV ECMO following cardiac surgery evaluation between the years of 2013–2015 at an academic medical center. Following establishment of ECMO, the patients were followed until discharge. Exact logistic regression was used to estimate the odds and probability of survival.
Results: A total of 30 patients were placed on VV ECMO during this time and retrospectively underwent SOFA and RESP scoring, 21 participants were classified as evaluable. The study population included 61.9% (13) males and 38.1% (8) females. The average age was 49.95 (range 17–83) years. All patients were placed on VV ECMO. The average SOFA score was 12.19 (range 7–18). The average RESP score was -1.14 (range -13–6). The average length of stay was 30.10 days (range 14–63). The average length of cannulation was 11.37 days (range 5–22), and the average time from decannulation to discharge in the surviving population was 9.0 days (range 6–27). The regression of survival on SOFA adjusted for gender and surgery indicated that with the higher SOFA score, the odds of survival decreased by 3% (OR = 1.10, 95% CI: 0.78 - 1.39, *p*-value = 0.888), while the regression of survival on RESP adjusted for gender and surgery indicated that with the higher RESP score, the odds of survival increased by 9% (OR = 1.09, 95% CI: 0.89 - 1.40, *p*-value = 0.456). In conclusion, the RESP score demonstrated the potential ability to more accurately facilitate the prediction of in-hospital mortality in patients requiring VV ECMO for cardiopulmonary failure. Future studies will evaluate 30 and 90-day mortality rates and functional outcomes to improve our use of ECMO in this acutely unwell and complex patient population.

270

Hemodynamic Impacts of IABP on VA ECMO in Porcine Heart Failure Model

J. Kim, S. Chung, D. Kim, C. Lim, K. Park, Y. Kim, S. Jheon. *Thoracic and Cardiovascular Surgery, Seoul National University Bundang Hospital, Seongnam, KOREA, REPUBLIC OF.*

Study: Intra-aortic balloon pump (IABP) might be helpful to reduce afterload on left ventricle when pulmonary congestion exists on veno-arterial extracorporeal membrane oxygenation (ECMO) support. This animal experiment is aimed to elucidate the hemodynamic impacts of IABP on ECMO with porcine heart failure model.
Methods: With 69~85kg pigs, we cannulated on femoral artery and vein for ECMO support by percutaneous or open technique. Left lateral thoracotomy via 4th intercostal level was performed for invasive catheterization and cardiac intervention. We checked various hemodynamic parameters including left atrial pressure and coronary blood flow on left anterior descending coronary artery and left subclavian artery blood flow with Doppler. We ran ECMO for one hour and added IABP on counterpart femoral artery for another one hour. In heart failure model, we induced heart failure by pulmonary artery banding to make mean arterial blood pressure below 60mmHg before ECMO support. We compared the IABP effect between normal heart (n=4) and failing heart (n=4).
Results: In normal heart model, IABP did not affect hemodynamic change such as mean blood pressure (118.3 ± 25.2 ECMO only vs. 86.8 ± 17.1mmHg ECMO+IABP, p=0.068), left atrial pressure (9.3 ± 7.4 vs. 3.3 ± 2.6mmHg, p=0.068) nor coronary blood flow (28.4 ± 5.4 vs 23.6mL/min, p=0.068), left subclavian artery flow (161.9 ± 55.8 vs. 123.3 ± 45.9 mL/min, p=0.465). In heart failure model, IABP showed no significant hemodynamic advantage over ECMO only support; mean blood pressure (93.8 ± 20.5 vs. 89.3 ± 19.6mmHg, p=0.716), left atrial pressure (7.5 ± 3.3 vs. 5.5 ± 2.5mmHg, p=0.144), coronary blood flow (26.4 ± 9.4 vs. 21.7 ± 3.4mL/min, p=0.197), left subclavian artery flow (125.6 ± 52.4 vs. 122.3 ± 53.4mL/min, p=1.000). IABP does not affect hemodynamic change on veno-arterial ECMO support even in heart failure model. The effect of IABP is seemed to be minimal during maximal support of ECMO. However, this study has limitation of small number experiment and short period support.

271

***In-vitro* Mock Circulation Study for Identifying the Optimal Pump Speed in Evaheart LVAS**

T. Motomura,[1] R. Benkowski,[2] F. Nestler,[3] D. Timmes.[3] *[1]Evaheart, Inc., Houston, TX; [2]B-squared Medical Device Solutions LLC, Fort Worth, TX; [3]BiVACOR Pty. Ltd, Wilston, AUSTRALIA.*

Study: Continuous flow LVAD (CF-LVAD) is a pump-speed dependent circulatory assist device. In order to meet the physiological demand, pump speed can be incremented accordingly based upon hemodynamic parameters and non-invasive cardiac imaging modality. However, inappropriate speed management can result in variety of adverse events such as right heart failure (RHF) or aortic valve insufficiency (AI), hence, determination of the optimal pump speed is crucial for better clinical outcomes. This in-vitro study aims to investigate the pressure stress level of the aortic valve and ventricular left septum shift across a range of pump speeds to identify the optimal pump speed based on those parameters.
Methods: EVAHEART LVAS was installed into the mock circulation system (BiVACOR, pty, LTD), which simulated moderate and severe heart failure (SHF) including systemic, pulmonary, and coronary circulation. The mock system was set to simulate normal heart function (CO=4.9L/min) and heart failure (CO=2.9), with no support, and then ramp the EVAHEART pump speed from 1,500 RPM to 2,300 RPM (increment by every 100 RPM).
Results: By increasing the pump speed, the aortic valve stress (SAvBN) gradually increased to reach the baseline value (SAvBN=60 mmHg) at 1,800 RPM. In contrast, stress of the ventricular septum left shifting (SSpLN) increased from 1,800 and linearly increased till 2,300. Systemic flow returned nearly normal at 1,800 (85% of normal cardiac output)-1,900 RPM (96% of normal cardiac output). This methodology may be useful to pre-determine the optimal pump speed in conjunction with post-operative echocardiography.

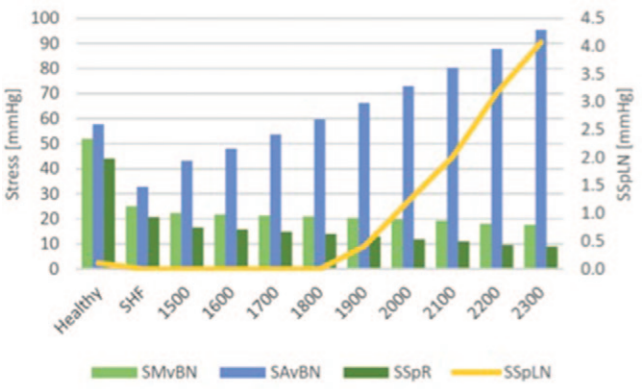

273

Fluid Structure Interaction Model Analysis of Cerebrospinal Fluid in Patients with Continuous-Flow Left Ventricular Assist Devices

C. A. Pierre,[1] Y. S. Vahedein,[2] S. W. Day,[2] A. S. Liberson,[2] V. Tchantchaleishvili.[3] *[1]Department of Neurosurgery, University of Rocheseter Medical Center, Rochester, NY; [2]Department of Mechanical Engineering, Rochester Institute of Technology, Rochester, NY; [3]Division of Cardiac Surgery, University of Rocheseter Medical Center, Rochester, NY.*

Study: The flow of cerebrospinal fluid (CSF) is driven by pulsatile flow regulated by arterial blood flow, and bulk flow produced by CSF secretion. However, in patients supported on continuous-flow left ventricular assist devices (CF-LVAD) arterial pulse is greatly diminished or absent. The current one-dimensional fluid structure interaction model (FSI) used to describe CSF flow, has not been applied to CF-LVAD patients. This study aims to characterize the effects of FSI on CSF pressure and flow in CF-LVAD patients.
Methods: Using the FSI model, we account for the curvature, variable cross sections of the CSF flow path, and friction. CSF production in choroid plexuses of the four ventricles was specified as a boundary condition for the model. The other source of production from capillary ultrafiltrate spaces was accounted for in the mass conservation equation. The primary CSF absorption sites were treated as the outlet boundary conditions.
Results: From existing model, absent pulse conditions resulted in no CSF flow because CSF production is not accounted for. Based on the fact that LVAD patients remain free of neurologic symptoms, the assumption of the role of pulsatility in the existing model must not play an important role in LVAD patients with continuous flow. To find the rigorous answer the versatile FSI model has been created. Preliminary analysis reveals that a simplified cylindrical computational fluid dynamics model is not a good representation of CSF generation and absorption, and a model with complex geometry needs to be implemented in order to account for the flow generation and absorption in each site.
Conclusions: The existing FSI model is not a suitable representation of CSF flow in CF-LVAD patients. We deduce that CSF flow is compensated by changes in CSF production and absorption that are not accounted for with existing model. The versatile FSI model simulates CSF in a variety of conditions, including application to CF-LVAD patient population.

276

Reduction of Stroke Risk from Embolic Shower Following Cardiac Surgery Using Cardiac Compression

P. Isingoma, J. Moon, R. Montes, K. May-Newman. *Bioengineering, San Diego State University, San Diego, CA.*

Study: Every year over 500,000 cardiopulmonary bypass (CPB) surgical procedures are performed in the United States. Unfortunately, they have been found to produce clinical, subclinical and silent neurologic injuries. The cause of these injuries is thought to be a surge of emboli released into circulation during the transition from CPB to the normal circulation following surgery. The hypothesis of this study is that brief external compression of the external carotid arteries will deflect particles from entering vessels that branch from the aorta to the brain. Thus, our objective is to visualize the flow pattern in the aorta by simulating the release of the aortic cross clamp following CPB surgery, and evaluate the impact of compression duration on the flow of particles into the vessel branches.
Methods: Flow visualization experiments are performed with an aortic arch model in a mock cardiovascular system. Fluorescent particles (20μm) are used to simulate emboli that are released into circulation immediately after carotid compression. Aortic flow is maintained at 4.0 ± 0.5L/min during baseline conditions, and pressure in the aorta and proximal branches at 65.0 ± 5.0mmHg. Flow through the branches was set to 10% of the aortic flow. Flow patterns of particles are visualized using DaVis imaging, and analyzed with ImageJ particle analysis tool to track, count, and record particle properties.
Results: The results tabulated the particle count for each condition from background-subtracted images. For 10 seconds carotid compression, particle count was reduced by 83% compared to the baseline; 84% for 15 seconds, and 81% for 20 seconds. Recirculation of the particles is observed in the compressed carotids proximal to the aortic arch, which results in the increase of particle count as the waiting period is increased. There is no significant change in the particle count through the innominate artery when compared to the baseline, which implies that most of the flow is diverted into the descending aorta.

278

Safety and Efficacy of Activated Prothrombin Complex Concentrates (PCC) for Patients with Intracranial Hemorrhage and Left Ventricular Assist Devices: A Novel Approach

G. P. Macaluso, G. Gavrilos, K. Meehan, R. Siemeck, W. Cotts, G. Bhat, S. Pauwaa, S. Zalawadiya, A. Tatooles, P. Pappas. *Advocate Christ Medical Center, Oak Lawn, IL.*

Study: Bleeding events and thromboembolism in patients with left ventricular assist devices (LVADs) contribute to significant morbidity and mortality. Management of intracranial hemorrhage (ICH) requires hemostasis through surgical or pharmacologic intervention or both. Accepted reversal of warfarin includes a combination of Vitamin K and fresh frozen plasma. This strategy, though effective, is a laborious process. More timely therapies include administration of recombinant activated factor VII (rFVII) or activated prothrombin complex concentrates (PCC). Ideal reversal of anticoagulation would include an agent that is immediately available, results in rapid reversal, and is devoid of thromboembolic complications. One approach to hemostasis is the administration of activated prothrombin complex concentrates (PCC). PCCs, like FEIBA, contain non-activated clotting factors II, IX, X, and to a lesser degree, activated factor VII. For patients with life-threatening bleeds with an INR less than five, 500 units of FEIBA has been shown to be safe and effective in achieving hemostasis while reducing incidence of thromboembolic events.
Methods: Retrospective, single-center, chart review, of LVAD patients with intracranial hemorrhage were evaluated after administration of PCC for 30 day mortality, clinical thromboembolism, and LVAD pump thrombosis.
Results: Three patients were treated using 500 units of FEIBA and 10mg of vitamin K. One patient required concomitant surgical intervention. After 30 days, mortality was 0% and no clinical thromboembolism and pump thrombosis was observed. This retrospective analysis is the first series of LVAD patients with ICH who underwent reversal of anticoagulation with FEIBA. Further prospective studies are needed to validate this analysis. FEIBA may offer an alternative approach to the management of hemorrhagic stroke in LVAD patients.

283

Risk Stratification of 30 Day and 360 Day Mortality of Patients Requiring ECMO

T. Yousuf, A. Rifai, A. Tatooles, W. Cotts, G. Bhat. *Advocate Christ Medical Center, Oak Lawn, IL.*

Study: To examine the 30 and 360 day mortality of patients requiring ECMO due to profound cardiogenic shock and to risk stratify these patients.
Methods: We retrospectively collected data on 95 patients admitted between 2005–2015 requiring ECMO. The 30 and 360 day mortality rate was 47.3% and 65.3%, respectively.
Results: Significant risk factors for increased mortality over 30 days in the univariate model included hypertension, coronary artery disease and elevated weight. Bilirubin and lactic acid after ECMO placement were significant univariate laboratory factors. In the multivariate model, increased weight HR 1.018(95% CI = 1.006–1.03, p=0.004) and elevated bilirubin HR 1.094(95% CI=1.021–1.173, p=0.011) after ECMO placement were significant predictors for 30 day mortality. Risk factors for increased mortality over 360 days in the univariate model included hypertension, chronic kidney disease and elevated weight. Laboratory findings that suggested a higher mortality rate were elevated bicarbonate, bilirubin and lactic acid. Increased weight, HR 1.015(95% CI = 1.004–1.027, p=0.01) was a significant predictor in the multivariate model. Mortality at one year after initial ECMO support is highest in the first 30 days. Increased weight is an important risk factor in both 30 day and one year survival.

Figure 1. Kaplan Meier Analysis for 30 and 360 day survival

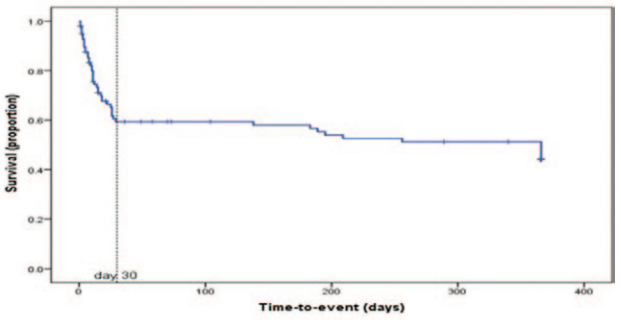

286

Optimized Rapid Electrolytic Processing of Nitinol Wire Components within Tissue for Paraffin Embedded Histology

A. V. Nguyen,[1] M. T. O'Brien,[2] B. R. Weeks,[2] F. J. Clubb. Jr.[2] *[1]Biomedical Engineering, Texas A&M University, College Station, TX; [2]Veterinary Pathobiology, Texas A&M University, College Station, TX.*

Study: Previous studies have demonstrated that utilizing electrolysis to dissolve metallic stents within tissue can allow for traditional processing with paraffin embedding and routine staining without compromising the surrounding tissue interface. However, these studies do not clarify what voltage, current, or solution concentration optimizes the dissolution of metallic components within tissue. Frequently, minute metal fragments remain throughout the tissue following electrolysis that can interfere with histological sectioning. This study was undertaken to determine the optimum conditions for electrolytic dissolution of metallic components within tissue. Compared to plastic embedding, electrolytic removal of metal from tissue is faster and allows vastly greater versatility for histological processing of tissues containing implanted metallic devices.
Methods: Nitinol wire was placed into blocks of formalin-fixed tissue. Varying currents were applied to the wire while the tissue was submerged in a citric acid and electrolyte solution. Additionally, citric acid solutions at different concentrations were evaluated. Electrolytic dissolution of the wire was verified by micro X-ray and paraffin-embedded histology. Through these assessments, optimal ranges for voltage, amperage, and citric acid were established for dissolution of nitinol wire within formalin-fixed tissue while preserving the tissue interface.
Results: An optimization table for electrolytic dissolution of nitinol wire within formalin-fixed tissue was created, with optimum ranges for citric acid concentration, voltage, and amperage.

288

The Effect of Reverse Remodeling on Intraventricular Flow in the LVAD-Assisted Heart Studied in a Mock Circulatory Loop

J. Moon, R. Montes, V. Ramesh, A. Newman, K. May-Newman. *Bioengineering, San Diego State University, San Diego, CA.*

Study: Advanced heart failure patients may receive a Left Ventricular Assist Device (LVAD) to improve blood flow. LVAD is a surgically implanted mechanical pump that connects the left ventricle (LV) to the aorta. After a LVAD is implanted, the heart often undergoes volume reduction and exhibits signs of restoration of normal cardiac geometry and function. Clinical studies show a reduction in LV vortex circulation and kinetic energy (KE) after LVAD implantation, which we hypothesize is due to LV volume (LVV) reduction. The goal of this study is to measure the LV flow and vortex dynamics in LV models representing the LVV reduction in the LVAD-assisted heart using Particle Image Velocimetry.
Methods: Two silicone LV models were created with volumes of 180 and 100ml, and studied separately in the SDSU cardiac simulator. The LV was connected to a Thoratec Heartmate II LVAD and the 2D velocity field in the LV mid-plane was measured for Pre-LVAD conditions (baseline) and several levels of LVAD support. This field was further analyzed using MATLAB to calculate circulation, kinetic energy (KE), position, and size of the large clockwise (CW) and smaller counter-clockwise (CCW) vortices that form in the LV during the cardiac cycle. Pulsatility index (PI) was calculated as the range divided by the mean of aortic flow.
Results: The baseline conditions for both models correspond to a cardiac output of 3.67 ± 0.11 L/min and mean aortic pressure of 63.5 ± 3.0. Vortex analysis showed that circulation and KE of the CW vortex was relatively unchanged with LVV reduction, but the smaller CCW vortex exhibited increased circulation and KE. CCW vortex circulation increased by approximately 60%, and CCW KE increased by 98% from 4.0 to 7.9$(m/s)^2$. The results support the observations of clinical studies.

289

Computational Prediction of Effects of LVAD and CRT Treatments on Ventricular Electromechanical Delay

A. Heikhmakhtiar. *Kumoh National Institute of Technology, Gumi, KOREA, REPUBLIC OF.*

Study: Clinically there are tools commonly used for patient who is suffering from HF: cardiac resynchronization therapy (CRT) and LVAD (Left Ventricular Assist Device). The main role of the CRT is as a pacemaker of the cardiac muscle. On other hand, the function of LVAD generally are mechanical unloading in the ventricle, increasing the blood absorption in the coronary artery, and optimizing the cardiac output. The goal of this study was to analyze the combined effect of CRT pacemaker and the LVAD to the electromechanical delay in cardiac muscle computationally.
Methods: To construct the electro-mechanical model, we used canine ventricle based on 3D MR image and integrated it to the lump model of the circulatory system and LVAD function. We simulated 14 ventricle unique cases. The subjects categorized into two groups, the first 7 models are LVAD groups and the other 7 models are non-LVAD group. Each model in each group has unique CRT pacing site shown in Figure below. To observe the electromechanical delay (EMD), we compute the interval of electrical activation time (EAT) and mechanical activation time (MAT). EAT defined as the membrane voltage of the local myocite exceeded above 0 mV and MAT defined as when the myofiber shortened at 10% of its maximum value.
Results: The results shows that overall the LVAD group models consumed lower energy (generally more than 50% of the ATP consumption). In terms of electrical activation, obviously, the tripacing model has the fastest or the lowest average EAT which was approximately 65 ms since it has three pacing sites. The sinus pacing has the highest output in terms of LV pressure, stroke work and stroke volume. The MAT and electromechanical delay (EMD) were also observed. Overall, other than the sinus pacing, the fastest MAT and EMD was from the tripacing site. This is the optimize option to maintain the hemodynamic in terms of electrical conduction pattern and contraction in the cardiac muscle.

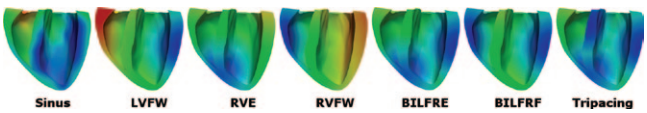

290

A Miniature Platform Technology for Multiple Applications of Chronic Mechanical Circulatory Assistance

R. K. Wampler,[1] J. W. Long,[2] T. A. Snyder,[3] J. R. Stanfield.[3] *[1]Oregon Health & Science University, Portland, OR; [2]Advanced Cardiac Care, INTEGRIS Baptist Medical Center, Oklahoma City, OK; [3]VADovations, Oklahoma City, OK.*

Study: Ventricular assist device (VAD) therapy remains limited due complexity, cost, and complications. Expansion of this therapy requires a new generation of smaller, safer, and more cost-effective technologies. Thus, we sought to develop a small, durable blood pump with superior hemocompatibility and reduced costs of manufacturing and use.
Methods: We have developed a platform technology for LVAD, RVAD, or Pediatric VAD applications retaining the same motor and bearing designs, while swapping out rotor/stator configurations designed for the physiology with each clinical application. The 9 mm OD pump housing incorporates modular hydraulics on one end and the motor with a magnetically stabilized, hydrodynamic bearing on the other end. This "inline" configuration allows for optimizing hemocompatibility by separating the bearing and primary flow paths and maximizing flow relative to diameter, given that the rotor is not surrounded by a motor. Through CFD optimization we developed RVAD, adult LVAD, and Pediatric LVAD hydraulics (rotor & stator blade combinations). The bearing was optimized for stability, improved hemocompatibility, and thermal management.
Results: The devices have been implanted in in acute and chronic animal studies up to 3 months in duration generating flows of 2 - 5.5 LPM adult and 1 - 3 LPM in pediatric configurations. The devices have demonstrated good hemocompatibility including very low hemolysis, < 5mg/dL, and preservation of von Willebrand Factor function. The issues encountered during development were electrical (early non-hermitic pumps and controller failure) and manufacturing (out of spec parts and polishing). Efforts continue to develop rapid implant and deployment tools and methods, and peripheral support equipment. Overall, we have developed a versatile, miniature blood pump platform for application in multiple configurations offering less invasive implant and expectations of superior hemocompatibility and cost-effectiveness.

291

Computational Quantification of LVAD Function During Ventricular Fibrillation Using 3D Cardiac Electromechanics Model

A. R. Yuniarti. *Medical IT Convergence, Kumoh National Institute of Technology, Gumi-si, KOREA, REPUBLIC OF.*

Study: LVAD has been used for patients who suffered weakened heart or congestive heart failure (HF), however, there are limited study which analyze the effect of LVAD to the heart which has arrhythmia. The goal of this study is to predict computationally the heart response during arrhythmia with implanted LVAD model to the electromechanical heart model. We concentrated to observe onto the fast arrhythmia or tachycardia which the heart has fast rhythm and altered electrical conduction pattern thus low effectiveness of contraction.
Methods: To construct electromechanical heart model, we used and MRI based mechanical model of heart failing ventricle with dilated geometry of the heart. The dilated geometry, fiber and laminar sheet structure were constructed from high-resolution MRI and DTMRI scans of HF canine ventricle. The electromechanical model consisted of two components which are electrical component and mechanical component. In addition, the mechanical model was also attached to the lumped cardiovascular system and LVAD model. To integrate the electrical component to the mechanical component, Ca^{2+} transient was used as a bridge. To conduct arrhythmia in the ventricle, we used s1-s2 stimulation. The conduction velocity was 60 cm/s. Using these parameter, we compare two arrhythmia subjects with and without LVAD in order to see the behavior of the LVAD to the arrhythmia ventricle.
Results: The result showed that, the arrhythmia ventricle with LVAD support has low energy consumption rate (ATP) and LV pressure compared to the arrhythmia ventricle without LVAD treatment. Even though the model without LVAD maintain mild pressure and appropriate volume, the cardiac output is insufficient compared to the LVAD case. It is because during the arrhythmia the heart is quivering instead of contracting. But the in the case of LVAD, The cardiac output is almost sufficient in order to distribute rich oxygenated blood through out the body.

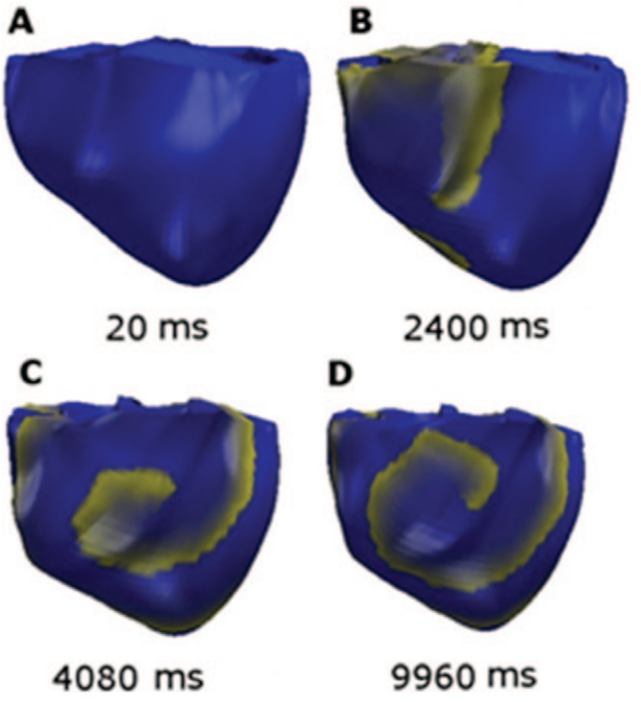

293

Trend Analysis of Intellectual Properties Relating to the Medical Devices Creating from Japanese Academic Institution

E. Akagawa. *Intellectual Asset Management, National Cerebral & Cardiovascular Center, Suita, JAPAN.*

Study: In order to lead to the commercialization of medical devices, intellectual property (IP) resulting from the study must have been evaluated quantitatively under the consideration of clinical situation. Thereby, there is a possibility to promote technology transfer (TT) from academia to industry. In the conventional generic IP evaluation in Japan, patentability and business feasibility have been positioned as key indicators. In the case of TT of medical devices, it should also be considered in medical significance except for above two indicators. To assist in the review and decision making process of IP of medical devices deliberation, we developed the scoring evaluation tool which consisted of three major criteria (1. patentability, 2. business feasibility, and 3. social aspects). The objective of this study is to analyze the IP for the medical devices creating from Japanese academic institution using the scoring evaluation tool.
Methods: The 26 patent applications that were extracted randomly from the published applicant information (not include companies at applicant) were analyzed. Three points to the high evaluation in the minor item, 2 points to the moderate one, the low one was arrange one point.
Results: In these results, the highest is 44 points, the lowest is 30 points, and the standard deviation was 3.3 points at the average 37.9 points. When comparing the scores for patentability, business feasibility, and social aspects listed in the main item, those were observed that patentability had high tendency (10.7 points / 12 points) and social aspects had low tendency (19.9 points / 30 points). In particular, because of some items were large standard deviation, it was suitable to evaluation tools has been suggested.

11

Is Single Ventricle Still a Risk Factor for Extracorporeal Membrane Oxygenation After Pediatric Cardiac Surgery?

Y. Kotani, S. Kasahara, S. Arai, Y. Kuroko, Y. Fujii, H. Taka, T. Douguchi, A. Miyamoto, S. Sano. *Cardiovascular Surgery, Okayama University, Okayama, JAPAN.*

Study: Extracorporeal membrane oxygenation (ECMO) is used for the bridge to recover from cardiopulmonary failure after a repair of congenital heart defects. Because of its complexity of hemodynamics, single ventricle (SV) is known as a risk factor for mortality in ECMO after pediatric cardiac surgery. This study is to elucidate if SV is risk for mortality.
Methods: Between January 2005 and September 2014, 74 patients had ECMO support after pediatric cardiac surgery. Median age and body weight was 2.0 (0–17.5) months and 3.2 (2.9–6.7) kg, respectively. Reason for ECMO was failure to wean cardiopulmonary bypass (CPB) in 21, low cardiac output in 24, E-CPR in 16, hypoxia in 10, arrhythmia in 2, and sepsis in 1. SV was seen in 42 patients, including 23 patients with hypoplastic left heart syndrome (HLHS). Data were compared between patients with SV and biventricular physiology (BiV).
Results: There were no statistical differences in reason for ECMO, timing of induction, and duration of ECMO between SV and BiV. Weaning from ECMO was successful in 28 of 42 (67%) in SV compared to 23 of 32 (72%) in BiV without a statistical significance (p=0.632). Survival rate to discharge tended to higher in BiV but did not reach to statistical significance (33% in SV vs. 47% in BiV). Logistic risk analysis showed induction other than operating room as a significant risk factor for mortality (p=0.030). However, HLHS as diagnosis, body weight, CPB time, and cardiac arrest time were not identified as risk for death. In conclusion, SV is not shown as risk for failure to wean from ECMO after pediatric cardiac surgery. Overall survival in SV; however, is slightly lower than BiV, suggesting earlier application and refinement of management for end-organ injury and bleeding would be a key to improve survival in this entity.

18

Prolonged Use of a Thoratec CentriMag RVAD with Oxygenator for Severe Acute Lung Injury

K. Nelson McMillan,[1] J. Young,[1] D. Stewart,[1] H. Lenker,[1] J. Jung-D'Amico,[1] K. McDonald,[2] N. Hibino,[1] C. Sciortino,[1] R. H. Bartlett,[3] L. Vricella.[1] *[1]Johns Hopkins University School of Medicine, Baltimore, MD; [2]Thoratec/St Jude Medical, Baltimore, MD; [3]University of Michigan, Ann Arbor, MI.*

Study: We report use of an RVAD in conjunction with an oxygenator, following insufficient peripheral ECMO support for refractory respiratory failure.
Methods: A 7 year old female presented to the pediatric ICU due to burns suffered during a house fire and subsequently developed severe acute respiratory distress syndrome (ARDS). On post-burn day 7, she experienced a cardiac arrest and was placed on VA-ECMO for 6 days, at which time she had cardiac recovery with ongoing respiratory failure, allowing transition to VV-ECMO. Despite maximal ECMO oxygenator support, consistent saturations above 80% could not be achieved. She underwent serial bronchoscopies revealing complete airway obstruction, prompting use of perfluorocarbon with intratracheal activated factor 7. While these strategies resulted in improvement in alveolar function, she continued to have inadequate gas exchange, as well as significant RV dysfunction and pulmonary hypertension (PH). An RVAD (Thoratec CentriMag) with an oxygenator was placed to allow for unloading of her RV as well as improve gas exchange. Serial ECHOs revealed improvement in RV function and PH as we weaned from full CentriMag support, ultimately transitioning to Thoratec PediMag support. Once she had adequate oxygenation from her native lungs, her RVAD was removed and an Avalon cannula was inserted in her IJ vein connected to the PediMag for use as an extracorporeal CO2 (ECCO2) removal device, as she continued to have a ventilatory defect. In total, she required 605 days of mechanical support (62 days of ECMO, 491 days of RVAD with oxygenator and 52 days of ECCO2 support). Over the course of time she was on mechanical support, she was able to fully participate in her rehab, including bike riding and attending school.
Results: It is often believed that ability to recover lung function following severe ARDS reaches full capacity within a few months. This case illustrates the potential of previously healthy pediatric lungs to undergo a protracted recovery following severe injury.

32

Glial Fibrillary Acidic Protein (GFAP) as Neurobiomarker in Pediatric Patients on Mechanical Circulatory Support (MCS)

J. C. McPhaul,[1] A. Lorts,[1] D. L. Morales,[1] A. Everett,[2] I. Wilmot.[1] *[1]Cincinnati Children's Hospital Medical Center, Cincinnati, OH; [2]The Johns Hopkins Hospital, Baltimore, MD.*

Study: Mechanical circulatory support (MCS) is becoming an increasingly common treatment modality in pediatric end-stage heart failure. MCS has been associated with an Increased risk of neuroinjury. Identifying brain injury and quantifying the extent of the damage with just the use of clinical and imaging assessments is imperfect. To continue to improve neurologic outcomes, a biomarker that can identify neuronal injury early is an important next step to both measure the extent of injury and provide prognostic information.
Methods: A prospective pilot study was performed on patients <25 years of age who were placed on MCS between 1/2015 and 9/2015 at Cincinnati Children's Hospital. GFAP levels were measured prior to ventricular assist device (VAD) implantation, 24 hours post-implantation, and on a weekly basis thereafter until transplant or decannulation.
Results: Data was collected on 4 initial patients who were male, ranged in age from 13–25 years, and from a variety of ethnic backgrounds (2 white, 1 Hispanic, 1 African-American). Presenting diagnoses included idiopathic dilated cardiomyopathy (A and B), prior heart transplant with coronary artery vasculopathy (C), and prior heart transplant with hemodynamically significant rejection (D). MCS devices included Heartware HVAD®(1), SynCardia TAH(2), and Centrimag®(1). No patients had neurologic injury after being placed on VAD. One patient (B) had a subclinical cerebral infarct found on Head CT (while on ECMO), which correlated with an elevation of GFAP prior to VAD initiation. Pre-VAD neuroimaging was performed and normal in 2 of the other patients (A and C), including 1 patient (C) whose course was complicated by cardiac arrest and emergent ECMO.
Conclusion: While none of the patients had neurologic injury while on VAD, GFAP was elevated in the one patient with a confirmed neurologic injury following an ECMO course. GFAP shows promise as a biomarker for neuroinjury in pediatric cardiac patients who require MCS.

GFAP Levels in Patients on MCS

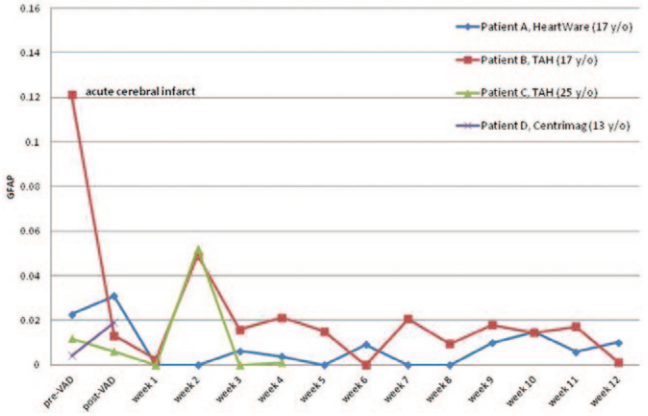

49

PC-MRI of Mechanical Cavopulmonary Assist Using an Intravascular Blood Pump

S. Chopski,[1] K. Whitehead,[2] R. Stevens,[3] A. Throckmorton.[1] *[1]Biomedical Engineering, Drexel University, Philadelphia, PA; [2]Pediatric Cardiology, The Children's Hospital of Philadelphia, Philadelphia, PA; [3]Pediatrics, Cardiothoracic Surgery, Drexel University, Philadelphia, PA.*

Study: The limit of therapeutic options for the treatment of failing or dysfunctional single ventricle physiology in the adult congenital population poses a new challenge for clinicians. A pressure boost of only 1–5 mmHg that augments pulmonary arterial perfusion, while not facilitating retrograde flow into the superior vena cava (SVC), is desired for cardiovascular benefit. In an effort to address this unmet therapeutic need, fluid dynamic studies were conducted on a patient-specific cavopulmonary circuit having an MRI-compatible, intravascular, axial flow blood pump in the inferior vena cava (IVC). The purpose of this study was to investigate the complex 3-D velocity profile of mechanical cavopulmonary assistance using high-resolution, cardiac magnetic resonance.
Methods: Phase contrast-MRI fluid dynamic studies were performed using a circulatory mock loop of Fontan and an axial flow blood pump in the IVC. Physiologic cardiac outputs were achieved with a 40%/60% flow split between the SVC and IVC, a 50%/50% flow split between the pulmonary arteries, and operational rotational speeds of 1000–4000 RPM with flow rates of 2–4 L/min.
Results: The intravascular blood pump was able to promote blood flow into the cavopulmonary junction and washout areas of stagnant blood. This study also demonstrates the benefits of PC-MRI as an application to evaluate intravenous mechanical cavopulmonary assistance.

51

Rotational Fluid Dynamics of Mechanical Cavopulmonary Assistance

A. Throckmorton,[1] S. Chopski,[1] S. Birewar,[1] P. Huang,[1] R. Stevens,[2] J. Kresh.[3] *[1]Biomedical Engineering, Drexel University, Philadelphia, PA; [2]Pediatrics, Cardiothoracic Surgery, Drexel University, Philadelphia, PA; [3]Cardiothoracic Surgery, Drexel University, Philadelphia, PA.*

Study: Surgical optimization of the cavopulmonary connection and pharmacological therapy for dysfunctional single ventricle physiology continue to advance, but only slow the progression of decline to end-stage heart failure. As a therapeutic option for these patients, we seek to develop a versatile mechanical cavopulmonary assist device that will provide bridge-to-transplant or stabilization support. We hypothesize that rotational blood flow, delivered by an implantable axial flow blood pump, could effectively assist the venous circulation in Fontan patients by mimicking vortical blood flow patterns in the cardiovascular system.
Methods: This study investigated seven new models of mechanical cavopulmonary assistance (single and dual-pump assist), created combinations of pump designs that deliver counter rotating vortical flow conditions, and analyzed pump performance, velocity streamlines, and energy augmentation in the cavopulmonary circuit for each support scenario.
Results: All models indicated strong pump performance and adequate pressure generation for Fontan patients. The model having an axial clockwise-oriented impeller in the inferior vena cava and an axial counterclockwise-oriented impeller rotating in the superior vena cava outperformed all of the support scenarios by enhancing the energy of the cavopulmonary circulation an average of 10% over the range of blood flow rates and a maximum of 27% at higher flow rates. This research is intended to serve as a guide in the development of axial flow blood pumps for Fontan patients. The findings demonstrated the strong probability of a cardiovascular benefit using counter rotating pumps in a dual support scenario, but that this could be dependent upon the patient-specific anatomy.

61

At-home Compression Therapy for Patients with Single Ventricle Physiology

J. Hernandez,[1] S. Lee,[2] W. Moskowitz,[2] S. Chopski,[3] A. Throckmorton.[3] *[1]Biomedical Engineering, Virginia Commonwealth University, Richmond, VA; [2]Pediatric Cardiology, Virginia Commonwealth University, Richmond, VA; [3]Biomedical Engineering, Drexel University, Philadelphia, PA.*

Study: To address the unmet need of a new treatment option for Fontan patients, we are investigating the feasibility of a non-invasive, at-home therapy to improve their hemodynamic status. Our hypothesis is that regularly and routinely applied compression therapy using pneumatically-driven trousers will augment systemic venous return, improve ventricular preload, and thus enhance cardiac output. In a clinical study (n=2), we employed the NormaTec Pneumatic Compression Device (PCD), which has received FDA510(k) premarket clearance for use to treat patients with venous insufficiency.
Methods: The PCD device is composed of trousers with air compartments that allow for circumferentially and uniformly applied pressure to the patient's lower extremities. It is operated by a programmable controller that enables the user to set the applied pressure level and interval for inflation and deflation of the trousers. Following an initial health screening, test subjects were pre-evaluated with a modified-Bruce, treadmill exercise stress test, and cardiorespiratory data baseline data was collected. They were fitted, trained, and evaluated on how to use the PCD. Test subjects then received 6 days of external compression therapy at-home. A final evaluation was conducted with a second treadmill stress test and hemodynamic assessment.
Results: Overall, both patients showed an improvement in exercise duration time, peak oxygen volume, and ventilator threshold as compared to baseline data. This data provides the groundwork for future studies that will focus on increasing the sample size and more accurately assess the clinical benefit of at-home compression therapy.

95

Artificial Placenta versus Mechanical Ventilation: Quantification of Lung Alveolarization

E. M. Perkins,[1] M. A. Coughlin,[1] N. L. Werner,[1] J. T. Church,[1] B. S. Bryner,[1] J. K. Bentley,[2] M. B. Hershenson,[2] A. Rojas-Peña,[1] R. H. Bartlett,[1] G. B. Mychaliska.[3] *[1]Department of Surgery, University of Michigan, Ann Arbor, MI; [2]Department of Pediatrics and Communicable Diseases, University of Michigan, Ann Arbor, MI; [3]Section of Pediatric Surgery, University of Michigan, Ann Arbor, MI.*

Study: Respiratory failure is the most common cause of mortality in neonates <27 weeks gestational age (GA). Current treatment with mechanical ventilation (MV) is costly and can cause lung injury. An Artificial Placenta (AP) using veno-venous extracorporeal life support (ELCS) would be a novel treatment for prematurity. We hypothesize the AP will allow for normal lung development compared to MV in a premature lamb model.
Methods: AP lambs of GA 119–121 days (term=145) were delivered and cannulated for ECLS (internal jugular drainage, umbilical vein reinfusion, n=4) with a goal of 7 days support. MV lambs (128–131 days, n=2) were placed on the ventilator with a goal of 48 hours support. Tissue controls (TC, 128–131 days) were immediately necropsied (n=4). Immunofluorescence was performed on lung tissue for α-actin and platelet-derived growth factor-α (PDGFR-α). Alveolarization was assessed using a morphometric technique. A grid was overlayed on lung micrographs using NIH Image. The ratio of points falling on the alveolar tips compared to the total number of reference points (area fraction) was calculated. To verify the identification of tips, we calculated the area fraction of α-actin and PDGFR-α-positive tips.
Results: MV lambs survived an average of 46.3 hours. Compared to TC, lungs of MV lambs showed thickened alveolar walls, and hypoalveolarization (Figure 1B, 1C). AP lambs survived an average of 7 days and lungs showed minimal trauma and normal alveolarization (Figure 1A). The average area fraction of alveolar tips was 0.015 ± 0.008 for AP, 0.008 ± 0.003 for MV and 0.016 ± 0.006 for TC. Average area fractions of double-positive tips were 0.013 ± 0.007 for AP, 0.003 ± 0.002* for MV and 0.013 ± 0.005 for TC (*significantly different from AP and TC, p<0.05, two-tailed t-test, Figure 2) Compared to TC, lung alveolarization was severely attenuated after MV but not after AP support. These data suggest the AP is superior to MV in supporting lung development in extremely premature lambs.

Figure 1: Lung Tissue From Premature Lambs Stained for α-actin (Red) and PDGFR-α (Green)

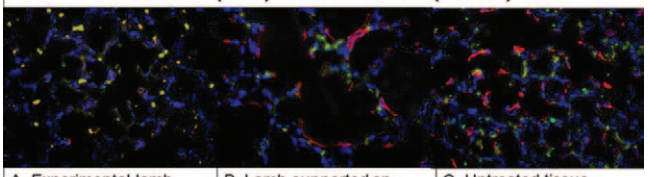

A. Experimental lamb supported on artificial placenta for 7 days. 40x.	B. Lamb supported on mechanical ventilation for 81 h. 40x.	C. Untreated tissue control. 40x.

Figure 2: Area Fraction Of Alveolar Tips Double Positive For α-actin and PDGFRα

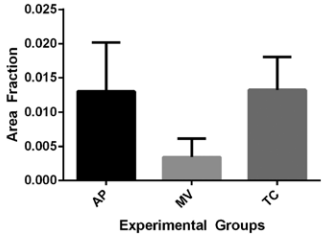

122

Prolonged Artificial Placenta Support with Transition to Mechanical Ventilation

J. T. Church, **M. A. Coughlin**, E. Perkins, H. Hoffman, R. H. Bartlett, G. B. Mychaliska. *University of Michigan Health System, Ann Arbor, MI.*

Study: Extremely premature infants face significant mortality and morbidity. An Artificial Placenta (AP) utilizing extracorporeal life support (ECLS) could support ELGANs for prolonged duration without mechanical ventilation (MV). The aim of this study was to extend AP support beyond 7 days and to transition to MV.
Methods: Lambs at 118 days gestational age (GA; term = 145 days) were placed in either AP or MV-control groups. AP lambs (n=8) were placed on venovenous ECLS with jugular drainage and umbilical vein reinfusion. Lungs remained fluid-filled. Lambs were supported for a goal of 10–12 days. Those lambs who survived to goal were transitioned to MV and given surfactant. MV-control lambs (n=5) were placed on MV support at the time of delivery and also given surfactant. Support continued in both groups until MV was inadequate to maintain adequate gas exchange, at which point lambs were euthanized.
Results: AP lambs survived a mean 186 ± 110 hours, with the longest survival 329 hours (13.7 days). MV-control lambs survived 5.7 ± 2.5 hours (p=0.002). Four lambs survived to 10 days AP support and were transitioned to MV. AP lambs underwent 36.8 ± 36.5 hours of MV lung recruitment, followed by withdrawal of AP support and continuation of MV alone for 11.5 ± 11.0 hours (see Figure). Despite adequate oxygenation and good compliance, inadequate ventilation and sedation limited MV duration. One AP sheep could not be weaned due to poor oxygenation. Of the four that did not survive to MV transition, two succumbed to oxygenator malfunction, one to hemorrhage following CPR, and one to sudden cardiac death of unclear etiology. These results show that the Artificial Placenta is capable of providing support for 10–12 days, with the potential for transition to mechanical ventilation.

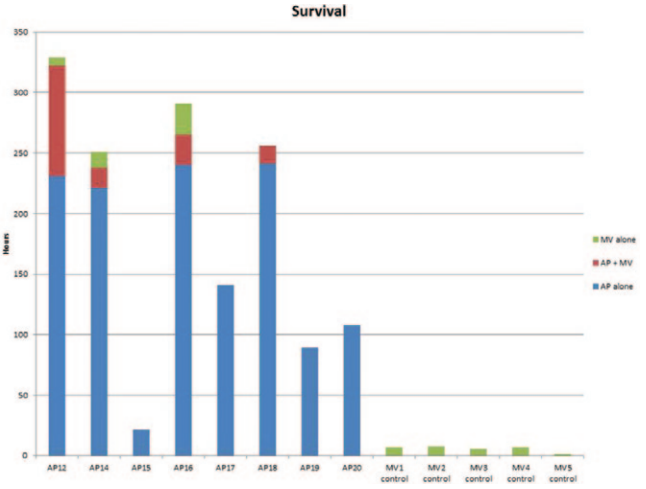

123

The Artificial Placenta Avoids Damage Caused by Mechanical Ventiliation

M. A. Coughlin,[1] N. L. Werner,[1] J. T. Church,[1] R. M. Rabah-Hammad,[2] R. H. Bartlett,[1] G. B. Mychaliska.[1] *[1]Extracorporeal Life Support Laboratory, University of Michigan, Ann Arbor, MI; [2]Department of Pathology, University of Michigan, Ann Arbor, MI.*

Study: The treatment of prematurity involves the use of mechanical ventilation (MV), which can lead to long-term pulmonary complications. Since an Artificial Placenta (AP) avoids the use of MV, we hypothesize that the AP will avoid lung injury.
Methods: AP lambs of gestational age (GA) 114–123 days (term=145, n=9) were delivered and placed on venovenous-ECLS (internal jugular drainage and umbilical vein reinfusion). They were intubated and the endotracheal tube clamped with a goal of 7 days AP support. MV lambs were delivered between 108–128 days (n=7), intubated, given surfactant, and placed on the conventional ventilator with transition to high frequency oscillatory ventilation as indicated. Tissue control (TC) animals were delivered between 105–130 days and immediately sacrificed (n=25). Lungs were procured and the airways filled to 30cm with formalin, sectioned and stained with hematoxalin and eosin. A pathologist blinded to groups evaluated the slides and scored injury based on infiltration, hemorrhage, edema, atelectasis, and necrosis on a 0–4 scale. Animals were grouped based on GA and student's t test used for comparison.
Results: Average survival of the AP animals was 7 days compared to 3.4 ± 2 hours for MV animals of similar GA. No statistically significant differences were found between AP and MV animals when evaluating edema, infiltration, or necrosis. The average hemorrhage score of all MV animals was 1.6 ± 0.7 vs. 0.75 ± 0.4 for AP (p=0.03) vs. 0.64 ± 1 for TC (p=0.02, Figure). The average atelectasis score of MV animals was 1 ± 0.8 vs. 0.3 ± 0.4 for AP (p=0.04) vs. 0.2 ± 0.5 for TC (p=0.005). These data suggest use of MV in extremely premature animals causes damage, especially in the form of hemorrhage and atelectasis. The use of AP avoids this early injury.

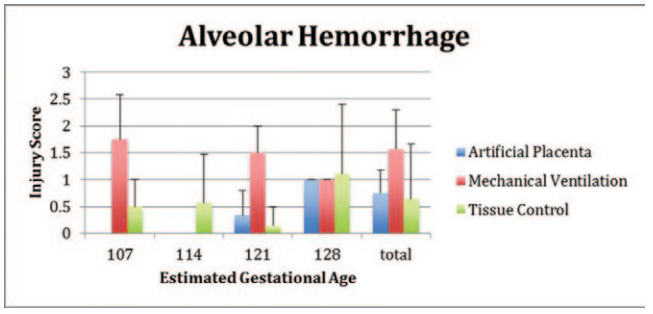

124

Maintaining Fetal Circulation in the Artificial Placenta Model

M. A. Coughlin, J. T. Church, N. L. Werner, G. E. Owens, R. H. Bartlett, G. B. Mychaliska. *Extracorporeal Life Support Laboratory, University of Michigan, Ann Arbor, MI.*

Study: By maintaining fetal circulation and avoiding mechanical ventilation an Artificial Placenta (AP) may solve many problems of prematurity. The aim of this study was to evaluate the effect of varying oxygen levels on long-term ductus arteriosus patency in the lamb model.
Methods: Five premature lambs (118 days gestation, term=145) were delivered via C-section and placed on veno-venous extracorporeal life support (drainage from the right internal jugular, reinfusion via the umbilical vein). An umbilical artery catheter was placed. Ultrasound with color Doppler was used to evaluate ductal patency and direction of flow at delivery and once a day. Two animals were managed with a goal SaO_2 of 70–80% (high) and three animals had a goal of 60–70% (low).
Results: Average survival of the lambs was 8 ± 3.5 days. All animals had a patent ductus arteriosus at delivery. Both animals in the high group showed closure of the ductus on day 2. One animal in the low group maintained a patent ductus for 9 days. Another animal had a closure of the ductus on day 2 after inadvertently high saturations, then showed reopening on day 5 with maintenance of lower saturations and remained open until day 8. Animals in the low group had an average pO_2 of 28.9 ± 5.1mmHg vs. 33.5 ± 3.9mmHg in the high group. Average saturation in the low group was 63.6 ± 6.4% vs. 72.9 ± 3.5% in the high group. All animals remained hemodynamically stable with lactate values that trended to normal. These data suggest that lower oxygen content may maintain or restore fetal circulation while on AP support without adversely affecting perfusion. This will be important as we assess lung development during AP support.

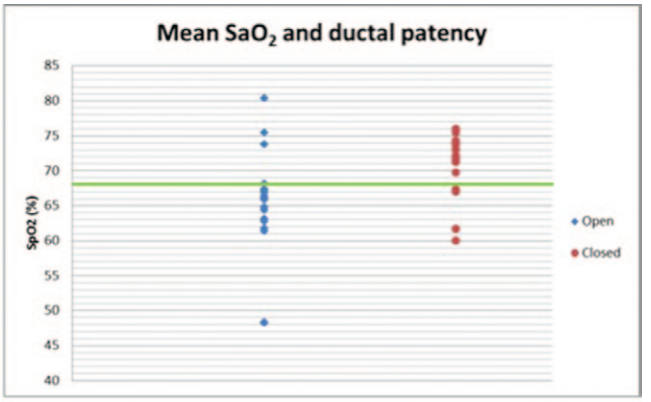

Figure: Cluster plot showing the average SaO_2 on days with an open vs. closed ductus. Line at 68%.)

134

What Do We Do with the School Age Children? A Comparison of Clinical Outcomes in School Aged Children Bridged to Transplant with Pulsatile and Continuous Flow Ventricular Assist Devices

C. Villa, J. Mathew, F. Zafar, R. Rizwan, D. L. Morales, A. Lorts. *Cincinnati Children's, Cincinnati, OH.*

Study: Continuous flow VADs (cfVADs) have quickly become the standard VAD technology used to bridge adolescent children to transplant. In smaller children, there is significant variability in device selection. Centers often debate when to use a pulsatile device and when to push size limits and use a cfVAD designed for an adult. We compared clinical outcomes of children (25–60 kg) bridged to transplant over the last decade with the currently used pulsatile and cfVADs.
Methods: The UNOS database was used to identify children ≤ 18 years that were 25–60 kg and who had an EXCOR, Heartmate II or Heartware at time listing between 6/2004 and 6/2014. Patients were stratified based on device type (pulsatile and cfVAD).
Results: A total of 79 patients were identified. Forty-five (57%) received a cfVAD (Table). Patients with a cfVAD were older and larger. cfVADs were less likely to have prior ECMO support, less likely to be ventilated and less likely to have BiVAD support. Despite these risk factors, waitlist outcome was similar between groups. There was no difference in post-transplant survival between groups (Figure). Conclusions: Over the last decade, waitlist and post-transplant survival is similar for school aged children 25–60 kg implanted with either a pulsatile or cfVAD. Information regarding quality of life and the potential for discharge home is needed to fully assess the potential risks and benefits of the available device technologies.

Table. Characteristics of children (25-60 kg) listed for transplant with a ventricular assist device stratified by flow type.

Variable	Continuous flow n=45	Pulsatile flow N=34	p-value
Female	21 (47%)	14 (41%)	0.654
Age (years)	13 (12 - 14)	11 (9 - 12)	<0.001
Height (cm)	160 (151 - 170)	146 (138 - 158)	<0.001
Weight (kg)	50 (43 - 56)	39 (30 - 47)	0.001
Body surface area (m^2)	1.52 (1.36 - 1.6)	1.26 (1.1 - 1.46)	<0.001
Caucasian	21 (47%)	18 (53%)	0.535
Diagnosis			
Cardiomyopathy	43 (96%)	28 (82%)	0.132
Congenital	2 (4%)	3 (9%)	
Other/Unknown	0 (0%)	3 (9%)	
ECMO at listing	0 (0%)	7 (21%)	0.002
BiVAD support	5 (11%)	16 (47%)	0.001
Status 1A at listing	41 (91%)	32 (94%)	0.822
Waitlist time (days)	45 (15 - 94)	48 (17 - 88)	0.843
Waitlist outcome			
Transplanted	40 (89%)	29 (85%)	0.827
Deteriorated	1 (2%)	2 (6%)	
Died	1 (2%)	2 (6%)	
Improved	2 (4%)	1 (3%)	
Censored	1 (2%)	0 (0%)	
Condition at transplant			
Creatinine (mg/dL)	0.6 (0.5-0.7)	0.5 (0.4-0.7)	0.307
Bilirubin (mg/dL)	0.7 (0.4-1.4)	0.8 (0.3-1.5)	0.928
On ventilator	1 (3%)	6 (21%)	0.037
Inotropic support	12 (32%)	6 (21%)	0.407

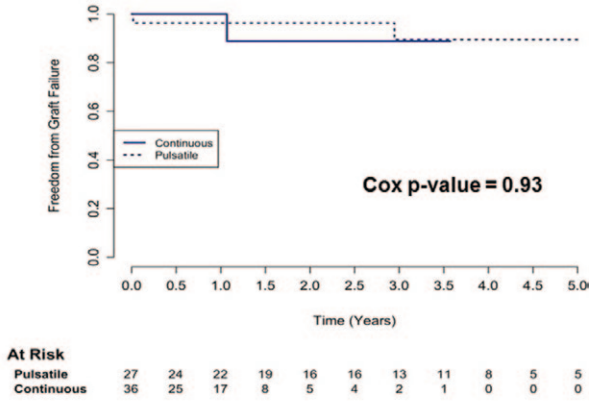

Figure. Post-transplant graft survival among children 25-60 kg bridged to transplant with a ventricular assist device stratified by device flow type.

140

Pediatric Artificial Lung: Effects on Right Ventricle Afterload in an Ovine Model of Pulmonary Hypertension

F. Alghanem, B. S. Bryner, U. P. Fernando, J. M. Trahanas, H. R. Hoffman, A. Rojas-Pena, R. H. Bartlett, R. B. Hirschl. *Extracorporeal Life Support Laboratory, Department of Surgery, University of Michigan, Ann Arbor, MI.*

Study: Chronic lung disease in children often results in pulmonary hypertension (PH) and right heart failure. The availability of an implantable pediatric artificial lung (PAL) would open new approaches to the management of these patients by bridging them to lung recovery or lung transplantation. This study investigates the efficacy of a novel PAL at alleviating a model of PH and increased right ventricle (RV) afterload in the acute setting.
Methods: Five juvenile lambs (20–30 kg) underwent PAL implantation via pulmonary artery to left atrium attachment (in-parallel). Induction of disease involved occlusion of the right main pulmonary artery. Systemic hemodynamics, pulmonary vascular input impedance, and RV efficiency were measured under (A) baseline, (B) disease, and (C) disease+PAL conditions.
Results: The disease model altered hemodynamic variables in a manner consistent with PH. Subsequent PAL attachment improved pulmonary artery pressure (29.3 ± 4.4 vs. 25.2 ± 4.9 mmHg, p=0.02), cardiac output (3.7 ± 1.0 vs. 4.2 ± 1.0 L/min, p=0.05), pulmonary vascular input impedance (Z.0: 4.8 ± 1.9 vs. 4.0 ± 1.8, p=0.03; Z.1: 11.7 ± 4.8 vs. 7.5 ± 3.5 mmHg/L/min, p=0.06), and RV efficiency (12.0 ± 1.7 vs. 14.0 ± 1.8 L/J, p=0.01). The PAL averaged blood flows of 1.3 ± 0.6 L/min and resistance of 2.3 ± 0.8 mmHg/L/min. Additional *in vitro* testing demonstrated average O2 transfer of 38.0 ± 2.2 mL/min and CO2 clearance of 122.6 mL/min at 1.5L/min blood flow. The PAL improves RV function in the setting of acute PH and may have potential for use as a bridge to lung recovery or transplantation in pediatric patients.

149

The Spectrum of General Surgery Interventions in Pediatric Patients with VADs

F. Kamel,[1] H. Buchholz,[2] B. Dicken,[3] J. Conway.[4] *[1]General Surgery, University of Alberta, Edmonton, AB, CANADA; [2]Cardiac Surgery, University of Alberta, Edmonton, AB, CANADA; [3]Paediatric Surgery, University of Alberta, Edmonton, AB, CANADA; [4]Paediatric Cardiology, University of Alberta, Edmonton, AB, CANADA.*

Study: Ventricular Assist Devices (VADs) revolutionized the therapy of heart failure. Despite their success, VADs come with a number of complications. In the adult population, up to 55% of patients with LVADs have abdominal complications. Although the literature describes LVAD complications in adults, there are no studies to date that directly focus on general surgical interventions in pediatric patients. This study aims to describe the general surgical interventions in pediatric patients with VADs at a single centre.

Methods: This was a retrospective descriptive study of the Stollery Children's Hospital Artificial Heart Program database. All pediatric patients (age < 17 years) having received VADs from 2005–2015 were included. A chart review was performed to determine general surgical interventions and outcomes. All patients undergoing general surgery had their anticoagulation held 30 minutes to 1 hour prior to the operation and resumed within two to six hours post-operatively.

Results: Fifty-four patients received VADs, including 40 Berlin Heart EXCORs, 15 Thoratec Centrimags, 7 Heartware HVADs and 1 Thoratec Heartmate II. Twenty-four patients (44%) underwent a general surgical procedure, including 2 emergency laparotomies for cannula site hemorrhage, 2 for bowel ischemia and 1 splenectomy for splenic infarct. There were 21 urgent procedures for vascular or dialysis access, 8 for long-term feeding tubes, and 2 for fundoplications. There were no deaths attributed to the general surgery interventions and no issues with the VAD were encountered.This is the first study to describe general surgical intervention encountered in pediatric patients with VADs with no mortality attributed to the direct surgical procedure and minimal associated morbidity. These findings are likely related to increasing comfort level with operating on these high risk patients and the emphasis placed on a multidisciplinary approach to their care.

150

Induction of ECMO in Operating Room Significantly Improves Survival in Infants With Congenital Heart Disease

Y. Fujii, S. Kasahara, N. Horio, S. Ishigami, &. Goto, M. Okuyama, J. Kobayashi, K. Etou, Y. Kotani, Y. Kuroko, S. Arai, T. Hiroshi, D. Takuma, A. Miyamoto. M. Nishimura, S. Sano. *Cardiovascular Surgery, Okayama University Graduate School of Medicine, Dentistry, and Pharmaceutical Sciences, Okayama, JAPAN.*

Study: Extracorporeal Membranous Oxygenation Support (ECMO) in infants with congenital heart disease (CHD) is still very high risk procedure although the clinical results of CHD has been remarkably improved. Aggressive use of ECMO before circulatory collapse may improve the outcomes. The purpose of this study was to describe the details of the current clinical results of ECMO for infants with CHD in this institution and describe the effect of planned ECMO induction before circulatory collapse.

Methods: Seventy-three infants underwent ECMO induction between January 1997 and December 2015. The chart reviews were performed retrospectively.The ECMO was induced in operative room in 30 patients (OR group) and in other places such as CCU or IVR in 43 patients (Not-OR group). Twenty-three patients in OR group took the ECMO induction immediately after cardiovascular operation, and the others in OR group underwent it because circulatory condition could not be managed well despite of intensive care. The clinical results were compared in the two groups. In addition, risk analysis for survival was performed.

Results: One patient in OR group and 22 patients in Not-OR group underwent cardiopulmonary resuscitation before ECMO induction (P<0.001). There was no significant difference in the other patients' backgrounds (See Table). OR group had a significantly higher rate of weaning from ECMO than Not-OR group (73% (22/30) vs 47% (20/43), P=0.023). Significantly higher rate of patients in OR group could discharge from the hospital (47% (14/30) vs 23% (10/43), P=0.036). There was no death in the all survivors with the average follow-up period of 4.2 ± 3.1 years (range, 0.1 - 11.2 years). With multivariate analysis, induction of ECMO in OR was a negative risk factor for failure of weaning from ECMO (P=0.033, CI; 1.095–8.563). In conclusion, induction of ECMO in OR before a serious circulatory collapse is very important to improve the survival in infants with CHD.

	Details of patient's characteristics		
	OR (n=30)	Not-OR (n=43)	P
before 2008	19 (63%)	20 (47%)	0.156
Age (days)	43 ± 12 (SE)	82 ± 16 (SE)	0.072
Neonate	19 (63%)	18 (42%)	0.071
Female	13 (43%)	23 (53%)	0.393
Body weight (kg)	3.28 ± 1.08	3.43 ± 1.37	0.632
Full Flow (ml/min)	537 ± 152	516 ± 215	0.643
Repair type	BV repair 9, 1st palliation 20, 2nd palliation 1	BV repair 10, 1st palliation 30, 2nd palliation 3	0.683
Pure respiratory failure	7 (23%)	5 (12%)	0.184
HLHS	12 (40%)	14 (33%)	0.514

182

Case Presentation: Berlin Heart EXCOR® Pump Exchanged on the Inpatient Cardiology Floor: "Can You Actually Do That?"

S. Zeigler, A. Winkie, S. Feehan, M. Gowen, E. Corpuz, B. Banys, P. Eustaquio, P. Church, N. La Croix-Agustin, M. Nguyen, P. Shuttle worth, S. Chen, K. Maeda, C. Almond, D. Rosenthal, **J. Murray**. *Lucile Packard Children's Hospital, Palo Alto, CA.*

Study: The Berlin Heart EXCOR® is widely used to support children as a bridge to transplant. Use of the Berlin Heart requires ongoing hospitalization but de-intensification of treatment is possible. During prolonged support, exchange of the pump may be required. We sought to describe a case of a 3 month old supported on a 10cc pump for whom exchange was successfully performed on the cardiology floor.
Methods: The patient had been on the floor for two weeks prior to exchange. His clot burden was significant despite therapeutic anticoagulation and triple antiplatelet therapy. The decision was made that the exchange would occur at the bedside jointly by the medical director and the surgeon. Our institution's pump exchange guideline was implemented by the involved staff to streamline and reinforce the process.
Results: The preparation time was about 2 hrs for education and obtaining supplies. The actual exchange was performed by the surgeon with assistance from the perfusionist and lasted approximately 1 min. The patient remained hemodynamically stable and no sedation was required. In patients maintained on stable EXCOR® support, pump exchange can be safely conducted on the cardiology floor. This can help expedite the exchange process which in turn may improve patient safety.

193

A Novel Test Bench to Simulate Failing Superior Cavo-Pulmonary Connection

F. De Gaetano,[1] M. Griselli,[2] M. Costantino.[1] [1]*Department of Chemstry, Material and Chemical Engineering "Giulio Natta", Politecnico di Milano, Milan, ITALY;* [2]*Department of Cardiac Surgery, King Faisal Specialist Hospital and Research Centre, Rhiad, SAUDI ARABIA.*

Study: Results for mechanical circulatory support in univentricular circulation have shown a worse success rate compared to biventricular circulation. Nowadays there is a growing interest in searching solutions for these patients. Great majority of research is focusing on patients with total cavo-pulmonary circulation, whilst children with failing superior cavo-pulmonary connection (SCPC) or Stage II Norwood remain an unsolved issue. Reasons are the scarcity of suitable assist devices for this small subgroup of univentricular patients and unsuitability for emergency types of mechanical cardiac support.
Methods: To define the best approach for these patients, we have developed a test bench model, *i.e.* a mock loop simulator (MLS), of SCPC which is working at standard physiological range of values, obtained from cardiac catheterization of 20 patients who have done well after SCPC. Previously reported MLSs have focused on a particular segment of the circulation adapting other values accordingly. In our model all segments need to reproduce physiological ranges allowing us to monitor responses while performing changes in the setting for mimicking different types of failure. A Berlin Heart Excor (BHE) 15ml pump was used as native heart, reproducing an ejection fraction of 66%. Standard settings were: BHE rate 130/min, cardiac output 1,3L/min, upper body flow ~ 450 ml/min, common atrial pressure 8 ± 2mmHg, SCPC pressure 12 ± 2mmHg, mean arterial pressure 50-60mmHg, pulmonary vascular resistance 1 WU.
Results: Four types of failure were tested: systolic dysfunction, diastolic dysfunction, cavo-pulmonary intrinsic failure, mixed type. The results obtained reproduced adequate the clinical scenarios of SCPC failure patients, however our test bench is only able to reproduce indirectly the neuro-humoral response noted in clinical practice. Next step will be the introduction of a ventricular assist device (VAD) function in the system to evaluate the interaction of VAD with the SCPC in different types of failure.

212

Evaluation of the New Polish ReligaHeart Pediatric VAD Family in Physical, *in-vitro* and *in-vivo* Pre-clinical Studies

P. Ciesla, **M. Gawlikowski**, M. Glowacki, M. Gonsior, K. Janiczak, A. Kapis, R. Kustosz. *Artificial Heart Laboratory, Foundation of Cardiac Surgery Development, Zabrze, POLAND.*

Study: The Berlin Heart Pediatric VAD is the gold standard in mechanical heart support for children, however is not free of thrombous formation risk. The new family of extracorporeal, pneumatic ReligaHeart (RH) PED VAD in sizes of 45, 30 and 20 ml of stroke volume (SV) was developed by Foundation of Cardiac Surgery Development. The pump construction is based on asymmetric shape of adult pump (RH EXT) and is equipped with original valves designed from the very beginning to work only in VAD application. RH PED construction provide a low risk of thrombogenicity, no hemolysis and good hemodynamic features. The evaluation was made in physical, in-vitro and in-vivo pre-clinical studies.
Methods: The first phase of development studies involved physical examination and long term durability tests. Next phase includes in-vitro blood studies conducted in accordance to the acute thrombogenicity method and determination of normalized index of hemolysis. The final phase consists of two stages: early pre-clinical stage which involves acute in-vivo experiments and 30 day pre-clinical studies. Both stages of in-vivo experiments include implantations (n=10) of two sizes of pediatric VADs; 45ml and 30ml SV in domestic pig model. During the experiment animals were monitored in the aspects of VAD performance, morphology, coagulology, hematology and presence of micro and macro biological material during the experiment and after deplantation inside the pump. Additionally, histopathological evaluation of vital organs was made.
Results: After successfully completed physical and in-vitro studies the results of pre-clinical in-vivo studies demonstrate low thrombogenicity, no hemolysis and good overall physical performance of RH PED VADs on animal model. In-vivo studies proved a lack of impact to vital organs and no sign of thrombus adhering to the pump. The pre-clinical examination results allow introducing pilot manufacturing of the RH PED 45ml and 30 SV VADs for clinical studies.

226

Continuing Development of a Single Ventricle Pediatric Mock Circulation for Student Instruction and Clinical Simulation

A. M. Swiergosz, B. Ngha, L. Pyles, A. Calhoun, K. Martin, K. Hughes-Miller, J. Sparks, G. M. Pantalos. *University of Louisville, Louisville, KY.*

Study: The simulation of clinical scenarios can maximize care team performance, minimize threats to patients, and improve overall outcomes. Simulation training is particularly beneficial for treating pediatric patients with less common congenital heart defects that result in single ventricle physiology. A functioning model of single ventricle physiology for pediatric critical care simulation has been created that is the first of its kind permitting learner interaction.
Methods: The simulator approximates key anatomic structures and elements of the infant cardiovascular system. The single ventricle model (with a stroke volume of 20 mL) was created from two pediatric ventricular assist devices resulting in two atrial inlets and one great vessel outlet like a patient with truncus arteriosus. Pulsatile, physiologic pressures and flows are created by pumping a blood analog fluid through the modeled vasculature. The model incorporates a compliant pulmonary artery (PA) segment for banding or atresia creation and a 4 mm Blalock-Taussig shunt. The simulator uses transducers from a patient monitor to display blood pressures and ECG adding fidelity to the simulation experience for the learner.
Results: By isolating the pulmonic (Qp) and systemic (Qs) circulations at a flow rate of 1.2 L/min, reasonable vascular resistances could be established for each circulation. Combining the circulations and adjusting the circulating fluid volume results in an unbalanced circulation (Qp/Qs >1) due to the lower resistance of the pulmonary circulation. Applying a critically adjusted PA band or opening a B-T shunt across an atretic PA, restored balance to the circulation (Qp = Qs), adding to the instructional and simulation value of the model. The addition of veno-arterial ECMO support, the presence of an atrial septal defect, and other scenarios are anticipated for the further development of the single ventricle simulation model.

231

Pediatric Use of Impella 5.0: Difficulty Removing Device Through Axillary Artery

D. Horne,[1] D. Parekh,[2] S. C. Tume,[3] A. Qureshi,[2] H. Justino,[2] C. M. Delauz,[2] A. Jeewa,[2] C. D. Fraser, Jr.[1] I. Adachi.[1] *[1]Congenital Heart Surgery, Texas Children's Hospital, Houston, TX; [2]Cardiology, Texas Children's Hospital, Houston, TX; [3]Intensive Care, Texas Children's Hospital, Houston, TX.*

Study: There is increasing use of Impella ventricular assist device in pediatric patients. The major limiting factor in pediatrics is the size of access vessels. Impella 5.0 is 7 mm in maximum diameter.
Methods: A 14-year-old male (BSA 1.7 m2) with monomorphic ventricular tachycardia presented with acute heart failure and progressive acute kidney injury. Placement of an Impella CP via the right femoral artery resulted in improvement in renal function. For better decompression of the left ventricle, Impella CP was subsequently replaced with Impella 5.0 via a right axillary artery graft without difficulty. This resulted in a decrease in pulmonary arterial wedge pressure (12 to 8 mmHg) and an increase in device-assisted flow (3.1 to 4.8 L/min). Cardiac function and rhythm significantly improved over the next 10 days, which lead to discontinuation of support. During the device removal, it unexpectedly got lodged once past the innominate artery. Under fluoroscopy guidance, right arm traction and shoulder manipulation were attempted along with multiple forceful traction and rotation maneuvers of the device catheter. This eventually delivered the device. Post-operative CT-angiogram ruled out dissection and confirmed vascular integrity. The CT was remarkable for narrow anterior-posterior chest diameter and multiple points of angulation from the ascending aorta to the right axillary graft, which might have posed technical difficulty in device removal. The innominate, right subclavian and axillary arteries measured 8.5, 6.4, and 6.4 mm, respectively. The patient was discharged 3 weeks later with low normal cardiac function and normal neuro-vascular examination.
Results: Impella is inserted but not removed over a guide wire, which serves to straighten vascular structures. Thus, successful insertion of Impella may not guarantee effortless removal. Careful vascular assessment is recommended when using Impella 5.0 in pediatric patients.

251

Cost of Ventricular Assist Device Hospitalization in Children: Maintaining Value in the Era of Rapidly Expanding Use

R. Rizwan,[1] F. Zafar,[1] A. Lorts,[2] C. Villa,[2] D. L. Morales.[1] *[1]Division of Cardiothoracic Surgery, Cincinnati Children's Hospital Medical Center, Cincinnati, OH; [2]Division of Cardiology, Cincinnati Children's Hospital Medical Center, Cincinnati, OH.*

Study: The use of Ventricular assist devices (VAD) in children with end-stage heart failure has increased over time. VAD use has been shown to have a positive impact on waitlist and post-transplant outcomes. This study reports the cost of VAD hospitalizations and changes in cost over time among children in the United States.
Methods: The most recent (2012) Healthcare Cost and Utilization Project - Kids' Inpatient Database (HCUP-KID) was analyzed to identify VAD implants. This database is a cross sectional nationwide sampling of hospital discharges of patients less than 20 years old weighted to provide national estimates. Cost data was compared against inflation adjusted (consumer price index) costs in the 2006 HCUP-KID database.
Results: There were 266 VAD implants performed in the US in year 2012. This was a 42% increase from the year 2006 (187 VAD implants). High volume centers (>5 implants) have performed only 23.5% (63) of these cases, which is a significant decrease (p<0.001) from the year 2006 (40%). Mortality has remained similar between these years (2006, 30% vs 2012, 24%; p=0.14). Mortality is similar between the high-volume and low-volume center; however, likelihood of transplant in the same admission is significantly higher for patients at high-volume centers (43% vs 22%; p=0.001). Median cost per day (MCPD) of VAD hospitalization was not significantly different between 2006 and 2012 (Table). MCPD was similar between the high volume and low volume centers [$7,630 vs $7,321; p=0.197].
Conclusion: VAD utilization has increased over time with more cases being performed at low volume centers currently; however, the likelihood of being transplanted is significantly better at higher volume centers. Despite the increase in utilization, the cost of VAD hospitalization has remained the same over the years.

Table: Comparison of Median Per Day Cost (MPDC) for VAD patients with each of the following characteristics between 2006 (Inflation adjusted for 2012) and 2012

	2006 (Inflation adjusted for 2012)		2012		
	n	Median [IQR]	n	Median [IQR]	p-value
MCPD	187	8,073 [$5,239 - $11,555]	266	$7,592 [$5,075 - $11,446]	0.646
Heart transplant	49 (26%)	$8,663 [$6,548 - $10,848]	72 (27%)	$7,490 [$4,951 - $11,417]	0.056
ECMO	40 (21%)	$11,020 [$8,887 - $15,552]	64 (24%)	$11,590 [$7,324 - $14,992]	0.888
CHD	40 (21%)	$8,121 [$6,237 - $12,605]	83 (31%)	$7,630 [$5,003 - $11,111]	0.242
Stroke	20 (11%)	$8,919 [$7,645 - $9,732]	48 (18%)	$9,071 [$5,283 - $11,643]	0.769
Sepsis	47 (25%)	$7,150 [5,530 - $11,210]	61 (23%)	$8362 [$5,451 - $13,427]	0.409
Acute renal failure	60 (32%)	$9,040 [$5,963 - $14,540]	109 (41%)	$9,482 [$5,431 - $12,620]	0.330
Respiratory failure	66 (35%)	$9,375 [$5,581 - $11,204]	131 (49%)	$7,635 [$5,075 - $11,590]	0.571

253

A Novel, Miniature Implantable Continuous Flow Pediatric Ventricular Assist Device Assist Device

P. D. Wearden,[1] T. A. Snyder,[2] R. K. Wampler,[3] J. R. Stanfield,[2] P. A. Coghill,[2] J. Wu,[4] D. A. Crompton,[5] S. E. Olia,[5] V. Shankarraman,[5] T. J. Maul,[1] S. Madan,[6] M. V. Kameneva,[5] W. R. Wagner,[7] J. W. Long.[8] *[1]Nemours Cardiac Center, Nemours Children's Hospital, Orlando, FL; [2]VADovations, Oklahoma City, OK; [3]Oregon Health & Science University, Portland, OR; [4]Advanced Design Optimization, Irvine, CA; [5]Bioengineering, University of Pittsburgh, Pittsburgh, PA; [6]Children's Hospital of Pittsburgh, Pittsburgh, PA; [7]Bioengineering & Surgery, University of Pittsburgh, Pittsburgh, PA; [8]Advanced Cardiac Care, INTEGRIS Baptist Medical Center, Oklahoma City, OK.*

Study: There is a growing need for a durable, implantable continuous flow ventricular assist device (VAD) suitable for use in children and infants. Herein, we describe efforts to develop a pediatric VAD, building on a miniaturized blood pump core technology designed for hemocompatibility and cost-effectiveness.

Methods: The core blood pump exists within a 7 mm diameter hydraulic flow pathway with modular hydraulics, and incorporates unique inline hydrodynamic bearing and magnetic stabilization of the rotor. The pump was designed to generate 0.8 - 3 LPM of blood flow against systemic pressure. Hydraulic performance and bearing design were evaluated in vitro. Anatomic fit was assessed using imaging from children from 2.5 - 25 kg imported into Mimics (Materialise, Plymouth, MI). Acute and chronic implants were performed in seven sheep. Hemocompatibility was assessed by blood chemistry, plasma free hemoglobin (PFH), advanced flow cytometric assays of platelet and leukocyte activation, aggregation, and microparticles, and by von Willebrand Factor function and distribution.

Results: From anatomic studies, intraventricular pump placement is acceptable for children <10 kg and for infants, intracardiac, trans-mitral LV-LA appears feasible, as does extracardiac placement. In vitro hemolysis testing confirmed low hemolysis (NIH < 0.08 with 2–4 day old sheep blood). During acute and chronic implant testing in 35–47 kg sheep, 1.2–3 LPM was generated with all of the final PFH < 15 mg/dL. There was no sustained increase in platelet or leukocyte activation or aggregation post-implant, and VWF function was preserved. Additional implants in smaller sheep are planned. Overall, this promising early experience demonstrates the feasibility of using a next-generation, miniaturized blood pump, designed for improved hemocompatibility, to support children and infants with heart failure.

266

Versatility of HeartWare HVAD ® Support in Pediatric Patients: Indications and Optimal Timing

K. Maeda, O. Reinhartz, D. N. Rosenthal, C. Almond, B. Kaufman, S. Chen, D. Bernstein, S. Hollander. *Cardiothoracic Surgery, Stanford University, Stanford, CA.*

Study: Despite wide acceptance of HeartWare HVAD® for support of adults, pediatric experience is limited. Herein we report use of HeartWare HVAD® in pediatric patients for left, biventricular, and single-ventricular support with a specific focus on preoperative characteristics.

Methods: We retrospectively reviewed all pediatric HeartWare HVAD® implants at our institution and analyzed indications, support configurations, and preoperative characteristsics, including end-organ function and nutritional status.

Results: Between 6/2013-12/2015, 16 patients underwent HVAD® implantation. Mean age was 14.5 years old (6.6–19.7), and mean BW and BSA were 51.2 kg (18–89) and 1.4 m^2 (1.4–2.0). Cardiac diagnoses included dilated cardiomyopathy 9, hypertrophic cardiomyopathy 2, end-stage biventricular heart disease 1, end-stage univentricular heart disease 2, ARVC 1, and transplant coronary vasculopathy 1. Two patients were on ECMO preoperatively and 4 had previously AICD. Support was left-ventricular in 11, biventricular in 3, and single-ventricular in 2. 3 patients were on mechanical ventilator support and 3 were on BiPAP, at the time of implantation. Mean serum albumin levels were 3.4 mg/dl (2.7–4.5). Body mass index percentile was 23.5 % (0.1–87.9). 11 were on single inotrope and 5 pts were on at least two inotropes. Median creatinine was 0.9 (0.6–4.9) mg/dl, AST 51.0 (15.0–9234) units/l, ALT 43.0 (19.0–6654) units/l, total bilirubin 1.3 (0.2–3.2) mg/dl and INR 1.3 (1.1–3.3). 10 patients were successfully transplanted, 2 patients died as outpatients due to cerebral hemorrhage, and 4 remain on device therapy.

Conclusion: Successful Heartware HVAD® implantation may be achieved in children for left ventricular, biventricular, and single ventricular support. Optimal timing of implant is critically important for these patients, and depends on multiple factors, and favors early implantation prior to end-organ dysfunction and cardiac cachexia.

285

Ventricular Assist Device Support for Systemic Right Ventricle: A Surgical Consideration

S. Burki, A. G. Cabrera, D. Horne, Z. M. Binsalamah, B. A. Elias, I. Adachi. *Texas Children's Hospital, Houston, TX.*

Study: To describe potential solutions for minimizing the risk of inflow cannula obstruction during HeartWare HVAD implantation in a child with systemic right ventricle (RV).

Methods: A 7-year-old male (BSA 0.8 m^2) with unbalanced RV dominant atrioventricular (AV) canal defect, malposed great arteries, and right atrial isomerism was referred to us for failing Fontan circulation. Echocardiogram showed severely depressed RV systolic function and a large RV thrombus. Clinical deterioration on inotropes required HVAD support as bridge to transplant. With cardiopulmonary bypass and aortic crossclamp, RV apical ventriculotomy was created through which the RV thrombus was removed. Intracardiac exploration revealed extensive apical trabeculations. Even after thorough excision of trabeculations, the ventricular cavity was still crowded by a prominent papillary muscle and its apparatus, which could potentially cause obstruction to an inflow cannula once HVAD was inserted. In an attempt at obtaining unobstructive pathway, a pledgeted 5-0 prolene suture was used to tack this papillary muscle to the lateral wall of the RV, thereby suspending it out from the mid ventricular cavity. The rest of the procedure was completed per our usual practice. Cardiopulmonary bypass was weaned off without difficulty as HVAD support was uptitrated. Transesophageal echocardiogram showed mild AV regurgitation (unchanged from prior) and no inflow obstruction. Chest CT angiogram demonstrated patency of the inflow channel despite heavily trabeculated RV cavity. A ramp test performed in the catheterization laboratory confirmed unobstructive inflow cannula, as evidenced by incremental decrease in the atrial pressure while HVAD RPM was sequentially increased. The patient was extubated on postoperative day 20 and has made steady progress.

Results: Extensive resection of apical trabeculations and papillary muscle suspension resulted in favorable HVAD support in a child with failing Fontan circulation.

38

High Efficiency Oxygen Transport Through a Silicon Micropore Membrane Oxygenator

A. Dharia,[1] E. Abada,[2] T. Yeager,[2] W. Moses,[3] J. Park,[2] C. Blaha,[2] N. Wright,[2] B. Padilla,[3] S. Roy.[2] *[1]Pulmonary Critical Care Medicine, UCSF, San Francisco, CA; [2]Department of Bioengineering and Therapeutic Sciences, UCSF, San Francisco, CA; [3]Department of Surgery, UCSF, San Francisco, CA.*

Study: Clinical use of extracorporeal membrane oxygenation (ECMO) is limited due to a significant risk of bleeding, mainly related to the need for high levels of anticoagulation. Improvements to device efficiency can lead to enhanced hemocompatibility, which, in turn, will lower the anticoagulation requirements and better outcomes. We have developed a flat sheet membrane oxygenator design to increase the gas transport efficiency of ECMO systems. The membranes are constructed from silicon micropore chips bonded to a thin layer of polydimethylsiloxane (PDMS); this arrangement results in membranes that are highly gas-permeable, while maintaining a liquid barrier and resisting mechanical deformation. In this study, we evaluated the oxygen exchange properties of the SμM in an *in-vivo* porcine model.

Methods: To determine our oxygenator's gas permeability, we cannulated the femoral and internal jugular veins of two systemically anticoagulated ~55kg Yorkshire pigs. Blood from the femoral vein was then pumped through a flow chamber that housed the membranes, and returned to the jugular vein. Blood gas analysis was performed on blood drawn from the circuit before and after the device to calculate net gas transport. This test was performed with two chamber designs at flow rates of 5-50ml/min and sweep gas pressures of 1.5–10 PSI.

Results: The gas permeability constant for the SμM oxygenator membrane was 177.6 ± 84.2 mL O_2 STP/min/m^2/cmHg (n=13). These proof-of-concept experiments demonstrate highly effective gas transport when compared to conventional ECMO membranes. This is significant because higher rates of gas transport result in decreased membrane surface area, which should translate to improved hemocompatibility of the ECMO system.

53

Normothermic Donor Lung Preservation with Portable EVLP Maintains IL-33-driven Epithelial Integrity Suppressing Inflammation in the Recipient

B. Wiegmann,[1] C. Falk,[2] M. Seyda,[2] C. Neudörfl,[2] C. Kühn,[1] I. Tudorache,[1] M. Avsar,[1] A. Haverich,[1] G. Warnecke.[1] *[1]Dpt. for Cardiothoracic, Transplantation and Vascular Surgery, Hannover Medical School, Hannover, GERMANY; [2]Institute of Transplant Immunology, Hannover Medical School, Hannover, GERMANY.*

Study: INSPIRE trial revealed significant reduction of PGD grade 3 using the Organ Care System (OCS) compared to standard of care (SOC) for lung preservation. To investigate immunological mechanisms initiated by cold vs. normothermic preservation, samples of INSPIRE patients were assessed for proteins involved in epithelial integrity, endothelial activation and immune response.

Methods: Blood plasma and perfusion solutions from 33 patients with OCS and 26 with SOC-preserved lungs were analysed for cytokines and angiogenic factors using multiplex protein assays. Donor and recipient demographics, cold ischemic times and PGD scores were assessed and correlated with plasma proteins.

Results: Clinical evaluation (OCS vs. SOC) revealed mean recipient age: 50 vs. 49, diagnosis: idiopathic fibrosis (n=17 vs. 10), cystic fibrosis (n=7 vs. 8), idiopathic pulmonary hypertension (n=3 vs. 3) and emphysema (n=6 vs. 5), mean total cold ischemic times: 257 vs. 531. In OCS, no PGD score > 2 was observed in contrast to 19% cumulative PGD 3 in SOC. Protein concentrations (e. g. IL-33) were significantly higher in OCS perfusion solutions ($p<0.05$). High IL-10 and IL-31 levels caused a shift towards an anti-inflammatory milieu resulting in significantly lower IL-6 and IL-8 levels in OCS-recipients at T0 ($p<0.05$). Only in SOC patients, IL-6, TNF-a and endoglin levels at T0 correlated with cold ischemic time ($p<0.05$) and IL-6 with PGD score >2. All plasma IL-6, IL-10, IL-8 and IL-33 concentrations peaked at T0, creating only favourable IL-10/IFN-g ratio in OCS patients. Summarizing, correlations of plasma IL-6, endoglin and IL-8 with cold ischemic times and PGD in SOC underline the clinical relationship between inflammation and graft function. During OCS preservation, IL-33 expression promotes an anti-inflammatory milieu guided by high IL-10 and IL-31 counterbalancing graft dysfunction and inflammatory reactions in the recipient.

62

Development of Combined Diagnostic Medical Device

W. Kim, **H. Kim**. *Department of Medicine, Division of Pulmonary and Critical Care Medicine, SMC(Samsung Medical Center), Seoul, KOREA, REPUBLIC OF.*

Study: The incidence of cardiopulmonary diseases is rapidly increasing as the aging of the population. For the early detection of the critical cardiopulmonary diseases, we plan to develop the device that can measure multiple bio-signals and detect the early cardiopulmonary illness.
Methods: Our research team is decided to manufacture a mobile medical device that has a diagnostic function of cardiopulmonary disorders. Through this device, patients can check their bio-signals by themselves and be advised for their health. First, we need to select useful bio-signals that can be obtained non-invasively and used for developing diagnostic algorithms. Several main signals, such as auscultation sound, electrocardiogram, pulse shape and pulse oximeter were selected.Second, for building a mainframe, we progress comparative analysis to select outstanding sensors. MEMS-based sensors were chosen with excellent frequency range and SNR, starting the hardware fabrication.Also, through a preliminary survey such as a market analysis and development strategy, we determined the prototype design focused on a strength of convenience and mobility.
Results: We developed the prototype of combined medical device derived from our research, which can measure multiple signals at the same time. The initial algorithms were also developed and under further upgrade by using patients' data, which were obtained from target disease patients by the aids of clinical trial team. Through the further upgrading of the algorithm, we will improve combined diagnostic medical device, and contribute the healthcare system as well as elevating our quality of life.This research is supported by the Ministry of Science, ICT and Future Planning and National Research Foundation of Korea (NRF-2014M3A9E2062267).

63

Evaluation of Pulsatlie Blood Flow in Oxygenators

L. Schraven,[1] A. Kaesler,[1] C. Flege,[2] R. Kopp,[2] T. Schmitz-Rode,[1] U. Steinseifer,[1] J. Arens.[1] *[1]Department of Cardiovascular Engineering, RWTH Aachen University, Aachen, GERMANY; [2]Department of Intensive Care, University Hospital RWTH Aachen, Aachen, GERMANY.*

Study: ECLA systems still have problems with thrombus formation, hemocompatibility, and inefficient gas exchange. One possible element of improvement of ECLA systems is pulsatile blood flow in the extracorporeal circuit. The general hypothesis is that especially the oxygenator works better with this form of flow as it provokes a better mixing and therefore, the thrombus formation is minimized and the haemocompatibility and gas exchange are improved.
Methods: A thorough literature review revealed positive and negative statements about the effects of pulsatile blood flow on oxygenators. Some studies state that pulsatile blood flow has negative effects on the efficiency of the oxygenator because the mechanical influence of geometry causes problems like high damping. Other publications about the systemic inflammation and oxygen gas transfer show similar results during constant and pulsatile flow. In contrast, there are studies which reveal a better gas exchange and perfusion. In order to get a valid statement about these controversial studies we planned a structured test series. For this we firstly designed a small oxygenator with a well-defined flow distribution inside the fiber bundle which gives us the additional opportunity for in-silico flow simulations, PIV-measurements, and in-vitro validation. This oxygenator has a gas exchange area of 0.25 m^2 with PMP fibers, designed for a mean blood flow of 100 to 800 ml/min. Subsequently, we conducted an exploratory test series with a limited combination of frequency, amplitude, and wave form of the pulsation parameters to get first hints about the effect on gas transfer and pressure drop.
Results: Previous studies described in literature, reveal controversy results on the effects of pulsatile flow with often no exact definition of the used pulsation parameters. In order to achieve a valid statement, we regard a well-structured test scenario as necessary. The results of this first series will be presented at the conference.

105

Determination of the Optimal Nitric Oxide Dose for Oxygenator Sweep Gas

C. T. Demarest, R. Ukita, C. Do-Nguyen, A. Lai, K. E. Cook. *Biomedical Engineering, Carnegie Mellon University, Pittsburgh, PA.*

Study: Artificial lungs fail due to clotting. To prevent this, our lab is investigating coupling nitric oxide (NO) delivery with anti-fouling zwitterionic coatings. The purpose of this study was to determine the optimal safe NO sweep gas concentration. At low doses, NO may not inhibit platelets, but at high doses, NO is toxic, resulting in methemoglobinemia and metabolic acidosis.

Methods: Miniature artificial lung (MAL) devices were attached to anesthetized rabbits (4.23 kg, average weight) in a venovenous extracorporeal membrane oxygenation configuration. The gas exchange surface was a bundle of silicone-coated polypropylene hollow fibers with a surface area of 0.1m^2. No anticoagulant was administered. Blood flow through the circuit was maintained at 35.7 mL/kg/min. Sweep gas flow was double that value and consisted of oxygen and various doses of NO (0, 250, and 500 ppm, n=3 ea). Data acquired included activated clotting time (ACT), arterial blood gases, and plasma p-selectin (PS). After 4 hours, the animals were euthanized and scanning electron micrographs (SEM) were taken of the fiber.

Results: All MALs demonstrated little visible clot over the test duration. Average ACTs were similar in all experiments. NO toxicity with methemoglobinemia resulted in metabolic acidosis, indicated by decreasing serum bicarbonate. As anticipated, 500 ppm NO resulted in the most acidosis (Fig 1A). Increasing doses of NO resulted in a smaller percent decrease in platelet count and smaller PS concentrations (Fig 1B), indicating less platelet adhesion and activation. SEMs indicate much greater clot formation on the fiber bundle weft fibers, which do not carry gas and do not release NO. Therefore, NO delivery via sweep gas prevents platelet activation and deposition at the fiber surface, but 500 ppm and likely 250 ppm are too toxic. Future studies will examine 100 ppm, which has been shown to be effective at reducing platelet activation when coupled with zwitterionic surfaces due to their synergistic action.

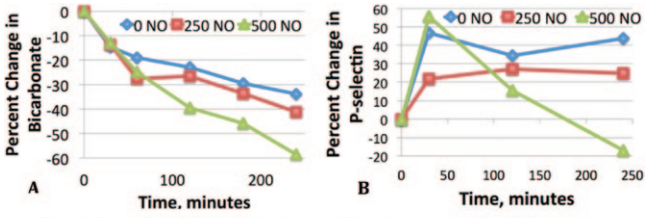

Figure 1: Percent change in A) serum bicarbonate and B) p-selectin.

106

Clot Formation and Functional Changes in the CardioHelp Oxygenator Over Time

C. T. Demarest,[1] S. J. Shoemaker,[1] S. R. Chicotka,[2] K. Fung,[3] M. D. Bacchetta,[2] J. F. Antaki,[1] K. E. Cook.[1] *[1]Biomedical Engineering, Carnegie Mellon University, Pittsburgh, PA; [2]Cardiothoracic Surgery, New York Presbyterian Hospital/Columbia University Medical Center, New York, NY; [3]Clinical Perfusion, New York Presbyterian Hospital/Columbia University Medical Center, New York, NY.*

Study: Despite advances, application of extracorporeal membrane oxygenation (ECMO) remains limited due to biocompatibility issues, including device failure via clot formation. However, little research to date is focused on where clots form within oxygenators and the conditions that accelerate this process. Greater understanding of this process and resulting changes in device performance will allow engineers to better design future devices.

Methods: All data come from Maquet CardioHelp oxygenator cases at a single institution. Data collected throughout the ECMO course include device blood flow (Q) and resistance (*R*), and arterial blood gases. Gas transfer (XFER) and inlet-outlet oxygen content differences (IOOCD) were calculated. Following device failure or patient weaning, the oxygenators were rinsed and photographed. The images were converted to binary using ImageJ, where clot is depicted as white and everything else is black. These binary images were then imported into MATLAB, which creates a heat map image depicting the frequency of clot formation, from blue (0% clot frequency) to red (100% clot frequency).

Results: An initial group of 12 cases was analyzed. Indications included cardiogenic shock (n=3), acute respiratory distress syndrome (n=7), pulmonary embolism (n=1), and cystic fibrosis (n=1). Device duration ranged from 5 to 21 days (mean: 13 ± 1.75). Three-day *R* averages increased linearly with time (Fig 1A) for the first 10 days. Thereafter, 4 of 12 devices had more extreme, exponential increases. Oxygen XFER decreases over time due to decreases in Q during weaning and O_2 exchange efficiency. Device IOOCD was stable for 10 days but decreased over days 13–21 (Fig 1B). Our image analysis reveals that clot forms at the device edges and in a standard pattern in the device center furthest from the inlets (Fig 1C,D). As additional cases are obtained, we plan to compare different oxygenators as well as patient conditions (i.e. diagnosis, clotting time, flow rate) that predict device failure.

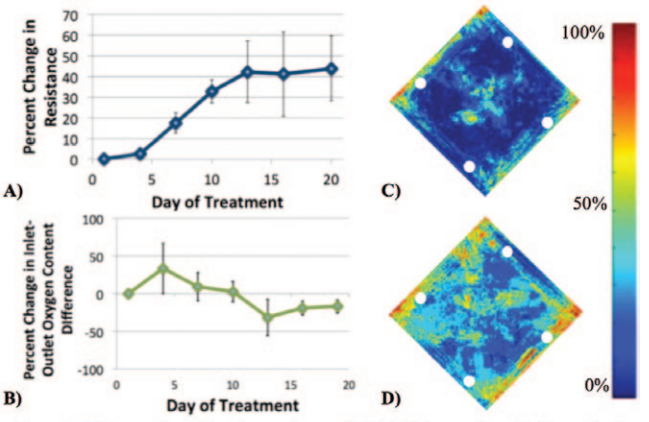

Figure 1: A) Percent change in resistance (mean ± SEM); B) Percent change in inlet-outlet O_2 content difference (mean ± SEM); Probability of clot formation at the device inlet at C) 5-11 days (n=6); D) 14-21 days (n=6). The white circles depict the four inlets of the device.

108

Qualitative Prediction of Hemolysis in an Integrated Pump/oxygenator Using CFD for Design Optimization

P. Albal. *ALung Technolgies, Pittsburgh, PA.*

Study: The development of reliable blood damage models is critical for in-silico design and optimization of blood pumps and oxygenators. Currently available hemolysis models are suitable for very simple geometries or for understanding fundamental mechanisms governing blood cell damage. However, they are not appropriate/practical for complex medical devices and hence, an alternative approach is necessary. In this study, we present a simplified qualitative approach to elucidate the primary parameters affecting hemolysis in an integrated pump/oxygenator (Hemolung, ALung Technologies, Pittsburgh, PA) without the need to quantifiably predict hemolysis.

Methods: For the CFD analysis, the fluid volume geometry of the device was created in SolidWorks (Concord, MA), exported as a parasolid, and meshed in ANSYS Workbench 15 (Canonsburg, PA). A mesh sensitivity analysis was performed. Different test cases were simulated for varying mass flow rates and pump speeds (RPM), corresponding to conditions tested on the bench. Hemolysis was measured experimentally using an in vitro blood loop according to ISO 7199 and represented as TIH (Therapeutic Index of Hemolysis) values.

Results: CFD results demonstrated that wall shear stress (WSS) remains constant with change in mass flow rate (Fig 1a) whereas it increases linearly with change in RPM (Fig 1c). The experimental TIH results corresponded with the WSS trends (Fig. 2b and 2d), where hemolysis (TIH) increased with pump speed (RPM), yet remained constant over the mass flow rates tested. The results indicate that hemolysis in this device is driven by WSS from the rotating pump. Hence, WSS optimization should be targeted as a critical design parameter for the next generation device. This technique enables identification the principal parameters affecting hemolysis without having to perform complex validation of a mathematical hemolysis model and will be greatly useful for optimization of devices in industry.

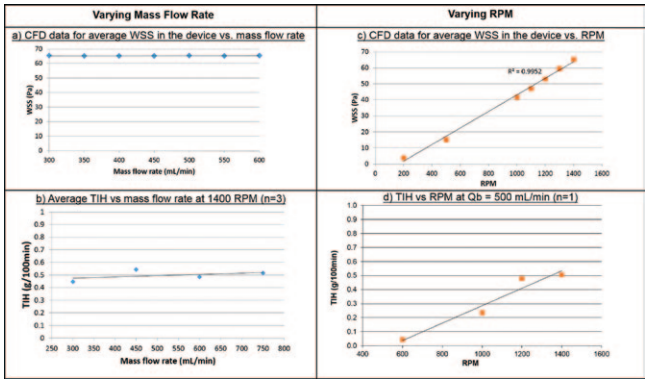

113

Development of an Ultra Compact ECMO System and Evaluation in a Long-term Animal Experiment

N. Katagiri, E. Tatsumi, Y. Takewa, T. Tsukiya, T. Mizuno, Y. Fujii, K. Togo, Y. Taenaka. *Artificial Organs, National Cerebral and Cardiovascular Center Research Institute, Suita, Osaka, JAPAN.*

Study: Some of cardiopulmonary support system have been employed a combination of an oxygenator and a pump those were approved for several hours use. In cases that require respiratory / circulatory support from days to weeks, however, lack of cardiopulmonary support system with an approval of long-term use caused prolonged use of conventional products with risks of complications related to thrombus and device exchange. We have been developing an ECMO system for long-term use in order to solve the current situation. In this study, we made a prototype of a compact ECMO system and evaluated its long-term durability and antithrombogenicity by a chronic animal experiment.

Methods: This ECMO system is consisted of a disposable unit, a driver unit and a gas bomb unit. The disposable unit was designed as a pre-connected ECMO circuit. A compact oxygenator (BIOCUBE6000), a novel hydrodynamically levitated centrifugal blood pump and tubes were arranged in order for being mountable on the driver unit. And its entire blood-contacting surface was treated with heparin bonding material (T-NCVC). A pump motor, measurement instruments and a display were integrated into the driver unit. Veno-arterial bypass ECMO with a prototype system was conducted for 18 days using an adult goat weighing 61 kg. Continuous heparin administration was conducted for keeping ACT in the range 150–200 sec.

Results: A dedicated pre-connected circuit design could provide one-touch mountable holder and reinforcement of kink-prone tubes to the disposable unit. The driver unit had a small size (W290 x D205 x H260 mm) and lightweight (6.6 kg). Chronic animal experiment could run continuously without device exchange. 2.5 L/min of bypass flow rate could be maintained stably. O_2 and CO_2 transfer rates were kept at sufficient levels (140 ± 14 and 90 ± 22 mL/min, respectively). After the experiment, no thrombi were observed in the ECMO circuit. The prototype of ultra compact ECMO system indicated the possibility of durability for over 2 weeks.

175

Developing a Biohybrid Lung: Ex vivo Testing of Limitations and Possibilities

E. M. Schumer,[1] K. Hoffler,[2] C. Kuehn,[2] S. Korossis,[2] M. S. Slaughter,[1] A. Haverich,[2] B. Wiegmann.[2] *[1]Department of Cardiovascular and Thoracic Surgery, University of Louisville, Louisville, KY; [2]Department of Cardiothoracic, Transplantation and Vascular Surgery, Hannover Medical School, Hannover, GERMANY.*

Study: The lack of donor organs has led to the development of alternative "destination therapies", such as a biohybrid lung (BH) for end-stage lung disease. Ultimately aiming at a fully implantable BH, general capabilities and limitations of different oxygenators were tested based on the model of BH positioning at the right upper lobe.
Methods: Three different sized oxygenators (neonatal, pediatric, adult) were tested in a mock circulation loop regarding oxygenation and decarboxylation capacities for three respiratory pathologies. Blood flows were imitated by a roller pump, and respiration was imitated by a mechanical ventilator with different levels of support. Pressure drops across the oxygenators and the integrity of the gas exchange hollow fibers were analyzed.
Results: The neonatal oxygenator proved to be insufficient regarding oxygenation and decarboxylation. Despite elevated pCO_2 levels, the pediatric and adult oxygenators delivered comparable sufficient oxygen levels, but sufficient decarboxylation across the oxygenators was ensured only at flow rates of 0.5 L/min (Figure 1). Only the adult oxygenator indicated no significant pressure drops. For all tested conditions, gas exchange hollow fibers remained intact. This is the first study showing the general feasibility of delivering sufficient levels of gas exchange to a BH via mechanical ventilation without damaging the gas exchange hollow fiber membranes.

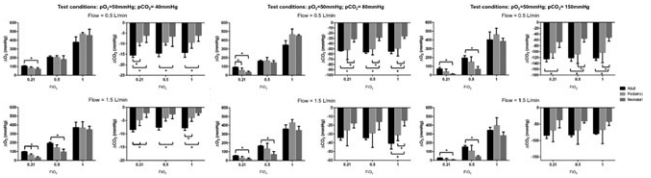

204

Rolled Construction and Scalable Design of Cylindrical Microfluidic Artificial Lungs

A. J. Thompson,[1] M. J. Goudie,[2] H. Handa,[2] A. Rojas-Pena,[3] J. A. Potkay.[1] *[1]VA Ann Arbor Healthcare System, Ann Arbor, MI; [2]Department of Biological Engineering, University of Georgia, Athens, GA; [3]Department of Surgery, University of Michigan Health System, Ann Arbor, MI.*

Study: Microfluidic artificial lungs (µALs) can potentially improve artificial lung technology by providing a high surface area to blood volume ratio for gas exchange and biomimetic blood flow paths. However, two major limitations of µALs are identified: 1) small rated blood flow and 2) lack of a large-scale manufacturing technique. In this work, a scalable method for combining many gas transfer units in a single device by rolling a patterned PDMS sheet around a cylindrical substrate is studied.
Methods: µAL preparation: Molds for µALs were fabricated using standard photolithography techniques, and devices are fabricated from a single mold. PDMS is spun to desired thickness, cured, and rolled/bonded around a silicone substrate to obtain a 4 layer µAL with blood flow, membrane, gas flow, and capping layers.

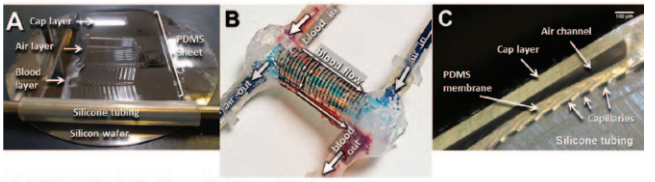

Fig 1. (A) Device before bonding, (B) a completed device, and (C) device cross-section.

In vitro studies: After confirming gross functionality, µALs were supplied with anticoagulated bovine blood (0.1–0.5 mL/min, 9.6 ± 0.3 Hb), and conditioned using either 100% O_2 or 21% O_2 (air) sweep gas (1 mL/min). Pressure drop and gas exchange were monitored (n=3 devices) and compared to theoretical values.
Results: Fabricated devices (n=3) had 12 µm high artificial capillaries and 50 µm thick PDMS membranes (Fig. 1). Oxygen saturation of blood varied inversely with blood flow rate, and ranged from 100 ± 0 - 97 ± 2.7% (pure O_2 sweep) and from 98.3 ± 1.7 - 87.7 ± 2.7% (air sweep, Fig 2). Blood pCO_2 levels ranged from 25.3 ± 4.4 - 45.5 ± 2.6 mmHg (air sweep, Fig 2), and pressure drop ranged from 36.1 ± 2.8 - 114 ± 14 mmHg. Gas exchange efficiency (mL gas $\cdot m^{-2} \cdot min^{-1}$) is comparable to commercial ALs and reported µALs. This proof of concept is promising for scale-up of µAL to higher rated flows. Also, this method allows for gas exchange into intermediate blood channels from two sides, which can increase efficiency for devices with many gas exchange units.

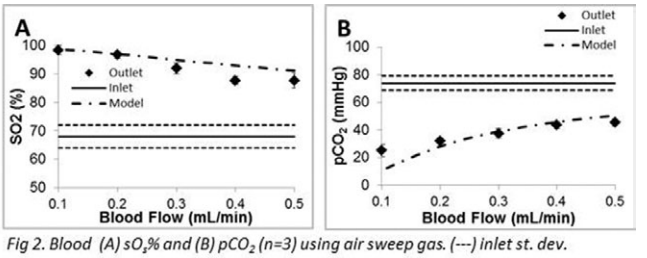

Fig 2. Blood (A) sO_2% and (B) pCO_2 (n=3) using air sweep gas. (---) inlet st. dev.

235

Changes in Pulmonary Artery Impedance and RV Pressure-volume Loop in Embolism-induced Pulmonary Hypertension-right Heart Failure Sheep Model

D. Wang,[1] C. Zhou,[1] P. Hsu,[2] Z. Du,[1] Y. Yang,[1] X. Huang,[1] K. Polley,[1] C. Ballard-Croft,[1] J. B. Zwischenberger.[1] *[1]Surgery, University of Kentucky, Lexington, KY; [2]School of Mechanical and Electrical Engineering, Soochow University, Suzhou, CHINA.*

Study: A pulmonary hypertension (PH)-induced right heart failure (RHF) large animal model is needed to evaluate right ventricular assist devices (RVADs). We are developing a sheep pulmonary artery (PA) embolism induced-PH-RHF model.
Methods: In adult female sheep (n=8), a perivascular flow probe was inserted via a 3rd intercostal thoracotomy for PA blood flow/waveform measurement. The RV pressure-volume (P-V) loop was measured with a conductance catheter. Intravenous boluses of 250 mg Polydextran beads (300 µm OD) were administered at 15 min increments. PA pressure (PAP), left atrial pressure (LAP), central venous pressure (CVP), arterial blood pressure (ABP), PA flow, and RV P-V loop were recorded 15 min after each beads infusion.
Results: All animals developed PH and died of RHF. An average 3.3 beads infusions (825 mg) resulted in PH (mPAP >25 mm Hg). The highest mPAP was 42 ± 6 mm Hg with a dosage of 9 beads infusions (2.25 g, Fig 1A). This dose also decreased CO (from 4.1 ± 0.7 to 3.0 ± 0.9L/min, Fig 1A), establishing stable PH with RHF. One additional beads dosage (2.5 g) was lethal. CVP was significantly increased only at RHF. Pulmonary vascular impedance significantly increased, with a 6 times increase in Z0 (increased vascular resistance), a 3.5 times increase in Z1 (decreased RV-PA coupling) and a right shifted f_{min}. The RV PV-loop progressively shifted up and to the right with shape change from triangle to rectangle (Fig 1B). The PV-loop Ea gradually increased, indicating increased total RV afterload. Ees/Ea showed significantly less RV-PA coupling along with decreased CO.
Conclusions: The beads-induced PA embolism resulted in PH and RHF with a very narrow dosage window between stable RHF and death. A progressive increase in PA impedance was observed while the RV P-V loop showed increased pre-afterload and decreased RV-PA coupling. This model closely parallels the clinical scenario, allowing an ideal model for RVADs.

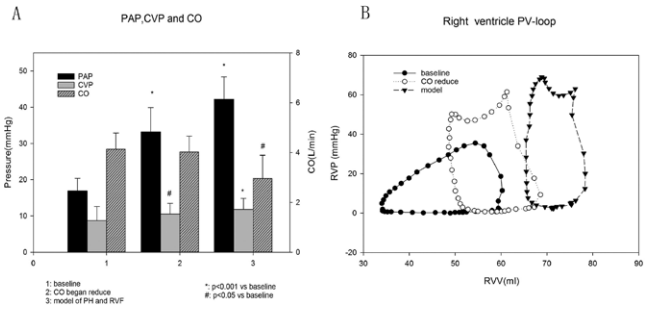

243

Hemodynamic Benefit of Intra-atrial Right-to-Left Shunt Flow for Pulmonary Hypertension Induced-Right Heart Failure: A Simulation Study

P. Hsu,[1] D. Wang,[2] C. Ballard-Croft,[2] A. Shafii,[2] J. B. Zwischenberger.[2] *[1]School of Mechanical and Electrical Engineering, Soochow University, Suzhou, CHINA; [2]Surgery, University of Kentucky, Lexington, KY.*

Study: Percutaneous atrial septostomy has been used in pulmonary hypertension induced-right heart failure to augment left ventricular (LV) output and unload the right ventricle (RV). A computer model was used to evaluate the quantitative relationship between right atrium to left atrium (R-L) shunt flow and LV output augmentation/RV unloading.
Methods: A numerical lumped-parameter model of the human circulation was employed to simulate pulmonary hypertension-induced right heart failure. This simulation model was characterized by decreased cardiac output (CO, 3.2 L/min) and elevated mean right atrial pressure (mRAP,19.4 mm Hg)/mean pulmonary artery pressure (mPAP, 74.4 mmHg). A R-L shunt flow (Qs) was created. This Qs was increased from 0.3 to 1.5 L/min in 0.3 L/min increments. At each Qs, RV/LV CO, left atrial pressure (LAP), mRAP, mPAP, RV, total work, and arterial saturation level (SaO2) were calculated.
Results: The results are shown in Fig. 1. Incremental increases in R-L shunt flow from 0.3 to 1.5 l/min: 1) progressively increased LAP and augmented the LV CO from 3.2 to 4.4 L/min, 2) decreased mRAP (RV preload) from 19.4 to 16.3 mmHg and reduced RV CO from 3.2 to 2.9 L/min, 3) decreased RV total work from 1.27 to 1.20 W, and 4) decreased SaO2 from 98% to 80%.
Conclusions: Our computer model shows that R-L shunt significantly augmented LV output and provided mild RV unloading. However, R-L shunt also significantly decreased SaO2. The optimal R-L shunt should be determined through a balance between LV CO augmentation and SaO2 reduction.

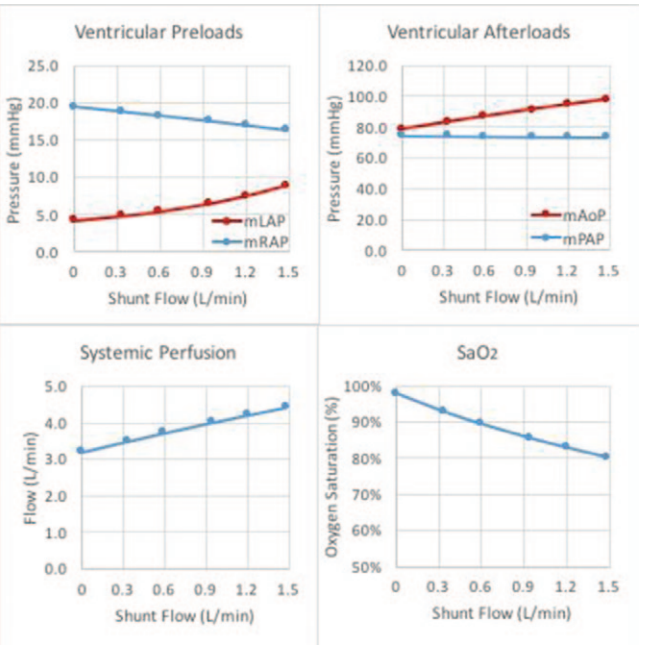

254

Extracorporeal CO_2 Removal by Hemodialysis for Hypercarbic Respiratory Failure: A Bench Feasibility Study

A. May,[1] A. Sen,[2] M. E. Cove,[3] J. A. Kellum,[4] W. J. Federspiel.[1] *[1]University of Pittsburgh, Pittsburgh, PA; [2]Department of Critical Care Medicine, Mayo Clinic Arizona, Scottsdale, AZ; [3]Department of Critical Care, NUHC, Singapore, SINGAPORE; [4]Department of Critical Care Medicine, University of Pittsburgh Medical Center, Pittsburgh, PA.*

Study: Extracorporeal CO_2 removal ($ECCO_2R$) is a treatment option for patients with acute lung failure, including ARDS and acute exacerbations of COPD. Respiratory hemodialysis is a form of $ECCO_2R$ that uses traditional hemodialysis to remove bicarbonate from blood. Metabolic acidosis resulting from the bicarbonate removal has limited the feasibility of respiratory hemodialysis. Here we apply Stewart's acid base chemistry to create a zero bicarbonate dialysate that maximizes bicarbonate dialysis without disrupting blood pH. This study investigates the feasibility of respiratory hemodialysis using our novel dialysate.
Methods: Bench studies were performed using a scaled down respiratory hemodialyzer in bovine or porcine blood. The scale factor for the bench studies was 22.5 (a 0.04 m^2 Gambro M10 dialyzer to a 0.9 m^2 M100 dialyzer). Dialysate flow rates ranged from 2.2 to 24 mL/min and blood flow rates were 11 and 18.7 mL/min. Blood inlet pCO_2 concentrations were 50 and 100 mmHg. CO_2 transfer was calculated as the sum of the changes in measured pCO_2 and calculated bicarbonate, using the Henderson-Hasselbalch equation, in the blood across the dialyzer.
Results: The results presented below are scaled up to those expected in standard hemodialyzers. CO_2 removal rates of 62.6 and 78.1 mL/min were obtained at blood flow rates of 248 and 420 mL/min, respectively, at an inlet pCO_2 of 50 mmHg. At an inlet pCO_2 of 100 mmHg the CO_2 removal rate was 117.8 mL/min at a blood flow rate of 248 mL/min. Increasing the dialysate flow rate from 67.5 to 450 mL/min resulted in a 103% increase in CO_2 removal at a blood flow rate of 248 mL/min. At a blood flow rate of 420 mL/min the CO_2 removal rate increased by 56% when the dialysate flow rate increased from 67.5 to 360 mL/min. None of the test conditions increased the blood pH by more than 0.08. These CO_2 removal rates were obtained at IHD dialysate flow rates, 400–500 mL/min. Ongoing work is being done to design a recirculation loop for the dialysate to allow for IHD flow rates.

256

***In-vitro* and Acute *in-vivo* Studies of an Integrated Wearable Pump-lung**

S. P. Madhani,[1] B. J. Frankowski,[1] G. Burgreen,[2] J. F. Antaki,[3] J. D'Cunha,[1] R. Kormos,[1] W. Federspiel. 15232.[1] *[1]Department of Bioengineering, University of Pittsburgh, Pittsburgh, PA; [2]CAVS, Missisipi State University, Starkville, MS; [3]Department of Biomedical Engineering, Carnegie Mellon University, Pittsburgh, PA.*

Study: We are developing the Paracorporeal Ambulatory Assist Lung (PAAL), intended to provide 70% to 100% lung support. The PAAL is an integrated and portable blood pump and gas exchange device designed to ambulate lung failure patients during bridge to transplant or recovery. The PAAL approach focuses on high gas exchange efficiency through the design of its hollow fiber membrane (HFM) bundle. Gas exchange efficiency is improved by increasing the mean blood flow velocity past fibers and allows for a reduction in HFM bundle size. This study investigates the in-vitro and acute in-vivo performance of the PAAL.
Methods: The PAAL features a 1.75 inch diameter cylindrical HFM bundle of stacked sheets, with a surface area of 0.65 m2. The centrifugal pump integrated into the device is designed to pump through a 27 Fr Maquet Dual Lumen Cannula (DLC). The PAAL was tested on the bench for gas exchange in accordance with AAMI 7199 standards as well as hemolysis in accordance with ASTM F1841 standards. The PAAL was then tested in 40–60 kg adult sheep (n=4) for 6h.
Results: The PAAL pumped 3.5 L/min against the DLC at 1900 RPM. Oxygenation performance met the target of 180 ml/min at 3.5 L/min of blood flow in vitro, at 277 ml/min/m2 efficiency. The normalized index of hemolysis for the PAAL and cannula was 0.054 g/100L at 3.5 L/min, as compared to 0.020 g/100L for control (DLC cannula and a Centrimag pump). In the acute animal studies, blood left the device fully oxygenated (100% sat) in vivo with inlet sat ranging from 50 to 70%. Oxygenation reached 155 ml/min at 3.5 L/min for an inlet sat of 69%. Plasma-free hemoglobin (pfHb) was unchanged from baseline (5-10mg/dL) for three animals. In one animal pfHb increased but plateaued under 20 mg/dL. A macroscopic thrombus characterization of the fiber bundle showed some small thrombi in some experiments but as the anticoagulation management improved the presence of thrombi was eliminated. The PAAL met in vitro and acute in vivo performance targets. 5 day chronic sheep studies are planned in the near term.

265

Early Tracheostomy in Patients Undergoing Veno-venous Extracorporeal Life Support Improves Survival

A. M. Bhatt,[1] R. S. Tripathi,[1] J. Crestanello,[2] A. Kilic,[2] S. Moffat-Bruce,[3] T. J. Papadimos,[1] **B. A. Whitson**.[2] *[1]Department of Anesthesiology, The Ohio State University, Columbus, OH; [2]Department of Surgery, Division of Cardiac Surgery, The Ohio State University, Columbus, OH; [3]Department of Surgery, Division of Thoracic Surgery, The Ohio State University, Columbus, OH.*

Study: Patients with respiratory failure who require veno-venous extra-corporeal life support (VV-ECLS) are ventilator dependent for prolonged periods of time. Endotracheal intubation has limitations on pulmonary toilet, ventilator weaning, and mobilization. We sought to determine if early tracheostomy had a significant impact on survival to decannulation in patients requiring VV-ECLS.

Methods: We retrospectively evaluated patients who underwent ECLS to include those with VV-ECLS for respiratory failure from January 1, 2012 through December 31, 2015. Type of ECLS, potential confounders, demographics, and risk scores at time of ECLS initiation were recorded. Tracheostomy during ECLS was noted. The primary outcome was survival to decannulation. Standard statistical methods were used.

Results: During the study period there were 151 patients received ECLS with 45 VV-ECLS patients meeting inclusion criteria. The overall survival for those patients who underwent VV-ECLS was 79.5%. There were 22 patients (48.9%) who received a tracheostomy. There were 22 men (48.9%). At the time of cannulation, median RESP score was 1 (range -13 to 6), and mean SOFA score was 11.5 +/- 3.8. In patients who had tracheostomy, survival was 95.5% (21/22) as compared to 63.6% (14/23) in those without tracheostomy (p=0.0058). The mean age of survivors was 40.7 compared to 43 in non-survivors (p=0.78). Gender, SOFA or RESP scores were not significant predictors of survival. There were no major bleeding or airway complications in those patients with tracheostomy. Early tracheostomy in VV-ECLS is safe and contributes to early mobilization and lung recovery. In a contemporary series of VV-ELCS patients with similar management, early tracheostomy has a significant positive impact on survival to ECLS decannulation.

46

Validity of a Kinetic Modeling for Continuous Renal Replacement Therapy (CRRT)

M. Mineshima. *Clinical Engineering, Tokyo Women's Medical University, Tokyo, JAPAN.*

Study: In CRRT, there are no guidelines for selecting modalities of the treatment, or for determining the treatment schedule, treatment time and operating conditions, such as dialysate flow rate (Q_D) and filtration flow rate (Q_F) for individual patient. In this paper, the solute removal characteristics of CRRT modalities and the optimal operating conditions for individual patients are examined from the viewpoint of a kinetic modeling.
Methods: An in vitro study using an aqueous solution involving several marker solutes was performed.
Results: From a result of the continuous hemodialysis (CHD) experiments, the dialysate flow rate Q_D should be required at least twice the patient's blood flow rate (Q_B) for sufficient removal of small molecular substances. CHD is of limited use for the removal of middle or more-sized molecules. During the continuous Hemofiltration (CHF) experiments in the post-dilution mode, the maximum filtration flow rate Q_F value can be determined as about 1/4 of the Q_B because of the existence of the formed elements, such as erythrocytes. From the continuous hemodiafiltration (CHDF) experiments, the Q_F is about 1/4 of Q_B value and the Q_D should be set up at least twice the Q_B value. The determination of adequate operating conditions for individual patients who receive CRRT can be summarized from a kinetic modeling viewpoint:(1)Determination of the targeted solute according to the patient's state.(2)Determination of the generation rate of the targeted solute by collecting spent dialysate and/or filtrate. (3)Determination of the minimal requirement treatment dose from the actual and targeted solute concentration levels. (4)Choice of treatment modality and determination of the treatment time according to the clearance value. Measurement of the removed amount of solute by collecting the spent dialysate and/or filtrate is recommended to maintain an adequate plasma level of the targeted solute in patients, who often have unstable states.

96

Surgical Considerations for an Implantable Renal Replacement System

W. Moses,[1] S. Kim,[2] Z. Iqbal,[3] J. Park,[3] N. Wright,[3] C. Blaha,[3] J. A. Heller,[3] M. Goodin,[4] K. Goldman,[5] J. Roberts,[1] G. Wieselthaler,[1] C. Owens,[1] W. H. Fissell,[6] S. Roy.[3] *[1]Department of Surgery, University of California, San Francisco, San Francisco, CA; [2]Division of Nephrology, University of California, San Francisco, San Francisco, CA; [3]Bioengineering & Therapeutic Sciences, University of California, San Francisco, San Francisco, CA; [4]SimuTech Group, Hudson, OH; [5]H-Cubed, Inc., Olmsted Falls, OH; [6]Division of Nephrology, Vanderbilt University, Nashville, TN.*

Study: Silicon nanopore membranes are key to the construction of a pumpless implantable renal replacement system. Through the development of an early-stage implantable prototype and subsequent preclinical feasibility testing in a large animal-model, we have attempted to examine key surgical and clinical factors.
Methods: An iterative proof-of-concept study was designed to develop the implantation procedure and to evaluate the blood-flow characteristics of the prototype. A swine model was selected because of the comparably sized vasculature and hematologic similarities with humans.
Results: A prototype was fabricated with a 3mm inlet and outlet, which was divided into three 1mm high blood channels defined by silicon parallel plates. The titanium-based device was 9.3cm x 5.7cm x 1.4cm with a dry weight of 189g. Autoclave was used for sterilization. Dacron (polyester) grafts with titanium connectors served as the blood conduits. Initial implantations were unsuccessful due to thrombosis. The Dacron grafts were not structurally rigid enough to prevent kinking. Moreover, inadequate anchoring and subsequent device shifting subjected the grafts to additional extrinsic forces. Iterative changes included replacing Dacron with a ringed two-layered graft (Polytetrafluoroethylene (PTFE) bonded to polyester) and reinforced with a silicone strain-relieving sleeve. Sections of the titanium exoskeleton were replaced with Polyether ether ketone (PEEK), which reduced movement of the implant and resulted in a 40% dry-weight reduction. . The anticoagulation regimen was modified to include Coumadin with a lovenox-bridge. These changes, along with refinement of the surgical procedure, allowed for successful implantation of the prototype with flow and patency confirmed via fluoroscopy on post-operative day 3.

133

A New Algorithm To Predict IDH Through A Multi-parametric Analysis On The Dialysis Project Data

C. Bianchi,[1] G. Casagrande,[1] D. Vito,[1] C. Minoretti,[2] G. Pontoriero,[3] G. Rombolà,[4] C. Schoenholzer,[5] M. Costantino.[1] *[1]Chemistry, Materials and Chemical Engineering Department, Politecnico di Milano, Milan, ITALY; [2]Azienda Ospedaliera Sant'Anna, San Fermo della Battaglia (CO), ITALY; [3]Ospedale Alessandro Manzoni, Lecco, ITALY; [4]Ospedale di Circolo e Fondazione Macchi, Varese, ITALY; [5]Ospedale Regionale di Lugano (EOC), Lugano, SWITZERLAND.*

Study: Intra-dialysis hypotension (IDH) is one of the most important short-term complications of haemodialysis. The aim of this work is to improve dialysis therapy outcomes by developing an algorithm, able to detect the risk of IDH onset, from multi-parametric dialysis data analysis.
Methods: Based on the literature and on data recorded during 434 dialysis sessions at Lecco Hospital (IT) and EOC (Lugano,CH), a set of shared criteria for the identification of IDH, were defined together with the clinicians.Statistical and sensitivity analyses on the acquired data allow highlighting and identifying physiological and etiological factors having a trigger role in IDH onset. A multi-parametric algorithm for IDH prediction was developed, as a function of intra-dialysis variations of blood pressure, blood volume, heart rate and potassium plasma concentration.The algorithm was used to predict IDH during further 311 sessions, involving a total of 4 dialysis units (Lugano-CH, Lecco, Como, Varese-IT). During these sessions, the IDH risk was detected, and a warning was recorded without alter clinical practice, so as to verify the effective IDH onset. After its onset, IDH was treated by using the usual management protocol.
Results: Sessions characterized by IDH were the 13% of the total in the 1st data set, and the 11% in the 2nd one. The application of the developed algorithm during the 2nd acquisition phase would have allowed the reduction of the 54% of the IDH episodes, with a specificity of 99.6%. In conclusion, the developed multi-parametric algorithm is a suitable IDH predictor and an easy tool to improve dialysis therapy outcomes.

144

Computational Study of AFE System Outflow Vein Blood Flow

D. B. Pike,[1] J. S. Richardson,[2] Y. Shiu,[1] L. W. Kraiss,[3] H. M. Loree, II[2] F. N. Franano,[4] A. K. Cheung.[1] *[1]Division of Nephrology and Hypertension, University of Utah School of Medicine, Salt Lake City, UT; [2]R&D, Flow Forward Medical, Inc., Lowell, MA; [3]Division of Vascular Surgery, University of Utah School of Medicine, Salt Lake City, UT; [4]Flow Forward Medical, Inc., Olathe, KS.*

Study: The purpose of this work is to understand cephalic vein blood flow and wall motion during treatment with the Arteriovenous Fistula Eligibility (AFE) System™ from Flow Forward Medical, Inc. The AFE System is a small, temporary, external blood pump designed to stimulate flow-mediated vein dilation prior to arteriovenous fistula (AVF) surgery, making more patients eligible for an AVF and increasing AVF maturation rates.
Methods: We investigated the velocity, wall shear stress (WSS), and pressure fields within a model of a curved 4 mm AFE System outflow conduit connected to a 4 mm cephalic vein through a 30° end (conduit) to side (vein) anastomosis using a computational fluid dynamics (CFD) simulation, with boundary conditions set to flow and pressure values measured during mock flow loop studies. Vessel wall motion was characterized using fluid-structure interaction (FSI) simulation. In the model, a nonpulsatile flow of 431 mL/min from the AFE System entered the cephalic vein and traveled only in the antegrade direction.
Results: CFD demonstrated spiral flow in the curved distal portion of the outflow conduit and into the anastomosis, with a flow jet impinging on the wall of the cephalic vein opposite the anastomosis (**Fig. 1A**). WSS peaks of ~ 20 Pa were observed within the curved conduit, at the toe of the anastomosis, and in the wall jet region (**Fig. 1B**). A mean WSS of 4 Pa was achieved about 20 mm downstream in the antegrade portion of the cephalic vein. A distinct pressure drop occurred along the entire flow path. Aside from distension of the walls of the antegrade portion of the cephalic vein, FSI did not result in any significant changes to the flow field. Ongoing studies of the AFE System will investigate the effects of anastomotic angle, vein diameter, and AFE System outflow conduit pressure on AFE System outflow vein blood velocity, pressure, WSS, and wall motion. Concurrent studies of conventional radiocephalic AVFs will investigate the effect of vein diameter and arterial blood pressure on these same parameters in the AVF outflow vein.

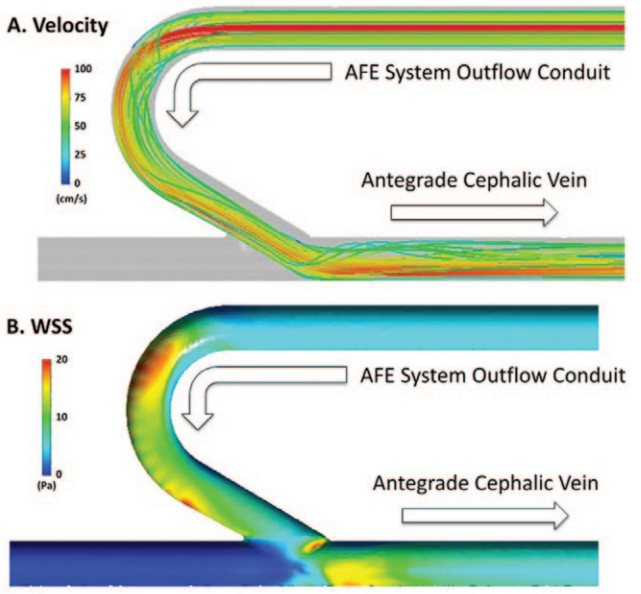

Fig. 1. Blood flow velocity (A) and WSS (B) in AFE System outflow conduit and cephalic vein by CFD

148

A Portable Hemofiltration System Newly Designed with aSmall Centrifugal Pump

T. Yamane,[1] Y. Kojima,[1] A. Tagi,[1] W. Yuasa,[1] A. Michiwaki,[1] T. Azuma,[2] O. Maruyama,[3] K. Yamamoto,[4] K. Matsuda.[5] *[1]School of Engineering, Kobe University, Kobe, JAPAN; [2]School of Medicine, Kobe University, Kobe, JAPAN; [3]Health Research Inst., AIST, Tsukuba, JAPAN; [4]Kawasaki University of Medical Welfare, Kurashiki, Okayama, JAPAN; [5]Dept. Emergency & Critical Care Medicine, School of Medicine, University of Yamanashi, Chuo, Yamanashi, JAPAN.*

Study: Population of dialysis patient is 310,000 at present in Japan. We are trying to replace a conventional roller pump with a small centrifugal pump to downsize the blood purification systems without using 120L dialysate. The first-stage aim of the present study is to develop a portable hemofiltration system having venous access for emergency care. This system can also be used for home care or for disaster care in the future.
Methods: We have developed small centrifugal pumps, DP3 and DP6, whose impeller diameters are 30 and 34 mm, respectively. Hemolysis tests were conducted and evaluated the plasma free hemoglobin with newly defined NIH(g/20min), which is extended for general flow assuming T=100L/(5L/min)=20min on NIH(g/100L) of ASTM standard. We also conducted an animal experiment with a pig to compare the hemofiltration characteristics of a centrifugal pump, DP3, with a conventional roller pump, Nipro MP-301.
Results: As a result, the indices of hemolysis turned out to be NIH(g/20min)=0.003 and 0.004, respectively. The NIH values were under 20% of that of a commercial centrifugal pump. In the animal experiment the transmembrane pressure, TMP, of DP3 pump was less than those of a roller pump. It can be understood that fouling in a centrifugal pump, representing degradation of the hemofilter, was less than that in a roller pump due to a steady flow instead of a pulsatile flow. [Conclusion] The results revealed that a developed centrifugal pump is not inferior in hemofiltration performance and has possibility to extend the filter lifetime compared to a conventional roller pump. Together with superiority of downsizing, a hemofiltration system with a centrifugal pump would be a superior system to the conventional system.

156

Design and Testing of Inflow Conduit Tip for Arteriovenous Fistula Eligibility (AFE) System

J. S. Richardson,[1] D. G. White,[2] B. S. Hutto,[3] J. M. Bernhard,[4] D. M. Groth,[5] G. D. Tansley,[6] H. M. Loree, II[7] F. N. Franano.[8] *[1]Flow Forward Medical, Inc., Lowell, MA; [2]White Enterprises, LLC, Rancho Santa Margarita, CA; [3]CIRTEC Medical Systems, LLC, Los Gatos, CA; [4]Bernhard Consulting, Framingham, MA; [5]Surpass, inc., Osceola, WI; [6]School of Engineering, Griffith University, Southport, AUSTRALIA; [7]R&D, Flow Forward Medical, Inc., Lowell, MA; [8]Flow Forward Medical, Inc., Olathe, KS.*

Study: The preferred form of vascular access for hemodialysis is the arteriovenous fistula (AVF). Flow Forward Medical's Arteriovenous Fistula Eligibility (AFE) System™ is designed to pump non-pulsatile blood into peripheral veins for 10 - 14 days prior to AVF creation and promote rapid peripheral vein dilation, thereby increasing AVF eligibility and improving AVF maturation. The AFE System comprises a small extracorporeal centrifugal blood pump, cuffed and heparin-coated inflow and outflow conduits, and a wearable controller with rechargeable batteries. This study was designed to evaluate blood flow characteristics and hemolysis for various inflow conduit tip configurations.
Methods: Computational fluid dynamics (CFD) studies were performed to assess max wall shear stress (WSS) and surface washing for five inflow conduit tip configurations (blunt, beveled, tapered, crown, and duckbill) in the superior vena cava (SVC) or mid right atrium (RA) at flow rates of 250 and 1000 mL/min. Three conduit configurations were then subject to *in vitro* hemolysis testing (flow = 1000 mL/min, duration = 6 hrs, n = 5), including a commercially available pediatric ECMO venous return catheter (Maquet HKV23P). The design with the lowest hemolysis (duckbill tip) was evaluated in a 3-day nonclinical study of the AFE System in a porcine model (weight = 29.6 kg, flow = 250 - 450 mL/min, mid-RA placement, ACT = 150 - 300 s, n = 1).
Results: CFD demonstrated that the duckbill tip had the lowest max WSS of the designs tested and that mid-RA placement provided better surface washing than SVC placement. Hemolysis studies showed that the duckbill tip (N.I.H. 59 ± 36 mg) caused significantly less hemolysis than either the crown tip (N.I.H. 128 ± 44 mg) or the Maquet HKV23P catheter (N.I.H 146 ± 75 mg). Necropsy after *in vivo* use of an inflow conduit with a duckbill tip confirmed an absence of adherent thrombus. Additional nonclinical studies of longer duration are planned.

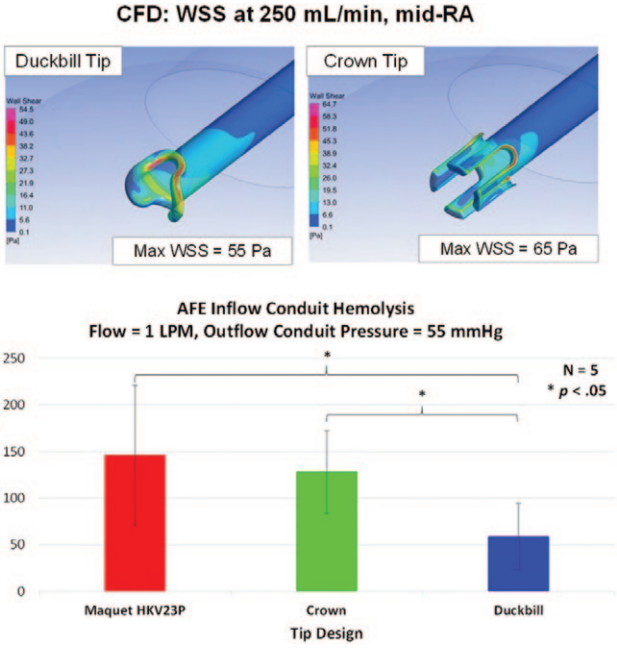

166

The Influence of Catheter Design on Convection-Dominated Heparin Leakage

M. C. Barbour,[1] K. Sansom,[1] K. Gow,[2] A. Aliseda.[1] *[1]Mechanical Engineering, University of Washington, Seattle, WA; [2]Seattle Children's Hospital and Department of Surgery, University of Washington, Seattle, WA.*

Study: The dominant mechanism in heparin leakage from central venous catheters (CVCs) has been shown to be convective flux of heparin from the catheter tip forced by the surrounding pulsatile blood flow, and instillation. Due to the rapid timescale of convection, the tip of a CVC is likely to contain negligible heparin concentration for the majority of the cycle. In the present study, we extend upon our previous work and investigate heparin egress from multiple catheter designs and sizes, under flow conditions representative of different patient ages. The goal of this study is to determine if convective leakage is the dominant mechanism driving heparin leakage across catheter types and patient characteristics, thus enabling a search for catheter designs that are less susceptible to forced convective transport and more capable of keeping an effective heparin lock.
Methods: Four catheters, in the 9.6 -13.5 Fr size, are studied: three with different side hole configurations and a Port-a-cath with no side holes. A fluorescent, heparin-mimicking fluid is instilled into the catheters and leakage from the catheter is measured using measurements of velocity (with Particle Image Velocimetry, PIV) and concentration (with planar laser induced fluorescence, PLIF). The catheters are placed inside of a pulsatile flow loop that matches the waveforms from 6–14 year old patient's superior vena cava. To investigate the influence of pulsatility and flow inertia, a second waveform with a 20% lower flow rate and 20% variation in heart rate is also studied.
Results: Results suggest that catheter tip geometry and side hole count and location do influence the rate of convectively-driven heparin leakage. Increases in pulsatility and inertia in the surrounding flow, increases the convective flux of heparin from the catheter tip. However, convective fluxes deplete the catheter tip much faster than heparin diffusion can reheparinize it. Thus, heparin concentration near the tip region is negligible after only 10-100s.

196

Four Methods to Reduce Exposure to Heparin During Hemodialysis

M. Skagerlind, Sr. **B. Stegmayr. Sr**. *Public Health and Clinical Medicine, Umea University, Umea, SWEDEN.*

Study: Heparin (UFH) is widely used to prevent clotting during hemodialysis (HD). For patients at risk of bleeding UFH has to be minimized. The aim was to clarify the efficacy and safety of 4 different low-dose UFH methods instead of a standard HD (SHD) using a tinzaparin bolus dose.
Methods: 23 patients on chronic HD were their own controls (case-control design); SHD was compared to HD without a bolus or maintenance dose of UFH using a heparin-coated filter (Evodial®, Gambro), or a solutions that was wasted after priming with 5000 units UFH/L saline (HS), HS + 1g albumin/L saline (HA), HA + citrate in the dialysate (HAC). Blood samples were collected at 0, 30 and 180 min during HD. Small heparin bolus doses were allowed during HD to avoid interruption by clotting.
Results: Compared to SHD (0/23 HD) extensive clotting caused interruption of HD in 7/20 using H (p=0.008), 3/21 with HA (ns), 1/19 with Evodial® (ns), 0/17 using HAC (ns). The mean Activated Partial Thromboplastin time (APT, ref 22–37 sec) at 30 and 180 minutes was with SHD 98 vs. 48 (sec). APT at 30 and 180 minutes did not differ between the other methods (H-priming: 39 vs. 38; HA: 35 vs. 32; HAC: 36 vs. 31; Evodial®: 32 vs. 31). Urea-Reduction-Rate (URR) was less with Evodial® at 30 and 180min vs. SHD (22 vs. 27% and 55 vs. 63%, p<0.01), H (25% at 30 and 57% at 180, p<0.01), HA (59% at 180 min, p=0.001), and HAC (61% at 180min, p=0.006). Mean UFH dose used: HAC:184 ± 299 Units, Evodial®:184 ± 506, HA:413 ± 695, H:642 ± 1442, SHD:4400 ± 1838 Units tinzaparin. No prolonged bleeding was noted.
Conclusion: The study indicated that sole heparin priming is least suitable. The URR was least with Evodial®. Individual and local experiences have to be considered.

241

Outside in Filter Design for Long Term Hemodialysis and Hemofiltration

M. E. Labib,[1] S. S. Dukhin,[1] Y. Tabani,[1] R. C. Lai,[1] P. Materna,[1] A. L. Zydney.[2] *[1]R & D, Novaflux Technologies, Princeton, NJ; [2]Department of Chemical Engineering, The Pennsylvania State University, University Park, PA.*

Study: In conventional hemodialysis (with blood flowing inside the hollow fibers), a single blood clot can permanently block a given fiber. In contrast to this situation, experiments have now been successfully performed in which the blood flows outside the fibers, in the space between the fibers and the housing. Any individual blood clot simply causes a redirection of blood flow, with minimal overall impact. For this, it is desirable to have the blood flow distribution in the fiber bundle be as uniform as possible, to avoid clumping of the fibers, to avoid or minimize blood flow stagnation points, and to stay within certain desirable numerical ranges of blood flow shear rate and velocity.
Methods: Relevant filter design variables to attain this include the packing fraction of fibers inside the housing, waviness of fibers, surface properties and chemistry of fibers, blood flow rates, and flow-related geometry at the ends of cartridges including the geometry of orbital distributors.
Results: Experiments show that much longer periods of treatment, including continuous treatment, are possible. This should allow long treatment times without clogging, and new modes of therapy. We will present the fundamentals of filter design and preferred operating conditions.

244

Predicting Removal of β-2-microglobulin in the Silicon Nanopore Membrane Based Artificial Kidney

B. J. Feinberg,[1] J. C. Hsiao,[1] J. Park,[1] A. L. Zydney,[2] W. H. Fissell,[3] S. Roy.[1] *[1]Bioengineering and Therapeutic Sciences, University of California, San Francisco, San Francisco, CA; [2]Department of Chemical Engineering, The Pennsylvania State University, University Park, PA; [3]Department of Medicine and Division of Nephrology and Hypertension, Vanderbilt University, Nashville, TN.*

Study: Recent research has demonstrated that low removal of middle molecular weight solutes such as β-2-microglobulin (B2M) is correlated with poorer clinical outcomes for kidney dialysis patients. Thus, in developing an implantable artificial kidney, the removal of these middle molecule solutes through hemofiltration membranes is of particular interest. However, at small pore sizes (5 to 15 nm) the influence of intermolecular forces such as van der Waals (vdW) and acid-base (AB) interactions can become important, significantly affecting the rate of transport. We present a mechanistic transport model accounting for the impact of these intermolecular forces in the unique slit pore geometry of silicon nanopore membranes (SNM), enabling the design of a robust artificial kidney with high middle molecule removal that would improve patient outcomes.
Methods: Goniometric measurement was conducted in order to characterize the vdW and AB surface tension parameters of B2M and polyethylene-glycol (PEG) modified SNM. Using these values, we applied the surface element integration method to numerically determine the solute partition coefficient and hindrance factors for transport of a spherical solute through a slit pore. Combined with existing membrane filtration models accounting for concentration polarization, the overall rate of transport of B2M through SNM was determined and validated experimentally by membrane sieving experiments over a range of pore sizes and operating pressures.
Results: AB and vdW interaction energy values between B2M and PEG modified SNM were determined to be 33.7 mJ/m^2 and -4.0 mJ/m^2, respectively. Data from sieving experiments correspond well with predicted model values (RMSSD = 2.75) over relevant operating pressures (1 to 4 psi) and pore size (8.5 nm). The model serves as a valuable tool in demonstrating how an artificial kidney with targeted membrane structure can optimize removal of clinically relevant middle molecular weight solutes.

255

Effect of the Blood Vessels Resistance in the Maturation of Grafts as Arteriovenous Fistula for Hemodialysis

K. T. Valencia Rivero,[1] A. P. Molano,[2] J. C. Briceño.[1] *[1]Bogotá D.C., Universidad de los Andes, Bogotá D.C., COLOMBIA; [2]Bogotá D.C., Fundación Cardioinfantil Instituto de Cardiología, Bogotá D.C., COLOMBIA.*

Study: Chronic Kidney Disease affects about 20 million people in the USA, with around 370.000 patients in Hemodialysis (HD) needing fistulae or grafts as vascular access for their treatment. Arteriovenous fistula (AVF) needs 6 weeks of maturation after surgical implantation to reach the required blood flow through it. The objective of this study was to analyze the effect of blood vessels resistance on AVF maturation by means of mathematical modelling.
Methods: Three mathematical models with different parameters and strategies were developed to evaluate resistances in the AVF, including arterial and venous sections upstream and downstream of the fistula. Model I used pressure heads and the Conservation of Energy and Mass in an ideal fluid. Model II implemented pressure drops, a Newtonian blood flow, geometrical relationships and friction losses. Model III was an analogy between the arteriovenous connection and an electrical circuit based on the Ohm's law, Kirchhoff's current law and Poiseuille's law. Doppler ultrasound examinations of patients with AVF were used for the calibration and validation of the mathematical models.
Results: The results show that during AVF maturation the resistance of the downstream artery increases and the resistances in the AVF and in the upstream vein decreases, promoting blood flow through the AVF, an arterialized vein and an ideal flow and proper AVF maturation. AVF with diameter smaller than 2.5 mm have a pressure drop directly proportional to blood flow, while larger AVF have a constant pressure drop close to 70 mmHg. Hypotension is a risk factor in the AVF maturation because the arterial resistance decreases and the venous increases, deflecting the blood flow away from the AVF. In conclusion, several mathematical models of the flow in the AVF have been implemented. These models allow to improve understanding of the maturation process and the changes in flow through the AVF. As a future work, model III can be a tool for predicting AVF maturation.

280

Impact of Sterilization Techniques on Polymer-coated Silicon for Renal Replacement Applications

W. Moses,[1] Z. Iqbal,[2] S. Kim,[3] E. Kim,[2] J. Park,[2] W. H. Fissell,[4] S. Roy.[2] *[1]Department of Surgery, University of California, San Francisco, CA; [2]Bioengineering & Therapeutic Sciences, University of California, San Francisco, CA; [3]Division of Nephrology, University of California, San Francisco, CA; [4]Division of Nephrology, Vanderbilt University, Nashville, TN.*

Study: Silicon nanopore membranes, functionalized with hemocompatible polymer-based coatings, show promise as a filter for an implantable renal replacement system. However, there is a paucity of information regarding how sterilization, necessary for clinical application, affects these membranes and their function. We aim to characterize the effects of five standard sterilization modalities on coated substrates.
Methods: Solid 1 x 1cm silicon chips were coated with polyethylene glycol (PEG) or poly-sulfobetaine methacrylate (pSBMA) and then exposed to one of five sterilization modalities (autoclave, dry heat (160 °C for 120 minutes), ethylene oxide (EtO), hydrogen peroxide (Sterrad˚) and x-ray). Uncoated and non-sterilized membranes served as controls. The surface coatings were analyzed by contact angle, x-ray photoelectron spectroscopy (XPS), ellipsometry and ELISA for albumin adsorption.
Results: After sterilization the presence of PEG and pSBMA was confirmed by contact angle and XPS. Autoclave was the only technique that caused a significant decrease in the thickness of the PEG layer (Δ0.327nm, p=0.0013). For pSBMA, each sterilization technique caused a significant decrease in thickness except EtO. X-ray resulted in the largest decrease in pSBMA thickness (Δ3.192nm, p=0.019). Moreover, compared to non-sterilized substrates, x-ray had the largest increase in albumin adsorption, particularly for pSBMA-coated silicon (+12.86%, p=0.0018). Sterilization of coated silicon wafers alters their surface chemistry and likely their biocompatibility. While in most cases the alterations appear to be relatively equivalent without major differences, x-ray, particularly of pSBMA-coated membranes, appears to be least favorable as it had the largest effect on protein adsorption and polymer thickness. Understanding the impact of sterilization on silicon substrates is essential to ensuring efficacy and hemocompatibility of implantable renal replacement systems.